The Interaction of $GABA_A$ Receptors with Synaptic Adhesion Proteins Regulates the Formation and Function of GABAergic Synapses

Yusheng Sui

Thesis submitted to University College London for the Degree of Doctor of Philosophy (PhD)

Supervisor: Prof Jasmina Jovanovic

School of Pharmacy

University College London

Declaration

I, Yusheng Sui, confirm that the work presented in this thesis is my own. Where information has been derived from other sources, I confirm that this has been indicated in the thesis.

Abstract

$GABA_A$ receptors are crucial for maintaining the balance between the excitation and inhibition in the brain. They mediate tonic inhibition at extrasynaptic locations or phasic inhibition by generating inhibitory postsynaptic currents at GABAergic synapses. Formation of GABAergic synapses during development involves complex protein-protein interactions between the presynaptic and postsynaptic elements. The focus of my thesis has been on interactions between $GABA_A$ receptors and Neuroginin-2 (NL2)/Neurexin, Dystroglycan/Pikachurin complexes and Diazepam Binding Inhibitor (DBI), using a co-culture approach.

I used stable HEK293 cell lines expressing synaptic ($\alpha_2\beta_2\gamma_2$) or extrasynaptic ($\alpha_4\beta_3\delta$) types of $GABA_A$ receptors in co-culture with GABAergic neurons to study synaptic contact formation by immunolabelling and confocal and super-resolution imaging. My results show that synaptic $GABA_A$ receptors can induce synaptogenesis on their own but also enhance synaptogenic effects of NL2. Extrasynaptic $GABA_A$ receptors do not induce synaptic contacts but can enhance synaptogenesis induced by NL2, although significantly less than synaptic $GABA_A$ receptors. Synaptic $GABA_A$ receptors and NL2 cooperativity is mediated by direct interactions between the $GABA_A$ receptors γ_2 subunit and NL2 via their intracellular domains. Functional assessment of synaptic contacts was done using electrophysiology and confocal imaging of the activity-dependent fluorescent labelling of presynaptic terminals forming contacts with HEK293 cells.

Using the same approaches, I have also shown that Dystroglycan, a well-

established synaptic adhesion protein, does not induce synaptic contacts but in combination with a synaptic matrix protein Pikachurin, can induce synaptogenesis in co-cultures. In a separate set of experiments, I have shown that expression of DBI, a multifunctional protein that inhibits allosteric modulation of $GABA_A$ receptors by benzodiazepines, can also promote synaptic contact formation in this system.

In summary, my studies indicate that synaptic $GABA_A$ receptors play an important structural role during synaptogenesis and provide evidence for the key interaction between these receptors and NL2 in this process.

Impact Statement

GABAergic synapses are the basic units of the neural circuits that regulate the activity of the central nervous system. They play a pivotal role in maintaining the excitation/inhibition balance, the disruption of which leads to a variety of neurological, neurodevelopmental, and psychiatric diseases including chronic pain, anxiety, depression, stroke, schizophrenia, and dementia. One important factor contributing to the normal functionality of GABAergic synapses is the clustering of specific $GABA_A$ receptors and scaffolding/adhesion proteins. Numerous studies have identified various proteins expressed in GABAergic synapses that facilitate their formation. Currently, we know very little about the cellular and molecular mechanisms underlying this process.

The current study uncovered a novel molecular mechanism underlying the formation of functional GABAergic synapses, which relies on a synergistic interaction between the $GABA_A$ receptors and Neuroligin-2. This mechanism extends our understanding of the regulation of GABAergic synaptogenesis and provides new targets for drug development for the neuropsychiatric disorders caused by dysfunction of GABAergic synapses.

In addition, I have characterized the synaptogenic effects of three proteins Pikachurin, Dystroglycan, and Diazepam binding inhibitor *in vitro*, which contributes to the current knowledge base for the proteins that regulate GABAergic synapse formation. These results can bring about further *in vitro* and *in vivo* studies that will reveal the exact roles of these proteins in neuronal

development. Moreover, Diazepam binding inhibitor acts by inhibiting the binding of benzodiazepines to $GABA_A$ receptors. Revealing how this protein regulates GABAergic synaptogenesis paves the way to potentially diminishing the adverse effects of benzodiazepines, which limit their clinic use.

In conclusion, the current study has extended our knowledge about the GABAergic synaptogenesis, which supports the downstream investigation on the treatment of neuropsychiatric diseases by expanding the basic knowledge and providing novel potential drug targets.

Acknowledgment

I would like to express my deepest appreciation to Prof Jasmina Jovanovic, for all your professional and endless help. This project would not have been possible without your patience, professionalism, encouragement, and inspiration. During my study, you were always there to help, timely but never too much. This has helped me to learn and progress at the same time, instead of passively receiving knowledge. I cannot think about any more than you did that a supervisor can possibly offer. Thank you, Dr. Audrey Mercer. Although we haven't worked so much together, your support for my experiment and encouragement during the study have been indispensable.

I also want to thank Dr. Martin Mortensen and Prof Trevor Smart. I have learned a lot from our collaboration. Thank you, Dr. Martin Nicholson, although you have left only a year after I joined the lab, you had been a fantastic colleague and a great mentor for the beginning of my PhD journey. Without your help, it would have definitely taken me much longer to start.

My acknowledgment also goes to my colleague and best friend in our lab Banghao Yuan, for your help in my research and learning technique. It was a great pleasure working with you. The experiments we conducted together and the discussion have inspired me a lot.

I would love to express my special thank you to Duanyi Chen, for always being by my side, for support and encouragement when things became tough,

and for the hot meal when I came back after late experiments. This journey must have been more difficult without you.

Last but absolutely not least, my parents, Xiaojing Liu and Kuiting Sui, deserve my endless and most sincere gratefulness for your constant love and support. Thank you for all the guidance that makes me a scientific person in childhood, and for supporting all my studies.

Table of Contents

List of Abbreviations:

ACBP - Acyl-CoA binding protein

AP2 - Clathrin adaptor protein 2

APS - Ammonium persulphate

Ara-C - Cytosine β-D-arabinoside

BCA - Bicinchoninic acid

BCIP - 5-Bromo-4-chloro-3-indolyl phosphate

BIC - Bicuculline

BIG2 - Brefeldin A-inhibited GDP/GTP exchange factor 2

BiP - Immunoglobulin heavy chain binding protein

BSA - Bovine serum albumin

CCK - Cholecystokinin

CDC42 - Cell division control protein 42

CNS - Central nervous system

DBI - Diazepam binding inhibitor

ddH_2O - Double distilled water

DGC - Dystrophin-Glycoprotein complex

DIA - Diazepam

DIV - Day in vitro

DMEM - Dulbecco's Minimum Essential Medium

DMSO - Dimethyl sulfoxide

DSP - Dithiobis (succinimidyl propionate)

DTT – Dithiothreitol

ECD - Extracellular domain

ECM - Extracellular matrix

EGF - Epidermal growth factor-like

EM - Cryo-electron microscopy

EPSP - Excitatory postsynaptic current

ER - Endoplasmic reticulum

ERM - Ezrin, Radixin, and Moesin

FBS - Fetal bovine serum

GABA - γ-Aminobutyric acid

GABARAP - GABA receptor associated protein

GAD - Glutamic acid decarboxylase

GEF - Guanine exchange factor

GFP - Green fluorescent protein

GODZ - Golgi-specific DHHC (Asp-His-His-Cys) zinc finger proteins

HBM - HEPES buffered incubation medium

HBSS - Hanks' Balanced Salt Solution

HRP - Horseradish peroxide

IgSF - Immunoglobulin superfamily

IPSC - Inhibitory postsynaptic currents

IQR - Interquartile range

KCC2 - Potassium-chloride cotransporter isoform 2

Lhfpl4/GARLH4 - Lipoma HMGIC fusion partner-like 4

LNS - Laminin-neurexin-sex hormone binding globulin

MDGA - Mucin domain-containing glycosylphosphatidylinositol anchor protein

Munc13 - Mammalian homolog of unc-13

NBT - Nitro blue tetrazolium

NKCC1 - Sodium-potassium-chloride cotransporter

NL2 - Neuroligin-2

NSF - N-ethylmaleimide-sensitive factor

ODN - Octadecaneuropeptide

PBS - Phosphate-buffered saline

PFA – Paraformaldehyde

pLGIC - Pentameric ligand-gated ion channels

PMSF - Phenylmethylsulfonyl fluorid

PSD - Postsynaptic density

PTP - Protein tyrosine phosphatase

PV - Parvalbumin

RIM-BP - RIM binding proteins

SB - Sample buffer

SDS - Sodium dodecyl sulphate

SDS-PAGE - Sodium dodecyl-polyacrylamide gel electrophoresis

SIM - Structured illumination microscope

Slitrk - Slit- and Trk-like

SNAP-25 - Synaptosomal-associated protein-25

SNARE - Soluble N-ethylmaleimide-sensitive component attachment protein receptor

S-SCAM - Synaptic scaffolding molecule

SVZ - Subventricular zone

TB - Transfer buffer

TBS-T - Tris buffered saline-Tween

TE - Tris-EDTA

TEMED - Tetramethyl ethylenediamine

TEMED - Tetramethylethylenediamine

TM - Transmembrane domains

TMB – Tetramethylbenzidine

TTN - Triakontatetraneuropeptide

VGAT - Vesicular GABA transporter

VGCC - Voltage-gated calcium channel

wt - Wild type

1. Introduction

Normal brain function is based on the information processed and transmitted by neural circuits. Synapses are highly specialized intercellular junctions that are the basic units of the neuronal circuits, which are crucial for the information exchange and storage between neurons (Mayford, Siegelbaum and Kandel, 2012). The term synapse was first described as a functional connection between excitable neurons, from the study of the spinal reflex by neurophysiologist C. S. Sherrington in the 1890s. There are two types of synapses: electrical and chemical. In the electrical synapses, the neighboring neurons are connected by gap junctions which are specialized intercellular channels permitting ions to flow directly between the cells and allowing reciprocal information exchange (Bennett and Zukin, 2004).

In the human brain, the majority of the interneuronal connections are chemical synapses that possess a more complicated structure, involving various proteins expressed in and between the pre- and postsynaptic specializations, allowing information exchange from a presynaptic cell to a postsynaptic cell. The chemical synapses utilize molecules called neurotransmitters, as the chemical messengers for the synaptic transmission. In the majority of the chemical synapses in the brain, glutamate or γ-aminobutyric acid (GABA) is used as the neurotransmitter. Glutamate induces excitatory postsynaptic currents (EPSPs) which increase the probability of action potentials, while GABA induces inhibitory

postsynaptic currents (IPSCs) which decrease the probability of action potential, of the postsynaptic cell. It is crucial to maintain a balanced excitation/inhibition ratio for the normal function of neural circuits. In a simplified view, either when excitation exceeds inhibition or when inhibition exceeds excitation, the balance in the neural circuit is broken, which will lead to pathological symptoms in later development stages (Rubenstein and Merzenich, 2003).

1.1 GABA and GABAA Receptors

GABA is the predominant inhibitory neurotransmitter in the brain, which specifically binds to three different types of receptors: ionotropic $GABA_A$ receptors, metabotropic $GABA_B$ receptors, and ionotropic $GABA_C$ receptors. $GABA_A$ and $GABA_C$ receptors are ligand-gated ion channels, which show a high level of homology in the genes that express them, with the latter being predominantly found in the retina (Lukasiewicz, 1996). $GABA_B$ receptors are G protein-coupled receptors that primarily regulate tonic inhibition in the central nervous system (CNS).

1.1.1 GABA Synthesis and Release

GABA is a four-carbon amino acid initially discovered in plants and later identified in animal brains. GABA is synthesized by decarboxylation of glutamic acid which is catalyzed by the enzyme glutamic acid decarboxylase (GAD), of which two isoforms encoded by two separate genes, GAD 65 and GAD 67, exist. The majority of neurons express both isoforms but the spatial distribution varies. GAD

65 localizes in the synaptic terminals and synthesizes GABA for release into the synaptic cleft, while GAD 67 is more widely distributed in the cell body (Soghomonian and Martin, 1998).

GABA is transported into the small synaptic vesicles by the activity of the vesicular GABA transporter (VGAT) which localizes to the membrane of these vesicles. GABA is released from the presynaptic terminal via vesicle exocytosis when the presynaptic membrane is depolarized in response to an action potential. This leads to an influx of calcium ions via the voltage-gated calcium channels, triggering the activity of the SNARE complex which mediates the fusion of the vesicle membrane with the plasma membrane and thus the release of GABA into the synaptic cleft (Barclay, Morgan and Burgoyne, 2005).

1.1.2 Structure of $GABA_A$ Receptors

$GABA_A$ receptors belong to a superfamily of the cys-loop pentameric ligand-gated ion channels (pLGICs) which also includes the nicotinic acetylcholine receptors, glycine receptors, and 5-hydroxytryptamine type 3 receptors (Olsen, 2018). $GABA_A$ receptors are heteropentamers, composed of subunits that have been classified according to the homology of the DNA sequence into α, β, γ, δ, θ, π, and ρ families. There have been six α, three β, three γ, three ρ, and one δ, θ, ε or π subunits discovered to form a variety of $GABA_A$ receptor subtypes that function differentially in the CNS (Sigel and Steinmann, 2012). Among these subunits, the ρ subunit is predominantly found in the retina and was previously considered to form $GABA_C$ receptors (Johnston, 1996). The $GABA_C$ receptor was

later categorized into a subfamily of $GABA_A$ receptor (Olsen and Sieghart, 2008).

The subunits share a common structure. Each subunit contains a large extracellular N-terminus, four transmembrane domains (TM1-4), a relatively large intracellular loop (between TM3-4), which interacts with the cytoplasmic proteins and is subjected to posttranslational modifications, and a small extracellular C-terminus (Figure 1.1A). The most common type of $GABA_A$ receptors in the brain is formed by two α, two β, and one γ or δ subunit in the order shown in Figure 1.1B. The extracellular N-terminal domains of these subunits are essential for the assembly and trafficking of the $GABA_A$ receptors (Wong, Tae and Cromer, 2015), as well as the binding of GABA and many other ligands that regulate their function. The structure of the $GABA_A$ receptors was first resolved with β_3 subunit homopentamers which showed consistency with the other pLGIC members (Miller and Aricescu, 2014). Later, several tri-heteropentameric $GABA_A$ receptor structures have been resolved with cryo-electron microscopy (EM) techniques, identifying multiple residues located on the α^-/β^+ subunit interfaces that contribute to the GABA binding by cation-π interaction, salt bridge, and a hydrogen bond (Phulera et al., 2018; Zhu et al, 2018; Laverty et al., 2019; Masiulis et al., 2019) (Figure 1.1B&C).

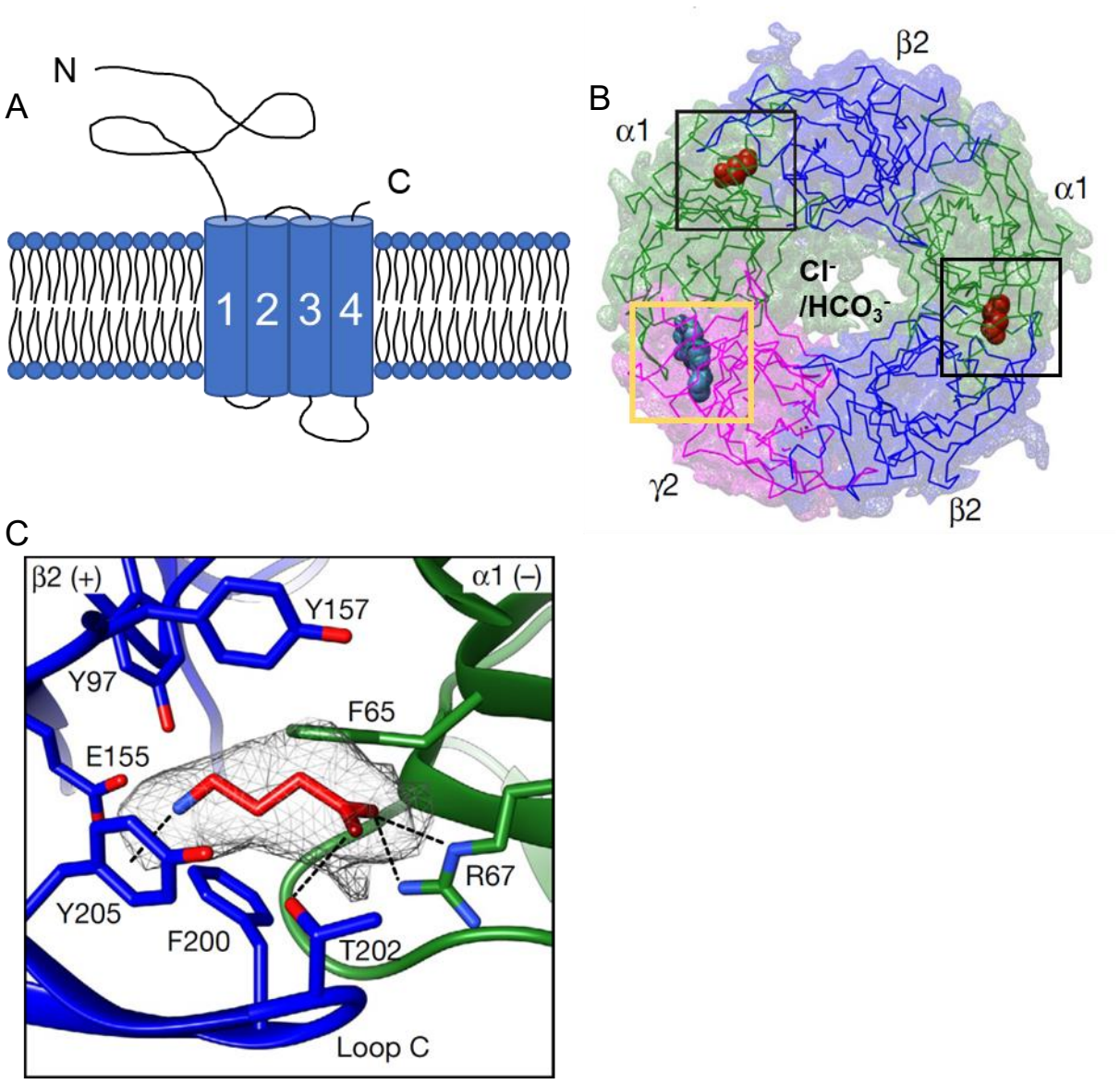

Figure 1.1

Structure of $GABA_A$ receptor and GABA-binding sites. (A) The structure of a $GABA_A$ receptor subunit. A single subunit is formed with a large N-terminal ECD, four TMs and a short C terminal extracellular domain. (B) Subunit organization of $\alpha_1\beta_2\gamma_2$-$GABA_A$ receptor by high-resolution EM (view from the extracellular domain) (Zhu et al., 2018). The location of GABA binding sites is shown in the black box and a benzodiazepine binding site is shown in the yellow box. A chloride/bicarbonate permeable pore is formed in the center of the five subunits. (C) Architecture of GABA-binding pocket (Zhu et al., 2018). The proposed hydrogen bonds and cation-π interactions are represented as dashed lines.

The TM2 helices from each subunit form the central pore which is permeable to chloride and bicarbonate ions (Gallagher, Higashi & Nisiii, 1978) in a 4:1 permeability ratio (Leonard et al., 1988). To be targeted to the cell surface, $GABA_A$ receptors need to contain the β subunits (Krasowski et al., 1998; Connor, Boileau and Czajkowski, 1998). The β_3 subunit can form homopentamers which can be efficiently targeted to the cell surface but these receptors are largely inactive and they do not respond to GABA (Cestari et al., 2000; Hannan and Smart, 2018). $GABA_C$ receptors are also composed of only one subunit type, ρ subunits, but these receptors are found most predominantly in the retina (Nelson et al., 1999).

A variety of molecules bind to $GABA_A$ receptors at distinct sites including GABA, barbiturates, benzodiazepines, neurosteroids, alcohol, and some anesthetics. There are two GABA binding sites on each functional $GABA_A$ receptor and these are located at the interfaces between the α and β subunits shown in the black boxes in Figure 1.1B (Sigel and Steinmann, 2012). When GABA binds to one of the two binding sites, the channel can open but the probability of the channel opening is greatly increased when both GABA binding sites are occupied (Sieghart, 2015). The benzodiazepine binding site is located at the ECD interface between α and γ subunits (Sigel and Buhr, 1997). Co-expression of γ_2 subunit with certain α and β subunits displays high Benzodiazepine affinity (Pritchett et al., 1989). Benzodiazepine binding to $GABA_A$ receptors exerts positive or negative allosteric modulation on the receptor function. A most recent study of $GABA_A$ receptors in complex with GABA and/or

benzodiazepines has revealed the structural basis of the positive allosteric modulation of $GABA_A$ receptors (Masiulis et al., 2019; Kim et al., 2020). Three new benzodiazepine binding sites were proposed in these two studies: two sites at the TM domain interfaces between β and α subunits (Masiulis et al., 2019), and one at the TM domain interface between γ and β subunits (Kim et al., 2020). The binding of Flumazenil to the benzodiazepine binding sites destabilizes the GABA binding possibly by creating a gap at the interface between γ and β subunits. The gap disappears in the presence of Diazepam, which dramatically stabilizes the GABA binding.

1.2 $GABA_A$ Receptor Function

When GABA binds to the binding sites on $GABA_A$ receptors, a series of conformational changes leads to the opening of the anion-permeable pore (Sigel and Steinmann, 2012). The exact conformational change in response to GABA binding remained debated for decades. A recent structural study of the GABA-bound $GABA_A$ receptors (Masiulis et al., 2019) revealed that upon GABA binding, an anticlockwise (when from the extracellular space) rotation of extracellular domains of all subunits occurs and is stabilized by hydrogen-bond networks. This locks the extracellular domains of the β subunits to the neighboring α interfaces leading to a concerted anticlockwise rotation of the transmembrane domains and thus opens the ion channel. The flow of the anions depends on the electrochemical driving force. The chloride gradient across the cell membrane is regulated by the expression of different types of ion transporters which are

dynamically regulated during development (Kuzirian and Paradis, 2011). Therefore, the function of the $GABA_A$ receptors is altered from excitation to inhibition during development, which is regulated by chloride homeostasis.

During the early development, the intracellular chloride concentration stays at a higher level (> 20 mM) relative to the adult brain due to the predominant expression of the sodium-potassium-chloride cotransporter (NKCC1) which transports the sodium, potassium, and chloride ions into the cell in 1:1:2 ratio (Yamada et al., 2004). Activation of $GABA_A$ receptors depolarizes the cell due to the outward chloride electrochemical gradient (Cherubini, Gaiarsa and Ben-Ari, 1991; Ben-Ari et al., 2007) and this can generate the inward calcium current via activation of voltage-dependent calcium channels, which is sufficient to remove the voltage-dependent magnesium blockade of NMDA receptors (Leinekugel, Tseeb, Ben-Ari and Bregestovski, 1995). These activities help promote the maturation of the neuronal circuits (Khazipov, Ragozzino and Bregestovski, 1995).

In the mature CNS (postnatal), the intracellular chloride concentration decreases due to the increased expression of the potassium-chloride cotransporter isoform 2 (KCC2) which pumps the potassium and chloride ions out of the cell generating an electrochemical gradient driving an inward flow of chloride ions. In the mature mammalian brain, the extracellular chloride concentration is 100 mM while the intracellular chloride concentration is ~5 mM (Bolsover, Shephard and White, 2011). Activation of $GABA_A$ receptors leads to hyperpolarization of the postsynaptic membrane (Ben-Ari et al., 2007) as the

influx of negatively charged chloride ions can further polarize the approximately -70 mV resting membrane potential. This effect decreases the probability of postsynaptic cell excitation and thus produces an inhibitory signal.

The dysfunction of $GABA_A$ receptors is related to several neuropsychiatric disorders. Thus, $GABA_A$ receptors have become one of the most intensively studied drug targets in the brain. As $GABA_A$ receptors are essential for the balance of excitatory and inhibitory signaling in the brain, the impaired $GABA_A$ receptor function is a major cause of epilepsy which is characterized by repeated seizures mainly caused by abnormal excitation in the brain. Thus, a large number of antiepileptic drugs have been developed over the years to potentiate the $GABA_A$ receptor inhibitory activity and inhibit seizures. (Perucca, 2005).

1.2.1 Phasic and Tonic Inhibition

The functional effects of $GABA_A$ receptors depend in part on their subcellular localization which is determined by the combination of incorporated subunits. The major type of $GABA_A$ receptors in the CNS is composed of α_1, β_2, and γ_2 subunits which can be found throughout the whole brain (Baur, Minier and Sigel, 2006). Most $GABA_A$ receptors containing $\alpha_{1\text{-}3}$ subunits are localized within GABAergic synapses (Tretter et al., 2008; Tretter et al., 2011; Mukherjee et al., 2011) where they mediate the fast synaptic inhibition while most of the receptors containing $\alpha_{4/6}$ subunits are extrasynaptic (Sieghart and Sperk, 2002). However, expression of the δ/θ/ε subunit may result in the receptor being expressed extrasynaptically, for example, the $\alpha_1\beta_2\delta$ and $\alpha_3\beta_3\theta$-containing $GABA_A$ receptors are found outside

of synapses (Sieghart and Sperk, 2002; Mortensen and Smart, 2006). The α_5-containing $GABA_A$ receptors are anchored by radixin to the actin skeleton in locations outside of synapses (Hausrat et al., 2015). However, the recent study showing the co-localization of the α_5 subunit and gephyrin in synapses as well as their co-immunoprecipitation (Brady and Jacob, 2015) indicated that α_5-containing $GABA_A$ receptors are also expressed synaptically.

Activation of $GABA_A$ receptors exerts two types of inhibition: phasic and tonic. The phasic inhibition is a point-to-point communication between inhibitory neurons and their synaptic targets which is mediated by the IPSCs generated by activation of synaptic $GABA_A$ receptors by GABA released into the synaptic cleft. In response to GABA binding, the synaptic $GABA_A$ receptors are activated to open the chloride channel for a very short time (milliseconds) which leads to a hyperpolarization of the postsynaptic cell. The tonic inhibition is achieved by the prolonged response of extrasynaptic $GABA_A$ receptors to the ambient GABA at low concentration spilled over from the synapses because they have a higher affinity for GABA binding than the synaptic $GABA_A$ receptors (Mortensen, Patel and Smart, 2012). The extrasynaptic $GABA_A$ receptors can also be activated by GABA released by glia cells by a non-vesicular mechanism (Yoon and Lee, 2014). The $GABA_A$ receptors are desensitized after prolonged activation by GABA (Bianchi, Haas and Macdonald, 2002), however, the extrasynaptic δ- or $\alpha_{4/6}$-containing $GABA_A$ receptors are desensitized at slower rate than synaptic $GABA_A$ receptors (Belelli et al., 2009).

1.3 Synthesis and Trafficking of $GABA_A$ Receptors to the Plasma Membrane

The majority of $GABA_A$ receptors in neurons are expressed at the plasma membrane. The synthesis and intracellular trafficking to the plasma membrane are tightly regulated processes that depend on the coordinated activity of many proteins (Figure 1.2).

$GABA_A$ receptors are assembled in the endoplasmic reticulum (ER), with the aid of the ER chaperone proteins calnexin and immunoglobulin heavy chain binding protein (BiP) (Connolly et al., 1996; Bradley et al., 2008). This process initiates with the assembly of α and β subunits followed by the assembling of the fifth subunit γ or δ, although single subunits and binary subunits can be oligomerized (Connolly et al., 1996). It has been also proposed recently according to the crystal structure of synaptic $\alpha_1\beta_3\gamma_2$-$GABA_A$ receptors that $\alpha_1\beta_3$ dimer and $\alpha_1\beta_3\gamma_2$ trimer form and subsequently assemble to form the full pentameric receptor according to the energy profile (Laverty, 2019). The homopentamers formed with β_1 or β_3 subunits can escape the ER for membrane insertion while the other misfolded receptors are retained in the ER (Krishek et al., 1996; Wooltorton et al., 1997). The exit of the $GABA_A$ receptors is negatively regulated by the ER-associated degradation which leads to the proteasomal degradation of the misfolded or homomeric (excluding β_1 or β_3 subunit homomers) $GABA_A$ receptor in the cytoplasm (Saliba et al., 2007; Bradley et al., 2008). The interactions between $GABA_A$ receptor α and β subunits with a ubiquitin-like

protein PLIC-1 inhibit ubiquitination of $GABA_A$ receptors that leads to degradation by the proteasome. This process facilitates the forward trafficking of the newly synthesized $GABA_A$ receptors and also the reinsertion of the recycled $GABA_A$ receptors into the cell membrane (Bedford et al., 2001). In the Golgi apparatus, the γ_2 subunit of the $GABA_A$ receptors acts as a substrate for palmitoylation by the Golgi-specific DHHC (Asp-His-His-Cys) zinc finger proteins (GODZ) (Keller et al., 2004), which indicates that γ_2 subunit may play an important role in forward trafficking of the $GABA_A$ receptors to the postsynaptic membrane. Knockout of GODZ is related to the loss of synaptic $GABA_A$ receptor clustering and inhibitory innervation (Kilpatrick et al., 2016). After the palmitoylation, $GABA_A$ receptors are packed in the vesicles formed by the activity of brefeldin A-inhibited GDP/GTP exchange factor 2 (BIG2), which acts as a guanine exchange factor (GEF) (Charych et al., 2004), and the ATPase N-ethylmaleimide-sensitive factor (NSF) by direct interaction via β subunits (Goto et al., 2005). The ubiquitin-like GABA receptor associated protein (GABARAP) is another protein present in the Golgi apparatus that regulates the surface expression of the $GABA_A$ receptors by interacting with the γ_2 subunit (Wang et al., 1999) via the intracellular domain between TM3-4 of the γ_2 subunit (Ye et al., 2021). Although the function of GABARAP remains unclear, it was reported that GABARAP can enhance GABAergic synapses when overexpressed in neurons (Leil et al., 2004) while the deletion of GABARAP did not have any significant effect (O'Sullivan et al., 2005). However, this protein is not specific to the $GABA_A$ receptor but interacts with a

variety of other intracellular proteins.

Both trafficking and synaptic anchoring of $GABA_A$ receptors are facilitated by the scaffolding protein gephyrin (Lorenz-Guertin and Jacob, 2017). $GABA_A$ receptor α_{1-3} and β_{2-3} subunits have been shown to localize at the postsynaptic membranes by binding to gephyrin (Groeneweg et al., 2018). Gephyrin is a 93-kDa polypeptide that self-aggregates to form a hexagonal complex lattice in the postsynaptic membrane (Groeneweg et al., 2018). Gephyrin is tethered to the cell membrane by binding to collybistin (Poulopoulos et al., 2009) and is critical in maintaining the $GABA_A$ receptor synaptic localization and density. A significant loss of synaptic $GABA_A$ receptors and reduced clustering were detected in gephyrin knock-out mice (Kneussel et al., 1999) while the total level of surface $GABA_A$ receptors expression was unaffected (Jacob et al., 2005). The expression of the γ_2 subunit and gephyrin are interdependent as inhibited gephyrin activity causes the loss of $GABA_A$ receptor clusters at the postsynaptic locations (Essrich et al., 1998), and the deletion of the γ_2 subunit results in the parallel loss of postsynaptic $GABA_A$ receptors and gephyrin clusters (Schweizer et al., 2003). The expression of extrasynaptic $GABA_A$ receptors depends on the interaction with radixin which belongs to the ERM (Ezrin, Radixin, and Moesin) protein family. Radixin provides the linkage between the $GABA_A$ receptors and the actin skeleton at the extrasynaptic locations at the plasma membrane (Mele, Leal and Duarte, 2016). How the other extrasynaptic $GABA_A$ receptors are restricted outside the synaptic area has not been fully elucidated.

The cell surface expression level of $GABA_A$ receptors is also regulated by endocytosis. The endocytosis is mostly clathrin-dependent and mediated by a GTPase dynamin-dependent invagination of the cell membrane (Kittler et al., 2000). The clathrin which forms endocytic vesicles is recruited to the $GABA_A$ receptors by the clathrin adaptor protein 2 (AP2) as the blockade of $GABA_A$ receptor interaction with AP2 leads to an increase of synaptic responses (Kittler et al., 2008). This interaction was shown to be inhibited by phosphorylation of $GABA_A$ receptor γ_2 and β subunits (Kittler et al., 2008).

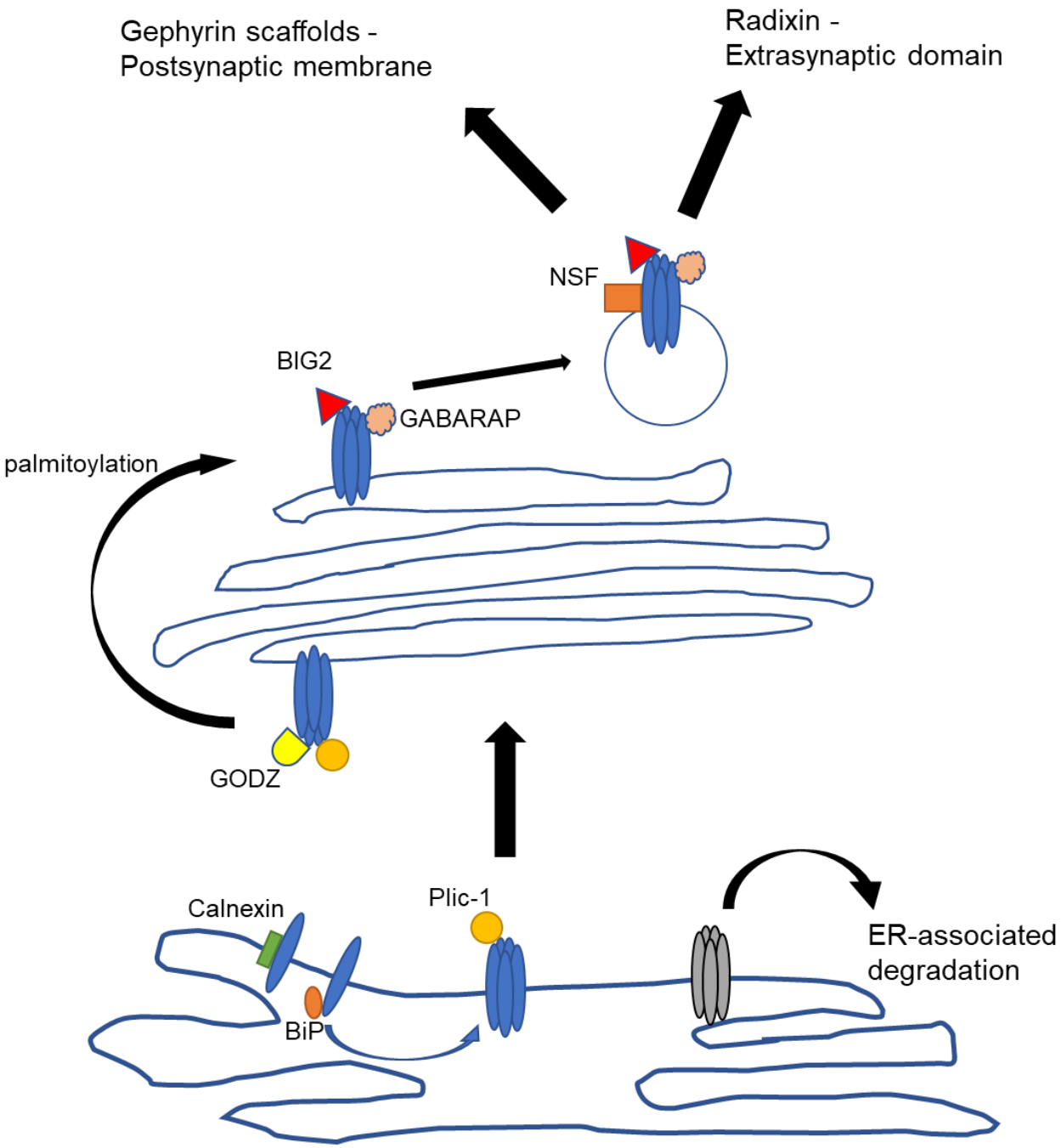

Figure 1.2

Synthesis and forward trafficking of $GABA_A$ receptors. $GABA_A$ receptors are assembled in the ER by the ER chaperones Calnexin and BiP. The misfolded receptors are degraded via ERAD. The assembled receptors are stabilized by interaction with PLIC-1, which inhibits ERAD, and transported to the Golgi apparatus. GODZ palmitoylates γ_2 subunit-containing $GABA_A$ receptors which is critical for their membrane insertion. The $GABA_A$ receptors are forward transported in the vesicular transporters with the aid of BIG2 and GABARAP, and inserted into the cell membrane by NSF of the SNARE-mediated fusion machinery. The subcellular localization of $GABA_A$ receptors is determined by the scaffolding protein Gephyrin (synaptic localization) and ERM protein Radixin (α_5 subunit-containing receptors).

1.4 Allosteric Modulation of $GABA_A$ Receptors by Benzodiazepines

Many ligand binding sites have been found on $GABA_A$ receptors that can regulate the function of $GABA_A$ receptors in different ways. Benzodiazepines are the most widely studied category of $GABA_A$ receptor ligands which act as positive allosteric modulators. The γ_2 subunit was identified to be essential for the high affinity binding of benzodiazepine (Shivers et al., 1989; Sontheimer et al., 1989). The benzodiazepine binding site has been targeted by a variety of drugs such as diazepam (Valium), flumazenil (Romazicon), alprazolam (Xanax) and zolpidem (Ambien). The occupancy of the benzodiazepine binding site leads to a change in the conformation of $GABA_A$ receptors which shifts the GABA concentration-dose curve to lower concentrations but does not change the maximum current response to GABA binding (Sigel and Ernst, 2018), because the inclusion of benzodiazepines strengthens the α/γ extracellular domain interface that facilitates the rotation of the extracellular domains in response to GABA binding (Masiulis et al., 2019). It has also been shown that several additional low-affinity binding sites exist which possibly locate in the transmembrane domains (Sieghart, 2015, Sigel and Ernst, 2018).

1.4.1 Exogenous Benzodiazepine Binding Site Ligands

Benzodiazepines have been used as drugs to treat a variety of neuropsychiatric diseases including anxiety, sleep disorders, depression, seizures, and muscle spasms (Ghit, Assal, Al-Shami and Hussein, 2021). Diazepam is one of the most

widely studied benzodiazepines which has been indicated for a wide spectrum of CNS diseases including anxiety, insomnia, muscle spasms, and epilepsy (Calcaterra and Barrow, 2014). As a positive allosteric modulator, diazepam potentiates the GABA binding affinity. The allosteric modulation by diazepam is inhibited by flumazenil, which is a competitive antagonist of the benzodiazepine binding site (Shoar and Saadabadi, 2019). The action of diazepam and its inhibition by flumazenil require the presence of the γ_2 subunit. A recent study reported that prolonged exposure of $GABA_A$ receptors to diazepam can induce the loss of GABAergic synapses via the $GABA_A$ receptor internalization (Nicholson et al., 2018). Alprazolam is another member of the benzodiazepine family that is one of the most commonly prescribed drugs for psychotropic disorders including panic and anxiety disorders in the US (George and Tripp, 2019).

Zolpidem is a widely-studied non-benzodiazepine drug that binds to the same site as diazepam. It has been widely prescribed as a hypnotic for the treatment of insomnia (Bomalaski et al., 2017). Zolpidem acts as a high-affinity positive allosteric modulator to $GABA_A$ receptors containing the α_1 subunits. Unlike diazepam, it has been reported that zolpidem can bind to the α_1-α_1 interface in binary αβ $GABA_A$ receptors, which suggests the existence of additional allosteric binding sites (Che Has et al., 2016).

1.4.2 Endogenous Diazepam Binding Inhibitor

Since the benzodiazepine binding site had been discovered, the search for

endozepines, the endogenous ligands that bind to this site, has been pursued. Diazepam binding inhibitor (DBI) was first isolated in 1983 (Guidotti et al., 1983; AIa and MI., 1983) and has become the most widely studied endozepine. Later on, it was found that DBI is identical to the acyl-CoA binding protein (ACBP) which serves as an important intermediate in lipid synthesis and fatty acid metabolism (Knudsen, 1991). In the brain, DBI is primarily secreted by astrocytes in the unconventional secretory pathway known as exophagy (Abrahamsen and Stenmark, 2010). The mechanism of DBI action at the benzodiazepine binding site on $GABA_A$ receptors has been shown to be largely due to negative allosteric modulation but with great variation in functions in different brain regions, which will be further discussed in Chapter 5.

1.5 The GABAergic Synapses

The two main categories of synapses in the brain were initially defined as asymmetric (Type I) and symmetric (Type II) synapses on the basis of the size of the postsynaptic density detected by high-resolution electron microscopy (Gray, 1969). With the identification of glutamate and GABA, the function of these two types of synapses was established to correspond to glutamatergic excitatory synapses and GABAergic inhibitory synapses, respectively. Compared to the glutamatergic synapse, GABAergic synapse (Type II synapses) possesses a less dense postsynaptic density, with the proteomic studies showing a 100-fold lower number of postsynaptic density proteins than in glutamatergic synapses (Charych, Liu, Moss and Brandon, 2009; Bayés et al., 2010).

The fast, point-to-point inhibitory synaptic transition is achieved by the temporal and spatial restriction of the neurotransmitter GABA binding to the postsynaptic $GABA_A$ receptors at a synaptic junction (Südhof, 2018). GABAergic synapses are formed by the adhesion of the presynaptic terminals at specific locations on the postsynaptic membrane. In the synaptic cleft, there is a variety of adhesion and scaffolding proteins that are important for the formation of the synapses and the maintenance of their normal function (Südhof, 2017). Although many transsynaptic proteins have been discovered and shown to regulate synapse formation, the question remains as to which of these proteins are absolutely essential for the initiation of synaptogenesis and thus how the GABAergic synapses are actually generated.

1.5.1 Structure of GABAergic Synapses

1.5.1.1 Presynaptic Active Zone

GABA is synthesized specifically for the release from axonal terminals by GAD 65. In most neurons, only one neurotransmitter is released depending on the presynaptic enzymes present, which are considered not to change over time (Dale, 1935; Strata and Harvey, 1999). However, co-transmission of glutamate (Root et al., 2014), acetylcholine (Takács et al., 2018), or dopamine (Maher and Westbrook, 2008) with GABA has been observed. Even in the same terminal, these neurotransmitters are transported into different vesicles and released from different active zones (Takács et al., 2018; Granger et al., 2020).

In response to the presynaptic action potential, GABA is released into the synaptic cleft by the exocytosis of the synaptic vesicles. This process is regulated by a group of proteins anchored to the presynaptic plasma membrane forming an electron-dense area called the active zone (Zuber and Lučić, 2019) (Figure 1.3). The active zone is the site for synaptic vesicle exocytosis and is composed of a matrix formed by detergent-insoluble proteins. The core of the active zone is called the SNARE (soluble N-ethylmaleimide-sensitive component attachment protein receptor) complex formed by proteins Syntaxin, Synaptobrevin, and Synaptosomal-associated protein-25 (SNAP-25). This complex is essential for the synaptic vesicle docking and fusion with the plasma membrane (Zhen and Jin, 2004). The structure of the active zone is maintained by a complex of proteins Piccolo, Bassoon, RIMs, RIM binding proteins (RIM-BPs), α-Liprin, and ELKS proteins (Südhof, 2012).

The active zone is composed of three components: the plasma membrane aligned to the postsynaptic membrane through transsynaptic adhesion molecules, the cytomatrix immediately attached to the plasma membrane, and the electron-dense projections protruding into the cytoplasm (Zhai and Bellen, 2004). This structure is common for both excitatory and inhibitory synapses. The dense projections are connected with thin fibrils to form a highly organized structure that provides docking spaces for the synaptic vesicles spatially near the plasma membrane (Lenzi and von Gersdorff, 2001).

The GABA molecules, produced by GAD catalyzed decarboxylation reaction,

are transported into the synaptic vesicles due to the action of VGAT. The vesicles are recruited and docked at the active zone where they undergo a priming reaction which is a pre-requisite for the fusion of their membrane with the plasma membrane. The priming reaction is regulated by the mammalian homolog of unc-13 (Munc13) with the aid of Bassoon and Piccolo (Leal-Ortiz et al., 2008). However, the action of Bassoon and Piccolo here might be redundant as the deletion of both proteins does not lead to an apparent phenotypic deficiency in the synaptic transmissions (Mukherjee et al., 2010). Moreover, Piccolo and Bassoon are important in maintaining the presynaptic cytoskeleton (Südhof, 2012). In the priming process, RIM protein prevents Munc13 from forming homodimers by binding to it and forming a heterodimer (Deng, Kaeser, Xu and Südhof, 2011). This heterodimer also forms a tripartite complex with a small GTPase, Rab3, from the synaptic vesicles to facilitate the docking of the vesicles (Gracheva et al., 2008). Once the action potential arrives in the presynaptic terminal, the voltage-gated calcium channels (VGCCs) open to allow an influx of Ca^{2+} ions. These VGCCs are tethered to the presynaptic domain plasma membrane by the RIMs and the RIM-BPs (Brünig et al., 2002). The Ca^{2+} ions trigger the fast opening of the fusion pore leading to the fusion of the vesicles with the plasma membrane to release GABA into the synaptic cleft.

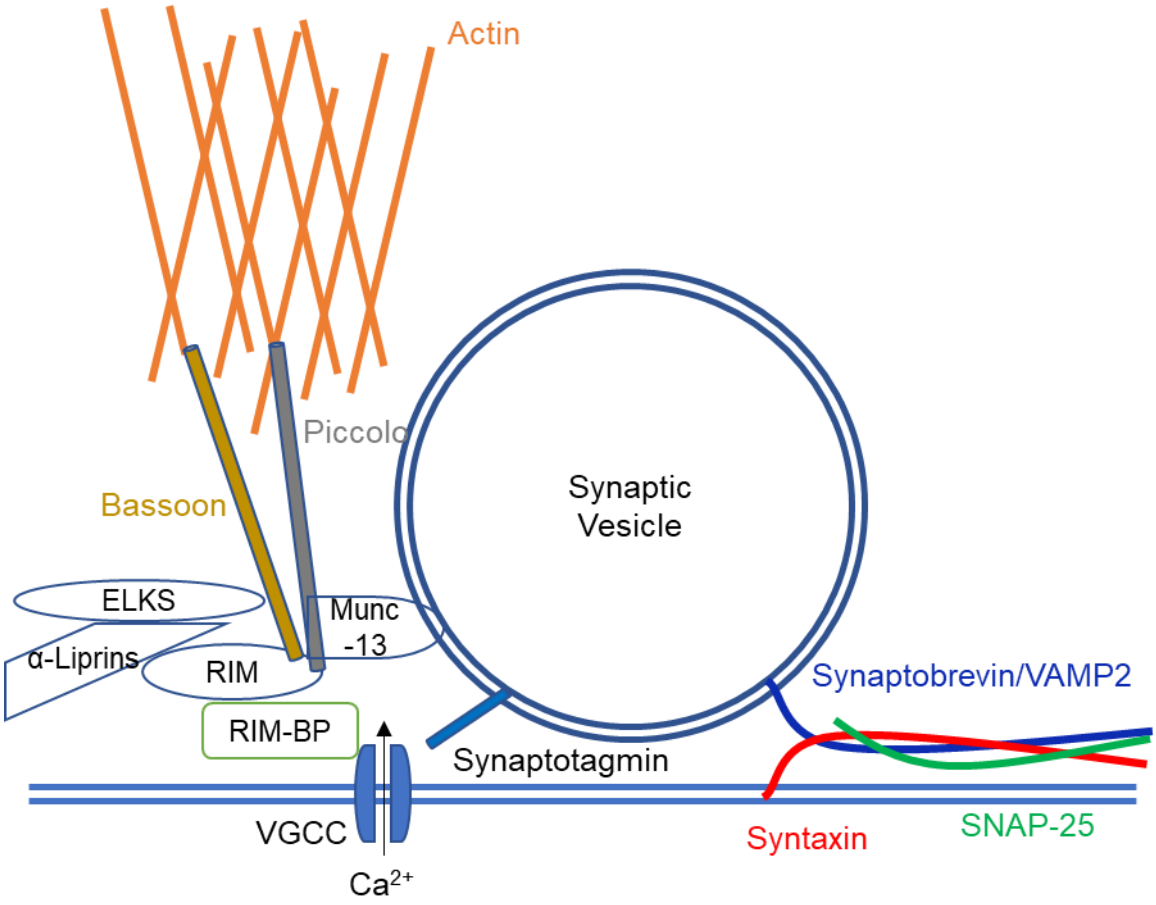

Figure 1.3

Schematic diagram of the presynaptic active zone. The SNARE complex formed by Syntaxin, Synaptobrevin and SNAP-25 is the core component of the active zone, which facilitates the Ca^{2+}-dependent release of GABA by docking and fusing the presynaptic vesicle to the presynaptic membrane. Five proteins RIM, Munc13, RIM-BP, α-liprin, and ELKS proteins maintain the basic structure of the presynaptic active zone. Bassoon and Piccolo are important in maintaining the presynaptic structure by linking the active zone to the Actin skeleton.

1.5.1.2 The Synaptic Cleft

The synaptic cleft is a narrow gap between the presynaptic axonal terminal and the postsynaptic cell membrane. It is a domain filled with extracellular matrix proteins and transsynaptic proteins that are important for synaptic adhesion and transmission of chemical signals (Figure 1.4). GABA molecules released from the presynaptic active zone diffuse through this dense network of proteins in the synaptic cleft to reach the postsynaptic receptors. Currently, little is known about these proteins due to difficulties in their biochemical isolation and characterization.

In the human brain, adhesion between the presynaptic and postsynaptic membranes is regulated by proteins produced by both the neurons and astrocytes which are closely associated with the synapses (Chung, Allen and Eroglu, 2015). The extracellular matrix (ECM) provides a periodically organized pattern in a net-like structure (Zuber et al., 2005), which is composed of a variety of proteins, proteoglycans and glycoproteins. The ECM provides the anchoring of the postsynaptic proteins which are linked to the intracellular skeleton. For instance, Laminin, the core component of the basal lamina, interacts with the postsynaptic transmembrane protein Dystroglycan to maintain the structural framework of the postsynaptic membrane and linkage to the synaptic cleft (Briggs et al., 2016). The ECM plays crucial role in maintaining the inhibitory synapse integrity. Knockout of ECM proteins results in a decrease in the density of GABAergic synapses and thus perturbs the excitation/inhibition balance (Gottschling et al., 2019).

1.5.1.3 The GABAergic Postsynaptic Density

The GABAergic postsynaptic specializations mostly localize on the dendritic shafts and the neuronal somas, but can also form on the axons. Apart from $GABA_A$ receptors which localize opposite to the GABAergic projection terminals on the postsynaptic cell membrane, there have been numerous proteins identified in the same domain. The postsynaptic density can be defined as a specialized microdomain that is maintained by core scaffolding proteins, such as Gephyrin, that anchor the $GABA_A$ receptors and other cell adhesion molecules, including NL2, to the subsynaptic cytoskeletons. On the presynaptic membrane, the synaptic adhesion proteins are mostly multifunctional, such as Neurexins, which play distinct roles at different synapses (Sudhof, 2021). In comparison, the postsynaptic adhesion proteins are less “hub”-like proteins, and more diverse with specific roles in synapse formation. These postsynaptic density proteins include receptors, transmembrane cell adhesion molecules, and submembrane scaffolding protein complexes. (Figure 1.4)

Among these proteins, Gephyrin has been shown to play a central structural role as a postsynaptic density protein (Tyagarajan and Fritschy, 2014). Gephyrin is one of the most important postsynaptic scaffolding proteins which plays a pivotal role in maintaining the organization of GABAergic synapses in the CNS. The name “Gephyrin” originates from the Greek word “Gephura” which means a bridge. As its name suggests, Gephyrin was initially discovered to cluster together with the postsynaptic glycine receptors, another inhibitory cys-loop LGIC, and

form a bridge between these receptors and the submembrane microtubules (Prior et al., 1992). It was later found that the expression of Gephyrin is far beyond the glycine receptors because Gephyrin is also co-localized with synaptic $GABA_A$ receptors and it regulates their postsynaptic clustering (Essrich et al., 1998). From the N-terminal to the C-terminal, Gephyrin possesses three functional domains: a G-domain which can form trimerization, an unstructured C-domain, and an E-domain which can mediate dimerization (Sander et al., 2013). The Gephyrin trimers connected with the G-domains are linked via E-domains to form a hexagonal structure that directly binds to the postsynaptic glycine or $GABA_A$ receptors (Sola et al., 2004). The structure of the C-domain is flexible, resulting in different structures in different postsynaptic densities. Compared to Gephyrin in glycinergic synapses, in the GABAergic synapses, the C-domain structure is less compact (Specht et al., 2013) which suggests a different mechanism of clustering of Gephyrin within GABAergic synapses.

Gephyrin clustering appears to be less dense in the GABAergic synapses possibly due to a lower affinity of gephyrin-$GABA_A$ receptor interactions (Pennacchietti et al., 2017). The postsynaptic localization of $GABA_A$ receptors is largely but not completely dependent on interactions with Gephyrin (Kneussel et al., 2001). Unlike the $GABA_A$ receptors containing $\alpha_{2/3}$, $\beta_{2./3}$, and γ_2 subunits, those containing $\alpha_{1/5}$ subunits were reported to be localized to inhibitory synapses even in the absence of Gephyrin, although the α_1 subunit and Gephyrin can interact directly in vitro (Mukherjee et al., 2011). However, the $GABA_A$ receptors

containing γ_2 subunits require Gephyrin for their postsynaptic localization (Kneussel et al., 2001), and, conversely, these receptors are also required for postsynaptic Gephyrin clustering. Knockout of the $GABA_A$ receptor α_3 (Studer et al., 2006) or γ_2 (Essrich et al., 1998) subunits in mice results in loss of Gephyrin clustering.

Collybistin is a brain-specific GEF selectively activating the Rho family cell division control protein 42 (CDC42), which stabilizes the Gephyrin clusters at the postsynaptic domain by remodeling the actin cytoskeleton (Xiang et al., 2006). It was shown to be essential for the submembrane clustering of the Gephyrin-$GABA_A$ receptor aggregate (Kins, Betz and Kirsch, 2000). The deficiency of Collybistin results in the loss of gephyrin and $GABA_A$ receptors clusters in the hippocampus and thus impairs both the formation and maintenance of GABAergic synapses in the Collybistin gene inactivated mouse model (Papadopoulos et al., 2008). The SH3-domain of collybistin is conformationally closed to exert an autoinhibitory effect on the submembrane clustering of the Gephyrin-Collybistin complex. This inhibitory effect can be removed by expression of other postsynaptic density proteins (Kins, Betz and Kirsch, 2000; Soykan et al., 2014).

The complex formed by NL2, Gephyrin, and Collybistin is essential for the tethering to the cell membrane and thus the formation of the GABAergic postsynaptic specialization. In the hippocampus of the NL2 knockout mice, the GABAergic synapses are disrupted in a subcellular region-specific manner: the

GABAergic synapses were fully preserved at the dendrites while at the perisomatic region the GABAergic synapses were dramatically reduced due to a loss of postsynaptic gephyrin-collybistin clustering (Poulopoulos et al., 2009). This is due to the loss of recruitment of Gephyrin and Collybistin to the postsynaptic submembrane domain. The binding of NL2 to Collybistin was shown to eliminate the autoinhibitory effect of the SH3-domain of Collybistin and thus associate the Gephyrin-Collybistin complex to the postsynaptic membrane (Poulopoulos et al., 2009). At the dendrites, it is likely that the loss of NL2 is compensated by another protein that can prevent the action of the Collybistin SH3-domain such as the small GTPase TC10 (Mayer et al., 2013).

The Dystrophin-Glycoprotein complex (DGC) is a transmembrane signaling complex that mechanically links the intracellular cytoskeleton to the extracellular matrix (Culligan and Ohlendieck, 2000). The DGC is widely expressed in the human body and can be found in striated and cardiac muscle, neurons, astrocytes, and kidney epithelial cells (Haenggi and Fritschy, 2006). In the brain, the DGC comprises Dystrophin, Syntrophins (α_1, $\beta_{1/2}$, and $\gamma_{1/2}$), Dystroglycan (α and β), Sarcoglycans, and Sarcospan to form a large molecularly heterogenous transmembrane complex (Pilgram et al., 2009). It has been suggested that the DGC can form a postsynaptic scaffolding complex that is independent of the Gephyrin-Collybistin complex. The WW domain of the synaptic scaffolding molecule (S-SCAM) binds to the proline-rich sequence of the β-Dystroglycan in the DGC and the PDZ domain of S-SCAM binds to the intracellular tail of NL2 to

link DGC with the NL2-Neurexin complex (Sumita et al., 2007), which results in the expression of the DGC at the GABAergic postsynaptic density even in the absence of $GABA_A$ receptors (Brünig et al., 2002). In a $GABA_A$ receptor α_2 subunit knockout mouse model, the GABAergic synapse is not perturbed in the perisomatic regions in the hippocampus, with a loss of postsynaptic gephyrin clusters (Panzanelli et al., 2011). The pyramidal cell specific ablation of Dystroglycan results in a minor change in the postsynaptic clustering of Gephyrin and γ_2 subunit-containing $GABA_A$ receptors (Früh et al., 2016). This observation can further support that the DGC postsynaptic scaffolding model is independent of the Gephyrin-Collybistin complex.

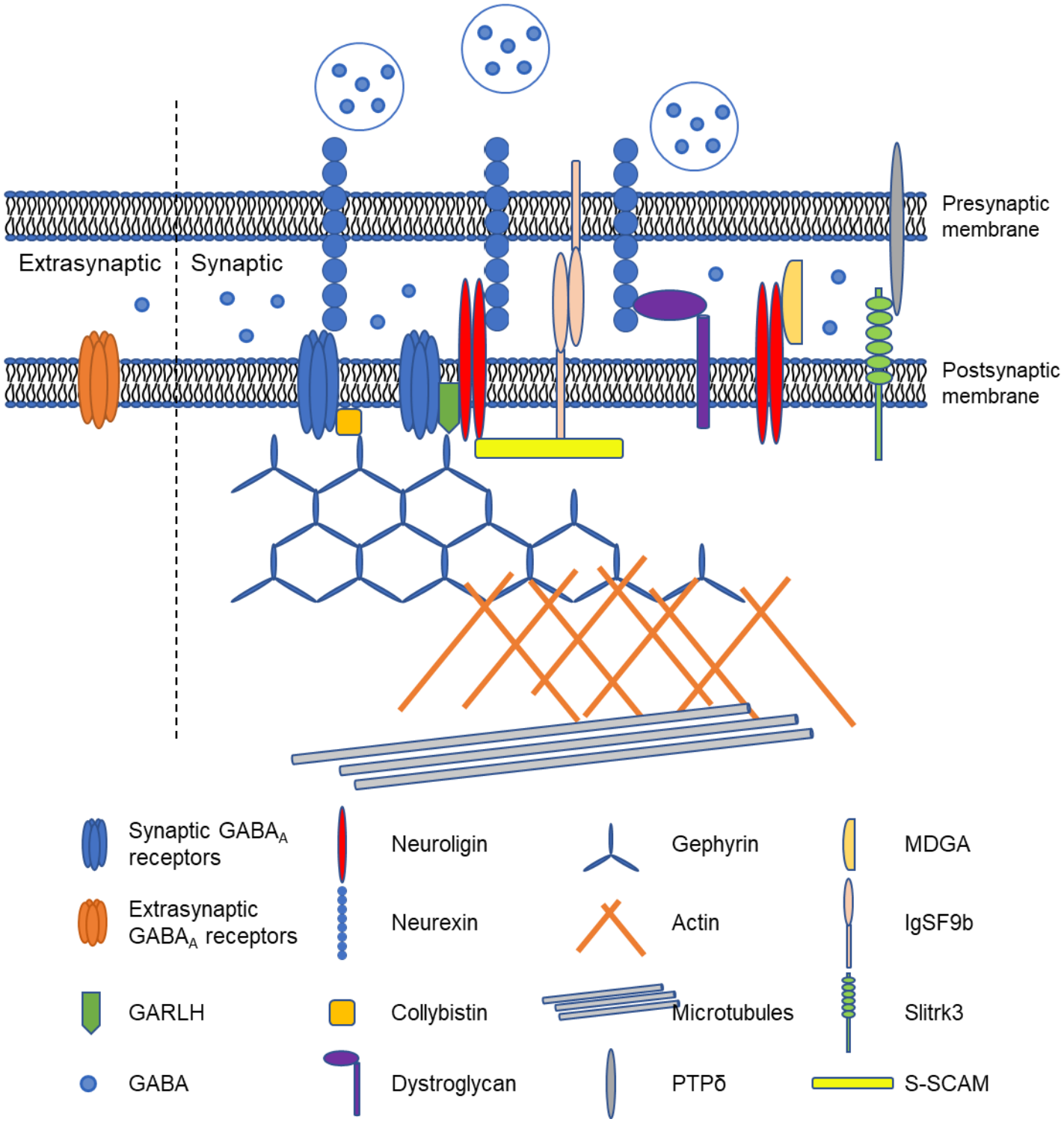

Figure 1.4

Schematic diagram of GABAergic postsynaptic scaffolding proteins and adhesion protein interactions that are important in the formation of GABAergic synapses. GABA molecules are packaged into the presynaptic vesicles and released to the synaptic cleft by the fusion of the vesicles to the presynaptic cell membrane. The structure of the synapse is maintained by several transsynaptic protein complexes. Neurexin acts as a presynaptic hub of multiple transsynaptic interactions and signalling. Synaptic $GABA_A$ receptors receive GABA for signal transmission and provides structural role to maintain the GABAergic synapse by interaction with synaptic adhesion proteins Neurexin and NL2.

1.5.2 Dynamics of GABAergic Synapse Formation

During development, the newborn neurons extend their axons which migrate to find the targets through a process named axon guidance (Suter and Jaworski, 2019). Synapses are subsequently formed in excess followed by programmed pruning during the young age (Bourgeois and Rakic, 1993) for the establishment of the functional neural circuit. The plasticity of the GABAergic synapses is related to learning and memory (Malenka and Bear, 2004; Mayford et al., 2012). The balance between the excitatory and inhibitory synapses is maintained in the brain by the dynamic regulation of formation, maintenance, and elimination of the synapses, either spontaneously or in response to the change in circumstances (Wierenga, Becker and Bonhoeffer, 2008; Dobie and Craig, 2011; Paolicelli et al., 2011).

Live imaging studies show that the formation of GABAergic synapses along the axons is a dynamic and non-linear process, which involves repeated assembly and disassembly of the synaptic boutons (Wierenga, Becker and Bonhoeffer, 2008; Wierenga, 2017). It appears that the sites of these dynamic synaptic boutons are unchanged during this process, which express pre- and postsynaptic synaptic proteins after the “first touch” (Sabo, Gomes and McAllister, 2006; Schuemann et al., 2013). This suggests that an unknown mechanism may underlie the decision of the site of synaptic contacts along the axon shaft, possibly due to a preceding structural change or expression of certain proteins that may induce the formation of pre- or postsynaptic specializations.

1.5.3 Formation of GABAergic Synapses

Currently, little is known about the exact cellular and molecular mechanisms that drive the formation of GABAergic synapses. As suggested by the live imaging results, the formation of GABAergic synapses is not a direct “meet-and-touch” process but may involve several steps of assembly and disassembly of the synaptic boutons.

A model was proposed that the neurotransmitter, GABA, can directly regulate synaptogenesis (Burlingham et al., 2022). The postsynaptic cell may recruit specific scaffolding and adhesion proteins and $GABA_A$ receptors in response to the presynaptic GABA release. This hypothesis is supported by the fact that neurons that co-express GABA and glutamate release these neurotransmitters from distinct active zones, and form separate synapses with distinct neurotransmitters (Root et al., 2014, 2018). This suggests that the presynaptic neurotransmitter release at least instructs the type of postsynaptic specializations. For the neurons that switch the expression of neurotransmitters during development, new synapses are formed in response to the new neurotransmitter (Spitzer, 2017; Li and Spitzer, 2020), which further supports that postsynaptic specialization is determined by the presynaptic neuron. In support of this statement, a most recent study showed that ectopic expression of GAD and VGAT in pure glutamatergic neurons is sufficient to produce GABA and effectively induce the formation of functional GABAergic synapses both *in vitro* and *in vivo* (Burlingham et al., 2022). Moreover, rapid local release of GABA was shown to

be sufficient to drive the formation of GABAergic synapses by inducing postsynaptic clustering of Gephyrin (Oh, Lutzu, Castillo and Kwon, 2016). Furthermore, this theory is strengthened by the importance of functional $GABA_A$ receptors on GABAergic transmissions (Essrich et al., 1998; Fritschy et al., 2006; Nguyen and Nicoll, 2018; Duan et al., 2019). However, in some studies, although GABAergic transmission is impaired due to the disrupted long-term maintenance of the GABAergic synapses, the initial establishment of the GABAergic synapses is not significantly affected (Fritschy et al., 2006).

It is important to note that $GABA_A$ receptors are synaptogenic via a structural role of the subunit ECDs, which is not activity-dependent (Fuchs et al., 2013; Brown et al., 2016). Because the synaptic puncta of the synaptic adhesion protein NL2 are not altered by $GABA_A$ receptor deletion (Patrizi et al., 2008), the structural function of $GABA_A$ receptors may be downstream of NL2 interactions during the GABAergic synapse formation. NL2 is a postsynaptic transmembrane protein that has been shown to play pivotal roles in GABAergic synapse formation and maintenance.

Therefore, another model is that the synaptic adhesion proteins induce the formation of the GABAergic synapses by forming the transsynaptic interaction (Missler et al., 2012; Südhof, 2021) (Figure 4). Extensive efforts have been devoted to the search for the key interactions facilitating this synaptogenesis process. Yet, no protein has been proposed to signal the initiation of this process, albeit several transsynaptic protein-protein interactions have been identified.

Currently, it appears that the synapse formation process is mediated by an interplay of multiple protein-protein interactions.

Neurexin is widely believed to be one of the most important presynaptic proteins in charge of synaptic adhesive interactions. Neurexin is not only essential for the presynaptic Ca^{2+}-dependent neurotransmitter release by clustering the VGCCs (Missler et al., 2003; Luo et al., 2020), but also acts as a "hub" for multifarious protein bindings (Südhof, 2017) including $GABA_A$ receptors (Zhang et al., 2010), Dystroglycan (Sugita et al., 2001; Reissner et al., 2014) and NL2 (Craig and Kang, 2007). Neurexin may not be essential for the formation of GABAergic synapses but it plays a crucial roles in GABAergic transmissions. The constitutive knockout of Neurexins significantly impairs the synaptic transmission in the neocortex and brainstem (Missler et al., 2003). However, in parvalbumin-positive interneurons, the deletion of Neurexin decreases the number of inhibitory synapses but not the presynaptic Ca^{2+} influx in the medial prefrontal cortex (Chen et al., 2017). Therefore, Neurexin regulates the GABAergic synapse transmissions by distinct mechanisms in different brain regions. This is because Neurexin exists in more than 1000 isoforms due to alternative splicing (Ullrich, Ushkaryov and Südhof, 1995) and interacts with multiple proteins in the synapse. The role of Neurexin may vary depending on the ligand interactions.

NL2 interaction with presynaptic neurexin has been extensively studied, which has been considered the core interaction in maintaining the functional GABAergic synapses. The constitutive triple knockout of NL1/2/3 is lethal and it

impairs the GABAergic synaptic transmission, but has little effect on the number or ultrastructure of the GABAergic synapses (Varoqueaux et al., 2006; Zhang et al., 2015). Moreover, the number of GABAergic synapses is not changed when the GABAergic transmission is impaired by the conditional knockout of NL2 (Chanda et al., 2017). In this knockout model, the impaired GABAergic transmission is predominantly caused by loss of postsynaptic $GABA_A$ receptor clustering rather than altered presynaptic release parameters or GABAergic synapse formation. Overall, the NL2-Neurexin interaction plays crucial role in maintaining GABAergic synapse structure and signal transmission. However, it seems not to be involved in the initiation of the formation process.

Calsyntenin3 is another postsynaptic type I transmembrane protein which has been shown to interact indirectly with both α- and β-neurexins (Kim et al., 2020), suggesting a potential synaptogenic role. It has 2 isoforms calsyntenin1 and calsyntenin2 belonging to the Ca^{2+}-dependent cell adhesion molecule family. While calsyntenin3 is able to induce both excitatory and inhibitory synapse formation in co-culture assay (Pettem et al., 2013a), the knockdown of Calsyntenin does not affect the synaptic density (Um et al., 2014). However, the triple knockdown of all Calsyntenin isoforms selectively reduces the GABAergic synapse density and impairs the GABAergic synapse transmission (Um et al., 2014). This suggests a redundancy of Calsyntenin isoforms in the GABAergic synaptogenesis.

Dystroglycan is the central component of the DGC. The DGC interacts with

presynaptic neurexins via the α-dystroglycan (Graf et al., 2004). The transsynaptic interaction of Dystroglycan may play an essential role in the formation of GABAergic synapses. It has been shown that by binding to Pikachurin and GPR179, Dystroglycan is essential for the formation and signal transmission of the ribbon synapse in the retina (Orlandi et al., 2018). Ablation of Dystroglycan in early development does not disturb the DGC-mediated neuronal migration but impairs the formation of the inhibitory synapses formed by GABAergic cholecystokinin (CCK)-positive interneurons on pyramidal cells (Früh et al., 2016). The ablation in adults dramatically reduced the CCK-positive innervations, which suggests Dystroglycan is also important in maintaining the GABAergic synapses (Früh et al., 2016). Furthermore, conditional knockout of Dystroglycan in pyramidal cells results in the CCK-positive interneuron cell death and failure (Miller and Wright, 2021). The remaining CCK-positive interneuron axonal terminals were retargeted to the striatum where expression of Dystroglycan was retained (Miller and Wright, 2021). These data strongly suggest that Dystroglycan may play an essential role in GABAergic synapse formation process.

Furthermore, a variety of postsynaptic adhesive proteins have been show to regulate GABAergic synapse formation. The immunoglobulin superfamily (IgSF) proteins are a class of neuronal cell adhesion proteins characterized by the expression of Ig domains which contribute to the synaptic adhesion of the pre- and postsynaptic membranes (Barclay, 2003). IgSF9b is an inhibitory synapse-

specific adhesion protein linked to NL2 via the multiple PDZ-domain-containing S-SCAM to promote the GABAergic synapse development (Woo et al., 2013). Membrane-associated mucin domain-containing glycosylphosphatidylinositol anchor proteins (MDGAs) are another subfamily of IgSFs related to several neurodevelopmental disorders linked to the development of the GABAergic synapses (Wang et al., 2019). MDGA exerts a negative regulation specifically on GABAergic synapse formation by inhibiting NL2 interaction with Neurexin (Lee et al., 2012; Pettem et al., 2013b). Overexpression of MDGA decreases GABAergic synaptic transmission, while knockdown of MDGA increases GABAergic synapse formation in cultured hippocampal neurons (Lee et al., 2012).

In addition to the IgSF protein family, Slitrk3 is a member of the Slit- and Trk-like (Slitrk) family of postsynaptic proteins, which has been shown to selectively regulate the formation of GABAergic synapses by transsynaptic interaction with the presynaptic protein tyrosine phosphatases (PTPs) (Takahashi et al., 2012). The knockout of Slitrk3 results in decreased GABAergic synapse numbers but has no effect on the morphology of the synapses. On the contrary, gain-of-function assays in co-culture models proved that overexpression of Slitrk3 selectively increases the GABAergic synapse formation without changing the size or strength of the synapses (Yim et al., 2013). Slitrk3 is tethered to Gephyrin which is phosphorylated in response to adenosine A_{2A} receptor activation (Gomez-Castro et al., 2021). The physical interaction of Slitrk3 and the presynaptic transmembrane protein PTPδ has been found to be specifically

occurring at GABAergic synapses to induce the presynaptic specialization development (Takahashi et al., 2012). It remains to be investigated if this transsynaptic interaction exists in parallel to the NL2-Neurexin interaction in the same type of GABAergic synapses.

Despite the rich understanding of the composition of presynaptic active zones and the postsynaptic specializations, the core question remains as to what induces the formation and assembly of these complexes. Further, the mechanism underlying the synaptogenesis process, involving the initial formation, specificity, and plasticity of the GABAergic synapses, remains largely unknown.

The two models describing the formation of the GABAergic synapses are different, but not fully separated from each other. Overall, the synapse formation process is a highly dynamic process (Wierenga, 2017), which may involve an establishment of the specific pre- and postsynaptic binding partners or the assembly of “general synaptic contacts” followed by the elimination of noncognate synapses. In either case, the functional GABAergic synapses require maintenance by transsynaptic interactions by various synaptic adhesion proteins (Sudhof, 2018). An orchestra of these synaptic adhesion protein interactions and signaling has been believed to be a core component of the GABAergic synapse formation process. Despite the advances in the currently available research methodologies, it is still a major challenge to draw a whole picture of the mechanisms underlying the GABAergic synapse formation.

1.6 Aim and Hypothesis

Although the formation of the GABAergic synapses is a complex process involving interactions between many proteins, pre-, trans- and post-synaptically, and numerous signaling mechanisms, it seems that individual proteins have their unique effects on the formation of the GABAergic synapses, but they may even produce opposite effects in different brain regions which can be partially explained by the heterogeneity of $GABA_A$ receptors. A well-established co-culture model system of HEK293 cell and embryonic rat medium spiny neurons has been designed and extensively used in our lab for the study of GABAergic synapse formation (Fuchs et al., 2013; Brown et al., 2014; 2016).

In this project, I have hypothesized that the formation of GABAergic synapses is regulated by synaptic adhesion proteins, including NL2, Pikachurin, Dystroglycan, and DBI, and their interactions with synaptic types of $GABA_A$ receptors. In order to test and verify this hypothesis, the following aims were investigated:

1. Development of a HEK293 cell line stably expressing extrasynaptic $\alpha_4\beta_3\delta$-$GABA_A$ receptors.
2. Characterization of the role of different $GABA_A$ receptors in GABAergic synapse formation process.
3. Investigation of the mechanism underlying the synergistic effect and functional maturation of GABAergic synapses mediated by NL2 and $GABA_A$ receptors.
4. Testing the role of Pikachurin, Dystroglycan, and DBI in GABAergic synapse

formation with/without $GABA_A$ receptors.

2. Materials and Methods

2.1 Cell Culture Maintenance

2.1.1 Human Embryonic Kidney (HEK) 293 Cell Line

Dulbecco's Minimum Essential Medium (DMEM; Thermo Fischer) was used to maintain the HEK293 cells wild type and HEK293 cells (CRL-1573, ATCC) stably expressing $GABA_A$ receptors (Brown et al., 2016). To make complete DMEM, 10 % fetal bovine serum (FBS; Thermo Fischer), 10 mM L-Glutamine (Thermo Fischer), 50 units/ml penicillin (Thermo Fischer) and 50 µg/ml streptomycin (Thermo Fischer) were added. HEK293 cell lines stably expressing $GABA_A$ receptors were kept in complete DMEM with the addition of suitable antibiotics. Geneticin G418 sulphate (Thermo Fischer) was used for selection of cells expressing α_2 and α_4 subunits at 800 µg/ml; Zeocin (Invitrogen) for β_2 and β_3 subunits at 800 µg/ml; and hygromycin B (Invitrogen) for γ_2 and δ subunits at 800 µg/ml expressing HEK293 cells.

At the start of a new culture, a vial containing frozen HEK293 cells in 1 ml of complete DMEM with 10 % dimethyl sulfoxide (DMSO) was taken from -140 ℃, and warmed up to 37 ℃ quickly. Cells were resuspended in complete DMEM and spun down to remove DMSO, and then plated in complete DMEM for 24 hours in the 37 ℃ 5 % CO_2 humidified incubator. For cells stably expressing $GABA_A$ receptors, the medium was changed with a suitable selection medium after 24 hours. Once the cells were 70-80 % confluent, they were detached using Versene

(Thermo Fischer) and seeded onto a new flask or plate at around 15-30% confluency.

The HEK293 cell line was maintained in CELLSTAR® T-75 cell culture flask (Greiner) with 10 ml complete DMEM (with selection for $GABA_A$ receptor expressing cell lines) in the 37 ℃ 5 % CO_2 humidified incubator. The confluency of HEK293 cells reaches > 70 % after ~3-day incubation. For passaging, the medium was aspirated and the HEK293 cells were washed with phosphate-buffered saline (PBS; Thermo Fischer). The HEK293 cells were subsequently incubated with Versene in the 37 ℃ 5 % CO_2 humidified incubator for 5 minutes. After incubation, DMEM was added to the flask and detached cells were collected and spun down at 3000 rpm for 5 min, at room temperature using a benchtop centrifuge (Mikro 2r, Hettich). The pellet was resuspended in complete DMEM medium and were seeded to the new T-75 flask with 1/10 dilution for maintenance.

2.1.2 Embryonic Rat Medium Spiny Neuron Culture

The GABAergic medium spiny neurons were prepared from striatum of ~ E17 embryonic Sprague-Dawley rats (UCL-BSU) housed and sacrificed according to UK Home Office guidelines. The embryos were taken from the uterus followed by a series of washes with pre-chilled sterile PBS and brains were isolated. The brains were dissected in pre-chilled sterile Ca^{2+} and Mg^{2+}-free HEPES-buffered saline solution (HBSS; Thermo Fischer) to dissect the striatum. The striata were collected and cut into fine pieces in chilled sterile HBSS and then carefully triturated using fire-polished Pasteur glass pipettes (Fischer) to dissociate the

tissue until the medium appeared homologous. Dissociated cells were filtered through sterile 70 µm Corning® cell strainer (431751, Corning) to remove clumps. The isolated medium spiny neurons were stained with Trypan blue solution (15250061, Gibco), which only stains dead cells, and counted using hemocytometer (0610010, Neubauer), and plated into poly-D-lysine (0.1 mg/ml; P1149-10MG, Sigma Aldrich) coated tissue culture dishes (Z707686, TPP) or poly-L-lysine (0.1 mg/ml; P6282-5MG, Sigma Aldrich) coated 13 mm glass coverslips (631-0148P, VWR). For immunoblotting and immunoprecipitation experiments, ~ 3 million cells were plated in each 10 cm cell culture dish coated with 0.1 mg/ml poly-D-lysine. For immunocytochemistry and electrophysiology experiments, 100,000 cells were plated on each glass coverslip coated with 0.1 mg/ml poly-L-lysine and 0.01 mg/ml laminin (L2020, Merck). The medium spiny neurons were cultured in serum-free Neurobasal medium (Thermo Fischer) containing B27 supplement (Thermo Fischer), 2 mM L-glutamine, 50 units/ml penicillin, 50 µg/ml streptomycin and 10 % glucose (Thermo Fischer). After a 7-day incubation in the 37 ℃ 5 % CO_2 humidified incubator, the cells were treated with 5 µM cytosine β-D-arabinoside (Ara-C; Sigma Aldrich) to stop proliferation of glia cells.

2.1.3 Co-culture Preparation

HEK293 cells (wt or stably expressing $GABA_A$ receptors) were transfected with cDNAs of a protein of interest using Effectene (301425, Qiagen) (Brown et al., 2014). The transfection procedure is described in Section 2.2.1. The HEK293

cells were incubated in the 37 ℃ 5 % CO_2 humidified incubator for 24 hours. On 12th day in vitro (DIV) of the medium spiny neuron culture, the transfected HEK293 cells were detached with Versene and collected into 15 ml Falcon tube in which they were centrifuged at 3700 rpm for 2 minutes at room temperature in a benchtop centrifuge (Mikro 2r, Hettich). The supernatant was aspirated and the pellet was resuspended in warmed Neurobasal medium (150 µl for HEK293 cells from one well of 6-well plate). The resuspended HEK293 cells (3×10^4 cells) were added to each well of the medium spiny neuron culture. The co-cultures were incubated in the 37 ℃ 5 % CO_2 humidified incubator for 24 hours for immunocytochemistry and confocal imaging, and for 24 - 48 hours for electrophysiology recordings.

2.2 Transfection

2.2.1 Effectene

HEK293 cells were plated on poly-D-lysine (0.1 mg/ml) coated 6-well plate (3×10^5 cells/well) 24 hours before transfection. After 24-hour incubation of cells in the 37℃ 5% CO_2 humidified incubator, a total of 200 ng DNA was mixed in 252.6 µl EC buffer (Qiagen) with 8.1 µl enhancer (Qiagen) for 5 minutes at room temperature after briefly vortexing the mixture. Effectene (Qiagen) was then added into the mixture (25.25 µl per 200 ng DNA) and further vortexed. After a 10-minute incubation at room temperature, the DNA-Effectene mixture was added into the wells drop-by-drop. The transfected cells were incubated in the 37 ℃ 5 % CO_2 humidified incubator for 24 hours before they were detached and

plated on poly-L-lysine (0.1 mg/ml) coated glass coverslips (VWR) in 24-well plate or added to cultured striatal medium spiny neurons already growing on glass coverslips for 12-13 days to form co-cultures.

2.2.2 Nucleofection

Nucleofection is an electroporation-based transfection method which allows the DNA to directly enter the nucleus (Distler et al., 2005). Amaxa nucleofector (Lonza) was used to perform nucleofection of the $NL2^{HA}$ cDNA into the HEK293 cells stably expressing $\alpha_2\beta_2\gamma_2$-$GABA_A$ receptors. The cells were plated to be at around 70 % confluency 24 hours before transfection. The cells were detached with Versene and collected into a 15 ml Falcon tube in which they were centrifuged at 3700 rpm for 2 minutes using a benchtop centrifuge (Mikro 2r, Hettich). The cells were then washed twice with warmed OPTI-MEM and subsequently resuspended in 0.5 ml warmed OPTI-MEM. The resuspended cells were combined with DNA (2 µg for 1 × 10^6 cells) and made up to 100 µl with OPTI-MEM for each nucleofector cuvette. The cuvettes were inserted into the Amaxa nucleofector to perform nucleofection with program A-23. After nucleofection, 200 µl warmed DMEM was added to each cuvette to collect all transfected cells into a 15 ml Falcon tube. The transfected cells were then plated into poly-D-lysine (0.1 mg/ml) coated 24-well plate (90,000 cells/well) for 24 hours in the 37 ℃ 5 % CO_2 humidified incubator before fixation.

2.2.3 Calcium Phosphate-Based Transfection

The HEK293 cells were around 70 % confluency in T75 tissue culture flasks when ready for calcium phosphate-based transfection (Jordan and Wurm, 2004). The cDNAs for proteins of interest or empty vector control (5 µg each per T75 flask) were mixed with 100 µl 2.5 M $CaCl_2$, made up to 1 ml with 1/10 Tris-EDTA (TE) buffer and then shaken vigorously for 15 seconds. The mixture was added to 2 × HEPES-buffered saline (50 mM HEPES, 280 mM NaCl, 1.1 mM Na_2HPO_4), pH 7.4 (HBS) solution drop-by-drop, mixed and incubated for 45 minutes at room temperature. The mixture was added to the cells in flasks drop-by-drop and incubated in the 37 ℃ 5 % CO_2 humidified incubator for 24 hours.

2.3 Immunocytochemistry

The cells plated on 13 mm coverslips (VWR) were briefly washed with PBS twice and 4 % paraformaldehyde (PFA) with 4% sucrose in PBS was used to fix the cells for 10 min at room temperature. The PFA was aspirated and the cells were rinsed with PBS twice briefly followed by three 5-minute washes. All washes were performed on a rocket shaker at room temperature. The residual aldehyde groups of PFA were blocked with 0.3 M glycine in PBS for 10 min at room temperature, followed by multiple washes with PBS. The cells were blocked in 1% bovine serum albumin (BSA, SIGMA) in PBS for 30 min at room temperature. The primary antibodies were diluted in 1 % BSA in PBS, added to the cells, and incubated for 2 hours at room temperature or overnight at 4 ℃. After incubation, the cells were rinsed twice and washed multiple times with PBS. For labeling of

intracellular proteins, the cells were permeabilized with 0.5 % Triton-X-100 in PBS for 10 min at room temperature prior to the addition of the primary antibody mix. The cells were washed and blocked again with 1% BSA in PBS for 30 min at room temperature. Fluorescently-labelled secondary antibodies (AlexaFluor) were diluted in 1 % BSA in PBS (1:750) and added to the cells for 1 hour at room temperature protected from light. The coverslips were washed with PBS and mounted on glass slides with ProLong Gold antifade reagent (Invitrogen). The slides were dried at room temperature protected from light and kept at 4 ℃ in boxes.

2.4 Confocal Imaging and ImageJ Analysis

The coverslips were imaged using Zeiss confocal microscope LSM 700/710/880 with 63× oil immersion objective and analyzed using ImageJ (National Institute of Health) as described previously (Brown et al., 2016). Before acquiring images, the coverslips incubated with solely secondary antibodies were imaged for setting up the parameters which minimized the non-specific staining by secondary antibodies. The detector gain and offset were adjusted to show just no signal for secondary antibody control samples. Images were acquired at 12-bit depth with 512 × 512 or 1024 × 1024 frame sizes from 10 - 15 cells from each co-culture. For each image, a series of z-stack images were acquired from the bottom to the top of the HEK293 cell with optimal intervals of 0.7 µm.

For analysis of contacts formed between presynaptic GABAergic terminals of cultured neurons and HEK293 cells, I used ImageJ software. Images acquired in

Zen software (Carl Zeiss) were imported into ImageJ. The smallest square area that contains all parts of a single HEK293 cell was cropped and the individual channels were split. The co-localization was obtained by “Process → Image Calculator” function using the option “And”, which produced an image showing all the pixels that appeared in both channels. The threshold of the image was adjusted by the “Auto-Threshold” function. The data for co-localization were obtained by the “Analyze → Analyze Particles” function. For quantitative assessment of synaptic contacts formed between presynaptic GABAergic terminals and HEK293 cells, two parameters were considered, “Count” which represents the number of colocalized pixels between fluorescently-labelled terminals and HEK293 cells, and “% Area” which represents the surface area of each HEK293 cell with co-localized pixels normalized to the total surface area of the cell.

These parameters were imported into Origin Pro software for statistical analysis and graphical presentation of the data. The Count and % Area data from $N \geq 2$ independent experiments were individually pooled for each group. The data were plotted with Box-and-Whisker plots showing the median, standard deviation and outliers. The data were analyzed using Shapiro-Wilk normality test to test if the data show normal Gaussian distribution. Non-normally distributed data were subjected to non-parametric Mann-Whitney test for investigating the statistical significance of differences between each group. Normally distributed data were analyzed using a two-tailed student’s t-test for investigating the statistical

significance.

2.5 SDS-PAGE

Protein analysis using SDS-PAGE (sodium dodecyl-polyacrylamide gel electrophoresis) and immunoblotting has been used for over 40 years for the detection of protein expression levels by separating proteins according to their molecular weight. Proteins are unfolded: dithiothreitol (DTT) reduces disulfide bonds; sodium dodecyl sulphate (SDS) binds to the proteins which lose their secondary structure to linearize them and coat them with uniform negative charges. The electrophoresis is divided into two stages with different pore sizes and pH of the acrylamide gel. In the stacking gel with a relatively large pore size and pH 6.8, linearized and negatively charged proteins move towards the positive electrode. Glycine from the running buffer is positively charged at high pH (in the running buffer) but is negatively charged at pH 6.8 (in the stacking gel). Therefore, glycine is zwitterionic in the stacking gel and moves slower than the proteins. However, the chloride anions from Tris-HCl move faster than the proteins. This gradient in movement forms a ‘sandwich-like’ order of chloride ions in front, proteins in middle, and glycine at the end, which stacks proteins into a tight band. In the separation gel with a smaller pore size and pH 8.8, glycine is fully negatively changed and travels much faster toward the cathode. Due to the smaller pore size, proteins move slower than glycine and chloride ions. Therefore, proteins move towards the cathodes at a speed determined by their molecular weight (the smaller the faster).

Cultured cells were washed twice with PBS and lysed with 2 % SDS. The lysates were boiled at 95 ℃ for 5 minutes and sonicated at 60 Amps for 30 sec and centrifuged at 13,000 rpm for 10 minutes. The concentration of proteins was determined by BCA Assay (Thermo Fisher Scientifics) as per the manufacturer's instructions. For detecting proteins with molecular weight in the 50-100 kDa range, 100-150 µg of total protein were loaded into a stacking gel (125 mM Tris, pH 6.8, 0.1 % SDS, 5.1 % poly-acrylamide, 0.05 % ammonium persulphate (APS), 0.1% tetramethylethylenediamine (TEMED, Fisher Bioreagents)) and separated in a 10 % SDS-poly-acrylamide separation gel at 55 V overnight. The 10 % SDS-polyacrylamide separation gel was made with 0.375 M Tris pH 8.8, 0.1 % SDS, 10 % poly-acrylamide, 0.025 % APS and 0.05 % TEMED. For 8 % SDS-polyacrylamide separation gel the concentration of poly-acrylamide was adjusted to 8 %. For proteins with higher molecular weight, 8 % SDS-poly-acrylamide separation gel was used. Before being loaded into the gel, the protein samples were mixed with sample buffer (SB, 62.5 mM Tris, pH 8.0, 2 % SDS, 10 % glycerol, 0.0025% Bromophenol Blue, 1 M DTT).

2.6 Immunoblotting

Proteins separated using SDS/PAGE were transferred onto a solid nitrocellulose membrane (Whatman) in transfer buffer (TB) (20 mM Tris, 120 mM glycine, pH 8.6, 20 % methanol) for a minimum of 200 mA for 4 hours. Ponceau-S (Thermo Fisher Scientific) was used to reversibly visualize the protein bands on the nitrocellulose membrane, which detected the efficiency and quality of transferring

proteins.

The membrane was incubated in a blocking solution (1.5 % (w/v) milk, 10% tris buffered saline-Tween (TBS-T, 50 mM Tris pH 7.6, 200 mM NaCl, 0.05 % Tween-20)) for 30 minutes to block non-specific binding with primary antibodies. The blocking solution was aspirated and the membrane was incubated with primary antibodies diluted in the blocking solution for at least 1.5 hours at room temperature or overnight at 4 ℃ on a GYRO-Rocker rocking plate (Jencons-PLS). After incubation, the primary antibody was removed and the membrane was washed with the blocking solution. The secondary antibody conjugated to alkaline phosphatese (goat anti-rabbit, 1:1000, A16099, Invitrogen; rabbit anti-mouse, 1:2500, 31450, Invitrogen) was diluted in blocking solution and added to the membrane and incubated for 1 hour at room temperature on the rocking plate. When the incubation was finished, the membrane was washed with the blocking solution, TBS-Tween, and TBS (50 mM Tris pH 7.6, 200 mM NaCl), and the final wash was done using the alkaline phosphatase buffer (100 mM Tris pH 9.5, 100 mM NaCl, 10 mM MgCl2·6H_2O). The immunoreactive bands were revealed by incubation with 5-bromo-4-chloro-3-indolyl phosphate (BCIP, 0.175 mg/ml)/nitro blue tetrazolium (NBT, 0.35 mg/ml) (S3771, Promega) substrates for alkaline phosphatase at room temperature.

2.7 Protein Assays

2.7.1 BCA Assay

A standard curve correlating optical absorbance and protein concentration was obtained using 1 mg/ml BSA standard according to the table below. Each sample was duplicated.

SDS cell lysates (2 µl) were mixed with 100 µl double distilled water (ddH_2O) for each sample. Pierce™ BCA reagent A and B were mixed in 50:1 ratio and 2 ml of this mix was added to each sample. The mixture was incubated in 37 ℃ water bath for 30 minutes. In this assay, the Cu^{2+} ions are reduced to Cu^{+} ions by the proteins in the alkaline condition, which is known as Biuret reaction. The Cu^{+} ions are chelated by bicinchoninic acid (BCA) from the reagents to produce a soluble dark purple complex. The intensity of the color reaction should be in a

Table 2.1 Standard curve establishment for BCA assay.

Standard (µg/µl)	ddH_2O (µl)	1 mg/ml BSA (µl)	2 % SDS (µl)
0	100	-	2
1	99	1	2
2	98	2	2
3	97	3	2
4	96	4	2
5	95	5	2
10	90	10	2
15	85	15	2
20	80	20	2

linear correlation with the protein concentration and is measured as absorbance at 562 nm (Davis and Radke, 1987). The absorbance at 562 nm was detected using a DU800 spectrophotometer (Beckman Coulter).

2.7.2 Bradford Assay

A standard curve correlating optical absorbance and protein concentration was obtained using 1 mg/ml BSA standard according to the table below. Each sample was duplicated.

Table 2.2 Standard curve establishment for Bradford assay.

Standard (µg/µl)	ddH_2O (µl)	1 mg/ml BSA (µl)	Sample Buffer (µl)
0	100	-	2
5	95	5	2
10	90	10	2
15	85	15	2
20	80	20	2

Protein samples (2 µl) were mixed with 100 µl ddH_2O for each sample. The Bradford assay dye (Bio-Rad) was diluted with ddH_2O (1:5 vol/vol) and 2 ml was added to each sample. The peak absorbance of the Coomassie dye in this assay shifts from 465 nm to 595 nm when it binds to proteins in the sample. This shift is proportional to the amount of protein in the sample (Bradford, 1976). The absorbance at 595 nm was measured using a DU800 spectrometer.

3. Development of HEK293 Cell Line Stably Expressing Extrasynaptic $GABA_A$-α4β3δ Receptors

3.1 Introduction

3.1.1 Extrasynaptic $GABA_A$ Receptors

Extrasynaptic $GABA_A$ receptors mediate tonic inhibition in the brain in response to the ambient GABA at low concentrations spilled over from synapses as they have a higher affinity for GABA binding than synaptic $GABA_A$ receptors (Mortensen, Patel and Smart, 2012). The tonic inhibition resulting from the extrasynaptic $GABA_A$ receptors persistently increases the conductance of the neuronal plasma membrane and hence results in a decreased probability of action potential generation (Farrant and Nusser, 2005). Tonic inhibition can also occur by the spontaneous opening of the extrasynaptic $GABA_A$ receptors which does not require GABA binding (Wlodarczyk et al., 2013). This spontaneous activation may contribute significantly to the overall tonic inhibition (O'Neill and Sylantyev, 2018). The GABA-independent tonic inhibition caused by spontaneous $GABA_A$ receptors activation is also important for shaping the neural plasticity by its regulation of the neural signal filtering and integration (O'Neill and Sylantyev, 2018).

3.1.2 Localization and Functional Role of Extrasynaptic $GABA_A$ Receptors in the Brain

In the preferential combination with $\alpha_{4/6}$ and $\beta_{2/3}$ subunits, δ-containing $GABA_A$

receptors are predominantly expressed extrasynaptically in the thalamus, neostriatum and dentate gyrus to mediate tonic inhibition (Farrant and Nusser, 2005). The α_4 subunit was first cloned by Wisden et al. in 1991. The δ subunit was first identified to exist in different neuronal subpopulations from the γ_2 subunits by Shivers et al. in 1989 By continuously increasing the input conductance of the neurons, tonic inhibition by the extrasynaptic $GABA_A$ receptors regulates the amplitude and frequency of excitatory inputs to the neurons. By exerting the tonic inhibition in the brain and being a key target to anaesthetics, neurosteroids and alcohol, extrasynaptic $GABA_A$ receptors are crucial in modulating various aspects such as sleep, consciousness, stress and alcohol intoxication (Brickley and Mody, 2012). The extrasynaptic $GABA_A$ receptors expressed on the thalamic nucleus reticular cells were shown to be essential in modulating the thalamocortical oscillations which regulates the sleep-wake cycles (Belelli et al., 2005). Except for GABA, neurosteroids are also regulators of $GABA_A$ receptors in the CNS, having a higher affinity for the δ-containing $GABA_A$ receptors, which have been associated with stress and anxiety disorders (Brickley and Mody, 2012). Although tonic inhibition has been observed even in the absence of δ subunits, due to a shift of γ_2 subunits from synaptic to perisynaptic domains, these receptors do not appear to respond to neurosteroids as observed in an epileptic mouse model (Zhang, Wei, Mody and Houser, 2007). The δ-containing $GABA_A$ receptors have also been shown to regulate alcohol consumption in response to low concentrations (1 – 30 mM) of ethanol (Lobo and

Harris, 2008). Whilst the potentiation of extrasynaptic tonic inhibition by ethanol was not altered in α_4-KO mice, this effect was shown to significantly decrease in δ-KO mice (Liang et al., 2007).

3.1.3 Forward Trafficking and Plasma Membrane Insertion

After assembly in the ER, $GABA_A$ receptors are transported to the Golgi apparatus for translocation to the cell membranes (Lorenz-Guertin and Jacob, 2017). During this process, α and β subunits play major roles in interacting with proteins that regulates the trafficking of $GABA_A$ receptors (Bedford et al., 2001; Goto et al., 2005). In the Golgi apparatus, γ_2 subunit is believed to be essential for GABARAP-mediated postsynaptic targeting of $GABA_A$ receptors which is also regulated by PRIP (Wang et al., 1999). The localization of $GABA_A$ receptors once they are inserted into the plasma membrane depends on their subunit composition. Whilst $GABA_A$ receptors that contain α2 subunit usually have synaptic localization, those that incorporate the $\alpha_{4/6}$ and δ subunits are predominantly found outside of synaptic contacts where they contribute to tonic inhibition (Belelli et al., 2009). Recent studies have revealed that lipoma HMGIC fusion partner-like 4 (Lhfpl4, also named GARLH4) regulates the synaptic localization of $GABA_A$ receptors in a subunit-dependent manner (Yamasaki et al., 2017, Davenport et al., 2017).

The α_5 subunit has been shown to contribute to both synaptic inhibition and extrasynaptic inhibition (Zarnowska et al., 2008; Loebrich et al., 2006). Membrane localization of extrasynaptic α_5-containinig $GABA_A$ receptors depends

on the interaction with ERM protein radixin. Radixin provides the linkage between the $GABA_A$ receptors and the actin skeleton at the perisynaptic locations at the plasma membrane (Hausrat et al., 2015; Mele, Leal and Duarte, 2016). How the other extrasynaptic $GABA_A$ receptors are restricted outside the synaptic area has not been fully elucidated. Although the $GABA_A$ receptors show the ability to diffuse in and out of the postsynaptic domains, this diffusion seems to be restricted by the presence of certain subunits. The expression of the δ subunit is largely related to the α_6 subunit, which leads to its extrasynaptic localization (Jones et al., 1997; Nusser, Sieghart and Somogyi, 1998). Martenson et al. (2017) showed that the GARLH-$GABA_A$ receptor complex depends on the γ_2 subunits whilst the expression of the δ subunit inhibits such interaction and hence leads to the extrasynaptic localization of the $GABA_A$ receptors. A recent study shows that a chimera form of δ subunit which has the intracellular loop TM3-4 region swapped for γ_2 equivalent changes the extrasynaptic localization of δ-containing receptors to the synaptic regions, which suggests that δ-containing $GABA_A$ receptors are restricted to the extrasynaptic area by interacting with unknown protein via its intracellular domain (Hannan et al., 2020).

3.1.4 HEK293 Cell Line

The HEK293 cell line expression system has been used for more than 40 years for its various advantages. Most importantly, HEK293 cells can be transfected to express exogenous membrane-anchored proteins (Thomas and Smart, 2005) and support their synthesis, trafficking and insertion to the cell membrane.

HEK293 cells are convenient to maintain in a 37 ℃ incubator with 5% carbon dioxide. The supporting reagents are accessible via commercial sources such as Gibco. The passaging of the HEK293 cells is relatively quick as they are fast dividing cells reaching 70% confluency from ~10% in 2 – 3 days, which is advantageous for designing and performing experiments. However, this growth rate of HEK293 cells is not too fast to occupy the whole growing area very quickly. This provides a large operational window for experiments such as microscopic imaging of single cells and quantitative assays such as cell surface ELISA which require an optimal cell density for detection of cell surface immunoreactivity. Moreover, the HEK293 cells are roughly 20 – 30 μm in length which is favored by electrophysiologists to perform whole-cell recordings and the expression level of exogenous protein in HEK293 cells is high enough to differ from endogenous noise (Thomas and Smart, 2005). Therefore, the HEK293 cell line has long been used in our lab for expressing proteins of interest. When studying the effect brought by a single receptor subtype, a HEK293 cell line without any other receptors is a suitable platform. For example, Brown et al. (2017) examined the role of the $GABA_A$ receptor N-terminal extracellular domains in inhibitory synapses formation using a co-culture of primary embryonic rat medium spiny neurons and HEK293 cell line transfected to stably express specific subtypes of $GABA_A$ receptors. The level of innervation was analyzed by immunocytochemistry and confocal microscope imaging of single HEK293 cells and the functionality of the synapses formed was examined by electrophysiology

recordings. Immunoblotting of cell lysates and ELISA were also used for the analysis of the receptor expression.

3.1.5 Aim and Hypothesis

The aim of this chapter was to create a stable HEK293 cell line that will express the $\alpha_4\beta_3\delta$-$GABA_A$ receptors at the cell surface. This cell line was going to be used to test whether the extrasynaptic $GABA_A$ receptors can facilitate the formation of synaptic contacts in a HEK293-medium spiny neuron co-culture model in which we have previously characterized the effects of synaptic $\alpha_2\beta_2\gamma_2$-$GABA_A$ receptors on synaptic contact formation (Brown et al, 2014, 2016). After insertion of individual subunits into plasmids with different antibiotic resistance genes and selection of clones in the presence of antibiotics, immunoblotting, immunocytochemistry and electrophysiology were used to confirm the stable expression and functionality of $\alpha_4\beta_3\delta$-$GABA_A$ receptors in this cell line.

3.2 Material and Method

3.2.1 Preparation for Chemically Competent *E. coli* Cells

A small volume of *E.coli* cells were streaked from a glycerol frozen stock onto 2 % (w/v) agar plate and incubated at 37℃ overnight. The next day a single colony was inoculated into 5 ml LB medium (Invitrogen) in a 50 ml Falcon tube which was incubated at 37℃ with shaking at 225 rpm overnight. A small volume of the overnight culture (0.5 ml) was then inoculated into supplement LB medium (LB medium with 0.01 M $MgSO_4$ and 0.2 % (w/v) glucose) and incubated at 37 ℃ shaking at 225 rpm. When the optic density at wavelength 600 nm ($OD_{\lambda = 600}$) reached between 0.6 and 0.7, the culture was immediately transferred to a centrifuge tube and incubated on ice for 10 minutes followed by 10-minute centrifugation at 2500 rpm at 4 ℃. The pelleted *E.coli* cells were resuspended in 0.5 ml supplement LB medium and stored in 2.5 ml storage solution (36 % glycerol, 12 % (w/v) $PEG_{MW = 8,000}$, 12 mM $MgSO_4$ in LB medium) in 100 µl aliquot at -80 ℃ for up to 3 months.

3.2.2 Transformation of *E. coli* and Amplification of DNA Plasmids

α_4 and δ DNA in pUNIV (ampicillin resistant) was provided by Dr. Martin Mortensen (NPP, Biosciences, UCL). β_3 DNA in pcDNA3.1-zeocin was available in the lab. To achieve selection for all three subunits, α_4 DNA was cloned into pcDNA3-G418 (Invitrogen) and δ DNA was cloned into pcDNA3.1-hygromycin (Invitrogen) vectors.

A small amount of DNA (1 ng) was mixed with 100 µl competent *E.coli* in a chilled Falcon polypropylene tube and incubated on ice for 30 minutes. The mixture was heat shocked in a 42 ℃ water bath for 50 seconds followed by 10-minute incubation on ice. The cell suspension was shaken at 225 rpm in 1 ml LB medium at 37 ℃ for 1 hour. The cells were transferred into 1.5 ml centrifuge tube and centrifuged at 7,000 rpm for 1 minute. The pellet was resuspended in 100 µl supernatant and seeded on 1 % (w/v) agar plate with 100 µg/ml ampicillin incubated at 37℃ overnight.

The next day 10 single colonies were picked pipette tips and incubated in 5 ml LB medium at 37 ℃ shaken at 225 rpm for at least 6 hours. A small portion of the culture (1 ml) was used to perform miniprep (Qiagen kit) as per the manufacturer's instructions. The purified DNA was run on a 1 % agarose gel to check the quality. The culture giving the most promising result was grown in 200 ml LB medium with 100 µg/ml ampicillin at 37 ℃ shaken at 225 rpm overnight. On the next day the culture was processed for maxiprep (Qiagen kit) as per the manufacturer's instructions.

3.2.3 Restriction Digestion and Ligation

Both α_4 and δ cDNA were obtained by double restriction digestion using restriction enzymes and suitable buffers from Promega at 37 ℃ for 2 hours. The details are shown in Table 1.

Table 1 Restriction digestion of α_4 and δ subunit cDNA insert.

Construct	Restriction Digestion Buffer	Restriction Enzyme I	Restriction Enzyme II
α4 in pUNIV	Buffer C	BamHI	XhoI
δ in pUNIV	Buffer D	BamHI	NotI

The digestion product was run on 1 % agarose gel and the bands reflecting both DNAs were cut out and processed by Qiagen DNA extraction kit as per manufacturer's instructions. The extracted DNA was ligated with their destination plasmids, i.e. α_4 with pcDNA3-G418 and δ with pcDNA3.1-hygromycin in 1:1, 2:1, 3:1, 5:1 and 7:1 ratio using T4 DNA ligase and ligation buffer (Thermo Scientific). Ligation was performed in Thermo cycler (Thermo) overnight at 16 ℃. The products of the ligation were transformed into *E.coli* and plated on LB Agar plates. Following miniprep analysis of selected colonies, the constructs were amplified by maxiprep as per manufacturer's instructions. The sequence was confirmed by Source Bioscience Sequencing.

3.2.4 Stable Transfection

3.2.4.1 Lipofectamine LTX

HEK293 wild type cells were seeded on 10 cm tissue culture dish (TPP) (2×10^6 cells/dish) 24 hours before transfection. DNA of α_4-pcDNA3-G418 and β_3-pcDNA3.1-zeozin cDNA constructs (7.5 µg each) was mixed with 12.5 µl plus reagent and 500 µl OPTI-MEM® I reduced serum medium for 5 minutes at room temperature. Lipofectamine LTX (12.5 µl) was added and mixed by incubating at room temperature for 25 minutes. Warmed DMEM (3 ml) was added and the final

mixture was added to the 10 cm tissue culture dish dropwise. The cells were incubated in the 37 ℃ 5 % CO_2 humidified incubator for 48 hours before they were split into 10 cm tissue culture dishes at six dilutions: 1:3, 1:5, 1:7, 1:10, 1:15 and 1:20. Once the cells were settled in the 10 cm dishes G418 and zeocin antibiotics were added to the complete DMEM. The antibiotic-containing medium was changed every two days. Colonies were formed ~15 days after transfection. At least six colonies were picked from each plate and seeded into 24-well plate. The cells were transferred to 6-well plate, 60 mm tissue culture dish (Thermo Fisher Scientific) and 10 cm tissue culture dish once they were confluent which took 2~3 days for each step. The expression level was analyzed by immunoblotting and electrophysiology.

3.2.4.2 Effectene

The cells were seeded on 10 cm tissue culture dish and the amount of DNA and volume of reagent were adjusted according to the optimizing scheme from manual of Effectene transfection reagent kit given by the company (Qiagen). The transfected cells were maintained in complete DMEM + zeocin which was changed to complete DMEM + G418, zeocin and hygromycin after 48 hours. The cells were then split into 10 cm tissue culture dishes at six dilutions: 1:3, 1:5, 1:7, 1:10, 1:15 and 1:20. The medium was changed every two days. Colonies were formed ~14 days after transfection and further selection and amplification of clones was done as described in section 3.2.4.1.

3.3 Results

3.3.1 Development of HEK293 Cell Line Stably Expressing α4β3δ-GABAA Receptors

Development of stable HEK293 cell lines expressing $GABA_A$ receptors was based on transfection of three plasmid DNA constructs incorporating α_4, β_3 or δ subunit together with antibiotic resistance genes for G418, zeocin and hygromycin, respectively. The development of the stable cell line was carried out in two stages. The first stage involved transfection of α4 and β_3 subunits into HEK293-wt cells followed by selection with antibiotics G418 and zeocin. The second stage involved transfection of δ subunit into the HEK293 cell line stably expressing $\alpha_4\beta_3$-GABAA receptors followed by selection with antibiotics G418, zeocin and hygromycin together. The expression of all three subunits in the stable cell line was confirmed by electrophysiology, immunoblotting and immunocytochemistry experiments.

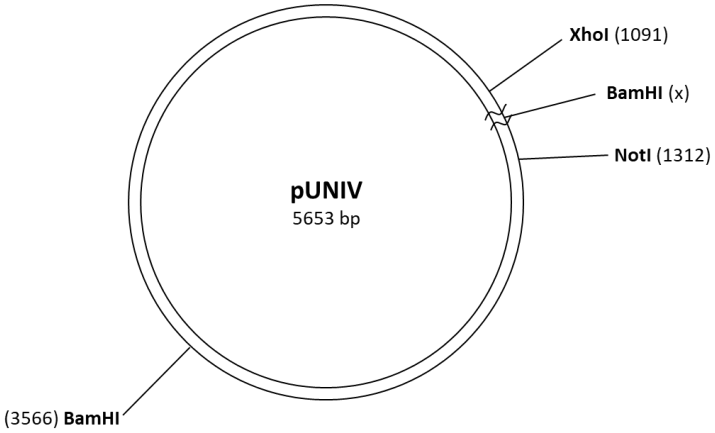

Figure 3.3.1
Representative pUNIV backbone showing the available restriction sites. An extra BamHI site was confirmed to be present in the sequence of δ cDNA insert by EMBOSS Needle pairwise sequence alignment analysis.

3.3.2 Preparation for α4-pcDNA3-G418 and δ-pcDNA3.1-hygromycin constructs

As β3-pcDNA3.1-zeocin was available in the lab, α4 and δ cDNAs, which were originally provided in pUNIV construct, needed to be subcloned into pcDNA3-G418 and pcDNA3.1-hygromycin plasmids respectively. The α_4-pUNIV and δ-pUNIV constructs were amplified by transformation into chemically competent E.coli cells followed by overnight incubation at 37℃. The cDNA inserts of α_4 and δ subunits were cut from pUNIV vector by restriction digestion. The selection of restriction enzymes was based on the comparison between the pUNIV and pcDNA3/3.1 vector maps. The restriction sites on pUNIV vector were obtained from published vector map (Venkatachalan et al., 2006) and Sanger sequencing (Source Bioscience). The restriction sites on pcDNA3/3.1 were obtained from the manufacturer manuals (Thermo Fisher Scientific). After sequencing, an extra BamHI site was found in δ sequence as shown in Figure 3.3.1. Figure 3.3.2 shows the evidence for successful digestion by selected restriction enzymes. The cDNA inserts for both subunits were extracted and ligated with pcDNA3/3.1 vectors to produce α_4-pcDNA3-G418 and δ-pcDNA3.1-hygromycin constructs.

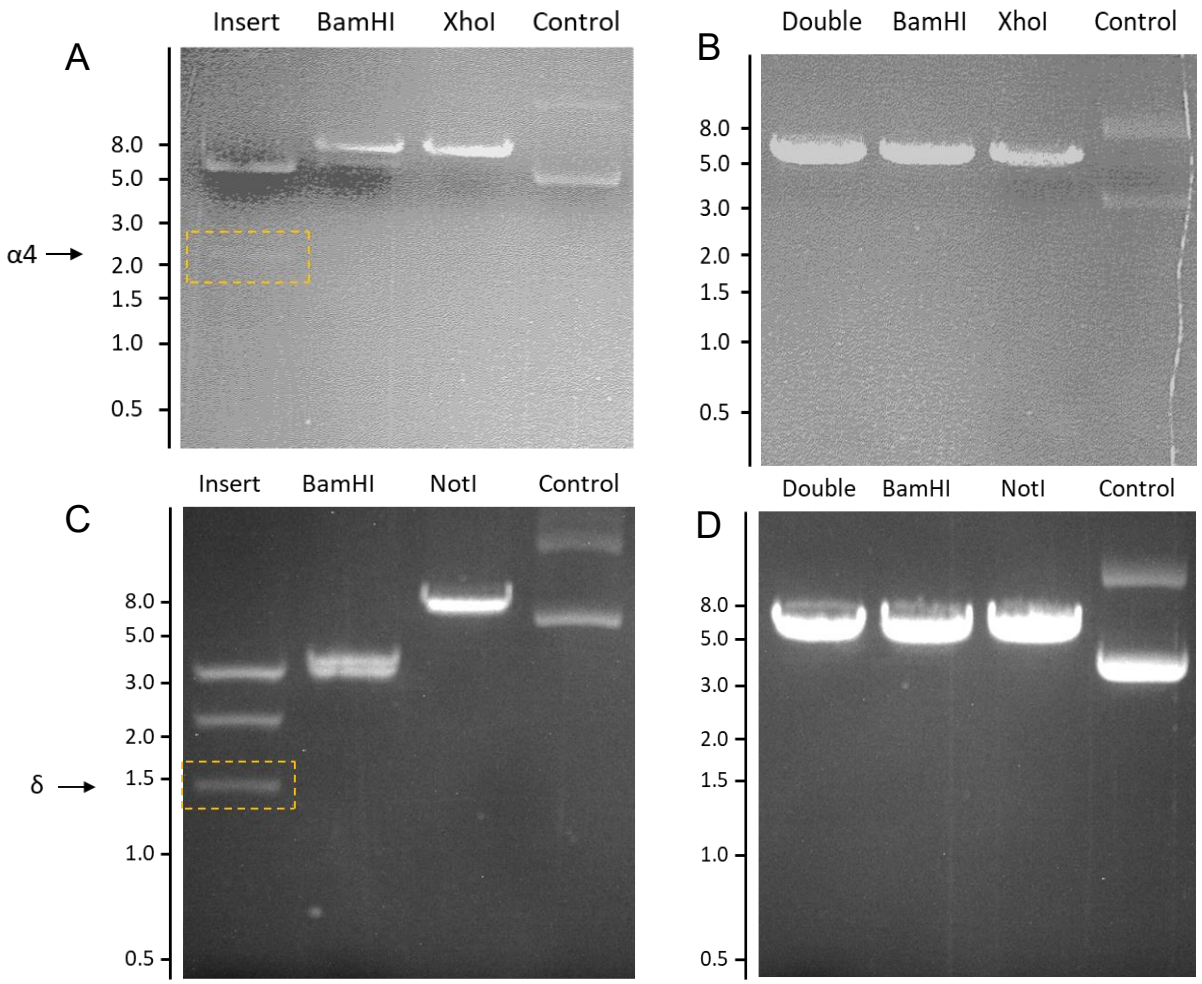

Figure 3.3.2

DNA electrophoresis to show successful restriction digestion of the α_4-pUNIV construct and empty pcDNA3-G418 vector (A, B) and δ-pUNIV construct and empty pcDNA3.1-hygromycin vector (C, D). (A) The double digestion with BamHI and XhoI produced a band at around 2.0kb (black arrow) in "insert" lane which corresponds to the size of α_4 subunit insert. (B) The double digestion with BamHI and XhoI produced only one band, suggesting that the vector was linearized. (C) The double digestion with both BamHI and NotI produced three bands between 3.0 and 4.0 kb, 2.0 and 3.0 kb and around 1.5 kb respectively. The ~1.5 kb band (black arrow) corresponds to the size of δ insert. (D) The double digestion with both BamHI and NotI produced only one band, suggesting that the vector was linearized.

3.3.3 Development of HEK293 Cell Line Stably Expressing α4β3-GABAA Receptors

α_4-pcDNA3-G418 and β_3-pcDNA3.1-zeocin constructs were transfected into HEK293-wt cells using lipofectamine LTX and plated at dilution 1:3, 1:5, 1:7, 1:10, 1:15 and 1:20. After ~2 weeks under antibiotic selection, six colonies from each dilution were picked and were labelled with a capital letter + number: A = colonies from 1:3 dilution, B = colonies from 1:5, C = colonies from 1:7, D = colonies from 1:10, E = colonies from 1:15 and F = colonies from 1:20, and transferred to 24-well plates. The cells were transferred to 35 mm dishes to further amplify the clones, followed by 60 mm dishes and 10 cm dishes. Fast growing colonies of cells were lysed with 2 % SDS and run on 10 % SDS-PAGE gel. The immunoblots indicated that α4 subunit was not expressed by any of the clones (Figure 3.3.3A), but clones A2, B2, B3, C3 and D1 expressed the β_3 subunit (Figure 3.3.3B). Clone B2 was selected for the next stage of transfection.

To test the cell surface expression of these two subunits, electrophysiological recordings were performed by Dr Martin Mortensen (NPP, Biosciences). As shown in Figure 3.3.4, the cells did not respond to the addition of up to 1 mM GABA but were depolarized by 1 mM picrotoxin. No response to GABA indicated that there were no $\alpha_4\beta_3$ assembled receptors expressed at the cell surface. The depolarisation caused by picrotoxin and the pattern of the recording indicated the closure of the spontaneously open homomeric receptors composed of the β_3

subunit (Cestari et al., 2000), which is consistent with our immunoblotting results (Figure 3.3.3).

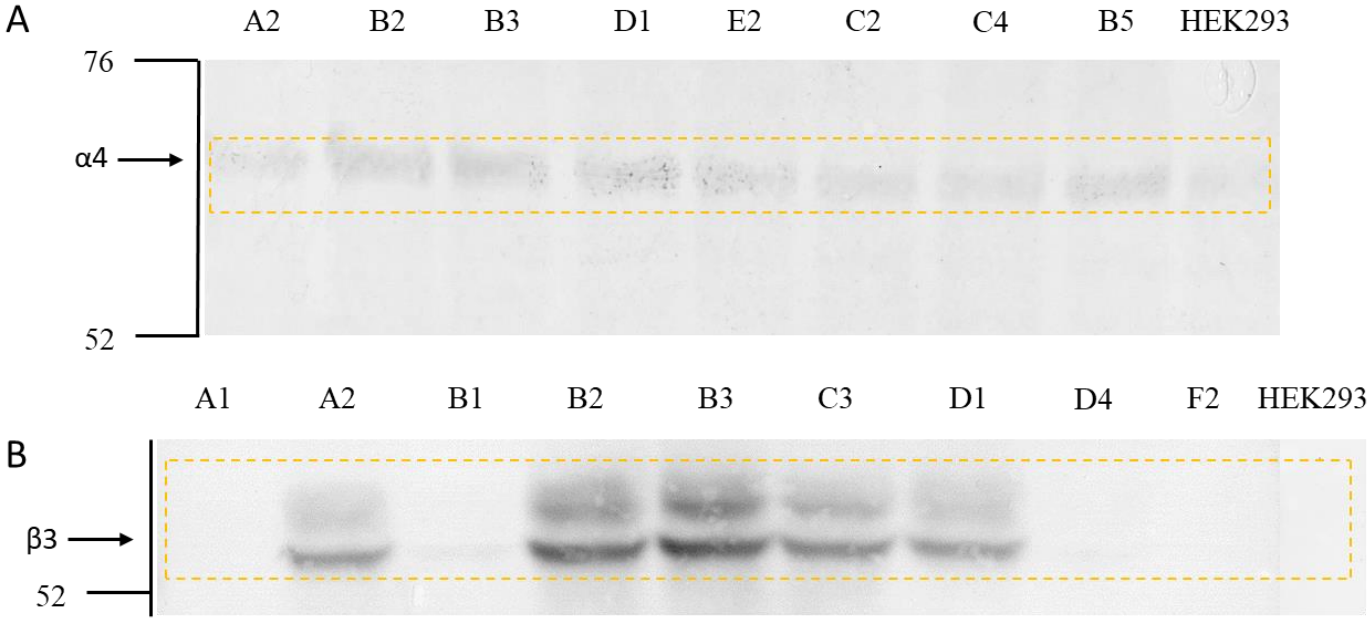

Figure 3.3.3

Immunoblot analysis of α_4 and β_3 expression in various clones of $GABA_A$ receptor-HEK293 stable cell. (A) Detection using the α_4 specific antibody. No specific band was detected at the molecular weight of the α_4 subunit. (B) Detection using the β_3 specific antibody. Bands slightly above 52 kDa correspond to the molecular weight of β_3 subunit for A2, B2, B3, C3 and D1 clones. Each lane was loaded with 100 µg protein. Expression for both subunits was visualized using alkaline phosphatase conjugated secondary antibodies and NBT/BCIP colour substrate reaction.

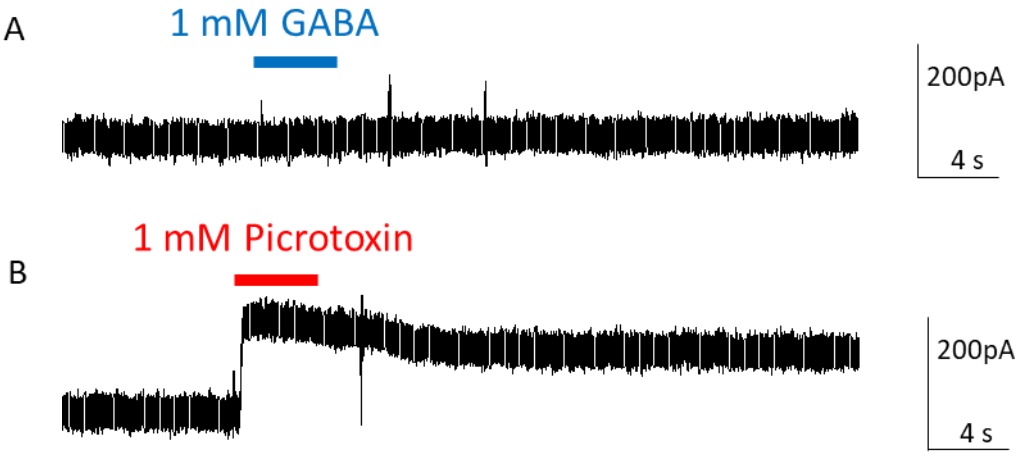

Figure 3.3.4

Whole-cell recordings of HEK293 cell line stably expressing $\alpha_4\beta_3$-$GABA_A$ receptors (cells were clamped at -60 mV). (A) Addition of 1 mM GABA caused no response. (B) Up to 1 mM picrotoxin application resulted in an upward current (depolarizing), which indicates closure of the spontaneously open homomeric $GABA_A$ receptors formed by the β_3 subunit. (n = 12 cells were tested in N = 2 independent experiments).

3.3.4 Development of HEK293 Cell Line Stably Expressing α4β3δ-GABAA Receptors

Because the expression of the α4 subunit was not detected in any of the clones following the first stage of selection, in the second stage δ-pcDNA3.1-hygromycin construct was transfected together with α_4-pcDNA3-G418 using Effectene and plated at increasing dilutions 1:3, 1:5, 1:7, 1:10, 1:15 and 1:20. Six colonies from each dilution were picked and labelled with capital letter + number': A = colonies from 1:3 dilution, B = colonies from 1:5, C = colonies from 1:7, D = colonies from 1:10, E = colonies from 1:15 and F = colonies from 1:20 and transferred to a 24-well plate. Fast growing colonies of cells were transferred to 35 mm dishes, followed by 60 mm dishes and 10 cm dishes to amplify the clones. Clone B2' was shown to be the only clone expressing the α4 subunit (Figure 3.3.5A). β_3 subunit was detected in many clones but at various levels. With the same amount of protein loaded in each lane, clone A2' failed to show expression of the α4 subunit and was used as a negative control in further experiments.

To further confirm the expression of the subunits in selected clones, the cDNA constructs with/without antibiotic resistance genes were transiently transfected into HEK293-wt cells using lipofectamine LTX. Figure 3.3.5B shows bands at the expected molecular weight for α4 subunit for clone B2' and HEK293 cells transiently transfected with both types of cDNA constructs. Figure 3.3.6B shows bands at the correct molecular weight for the β3 subunit in clones B2', A2' and HEK293 cells transiently transfected with α_4, β_3 and δ cDNA. Figure 3.3.7 shows

a band at the expected molecular weight for δ subunit in clones B2' and A2', but no corresponding band was detected in transiently transfected cells (data not shown).

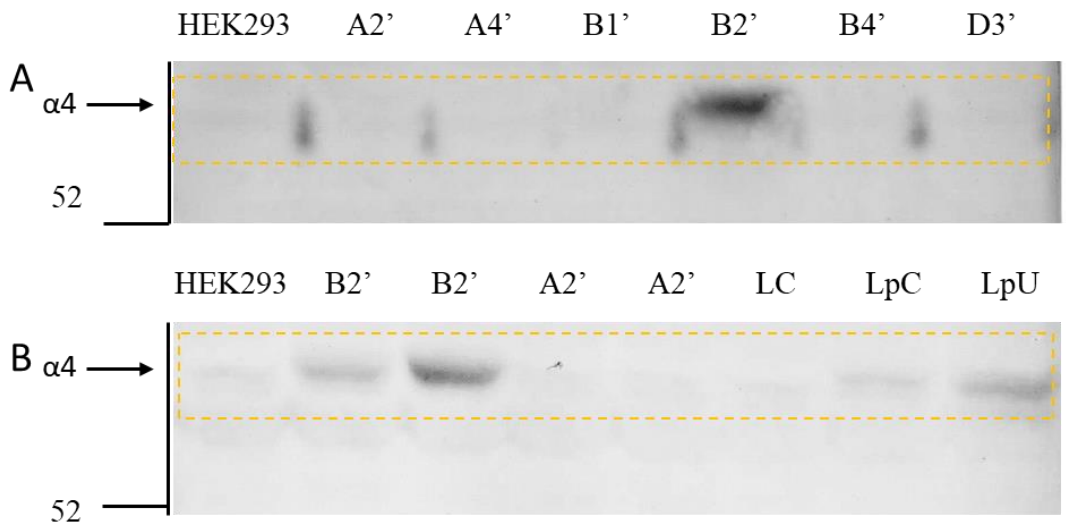

Figure 3.3.5

Immunoblot analysis of α_4 expression in various clones of $GABA_A$ receptor-HEK293 stable cell. (A) Detection of the α_4 subunit in $\alpha_4\beta_3\delta$ cell clone lysates at ~52 kDa corresponding to the molecular weight of α_4 subunit for B2' clone. (B) Detection of the α_4 subunit in $\alpha_4\beta_3\delta$ cell clone B2' compared to A2' and HEK293 cells transiently transfected with α_4, β_3 and δ subunits. LC = HEK293 cells negative control; LpC = HEK293 cells transiently transfected with α_4-pcDNA3-G418, β_3-pcDNA3.1-zeocin and δ-pcDNA3.1-hygromycin constructs; LpU = HEK293 cells transiently transfected with α_4-pUNIV, β_3-pcDNA3 and δ-pUNIV constructs. For each clone 100 µg protein was loaded. Primary antibody binding was visualised using alkaline phosphatase-conjugated secondary antibody and NBT/BCIP colour substrate reaction. This further confirms the expression of α_4 subunit in the B2' clone.

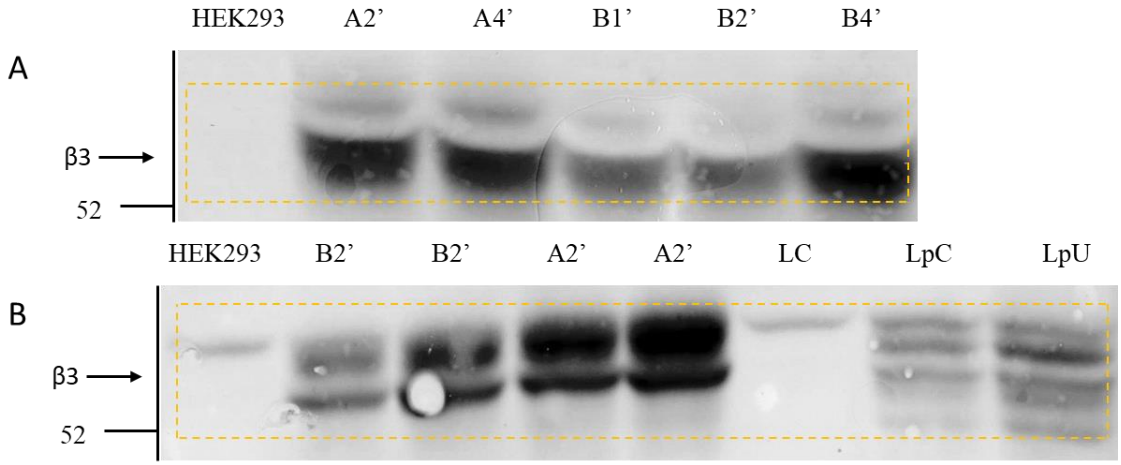

Figure 3.3.6

Immunoblot analysis of β_3 expression in various clones of $GABA_A$ receptor-HEK293 stable cell line. (A) Detection of β_3 subunit in $\alpha_4\beta_3\delta$ cell clone lysates. For each clone 100 µg protein were loaded producing a band around 52 kDa corresponding to the molecular weight of the β_3 subunit for all clones tested. (B) Detection of β_3 subunit in $\alpha_4\beta_3\delta$ cell clone B2' compared to A2' and HEK293 cells transiently transfected with α_4, β_3 and δ subunits. LC = HEK293 cells negative control; LpC = HEK293 cells transfected with α_4-pcDNA3-G418, β_3-pcDNA3.1-zeocin and δ-pcDNA3.1-hygromycin constructs; LpU = HEK293 cells transfected with α_4-pUNIV, β_3-pcDNA3 and δ-pUNIV constructs. For each clone 100 µg protein was loaded per lane. Primary antibody binding was visualised using alkaline phosphatase-conjugated secondary antibody and NBT/BCIP colour substrate reaction. This further confirms the expression of the β_3 subunit

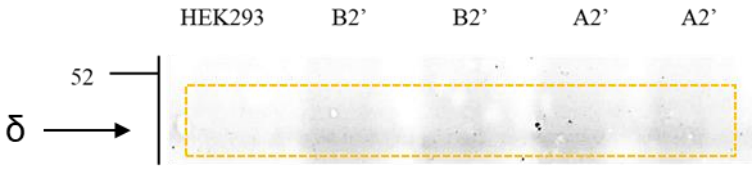

Figure 3.3.7

Immunoblot analysis of δ subunit expression in $\alpha_4\beta_3\delta$ cell clone B2' compared to A2' and HEK293 cells. Incubation with the δ subunit specific antibody produced bands at ~50 kDa corresponding to the expected molecular weight. Primary antibody binding was visualised using alkaline phosphatase-conjugated secondary antibody and NBT/BCIP colour substrate reaction. For each clone 100 µg protein was loaded.

In order to test the cell surface expression of the three subunits, 30,000 cells were plated on coverslips in 24-well plate for immunocytochemistry experiment. Zeiss confocal microscope LSM 710 was used to acquire fluorescent images. Clone B2', A2' and HEK293-wt cells were tested. Because the α_4 and δ subunit specific antibodies available in the lab were both raised in rabbits, the cells were double labelled with α_4 and β_3 subunit-specific antibodies at the same time (Figure 3.3.8) or β_3 and δ subunit-specific antibodies (Figure 3.3.9). In the clone A2', no signal for α_4 or δ subunit was detected, which produced the same image pattern as HEK293-wt cells. The expression of β_3 subunit was detected in all cells. In the clone B2', expression of all three subunits was detected in all the cells. The merged channels of Figure 3.3.8 and Figure 3.3.9 (middle panel) show the co-localization of α_4 and β_3 subunits and β_3 and δ subunits on the cell surface.

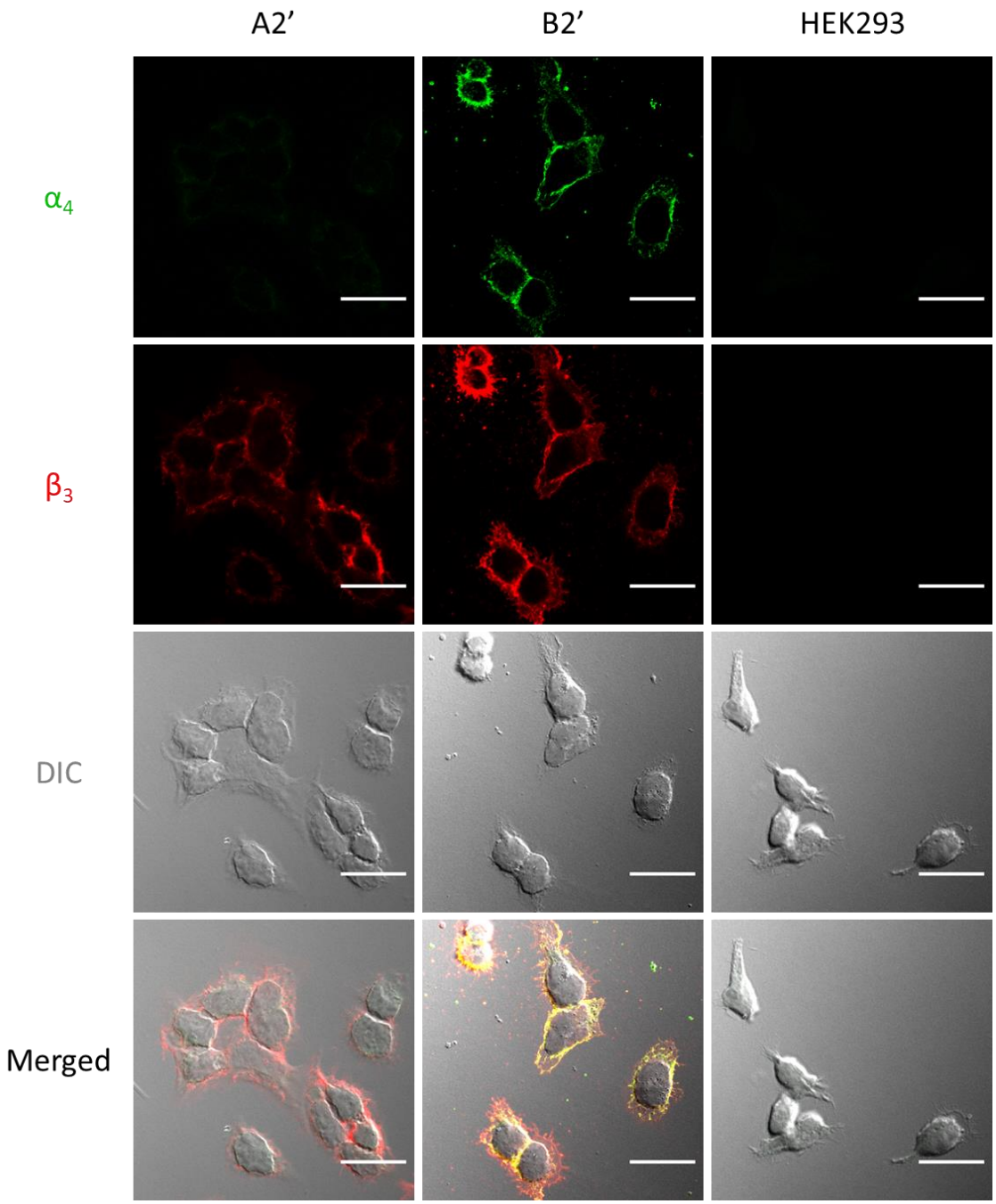

Figure 3.3.8

Fluorescent immunolabelling of α_4 and β_3 subunits on the cell surface of clones A2' and B2'. HEK293-wt cells were used as negative control. Clone A2' shows no expression of the α_4 subunit but expression of the β_3 subunit (red). Clone B2' shows expression of both α_4 (green) and β_3 (red) subunits. The merged channel shows the co-localisation of the two subunits on the cell surface. HEK293-wt cells show no expression of either α_4 or β_3 subunits. Scale bar = 20 μm. The DIC channel shows all the cells in the field. Fluorescent imaging was done using Zeiss 710 confocal microscope at 40 x magnification.

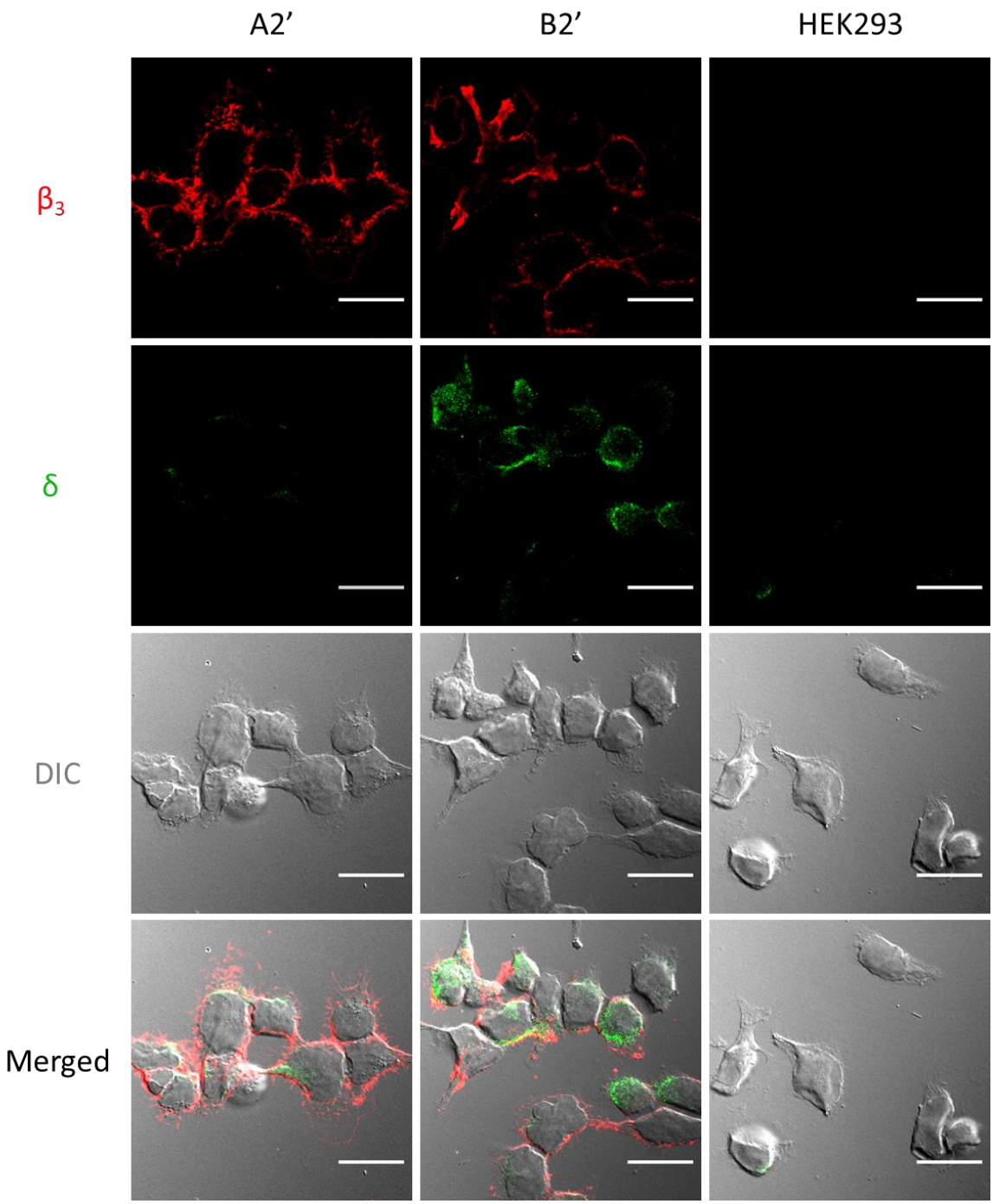

Figure 3.3.9

Fluorescent immunolabelling of β_3 and δ subunits on the surface of A2' and B2' clones. HEK293-wt cells were used as negative control. A2' clone shows expression of the β_3 subunit (red) but very low expression of the δ subunit. B2' clone shows expression of both β_3 (red) and δ (green) subunits. The merged channel shows the co-localisation of the two subunits on the cell surface. HEK293-wt cells show no expression of either β_3 or δ subunits. Scale bar = 20 µm. The DIC channel shows all the cells in the field. Fluorescent imaging was done using Zeiss 710 confocal microscope at 40 x magnification.

Once expression of the $\alpha_4\beta_3\delta$-$GABA_A$ receptors was confirmed, it was important to show that these receptors are functional. Expression of functional receptors in the clone B2' was confirmed in dose-response experiments with GABA resulting the average EC_{50} = 0.53 μM. Expression of the δ subunit was further confirmed by the significant potentiation of currents with DS2 which is a positive allosteric modulator for $GABA_A$ receptor containing δ subunits (Figure 3.3.10) (Jensen et al., 2013) (Experiments performed by Dr Martin Mortensen).

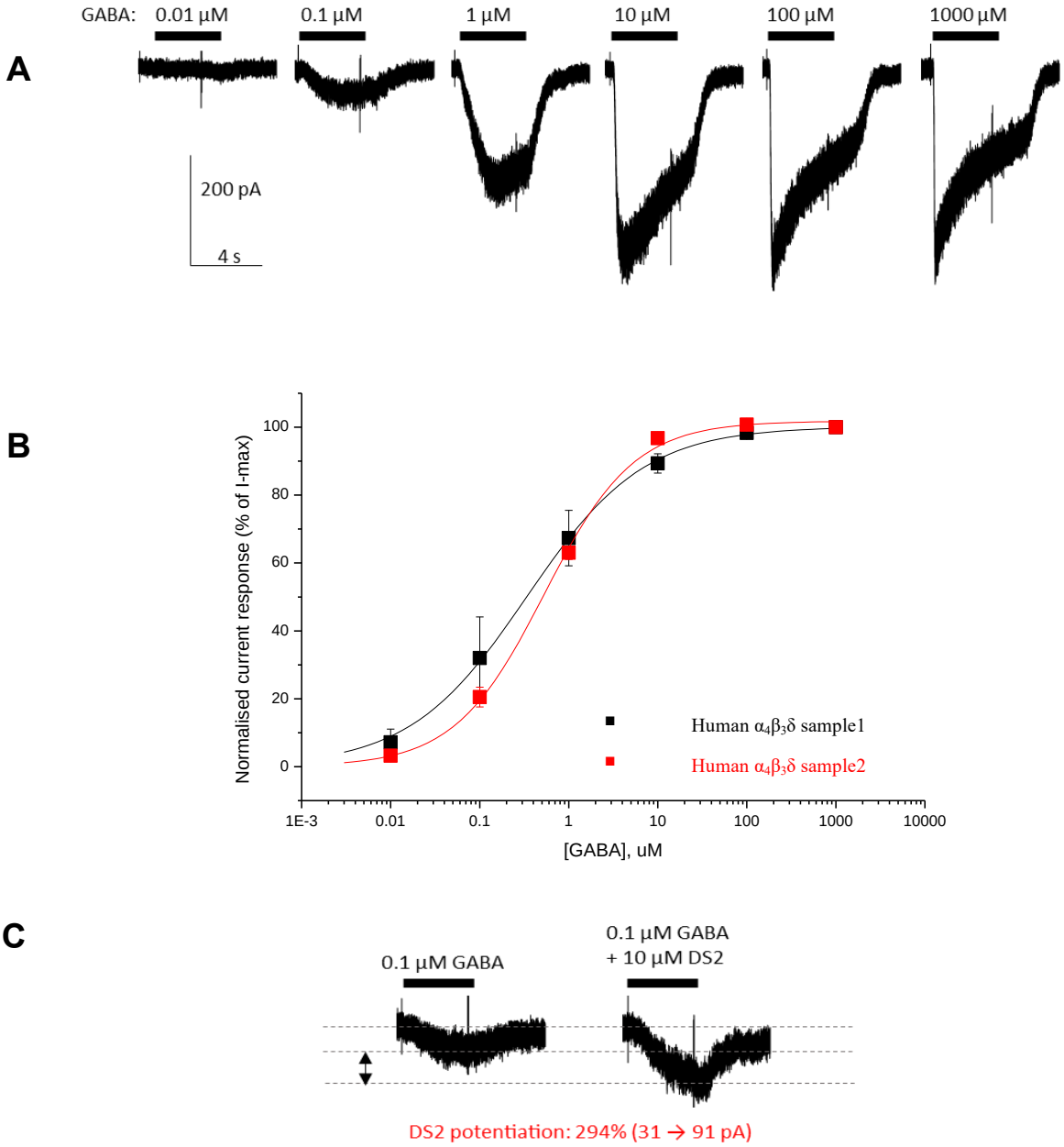

Figure 3.3.10

Whole-cell recordings of $\alpha_4\beta_3\delta$-$GABA_A$ receptors currents in the clone B2' (cells were clamped at -60 mV). (A) Typical recording trace of current responses of the $\alpha_4\beta_3\delta$-$GABA_A$ receptors evoked by various concentrations of GABA. (B) Dose-response curve. (C) Typical recording trace of current response of the $\alpha_4\beta_3\delta$-$GABA_A$ receptors in 0.1 µM GABA with/without 10 µM of a δ selective compound 2 (DS2). The 94 % potentiation of the current by DS2 confirms the presence of the δ subunit.

3.4 Discussion

Compared to transient transfection of proteins of interest, working with a stable cell line is a much more efficient method for the study of the surface receptors. Apart from the relatively low transfection efficiency and the cells being more fragile after transfection, the cost of transient transfection is much higher for long term use than creation of a stable cell line. For its ease of maintenance, limited expression of endogenous membrane receptors, ability of expression and forward trafficking of transfected exogeneous membrane receptors, HEK293 cell line has been extensively used for more than 40 years. In our lab, COS-7 and SF9 cells have also been used for expression of proteins. SF9 cells, grown in suspension culture, have been used for high-level expression of proteins (Schneider and Seifert, 2010). These were used for expression and purification of $GABA_A$ receptor N-terminal extracellular domains in the investigation of how they affect GABAergic synapse formation (Brown et al., 2016). COS-7 cell line derived from the kidney of the African green monkey (*Cercopithecus aethiops*) is another immobilized cell line for the expression of various proteins and the study of their function (Yasumura and Kawakita, 1963). It has been shown that there is no significant difference in transfection of foreign vectors between HEK293 and COS-7 cells (Douglas, Piccirillo and Tabrizian, 2008). However, due to the fact that Cos-7 cells attach to the cell culture dish much more firmly than HEK293 cells, trypsin is required in passaging or transferring such cell lines. For our future

experiments, especially in co-culture with primary cultured neurons, the presence of structurally and functionally intact $GABA_A$ receptors is necessary. Therefore, HEK293 cells were chosen to stably express $\alpha_4\beta_3\delta$-$GABA_A$ receptors.

For the study of cell surface distribution of typical extrasynaptic $GABA_A$ receptors and their contribution to GABAergic synapses in a co-culture model in comparison with the typical synaptic $\alpha_2\beta_2\gamma_2$-$GABA_A$ receptors, the δ subunit was chosen because it was shown to restrict the diffusion of $GABA_A$ receptors to areas outside of the postsynaptic domain in hippocampal neurons in culture (Hannan et al., 2020). Amongst the six α subunits, α_4 subunit is the one most frequently found in association with the δ and $\beta_{2/3}$ subunits (Farrant and Nusser, 2005), jointly forming the extrasynaptic $GABA_A$ receptors to mediate tonic inhibition in the Forebrain, particularly in the Dentate Gyrus cells and the Thalamic Relay neurons (Brickley and Mody, 2012). Although the α_6 subunit is also found to associate with the δ subunit, the expression of the α_6 subunit is the most prominent in the cerebellar granule cells (Nusser, Sieghart and Somogyi, 1998). The importance of α4 subunits has been examined using an α_4-knockout mouse model showing dramatically reduced tonic inhibition in the Dentate Gyrus and Thalamic Relay neurons (Chandra et al., 2006; Liang et al., 2007). In these mice, gaboxadol, a specific agonist to $GABA_A$ receptors which are not modulated by benzodiazepines, lost its effect. Moreover, the expression level of the γ_2 subunit was observed to increase in the Hippocampus and Thalamus, indicating a compensation mechanism in the absence of the α_4-containing $GABA_A$ receptors.

It has been shown that the β_2 subunit is the most abundant β subunit in the brain (Olsen and Sieghart, 2008), however, it appears that the β_3 subunit is more frequently found in the complex with α_4 and δ subunit (Sur et al., 1999).

Thus, it was decided to stably express the extrasynaptic $\alpha_4\beta_3\delta$-$GABA_A$ receptors for the study of GABAergic synapse formation. Development of the HEK293 cell line stably expressing $\alpha_4\beta_3\delta$-$GABA_A$ receptors involved the preparation of plasmids containing the $GABA_A$ receptor subunit cDNAs together with specific antibiotic-resistance genes, followed by transfection, antibiotic selection, and characterization of fast-growing clones. Plasmids with resistance to G418, zeocin and hygromycin were selected to deliver the α_4, β_3 and δ subunits, respectively, for the ease of selection and maintenance.

The fact that the β_3 subunit of the $GABA_A$ receptors can form homopentamers on the cell surface (Lorenz-Guertin and Jacob, 2017) brought a major challenge to the first stage of preparation of this cell line, and antibiotic selection, as the β_3 subunit was found to be expressed at the cell surface in several clones in the absence of the α_4 subunit according to our immunoblotting with specific antibodies (Figure 3.3). Expression of β_3-containing homopentameric receptors was confirmed by electrophysiological recordings that showed no response to GABA but blockade of the spontaneously open channels by picrotoxin with a similar current pattern compared to the literature (Cestari et al., 2000).

Therefore, in the second stage of transfection and antibiotic selection, α_4 subunit cDNA was reintroduced at the same time as the δ cDNA. Finally, after the

14-day antibiotic selection, the expression of all three subunits was detected in one clone using immunoblotting with α_4, β_3 and δ subunits specific antibodies (Figure 3.3.5 – 3.7). Their colocalization at the cell surface was confirmed by immunocytochemistry and confocal imaging with α_4, β_3 and δ subunit-specific antibodies (Figure 3.3.8, 3.9). The cell line was then tested with electrophysiological recordings. The current was recorded in response to GABA ranging from 0.01 μM to 1000 μM and aconcentration-response curve was established to confirm the normal functionality of the $\alpha_4\beta_3\delta$-$GABA_A$ receptors (Figure 3.3.10).

With immunocytochemistry and confocal microscope imaging, the cell surface expression of the subunits was demonstrated (Figure 3.3.8, 3.3.9). With the DIC images showing the HEK293 cell shape, the α_4, β_3 and δ subunits were labelled with respective antibodies which was visualized using AlexaFluoro™ secondary antibodies conjugated to a fluorophore. At the HEK293 cell surface, α_4 subunits were clearly shown to colocalize with the β_3 subunits, which suggests efficient expression and assembly of $\alpha_4\beta_3$ combinations (Figure 3.8). Although an obvious difference can be observed between A2' and B2' clones, the pattern of δ subunit expression was not always colocalized with the β_3 subunits (Figure 3.9). This could be due to the low quality of the δ subunit-specific antibody for both immunoblotting and immunocytochemical experiments. With electrophysiological experiments, the hyperpolarizing current in whole -cell recordings induced by GABA was potentiated ~3 fold in the presence of specific positive allosteric

modulator DS2, which successfully confirmed the expression of the δ subunits in the pentamers (Figure 3.3.10). This together with the fact that δ subunits cannot access the cell surface without assembly with the α and β subunits confirms that the majority of the surface receptors formed were composed of the $\alpha_4\beta_3\delta$ subunits. However, due to the fact that the β_3 subunits are able to be assembled into homopentamers and insert into the plasma membrane, a small proportion of the surface receptors in this stable cell line could be composed of the β_3 homopentamers. As these homopentamers do not have GABA binding sites, and their spontaneous opening seems to be minor in electrophysiology recordings (Figure 3.10), their effect could be minimal in co-culture experiments.

Apart from the use in electrophysiological recordings, immunocytochemistry and confocal imaging experiments, this stable cell line can be used in biochemical experiments. The expression level of $GABA_A$ receptors in these cells can be monitored for investigating the effects of different drugs or proteins on $GABA_A$ receptor assembly and forward trafficking.

Overall, the expression pattern of $\alpha_4\beta_3\delta$-$GABA_A$ receptors on the HEK293 cell surface is consistent with the observed pattern of expression in neuronal cells (Hannan et al., 2020). This indicates that the functional properties of extrasynaptic $\alpha_4\beta_3\delta$-$GABA_A$ receptors stably expressed in HEK293 cells are similar to those expressed in neurons. This was crucial for the use of this cell line in further studies. Thus, the role of $\alpha_4\beta_3\delta$-$GABA_A$ receptors in the formation of synaptic contacts will be investigated in the following chapter.

4. Formation and Functional Maturation of GABAergic Synapses is Regulated by Interactions between γ_2-containing $GABA_A$ Receptors, Neurexin and Neuroligin-2

4.1 Introduction

4.1.1 Formation of GABAergic Synapses is Regulated by Various Cell Adhesion Molecules

GABAergic synapses are the most important inhibitory inter-neuronal junctions that are essential for maintaining the excitation/inhibition balance in the brain. GABAergic synapses are formed by adhesion of the presynaptic terminals at specific locations on the plasma membrane of the postsynaptic neurons. This process is highly organized and regulated, and it involves the recognition of the contact region, recruitment of the pre- and postsynaptic adhesion proteins to these regions, and establishment of a functional synaptic transmission by the release and reception of the neurotransmitter GABA. In the synaptic cleft, there are many adhesion and scaffolding proteins that are important for the formation of synapses and maintenance of their normal function (Südhof, 2017). Although a large number of transsynaptic proteins has been discovered and shown to regulate synapse formation, the question remains as to which proteins are absolutely essential for the initiation of synaptogenesis and thus how the GABAergic synapses are actually generated. How is this process dynamically regulated also remains largely unknown. The complexity of this process brings

the major challenge to the investigators. One of the most widely used methods to study the role of individual synaptic proteins in this process is the co-culture model system in which neurons and non-neuronal HEK293 cells expressing proteins of interest are cultured together (Scheiffele et al., 2000). A protein can be defined as a cell adhesion molecule if it can induce synaptic contact formation when expressed on the surface of non-neuronal cells in this assay. Nevertheless, this model system provides information that is limited to the protein of interest.

4.1.2 The Neurexin-Neuroligin Complex

The Neurexin-Neuroligin complex is one of the most widely studied components of the GABAergic synapses. Neurexin was first discovered as a presynaptic receptor for α-latrotoxin which induces Ca^{2+}-dependent synaptic vesicle release (Ushkaryov, Petrenko, Geppert and Südhof, 1992). Neurexin is expressed by three genes Neurexin 1/2/3 and each neurexin contains a long α-Neurexin and a short β-Neurexin, which share an identical cytosolic domain and a single transmembrane domain (Südhof, 2017). The extracellular domain of α-Neurexin contains six LNS (laminin-neurexin-sex hormone binding globulin) domains with three epidermal growth factor-like (EGF) domains between LNS 1/2, LNS 3/4 and LNS 5/6 (Reissner, Runkel and Missler, 2013). The shorter β-Neurexin contains a single extracellular LNS domain (Reissner, Runkel and Missler, 2013). Neurexins play a crucial role in regulating the functional properties of GABAergic synapses. Deletion of α-Neurexins by constitutive knockout in mice dramatically impairs the action potential-induced Ca^{2+} influx and hence compromises synaptic

transmission due to loss of presynaptic vesicle release (Missler et al., 2003). Notably, the deletion of α-Neurexin is lethal to the mice due to the loss of signal transmission rather than the loss of GABAergic synapse formation (Missler et al., 2003). This indicates that neurexins may not be absolutely necessary for synaptogenesis but are essential for the functionality of synapses. Although the deletion of β-Neurexin is not lethal, the excitatory presynaptic vesicle release is significantly decreased in the presence of α-neurexins (Anderson et al., 2015). In the olfactory bulb, conditional knockout of Neurexin3β impairs the GABAergic synaptic signal transmission by decreasing the presynaptic release probability of GABA (Aoto et al., 2015). However, the role of Neurexin in the formation of GABAergic synapses has not been well studied.

One of the best characterized postsynaptic interactors of Neurexins are Neuroligins of which there are four isoforms: Neuroligin-(1-4) (NL1-4). NL1 is restricted to the excitatory synapses (Song, Ichtchenko, Sudhof and Brose, 1999). NL3 is found in both excitatory and inhibitory synapses (Budreck and Scheiffele, 2007). NL4 is expressed in glycinergic synapses (Hoon et al., 2011). NL2 is expressed in GABAergic, dopaminergic and cholinergic synapses (Varoqueaux, Jamain and Brose, 2004; Dong et al., 2007; Uchigashima, Ohtsuka, Kobayashi and Watanabe, 2016; Takács, Freund and Nyiri, 2013). This is possibly due to the role of GABA as a co-transmitter in the latter two types of synapses. NL2 plays an important role in GABAergic synaptic formation (Varoqueaux, Jamain and Brose, 2004; Dong et al., 2007). Same as the other family members, NL2 is a

type 1 membrane protein that includes a large extracellular domain. Two interaction sites have been recognized on the extracellular domain of NL2: a Neurexin binding site and an interface for Neuroligin dimerization which is not restricted to NL2 but is accessible to other Neuroligins due to the highly conserved sequence of the dimeric interface between extracellular domains of the Neuroligin family (Koehnke et al., 2008). Dimerization is required for clustering of the presynaptic Neurexin monomers and is essential for the functionality of the transsynaptic signaling (Bang and Owczarek, 2013). In the brain, the homodimeric NL2 is predominantly found. Although Neuroligin heterodimers are also detected (Poulopoulos et al., 2012), their functionality is currently unknown. The smaller intracellular domain of NL2 is different from that of other isoforms (Levinson et al., 2010). Different sequences in the intracellular domain of NL1-4 are thought to determine how these proteins interact with different postsynaptic scaffolding proteins which may impact on their localization to either excitatory or inhibitory postsynaptic sites. The intracellular region between amino acids 716 and 782 was shown to be critical for the Gephyrin interaction and the inhibitory clustering of NL2 at inhibitory synapses (Levinson et al., 2010).

NL2 is also critical for the recruitment of the postsynaptic scaffolding proteins Gephyrin and Collybistin. Gephyrin is a 93-kb polypeptide which self-aggregates to form a supermolecular hexagonal complex lattice beneath the postsynaptic membrane (Groeneweg et al., 2018). Gephyrin is tethered to the cell membrane

by binding to Collybistin, a brain-specific guanine nucleotide exchange factor (GEF) (Poulopoulos et al., 2009), and is critical in maintaining the $GABA_A$ receptors synaptic localization and density (Essrich et al., 1998). NL2 was shown to be essential for the submembrane localization of the Gephyrin-Collybistin complex (Poulopoulos et al., 2009).

4.1.3 The Role of $GABA_A$ Receptors in the Formation of GABAergic Synapses

Functional GABAergic synapses can form in co-culture model systems (Brown et al., 2016) and *in vivo* (Poulopoulos et al., 2009) in the absence of Neuroligins. Conversely, formation of the Neurexin-Neuroligin complex can trigger GABAergic synaptogenesis in co-culture model systems in the absence or presence of $GABA_A$ receptors (Craig and Kang, 2007). It has been demonstrated that this complex facilitates the clustering of $GABA_A$ receptors at the postsynaptic sites by interacting with Gephyrin and Collybistin, proteins important for the maintenance and function of GABAergic synapses (Poulopoulos et al., 2009). The knock-out of NL2 in mice showed severely impaired synaptic transmission and postsynaptic GABAergic structures, but not a deficit in synapse formation (Poulopoulos et al., 2009). This suggests that NL2 may be important for the functional maturation of GABAergic synapses but may not be crucial for the initiation of synaptic contacts.

It has been shown that $GABA_A$ receptors alone are able to initiate the formation of GABAergic synapses between GABAergic medium spiny neurons and HEK293 cells expressing these receptors in a co-culture (Fuchs et al., 2013).

The $GABA_A$ receptor subunit N-terminal extracellular domain (ECD) was shown to contribute to the formation of GABAergic synapses (Brown et al., 2014; 2016) possibly by interacting directly with some of the presynaptic proteins including Neurexin (Zhang et al., 2010).

Recently, GARLH4 was described as an auxiliary protein that forms a tripartite complex with NL2 and $GABA_A$ receptors selectively via the γ_2 subunit, which is important for the synaptic localization of $GABA_A$ receptors (Yamasaki et al., 2017, Davenport et al., 2017). This interaction can possibly explain the finding that co-expression of $GABA_A$ receptors and NL2 in HEK293 cells has a synergistic effect in facilitating synapse formation with the medium spiny neurons in the co-culture (Fuchs et al., 2013). However, the underlying molecular mechanisms involved in this process require further investigation.

It is important to note that neurexin-2β was shown to interact directly with the α_1 subunit of the $GABA_A$ receptors *in vitro* and, when applied exogenously to cultured neurons, it decreases the GABAergic postsynaptic currents independently from NL2 (Zhang et al., 2010). Thus, expression of NL2 may act as an “on” switch for synaptic transmission at these initial points of contact by recruiting the postsynaptic scaffolding proteins and stabilizing $GABA_A$ receptors. Therefore, it has been hypothesized that a tripartite interaction between γ_2-containing $GABA_A$ receptors, NL2 and Neurexin may be important for initiation and functional maturation of GABAergic synapses.

4.1.4 Aim and Hypothesis

The aim of this chapter was to investigate the role of Neurexin-$GABA_A$ receptor-NL2 interactions in the formation and functional maturation of GABAergic synapses. To test this hypothesis, a co-culture model system incorporating either a HEK293 stable cell line expressing $\alpha_2\beta_2\gamma_2$-$GABA_A$ receptors or HEK293 stable cell line expressing $\alpha_4\beta_3\delta$-$GABA_A$ receptors, and GABAergic medium spiny neurons was used. I investigated the following specific questions:

- Are extrasynaptic $\alpha_4\beta_3\delta$-$GABA_A$ receptors able to induce GABAergic synapse formation in the co-culture model system in the presence or absence of NL2?
- Are the synapses formed in the presence of NL2 with $\alpha_4\beta_3\delta$- or $\alpha_2\beta_2\gamma_2$-$GABA_A$ receptors functional?
- Which subunits mediate the synergistic effects of $GABA_A$ receptors and NL2 in inducing GABAergic synapses?
- What is the mechanism underlying this synergistic effect?

4.2 Materials and Methods

4.2.1 Cell Culture

Culturing of medium spiny neurons and HEK293 cells and preparation of co-cultures was described in Chapter 2 section 2.1. Immunocytochemistry protocol was described in Chapter 2 section 2.3.

4.2.2 Cell Surface ELISA

Cell surface ELISA was performed using a well-established protocol (Jovanovic et al., 2004). HEK293 cells stably expressing $GABA_A$ receptors were transfected with HA-tagged NL2 cDNA (Poulopoulos et al., 2009) as described in the Chapter 2 section 2.2.2, and incubated in 24-well plates coated with 0.1 mg/ml poly-D-lysine (Sigma Aldrich) in the 37 ℃ 5 % CO_2 humidified incubator for 24 hours. After incubation, the cells were fixed with 4 % paraformaldehyde (PFA)/4 % sucrose in phosphate-buffered saline (PBS) (w/v, pH 7.0) for 10 minutes at room temperature on a rocking plate. When the PFA was aspirated, the samples were washed with PBS first and then Hanks' Balanced Salt Solution (HBSS) (Thermo Fisher). The cells were incubated in 1 % BSA (Sigma Aldrich) in HBSS in order to block any non-specific interactions between the primary antibodies and other proteins. The anti-HA tag primary antibody (ab184643, Abcam) was diluted (1:10,000) in 1 % BSA in HBSS and added to the cells. The cells were incubated overnight at 4 ℃. The next day after the primary antibody was washed with HBSS, the cells were blocked in 1 % BSA in HBSS for 30 minutes at room temperature

on a rocking plate. The secondary antibody conjugated to horseradish peroxide (HRP) (31460, Thermo Fisher) was diluted in 1 % BSA in HBSS (1:2500) and added to the cells which were then incubated at room temperature for 1 hour on a rocking plate. The secondary antibodies were washed multiple times with HBSS. The HRP activity was detected using 0.5 ml Enhanced K-Blue® substrate (tetramethylbenzidine, TMB, Neogen), which was added to each well and transferred into 1.5 ml distilled H_2O after 5-10 minutes. The time of incubation between different wells in the 24-well plate was kept constant. The oxidation of TMB substrate by HRP produced blue color, the absorbance of which was measured at 650 nm by DU800 spectrophotometer (Beckman Coulter).

4.2.3 Calcium-Phosphate Based Transfection

The HEK293 cell cultures were ~ 70 % confluent in T75 tissue culture flasks when they were subjected to calcium phosphate-based transfection (Jordan and Wurm, 2004). For the study of interaction between NL2 and $GABA_A$ receptors, HEK293 cells were transfected with cDNAs of $\alpha_{1/2}$, β_3 and γ_2 subunits with myc-tag (Connolly et al., 1996) for the expression of $GABA_A$ receptors. Equal amount of $NL2^{HA}$ cDNA or control with empty PRK5 plasmid was mixed with the $GABA_A$ receptor cDNAs to make up to 20 µg (5 µg each) in total for transfection. The DNA mixture was mixed with 100 µl 2.5 M $CaCl_2$ and made up to 1 ml with 1/10 Tris-EDTA (TE) buffer and then shaken vigorously for 15 seconds. The mixture was added to 2 × HBS (50 mM HEPES, 280 mM NaCl, 1.1 mM Na_2HPO_4), pH 7.4 solution drop-by-drop slowly and mixed. The precipitates were incubated for

45 minutes at the room temperature, added to the cells drop-by-drop and incubated in the 37 ℃ 5 % CO_2 humidified incubator for 24 hours.

4.2.4 Detection of Presynaptic Activity by Uptake of Synaptotagmin Antibody

This method is based on the immunocytochemistry and confocal imaging of co-cultures of medium spiny neurons and HEK293 cells expressing proteins of interest as described in the Chapter 2, section 2.1.3 and 2.3. Synaptotagmin 1 is a synaptic vesicle associated protein which regulates their fusion with the presynaptic terminal membrane when activated by Ca^{2+} ions to release GABA into the synaptic cleft of GABAergic synapses (Chapman, 2008). During the fusion of synaptic vesicles synaptotagmin 1 is transiently expressed at the surface of active nerve terminals with its intraluminal domain facing the extracellular environment (Fernández-Alfonso, Kwan and Ryan, 2006), before it is endocytosed back into the pool of vesicles. While at the cell surface, synaptotagmin can be labelled with a Cy5-labelled anti-synaptotagmin 1 luminal domain-specific antibody which can be internalized together with synaptotagmin, thus allowing fluorescent labeling of active terminals. We have employed this method to study the activity of GABAergic terminals of medium spiny neurons in co-culture with HEK29 cells stably expressing $GABA_A$ receptors. After platting the HEK293 cells into the medium spiny neuron culture (12 days in vitro) the co-cultures were incubated in the 37 ℃ 5 % CO_2 humidified incubator for 24 hours. The medium was aspirated and replaced with Neurobasal medium containing

1:50 diluted anti-synaptotagmin 1 luminal domain-specific antibody (105311C5, Synaptic Systems) and incubated the 37 ℃ 5 % CO_2 humidified incubator for 30 minutes. The co-cultures were protected from light during the rest of the procedure. The cells were washed with PBS to remove excess antibody and fixed using 4 % PFA solution at room temperature for 10 minutes. The PFA was aspirated and the cells were rinsed with PBS twice briefly followed by three 5-minute washes. The residual aldehyde groups of PFA were then blocked with 0.3 M glycine in PBS for 10 minutes at room temperature, followed by multiple washes with PBS. The cells were permeabilized with 0.5 % Triton-X-100 in PBS for 10 min at room temperature, followed by multiple washes with PBS. The cells were blocked in 1 % BSA in PBS for 30 minutes at room temperature. After the blocking solution was aspirated, Anti-VGAT antibody (131003, Synaptic Systems) was diluted (1:500) in 1 % BSA and added to the co-culture for the detection of all presynaptic GABAergic terminals. The cells were blocked in 1% BSA in PBS for 30 minutes at room temperature. After the blocking solution was aspirated, fluorescently-labelled secondary antibodies (AlexaFluoro™) were diluted in 1 % BSA in PBS (1:750) and added to the cells for 1 hour at room temperature protected from light, followed by brief rinsing twice and multiple washes with PBS. The coverslips were mounted on glass slides with ProLong™ Gold antifade reagent (Invitrogen). The slides were dried at room temperature protected from light and kept at 4 ℃ in boxes. The coverslips were imaged using Zeiss confocal microscope LSM 700 with 63x oil-immerse objective. For single HEK293 cell

imaging, a z-stack with 0.70 µm interval series of images covering the whole HEK293 cell (~ 10 µm) were obtained with 12-bit depth.

4.2.5 Co-immunoprecipitation

4.2.5.1 Rat Brain Extracts

A male adult rat was sacrificed under Schedule 1 methods according to the UK Home Office. The brain was dissected with pre-chilled tools to obtain cerebral hemispheres on ice. The cortex and striatum were dissected and cut into small pieces and transferred into the glass-glass homogenizer (Wheaton) containing 2 ml pre-chilled lysis buffer (20 mM HEPES pH 7.4, 100 mM NaCl, 1 % TritonX-100, 2 mM $CaCl_2$, 1 mM $MgCl_2$). Protease inhibitors (phenylmethylsulfonyl fluorid (PMSF), 10 µM; leupeptin, chymostatin, pepstatin, 5 µg/ml each; Peptide Institute) were added to the lysis buffer before homogenization. The tissue was homogenized with the glass homogenizer up and down for 30 times on ice and then transferred into 15 ml Falcon tube. The homogenized lysates were agitated at 4 ℃ for 2 hours and then centrifuged at 21,000 rpm for 10 min at 4 ℃. The supernatant was collected and the concentration of protein was determined by Bradford assay (Bio-Rad). The input (1 mg total protein) was incubated with 10 µg of $GABA_A$ receptor $\alpha_{1/2}$ subunit-specific IgG (Duggan and Stephenson, 1990) or non-immune control IgG (31243, Invitrogen; from the same species as the specific antibody) for 2 hours at 4 ℃. The mixture was then incubated with 1 % BSA coated Protein-G-Sepharose beads (Generon) for 1 hour at 4 ℃. The mixture was washed with the lysis buffer 3 times quickly and 3 times for 10 min

at 4 ℃. The supernatant was removed and proteins pulled down with beads were denatured with Laemmli SB (62.5 mM Tris, pH 8.0, 2 % SDS, 10 % glycerol, 0.0025% Bromophenol Blue, 100 mM DTT) with 10-minute incubation at 95 ℃, and then separated using SDS/PAGE. The proteins were aligned in a stacking gel (125 mM Tris, pH 6.8, 0.1 % SDS, 5.1 % poly-acrylamide, 0.05 % APS, 0.1 % tetramethyl ethylenediamine (TEMED, Fisher Bioreagents)) and then separated in 8 % separation gel (0.375 M Tris pH 8.8, 0.1 % SDS, 8 % poly-acrylamide, 0.025 % APS and 0.05 % TEMED). Proteins were transferred onto a solid nitrocellulose membrane (10600011, Amersham) in TB (20 mM Tris, 120 mM glycine, pH 8.6, 20 % methanol) at the current of 200 mA for 4 hours. Ponceau-S (A40000279, Thermo Fisher Scientific) was then used to visualize the protein bands on the nitrocellulose membrane. After Ponceau-S was washed with water, the membrane was incubated in blocking solution (1.5 % (w/v) milk, 10% TBS-Tween (50 mM Tris pH 7.6, 200 mM NaCl, 0.05 % Tween-20)) for 30 minutes to block non-specific binding of the primary antibodies. The blocking solution was aspirated and the membrane was incubated with primary antibody specific to NL2 (129203, Synaptic Systems) or Neurexin 1/2/3 (175003, Synaptic Systems) diluted in blocking solution for at least 1.5 hour at room temperature or overnight at 4 ℃ on a GYRO-Rocker rocking plate (Jencons-PLS). After incubation, the primary antibody was removed and the membrane was washed with blocking solution. The goat anti-rabbit secondary antibody conjugated to alkaline phosphate (A16099, Invitrogen) was diluted (1:1000) in blocking solution and

added to the membrane and incubated for 1 hour at room temperature on the rocking plate. The membrane was washed and proteins were visualized with BCIP/NBT substrates reaction as described in Chapter 2 section 2.6.

4.2.5.2 Transfected HEK293 Cells

HEK293 cells were transfected with myc-tagged $GABA_A$ receptor subunits and $NL2^{HA}$ cDNAs as described in section 4.2.4. After 24-hour incubation, the DMEM was aspirated and cells were washed twice with pre-chilled PBS on ice. The HEK293 cells were lysed using lysis buffer (0.5 ml per T75 flask) with Protease inhibitors followed by homogenization, antibody/ Protein-G-Sepharose beads incubation and immunoblotting as described in section 4.2.5.1.

4.2.6 P2 Synaptosome Fractionation

The cortex was obtained using the same method as in section 4.2.4. The tissue was cut and homogenized in pre-chilled 320 mM sucrose (VWR) at 4 ℃ using Potter-Elvehjem tissue grinder with a motor-driven Teflon pestle rotated at 900 rpm using 8/10 up and down strokes. The homogenate was diluted two-fold and centrifuged at 5200 rpm for 2 min at 4 ℃ (Avanti J-20 XPI, Beckman). The supernatant S1 was centrifuged at 11400 rpm for 10 min at 4 ℃ to collect the pellet P2. The P2 pellet was resuspended in 30 ml HEPES buffered incubation medium (140 mM NaCl, 5 mM Na_2HCO_3, 1 mM $MgCl_2 \cdot 6H_2O$, 1.2 mM Na_2HPO_4, 10 mM HEPES, pH 7.4) (HBM) and centrifuged at 5180 rpm for 10 min at 4 ℃, which was repeated once. The pellet was then resuspended in 1 ml lysis buffer

for immunoprecipitation experiment as described in section 4.2.5.1 or lysed with 2 % SDS for immunoblotting analysis.

4.2.7 Super-Resolution Imaging

Super-resolution imaging using a structured illumination microscope (SIM) allows acquisition of images of fluorescently labelled samples with increased resolution which breaks the limit due to the diffraction barrier when using conventional widefield or confocal microscopes. The highly mathematical and computer based super-resolution SIM applies a Moiré fringe pattern which increases the resolution limit by at least two-fold due to the frequency mixing of the fluorophores nearby (Allen, Ross and Davidson, 2014). The raw data was then processed by Fourier analysis which reconstructs the high frequency information in reciprocal space to produce a structured illuminated output (Allen, Ross and Davidson, 2014). The image was processed to correct the chromatic aberration and deconvolved with the point scatter function for statistical analysis.

The HEK293 cells stably expressing $\alpha_2\beta_2\gamma_2$- or $\alpha_4\beta_3\delta$-$GABA_A$ receptors were transfected with $NL2^{HA}$ cDNA and co-cultured with embryonic rat medium spiny neurons. The co-culture coverslips were prepared in the same method as described for immunocytochemistry and confocal imaging in the Chapter 2, section 2.3. The $GABA_A$ receptors were labelled with α_2 (1:500; 224103, Synaptic Systems) or α_4 (1:200; Hörtnagl et al., 2013) subunit-specific antibodies, respectively. The synaptic contacts were labelled with presynaptic active zone marker bassoon-specific antibody (MA1-20689, Thermo Fischer). Images were

acquired using ELYRA PS.1 SIM (Carl Zeiss) at 63x oil lens following chromatic shift correction by recording fluorescent beads. A 4 µm z-stack with 0.110 µm intervals of the samples was acquired to keep the z-range in focus. The images were then processed by Structured Illumination and Channel Alignment function in Zen 2012 Software. The images were deconvolved and analyzed using SVI Huygens Professional software. After deconvolution, the background was eliminated using Coastes Optimized method (Coastes et al., 2004). The Manders coefficients M1, which represents the fraction of the Bassoon-positive pixels that are also positive to the $GABA_A$ receptor α_2 or α_4 subunits signals, and M2, which represents the fraction of $GABA_A$ receptor α_2 or α_4 subunits-positive pixels that are also positive to the bassoon signal were calculated using the software based on the algorithm described by Manders et al. in 1992.

4.3 Results

4.3.1 Formation of GABAergic Synapses can be initiated by $\alpha_2\beta_2\gamma_2$- but not $\alpha_4\beta_3\delta$-$GABA_A$ Receptors *in vitro*

The $\alpha_4\beta_3\delta$-$GABA_A$ receptors are prototypical extrasynaptic receptors with distinct physiological properties and subunit composition to the synaptic $GABA_A$ receptors. They have been shown to mediate tonic inhibition with their perisynaptic localization in neuronal cultures (Hannan et al., 2020). Given that synaptic $GABA_A$ receptors composed of $\alpha_1\beta_2\gamma_2$, $\alpha_2\beta_2\gamma_2$, $\alpha_1\beta_3\gamma_2$ or $\alpha_2\beta_3\gamma_2$ subunits have been demonstrated to facilitate the formation of GABAergic synapses (Brown et al., 2016), we wanted to test if the $\alpha_4\beta_3\delta$-$GABA_A$ receptors can initiate or regulate the formation of GABAergic synapses in the absence of other postsynaptic cell adhesion molecules, such as NL2, under similar experimental conditions as the synaptic receptors.

The $\alpha_4\beta_3\delta$-$GABA_A$ receptor stable cell line characterized in Chapter 3 was used to create a co-culture with the embryonic rat medium spiny neurons in which synapse formation can be studied as described previously (Brown et al., 2014). The $\alpha_4\beta_3\delta$-$GABA_A$ receptor-expressing HEK293 cells were first transfected with GFP cDNA to allow visualization of HEK cells under the confocal microscope and 24 hours later, the cells were transferred to cultures of differentiated embryonic medium spiny neurons (14 DIV) and further incubated for 24 hours in 37 ℃ in the 5 % CO_2 humidified incubator, which is the minimum time required for synaptic contacts to be formed (Brown et al., 2014). The cells were subsequently fixed and

subjected to immunolabeling with primary and fluorescently-labelled secondary antibodies to label the VGAT protein specific for the presynaptic GABAergic terminals. Fluorescent z-stack images of GFP labelled HEK cells which were in the vicinity of at least one or several medium spiny neuron projections were acquired by Zeiss confocal microscope LSM 710 using 63× lens (Figure 4.3.1). The interval between each z-stack was 0.70 µm.

Quantification of the % area of co-localized pixels (as described in section 2.4) that represents contacts between VGAT terminals and HEK293 cells demonstrated no significant difference between the wt-HEK293 cell line and $\alpha_4\beta_3\delta$-$GABA_A$ HEK293 cell line (median = 0.30 %; IQR = 0.04 - 0.46 %; n = 21 cells *vs.* median = 0.36 %; IQR = 0.24 - 0.63 %; n = 18 cells, respectively; from N = 2 independent experiments, $p > 0.05$, Figure 4.3.2).

Quantification of the number of co-localized pixels between VGAT terminals and HEK293 cells also demonstrated no significant difference between wt-HEK293 cell line and $\alpha_4\beta_3\delta$-$GABA_A$ receptor-expressing HEK293 cell line (median = 51; IQR = 20 – 106; n = 21 cells *vs.* median = 38; IQR = 25 – 53; n = 18 cells, respectively; from N = 2 independent experiments, $p > 0.05$, Figure 4.3.2).

These results indicate that $\alpha_4\beta_3\delta$-$GABA_A$ receptors do not promote the formation of inhibitory synapses in this model system, indicating that this activity is specific to synaptic $GABA_A$ receptor subtypes (Brown et al., 2016).

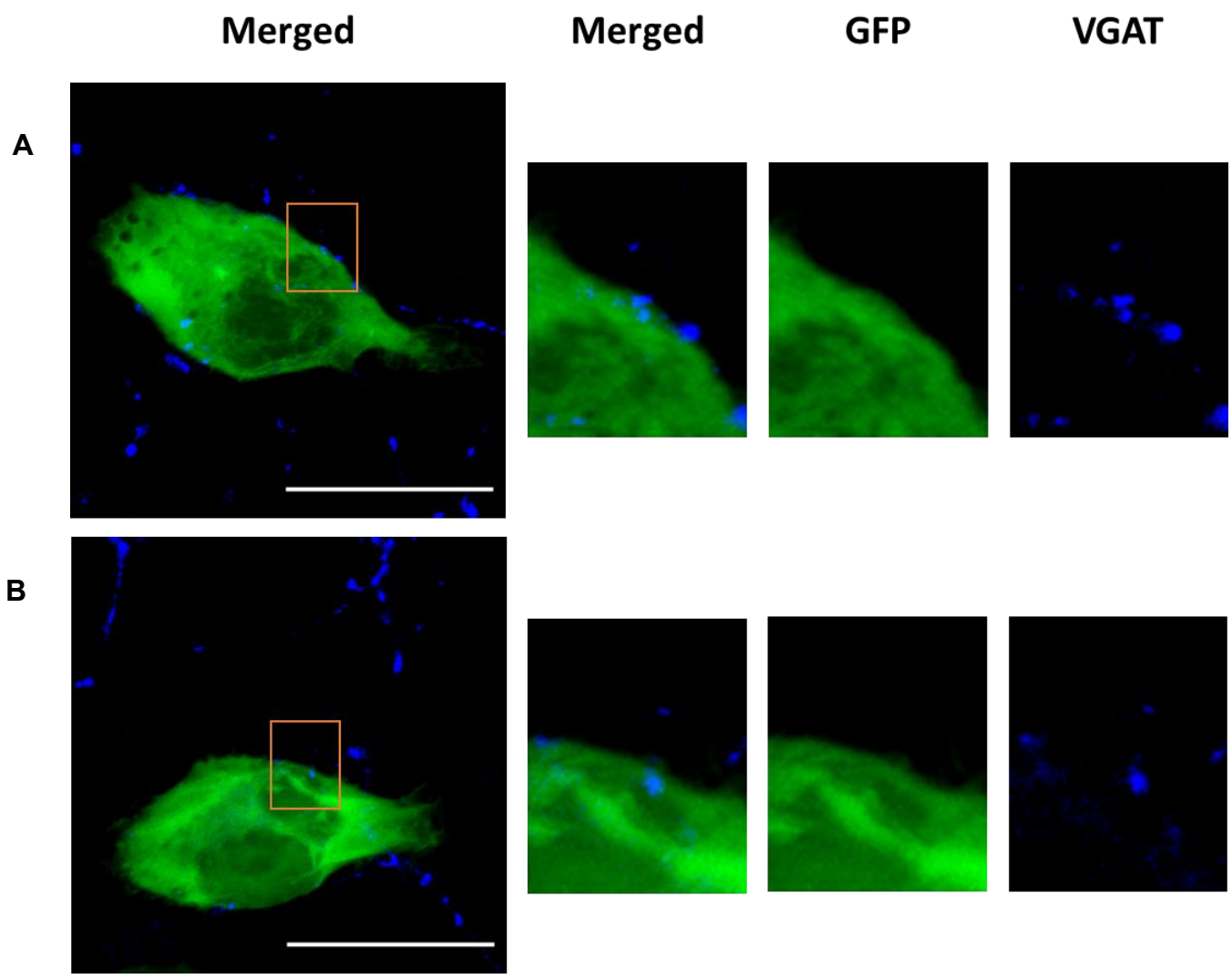

Figure 4.3.1

Synaptic contact formation in co-culture of (A) wt-HEK293 cells; (B) $\alpha_4\beta_3\delta$-$GABA_A$ receptor-expressing HEK293 cells and embryonic medium spiny neurons. HEK293 cell lines expressing GFP were incubated in co-culture with medium spiny neurons for 24 hours. The HEK293 cell body was visualized by GFP (green) and synaptic terminals of medium spiny neurons were labelled with VGAT antibody (blue). Scale bar = 20 μm. Fluorescent imaging was done using Zeiss 700 confocal microscope at 63 × magnification with image size 1024 × 1024. Max intensity projection of the z-stack images was shown. The enlarged images are 10 × zoom in.

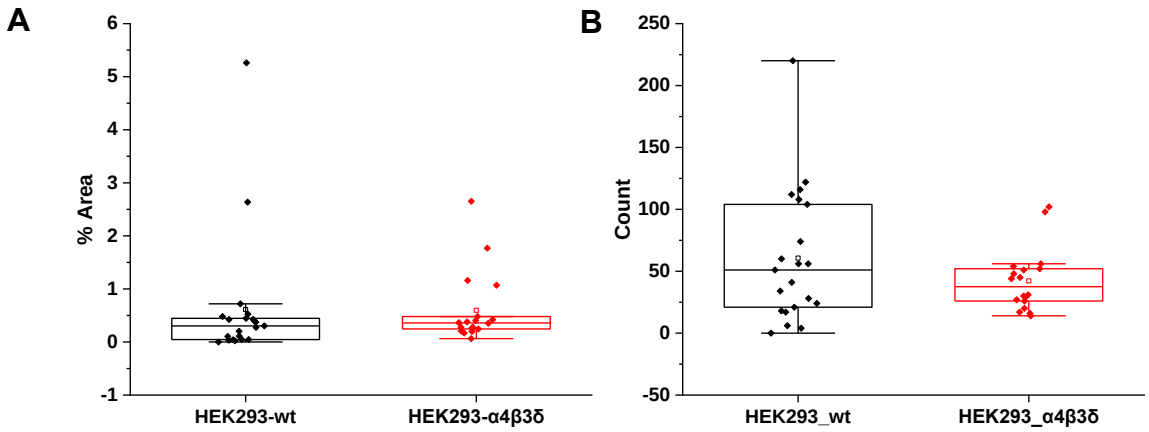

Figure 4.3.2

The $\alpha_4\beta_3\delta$-$GABA_A$ receptors expressed in HEK293 cells do not promote the formation of synaptic contacts with the medium spiny neurons in co-culture. Quantitative analysis of VGAT positive terminals in contact with HEK293 cells imaged using confocal microscopy. (A) The % area of co-localized pixels that represents contacts between VGAT terminals and HEK293 cells. (B) The number of co-localized pixels between VGAT terminals and HEK293 cells. The box and whisker plot show the mean (square dot with no fill), median (horizontal line), standard deviation (whiskers) and the outliers (square dot black fill). Data from n = 21 wt-HEK293 cells and n = 18 $\alpha_4\beta_3\delta$-$GABA_A$ receptor-expressing HEK293 cells; N = 2 independent experiments. Shapiro-Wilk normality test was used to test the normal distribution of the data and Mann-Whitney test was used to analyze statistical significance of the difference. (* $p < 0.05$)

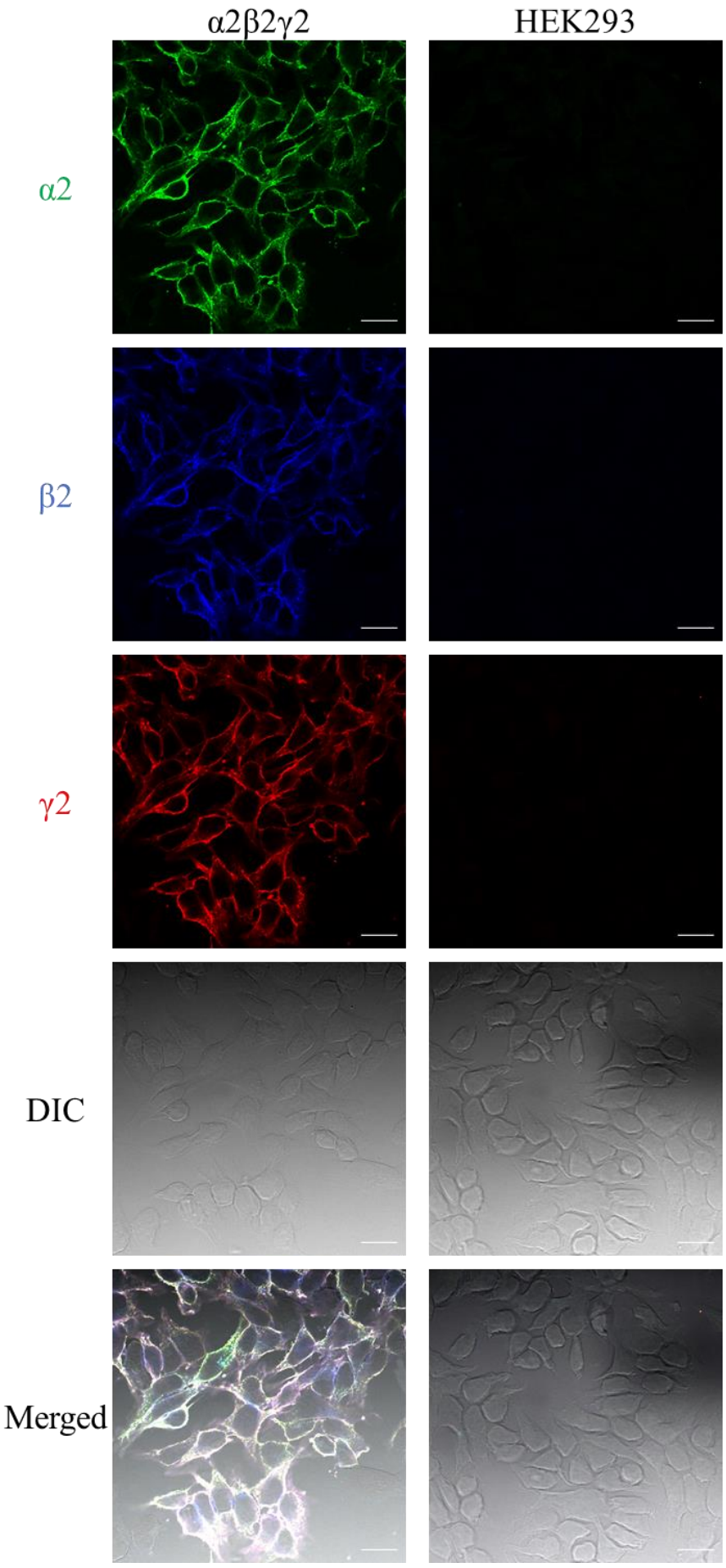

Figure 4.3.3

Fluorescent immunolabelling of α_2, β_2 and γ_2 subunits on the cell surface of $\alpha_2\beta_2\gamma_2$-$GABA_A$ receptor-expressing HEK293 cell line. wt-HEK293 cells were used as negative control. The three subunits were visualized using specific antibodies for: α_2 in 488 (green), β_2 in cy5 (blue) and γ_2 in 555 (red), respectively. The merged channel shows the co-localisation of the three subunits on the cell surface. wt-HEK293 cells show no expression of either α_2, β_2 or γ_2 subunits. Scale bar = 20 µm. The DIC channel shows all the cells in the field. Fluorescent imaging was done using Zeiss 700 confocal microscope at 40 x magnification.

HEK293 cells stably expressing $\alpha_2\beta_2\gamma_2$-$GABA_A$ receptors at the cell surface (Figure 4.3.3) were co-cultured with the medium spiny neurons (14 DIV) under the same conditions as previously described for the $\alpha_4\beta_3\delta$-$GABA_A$ receptor-expressing HEK293 cell line. The contacts were identified and quantified as described above. Figure 4.3.4 shows representative images of synaptic contacts formed in co-culture.

Quantification of the % area of co-localized pixels that represents contacts between VGAT terminals and HEK293 cells revealed a significant increase in synaptic contact formation in the presence of $\alpha_2\beta_2\gamma_2$-$GABA_A$ receptors in comparison with the wt-HEK293 cell line (median = 0.20 %; IQR = 0.16 % - 0.30 %; n = 17 cells *vs.* median = 0.08 %; IQR = 0.03 % - 0.21 %; n = 21 cells, respectively; from N = 2 independent experiments, $p < 0.05$, Figure 4.3.5).

Quantification of the number of contacts also showed that the difference between $\alpha_2\beta_2\gamma_2$-$GABA_A$ receptor-expressing HEK293 cells and wt-HEK293 cells is statistically significant (median = 45; IQR = 25 - 71; n = 17 cells *vs.* median = 24; IQR = 12 - 45; n = 21 cells, respectively; from N = 2 independent experiments, $p < 0.05$, Figure 4.3.5).

Together, the data show that with the expression of $\alpha_4\beta_3\delta$-$GABA_A$ receptors, the median of % area is 1.2 × higher than without expression of $GABA_A$ receptors (wt-HEK293 cells) albeit not significantly different (Figure 4.3.2) while with the expression of $\alpha_2\beta_2\gamma_2$-$GABA_A$ receptors the median of % area is 2.5 × higher than without expression of $GABA_A$ receptors (Figure 4.3.5). For the count of co-

localized pixels, the median is 0.75 × when $\alpha_4\beta_3\delta$-$GABA_A$ receptors are expressed in comparison with the wt-HEK293 cells, but not significantly different (Figure 4.3.2), while the median count for $\alpha_2\beta_2\gamma_2$-$GABA_A$ receptor expressing-HEK293 cells is 1.88 × higher than median obtained with the wt-HEK293 cells in which the difference was statistically significant ($p = 0.03$, Figure 4.3.5). These experiments indicate that the ability to promote synaptic contact formation is specific for the synaptic $GABA_A$ receptor subtypes, such as the $\alpha_2\beta_2\gamma_2$-$GABA_A$ receptors, while the extrasynaptic subtypes do not display this activity. This is in agreement with the previously published findings from our laboratory (Fuchs et al., 2013; Brown et al., 2016).

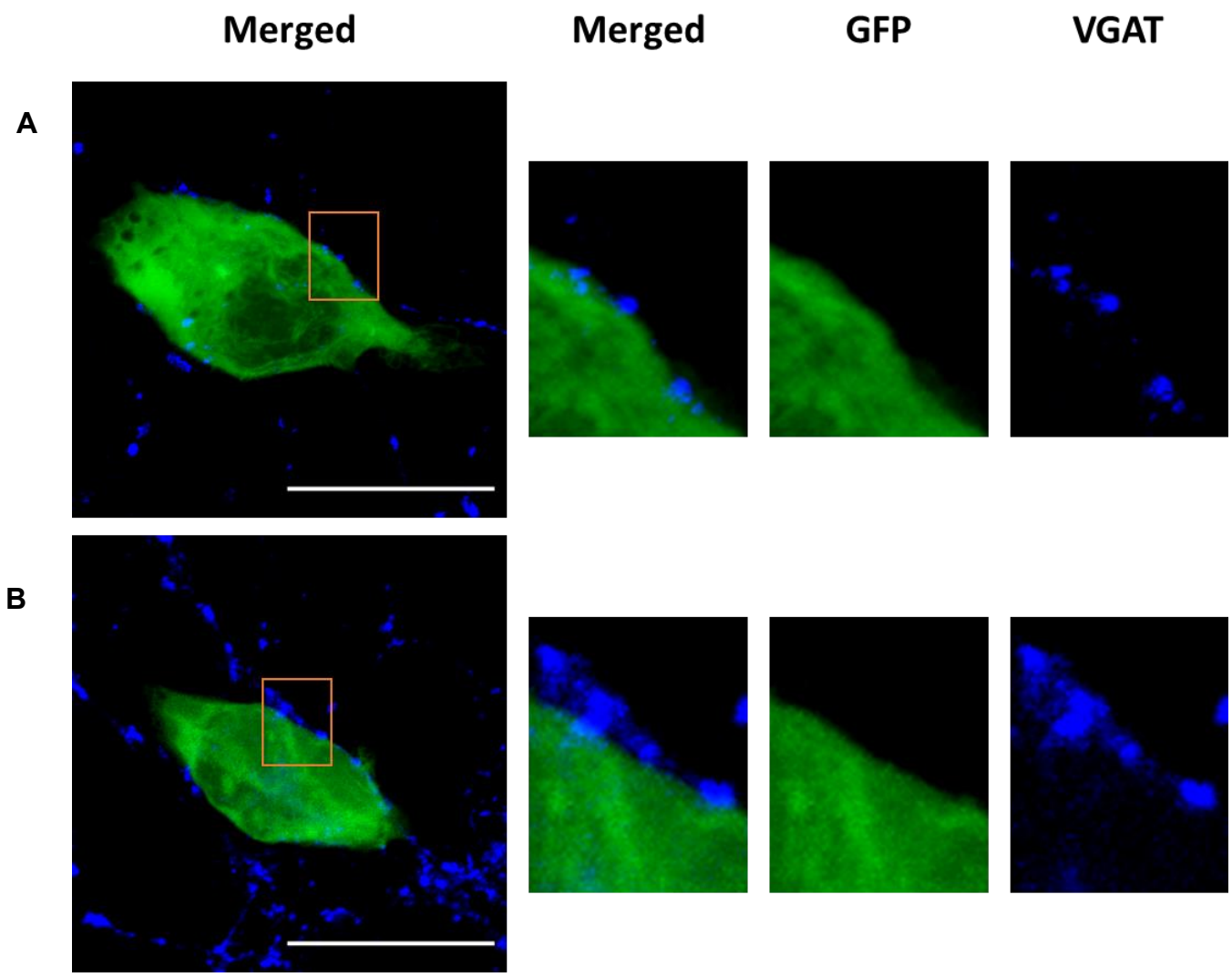

Figure 4.3.4

Synaptic contacts formation in co-culture of (A) wt-HEK293 cells; (B) $\alpha_2\beta_2\gamma_2$-$GABA_A$ receptor-expressing HEK293 cells and embryonic medium spiny neurons. HEK293 cell lines expressing GFP were incubated in co-culture with medium spiny neurons for 24 hours. The whole cell body was visualized by GFP (green) and synaptic terminals of medium spiny neurons were labelled with VGAT antibody (blue). Scale bar = 20 μm. Fluorescent imaging was done using Zeiss 700 confocal microscope at 63 × magnification with image size 1024 × 1024. Max intensity projection of the z-stack images was shown. The enlarged images are 10 × zoom in.

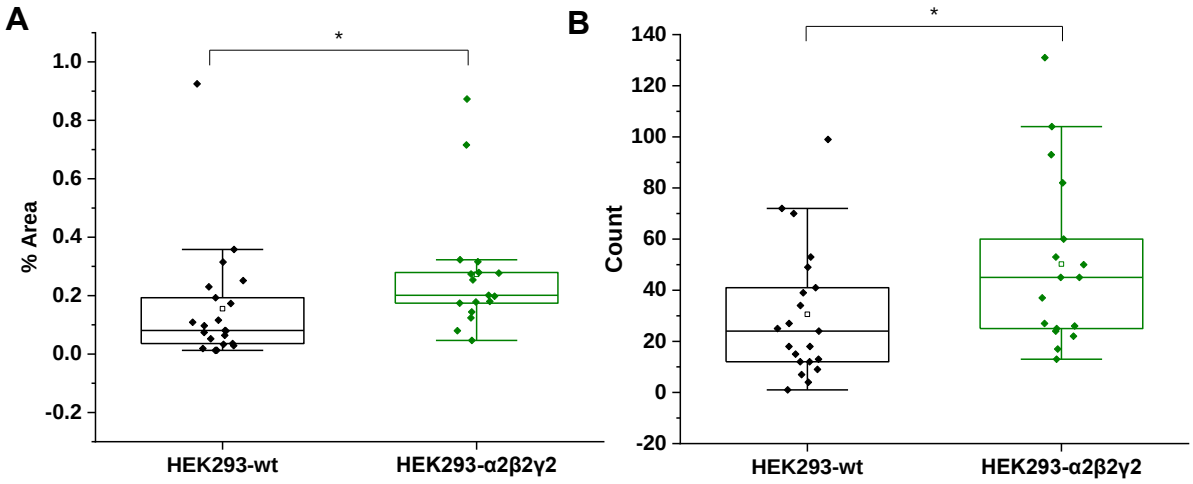

Figure 4.3.5

The $\alpha_2\beta_2\gamma_2$-$GABA_A$ receptors expressed in HEK293 cells can initiate the formation of synaptic contacts between these cells and medium spiny neurons in co-culture. Quantitative analysis of VGAT positive terminals in contact with HEK293 cells imaged using confocal microscopy. (A) The % area of co-localized pixels that represents contacts between VGAT terminals and HEK293 cells. (B) The number of co-localized pixels between VGAT terminals and HEK293 cells. The box and whisker plot show the mean (square dot with no fill), median (horizontal line), standard deviation (whiskers) and the outliers (square dot black fill). Data from n = 21 wt-HEK293 cells and n = 17 $\alpha_2\beta_2\gamma_2$-$GABA_A$ receptor-expressing HEK293 cells; N = 2 independent experiments. Shapiro-Wilk normality test was used to test the normal distribution of the data and Mann-Whitney test was used to analyze the statistical significance of the difference. (* $p < 0.05$)

4.3.2 Initiation of GABAergic Synapses in the presence of $GABA_A$ Receptors and NL2

The synaptogenic effect of NL2 have been well characterized by many groups (for review: Lu, Bromley-Coolidge and Li, 2017). I therefore aimed to characterize the synaptogenic effects of $GABA_A$ receptors in the presence of NL2 given that these proteins are co-localized at the majority of GABAergic synapses in the brain (Varoqueaux, Jamain and Brose, 2004; Dong et al., 2007; Yamasaki et al., 2017). To investigate this question, NL2 cDNA was transfected into wt-, $\alpha_2\beta_2\gamma_2$- or $\alpha_4\beta_3\delta$-$GABA_A$ receptor-expressing HEK293 cell lines and synaptic contact formation was assessed using the same approach as above.

4.3.2.1 Cell Surface Expression of NL2 in the wt-, $\alpha_2\beta_2\gamma_2$- or $\alpha_4\beta_3\delta$-$GABA_A$ Receptor-Expressing HEK293 cell lines

First, I have assessed whether intracellular processing and surface expression of NL2 may vary between the three HEK293 cell lines as this would have an impact on synaptic contact formation. In these experiments, $NL2^{HA}$ cDNA was transfected into the individual cell lines and its surface and total expression quantified using cell surface ELISA with an HA tag-specific antibody. The ELISA results showed no change in either surface or total levels of NL2 expression in the three HEK293 cell lines (Figure 4.3.6).

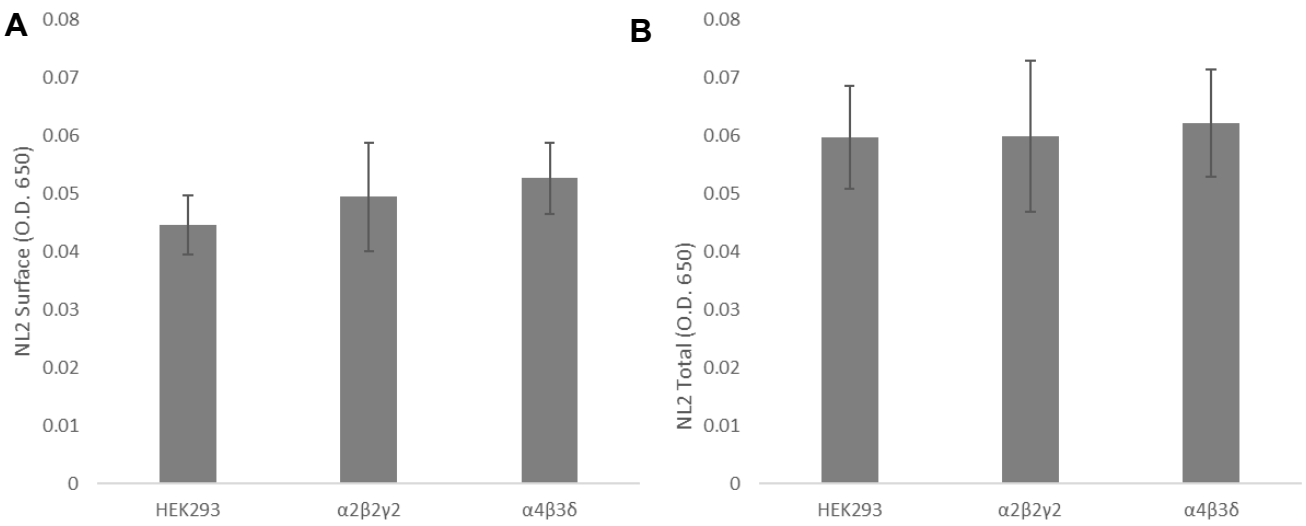

Figure 4.3.6

(A) Cell surface and (B) total expression of NL2 in the wt, $\alpha_2\beta_2\gamma_2$-$GABA_A$ receptor- or $\alpha_4\beta_3\delta$-$GABA_A$ receptor-expressing HEK293 cells. HEK293 cells were transiently transfected with $NL2^{HA}$ cDNA and 24 hours later fixed and incubated with an HA-tag specific antibody followed by an HRP-conjugated secondary antibody. The color substrate absorbance was measured at λ = 650 nm. NL2 surface and total expression showed similar values in all three groups indicating that co-expressed $GABA_A$ receptors do not influence how NL2 is processed in these cells. Data from N = 3 independent experiments. Each experiment was done in triplicates.

4.3.2.2 Synergistic effects of GABAA Receptor and NL2 in Synaptic Contact Formation

To investigate whether and how co-expression of $GABA_A$ receptors and NL2 in HEK293 cells regulates the formation of synaptic contacts, HEK293 cells stably expressing $\alpha_2\beta_2\gamma_2$-$GABA_A$ receptors or $\alpha_4\beta_3\delta$-$GABA_A$ receptors or the wt-HEK293 cells were transfected with GFP and mcherry-tagged NL2 cDNAs and co-cultured with ~E17 rat medium spiny neurons for 24 hours. The cells were fixed and immunolabeled with an VGAT-specific antibody to detect GABAergic terminals in contact with HEK293 cells using confocal microscopy. Synaptic contacts were defined based on signal colocalization between the VGAT and GFP (green and blue channel in Figure 4.3.7) and analyzed using Image J as described in the section 2.4.

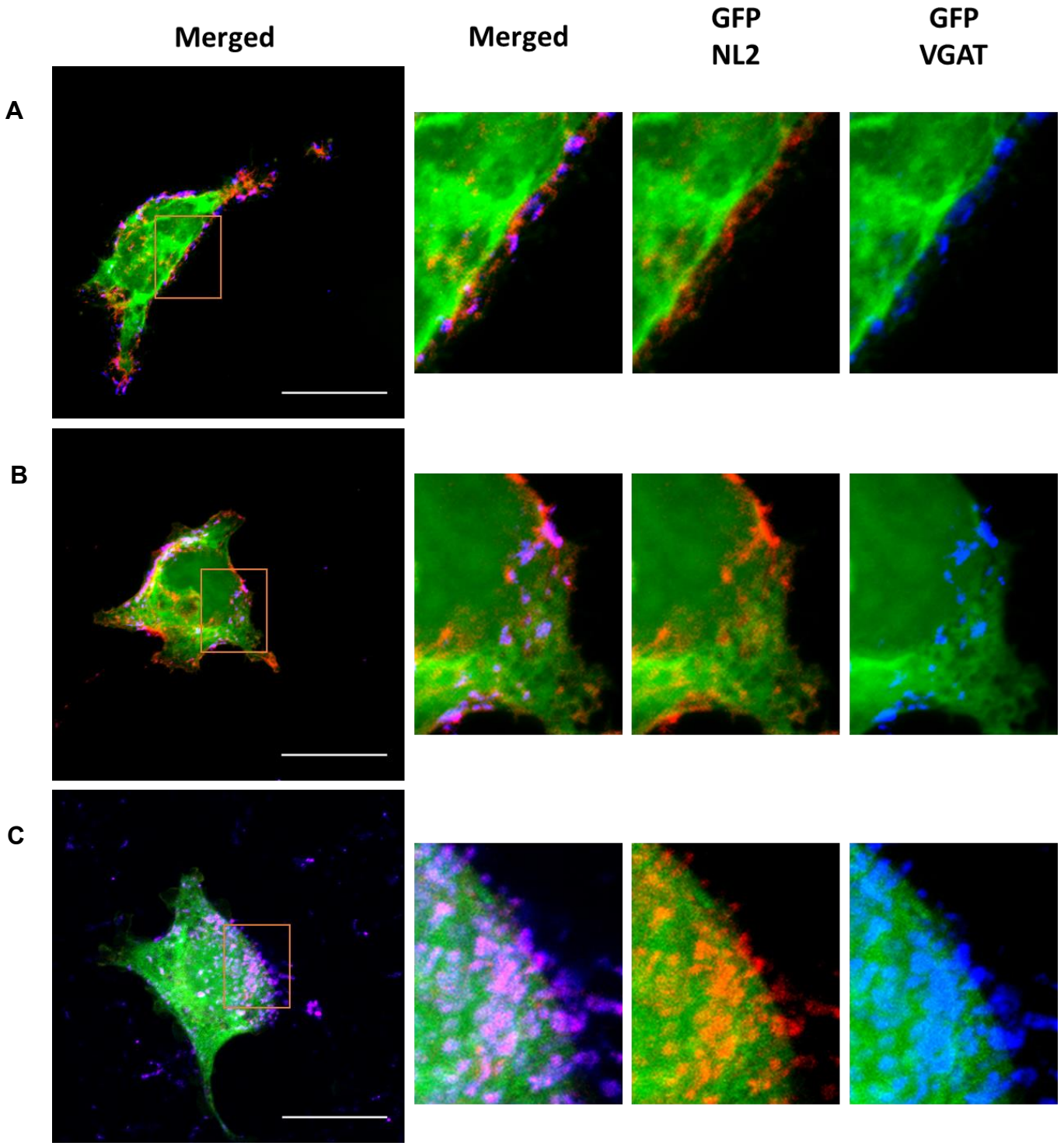

Figure 4.3.7

Synapse formation in co-culture of (A) wt-HEK293, (B) α4β3δ-$GABA_A$ receptor-expressing HEK293 and (C) $\alpha_2\beta_2\gamma_2$-$GABA_A$ receptor-expressing HEK293 cells and embryonic medium spiny neurons. HEK293 cells expressing GFP and NL2 were incubated in co-culture with medium spiny neurons for 24 hours. The whole cell body was visualized by GFP (green); NL2 was tagged with cherry-tag (red); and synaptic terminals of striatal neurons were labeled with VGAT antibody (blue). Scale bar = 20 μm. Fluorescent imaging was done using Zeiss 700 confocal microscope at 63 × magnification with image size 512 × 512. Max intensity projection of the z-stack images was shown. The enlarged images are 10 × zoom in.

Quantitative analysis of colocalization of presynaptic terminals and HEK293 cells was obtained using the method described in section 4.3.1. Furthermore, the data were normalized with the expression level of NL2 by the mean intensity expressed in the form of x 10^4 for the convenience in calculation to take into account variation due to transient transfection of NL2 in HEK293 cells.

Quantification of the % area of co-localized pixels that represents contacts between VGAT terminals and HEK293 cells revealed a significant increase in synapse formation in the presence of $GABA_A$ receptors and NL2 (Figure 4.3.8A). The presence of NL2 significantly increased the synapse formation in all three cell lines as observed previously (Scheiffele et al., 2000; Fuchs et al., 2013). Compared to wt-HEK293 cell line, the presence of $\alpha_4\beta_3\delta$-$GABA_A$ receptors significantly increased the formation of synapses in the presence of NL2 (median = 0.95 %; IQR = 0.52 % - 1.49 %; n = 53 cells *vs.* median = 1.81 %; IQR = 1.25 % - 3.02 %; n = 52 cells, respectively; from N = 4 independent experiments, $p < 0.05$). In the presence of $\alpha_2\beta_2\gamma_2$-$GABA_A$ receptors, the synapse formation was further increased significantly compared with the $\alpha_4\beta_3\delta$-$GABA_A$ receptor-expressing HEK293 (median = 3.28 %; IQR =1.96 % - 4.78 %; n = 52 cells *vs.* median = 1.81 %; IQR = 1.25 % - 3.02 %; n = 52 cells, respectively; from N = 2 independent experiments, $p < 0.05$). The difference between the wt- and $\alpha_2\beta_2\gamma_2$-$GABA_A$ receptor-expressing HEK293 cell lines was also significant ($p < 0.05$).

Quantification of the number of co-localized pixels between VGAT terminals and HEK293 cells demonstrated similar changes in synapse formation in the

presence of NL2 (Figure 4.3.8B). However, no significant difference was observed between wt-HEK293 and $\alpha_4\beta_3\delta$-$GABA_A$ receptor-expressing HEK293 cell lines (median = 51; IQR = 30 - 96; n = 53 cells *vs.* median = 47; IQR = 32 - 84; n = 52 cells, respectively; from N = 4 independent experiments, $p > 0.05$). In the presence of $\alpha_2\beta_2\gamma_2$-$GABA_A$ receptors, synapse formation was significantly increased when compared to that of $\alpha_4\beta_3\delta$-$GABA_A$ receptors (median = 72; IQR = 51 - 125; n = 52 cells *vs.* median = 47; IQR = 32 - 84; n = 52 cells, respectively; from N = 4 independent experiments, $p < 0.05$). The difference between wt- and $\alpha_2\beta_2\gamma_2$-$GABA_A$ receptor-expressing HEK293 cell lines was also significant ($p < 0.05$).

The count analysis showed consistent but more variable effects of $GABA_A$ receptors and NL2 expression on synapse contact formation in comparison with the % area analysis. The reason for this discrepancy could be the change in the morphology and size of HEK293 cells after transfection. We have observed that the wt-HEK293 cells had more uniform shape and size than the $\alpha_2\beta_2\gamma_2$-$GABA_A$ and $\alpha_4\beta_3\delta$-$GABA_A$ expressing cells. When using the % area analysis, as described in Chapter 2 section 2.4, the synaptic contacts were represented by the area they occupy on the surface of HEK293 cells normalized to the total surface area, which reduces the impact of variability in size and shape among the HEK293 cells on synaptic contacts analysis (Brown et al, 2016, 2015). On the contrary, the count analysis involved no consideration of the variation in size and shape among the HEK293 cells and the probability of receiving the larger number

of contacts by default due to the larger cell size and surface area. Therefore, remaining data included in this Chapter were quantified as the % area of HEK293 cell surface occupied by the nerve terminals forming the synaptic contacts.

Together, these results indicate that $GABA_A$ receptors and NL2 cooperate during the process of synapse formation. This was detected for both synaptic and extrasynaptic $GABA_A$ receptors, although the effects of synaptic $GABA_A$ receptors were significantly stronger. Whether these effects require active signaling through $GABA_A$ receptors or are mediated by direct protein-protein interactions between $GABA_A$ receptors and NL2 will be investigated further in this chapter.

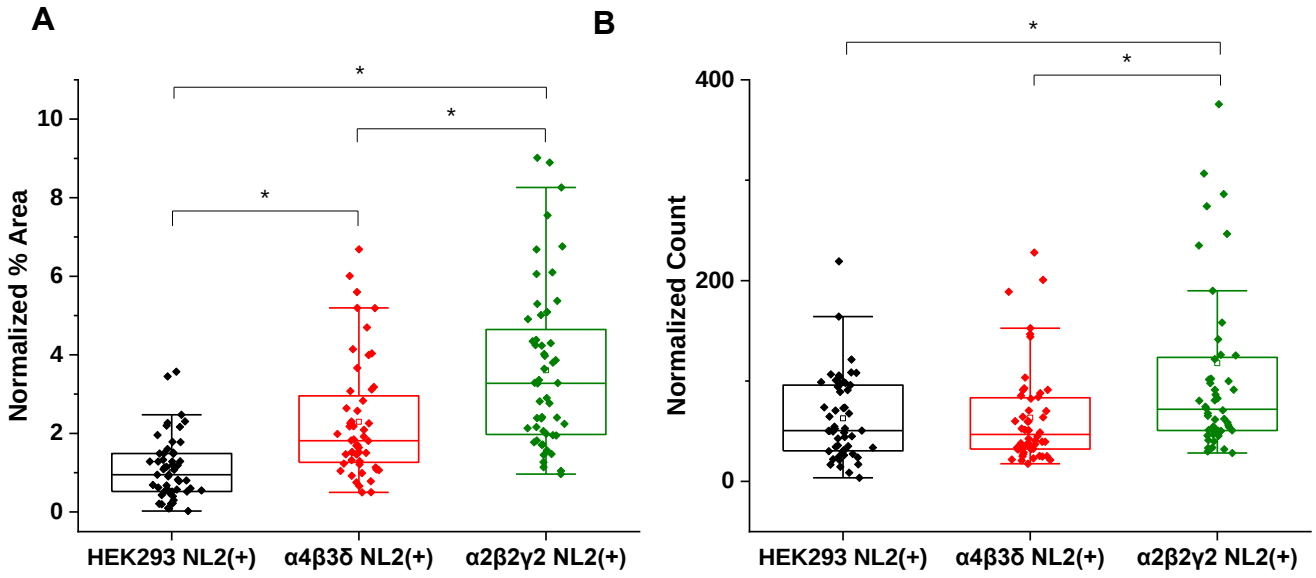

Figure 4.3.8

Quantitative analysis of HEK293 (wt, $\alpha_4\beta_3\delta$ and $\alpha_2\beta_2\gamma_2$) cell in contact with VGAT terminals in the presence of NL2. The % area and Count was normalized with expression level of NL2. (A) Normalized % area of colocalization. The synapse formation was significantly higher in the presence of NL2 with $\alpha_4\beta_3\delta$-$GABA_A$ receptors than in wt-HEK293 cells ($p = 0.00003$). The $\alpha_2\beta_2\gamma_2$-$GABA_A$ receptors promoted significantly higher synapse formation than $\alpha_4\beta_3\delta$-$GABA_A$ receptors ($p = 0.003$). (B) Normalized count of colocalization. The synapse formation was significantly higher in the presence of NL2 in $\alpha_2\beta_2\gamma_2$-HEK293 cell line than in $\alpha_4\beta_3\delta$-HEK293 ($p = 0.002$) cell line. The box and whisker plot shows the mean (square dot with no fill), median (horizontal line), standard deviation of the mean (whiskers) and the outliers (square dot black fill), with filled dots representing individual data. Data from wt-HEK293 cells (n = 53, from N = 4 independent experiments), $\alpha_4\beta_3\delta$-$GABA_A$ receptor-expressing HEK293 cells (n = 52, from N = 4 independent experiments) and $\alpha_2\beta_2\gamma_2$-$GABA_A$ receptor-expressing HEK293 cells (n = 52, from N = 4 independent experiments). Shapiro-Wilk normality test was used to test the normal distribution of the data and Kruskal Wallis ANOVA followed by Dunn's test was used to analyze the statistical significance of the difference. (* $p < 0.05$)

4.3.2.3 Synergistic Effects of $GABA_A$ Receptors with NL2 Depend on the Subunit Composition but not Activity of $GABA_A$ Receptors

Given a clear difference between the synaptic and extrasynaptic $GABA_A$ receptors in inducing synapse formation in the presence of NL2, my next aim was to define which subunits of $GABA_A$ receptors mediate these effects. In these experiments, I have employed a stable cell line expressing the β_3 subunit (B2 clone) initially described in the Chapter 3, section 3.3.3. These cells were transiently transfected with α_2, α_4, γ_2 or δ subunits together with NL2 to produce the following receptor subtypes: $\alpha_2\beta_3\delta$, $\alpha_2\beta_3\gamma_2$, $\alpha_4\beta_3\delta$ or $\alpha_4\beta_3\gamma_2$ (Figure 4.3.9). The cells were co-cultured with the medium spiny neurons for 24 h, fixed and immunolabelled with a Bassoon-specific antibody and VGAT-specific antibody to detect GABAergic terminals forming contacts with HEK293 cells using confocal microscopy. The immunolabeling of Bassoon provides visualization of the presynaptic active zone in GABAergic terminals while immunolabeling of VGAT reveals the intraterminal small synaptic vesicle clusters (Fernández-Alfonso, Kwan and Ryan, 2006). NL2 was labelled with cherry-tag. Synaptic contacts were defined based on signal colocalization between the Bassoon and NL2 (cyan and red channel in Figure 4.3.9) and analyzed using Image J. The γ_2 subunit was visualized using γ_2-specific antibody (Mohler et al., 1995) and the δ subunit was tagged with GFP-tag (Hannan et al., 2020). The presynaptic marker VGAT was also imaged. The HEK293 cells expressing heteropentameric $GABA_A$ receptors were confirmed with the expression of γ_2 or δ subunit on the surface (Figure

4.3.10) as these two subunits can only be inserted into the plasma membrane when co-assembled together with the α and β subunits.

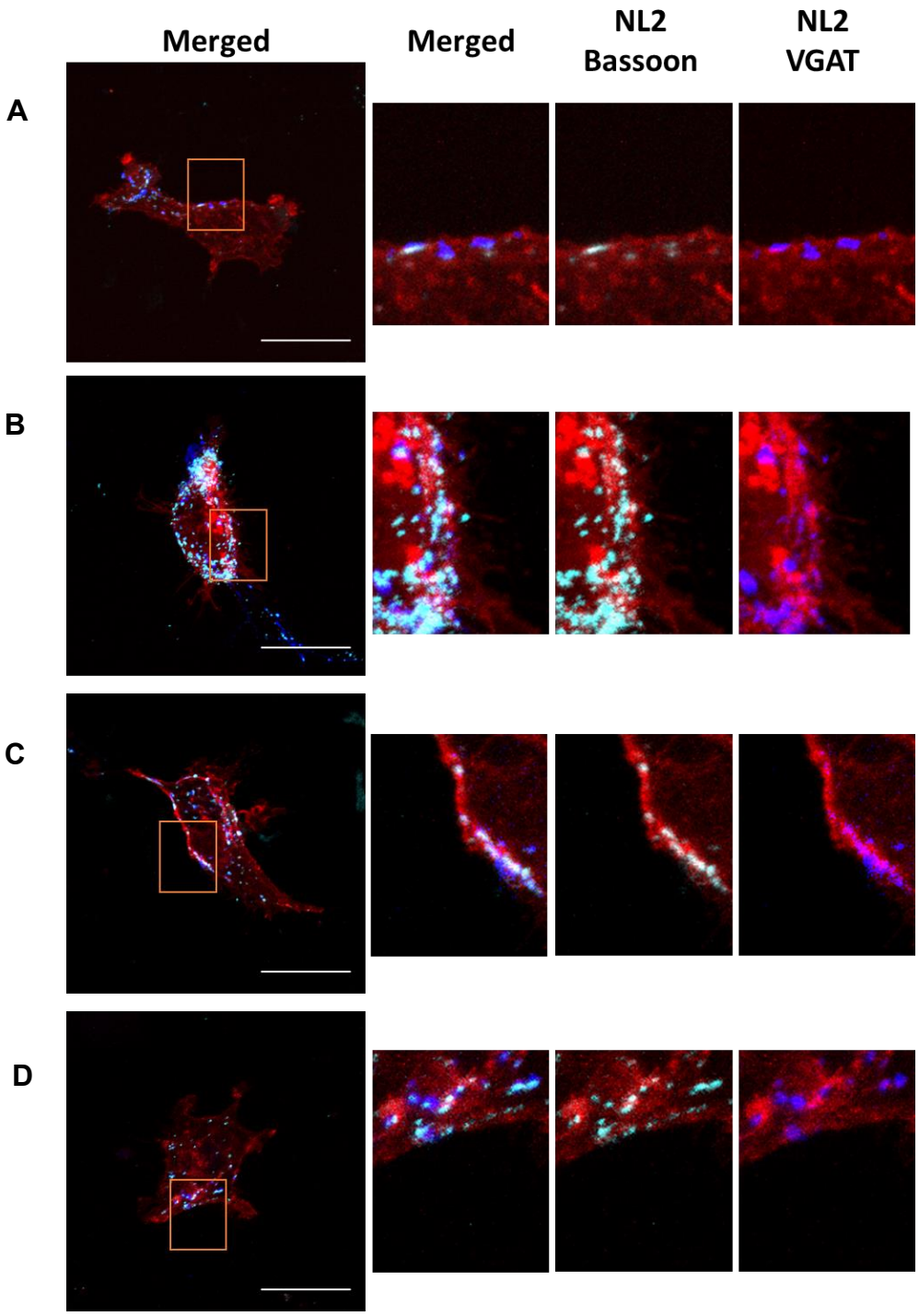

Figure 4.3.9

Synaptic contact formation in co-culture of HEK293 cells and embryonic medium spiny neurons. HEK293 cells expressing (A) $\alpha_2\beta_3\delta$-, (B) $\alpha_2\beta_3\gamma_2$-, (C) $\alpha_4\beta_3\delta$- and (D) $\alpha_4\beta_3\gamma_2$-$GABA_A$ receptors and NL2 were incubated in co-culture with medium spiny neurons for 24 hours. NL2 was tagged with cherry-tag (red); GABAergic terminals were labelled with VGAT antibody (blue) and Bassoon antibody (cyan). Scale bar = 20 μm. Fluorescent imaging was done using Zeiss 700 confocal microscope at 63 × magnification with image size 1024 × 1024. Max intensity projection of the z-stack images was shown. The enlarged images are 10 × zoom in.

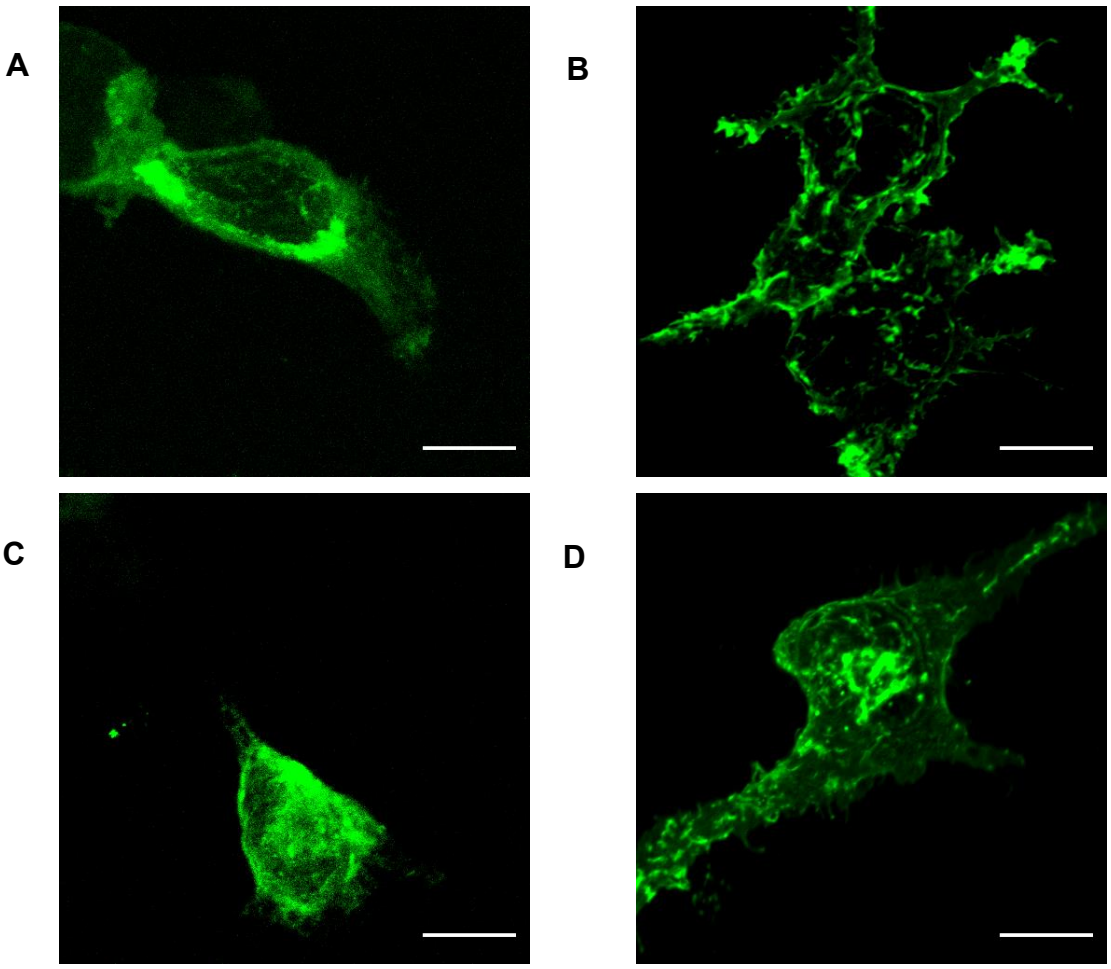

Figure 4.3.10

Surface expression of $GABA_A$ receptor δ or γ_2 subunits in HEK293 cells expressing NL2 and (A) $\alpha_2\beta_3\delta$-, (B) $\alpha_2\beta_3\gamma_2$-, (C) $\alpha_4\beta_3\delta$- and (D) $\alpha_4\beta_3\gamma_2$-$GABA_A$ receptors in co-culture with embryonic medium spiny neurons. Note that the fluorescent labelling of δ and γ_2 subunits is not directly comparable because the former was visualized with the GFP tag while the latter was visualized using specific antibody. Fluorescent imaging was done using Zeiss 700 confocal microscope at 63 × magnification with image size 1024 ×1024. Max intensity projection of the z-stack images was shown.

Quantification of the % area of co-localized pixels that represents contacts between presynaptic Bassoon and postsynaptic NL2 on HEK293 cell surface demonstrated that the level of synapse formation was significantly higher with $\alpha_2\beta_3\gamma_2$ combination (median = 1.22 %; IQR = 0.54 % – 1.96 %; n = 45) than $\alpha_2\beta_3\delta$ (median = 0.62 %; IQR = 0.17 % – 1.19 %; n = 43), $\alpha_4\beta_3\delta$ (median = 0.69 %; IQR = 0.34 % – 1.01 %; n = 43) or $\alpha_4\beta_3\gamma_2$ (median = 0.78 %; IQR = 0.36 % – 1.20 %; n = 43) (from N = 3 independent experiments, $p < 0.05$; Figure 4.3.11). No significant difference was observed with the other subunit combinations.

These data indicate that $GABA_A$ receptor α_2 and γ_2 subunits are important for the further induction of synaptic contact formation in the presence of NL2

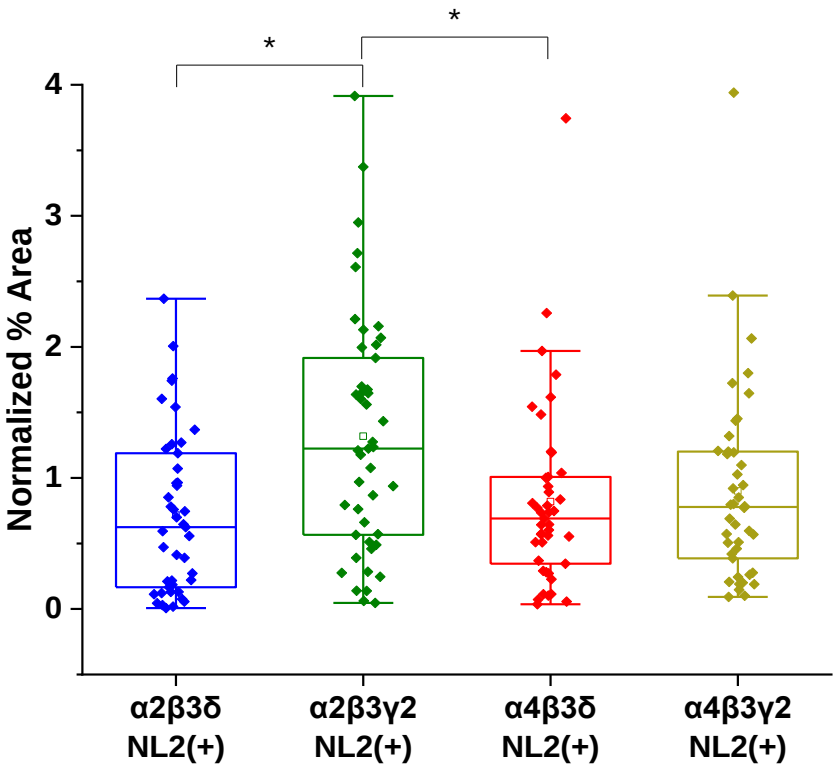

Figure 4.3.11

Quantitative analysis of HEK293 ($\alpha_2\beta_3\delta$, $\alpha_2\beta_3\gamma_2$, $\alpha_4\beta_3\delta$ and $\alpha_4\beta_3\gamma_2$) cell area in contact with striatal terminal bassoon in the presence of NL2. The % area and Count were normalized with expression level of NL2. (A) Normalized % area of colocalization. The synapse formation was the highest in the presence of $\alpha_2\beta_3\gamma_2$-$GABA_A$ receptors. The difference was statistically significant ($\alpha_2\beta_3\delta$ $p = 0.003$; $\alpha_4\beta_3\delta$ $p = 0.03$), except for comparing with $\alpha_4\beta_3\gamma_2$-$GABA_A$ receptors. (B) Normalized Count of colocalization. The synapse formation was significantly higher in the presence of $\alpha_2\beta_3\gamma_2$-$GABA_A$ receptors than $\alpha_2\beta_3\delta$-$GABA_A$ receptors ($p = 0.01$). The box and whisker plot shows the mean (square dot with no fill), median (horizontal line), standard deviation of the mean (whiskers) and the outliers (square dot black fill), with filled dots representing individual data. Data from N = 3 independent experiments. Shapiro-Wilk normality test was used to test the normal distribution of the data and Kruskal Wallis ANOVA followed by Dunn's test was used to analyze the statistical significance of the difference. (* $p < 0.05$)

4.3.2.4 Synergistic Effects of $GABA_A$ Receptors and NL2 do not Require $GABA_A$ Receptor Activation by GABA or Potentiation by a Positive Allosteric Modulator Diazepam

We next examined if the $GABA_A$ receptor activity affects these observed synergistic effects between $GABA_A$ receptors and NL2 in synapse formation. HEK293 cells stably expressing $\alpha_2\beta_2\gamma_2$- or $\alpha_4\beta_3\delta$-$GABA_A$ receptors or the wt-HEK293 cells were transfected with $NL2^{cherry}$ cDNA. In the co-culture system, bicuculline (BIC, 25 μM), a $GABA_A$ receptor antagonist, or DMSO as control, was applied 30 minutes after the HEK293 cells were plated into the medium spiny neuronal cultures and incubated for 24 h (Figure 4.3.12).

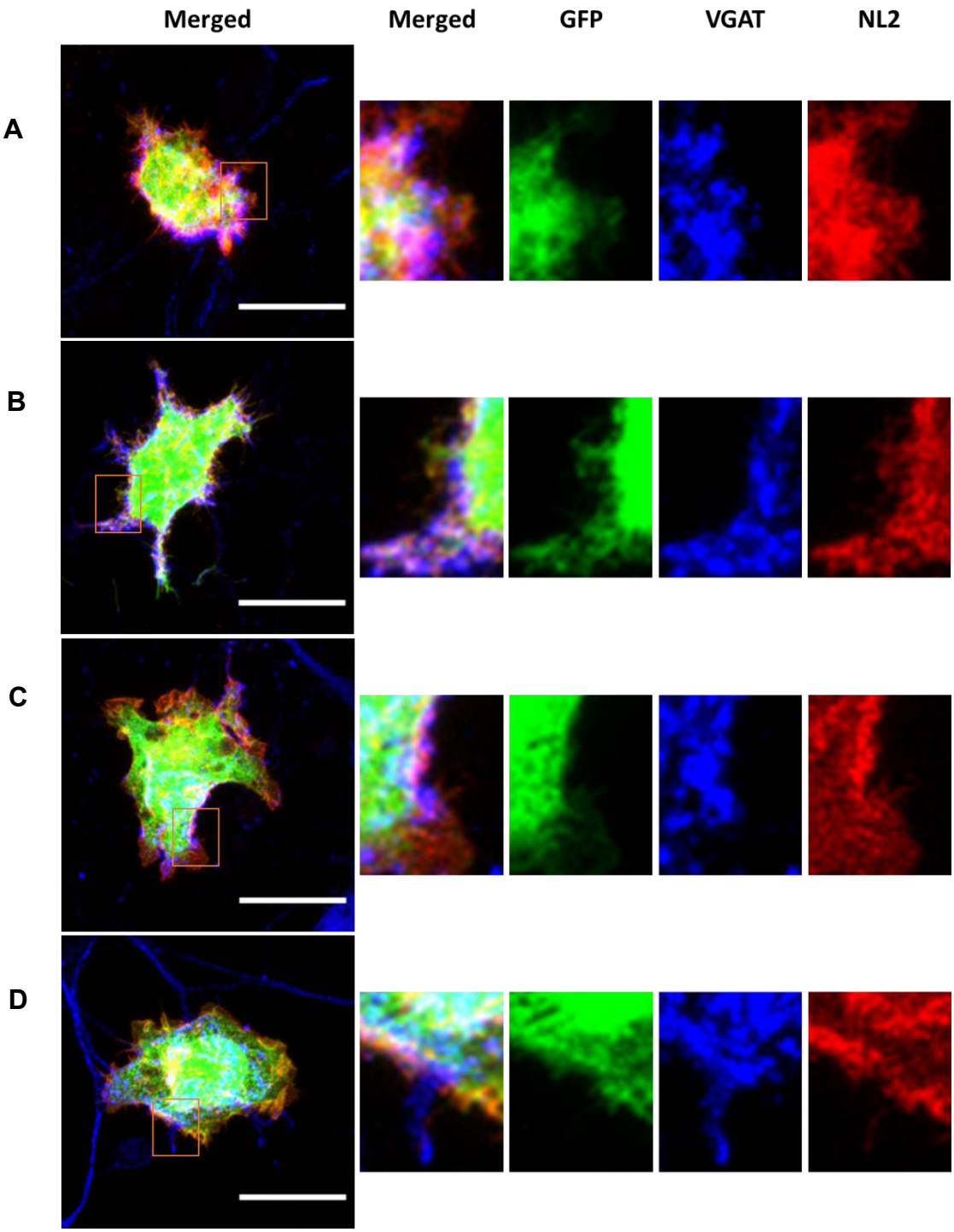

Figure 4.3.12

Synaptic contact formation in co-culture of HEK293 cells and embryonic medium spiny neurons in the presence of DMSO control or bicuculline (25 μM). HEK293 cell body was visualized with GFP expression (green) and the presynaptic terminals were visualized with VGAT-specific antibody (blue). NL2 was tagged with cherry-tag (red) (A) wt-HEK293 cells expressing NL2 in co-culture treated with bicuculline; (B) wt-HEK293 cells expressing NL2 in co-culture treated with DMSO; (C) $\alpha_2\beta_2\gamma_2$-$GABA_A$ receptor-and NL2-expressing HEK293 cells in co-culture treated with bicuculline; (D) $\alpha_2\beta_2\gamma_2$-$GABA_A$ receptor and NL2-expressing HEK293 cells in co-culture treated with DMSO. Scale bar = 20 μm. Fluorescent imaging was done using Zeiss 700 confocal microscope at 63 × magnification with image size 512 ×512. Max intensity projection of the z-stack images was shown. The enlarged images are 10 × zoom in.

Quantitative analysis of colocalization of presynaptic terminals and HEK293 cell body was obtained using the same method described in section 4.3.1. Furthermore, the data were normalized with the expression level of NL2 by the mean intensity at x 10^4.

Quantification of the % area of co-localized pixels of VGAT and GFP that represents contacts between the presynaptic terminals and HEK293 cells showed significant increase in the presence of $\alpha_2\beta_2\gamma_2$-$GABA_A$ receptors irrespective of whether the cultures were incubated with DMSO or bicuculline (Figure 4.3.13). In the case of the wt-HEK293/NL2 cells in co-culture, the % area values for DMSO-treated cultures were median = 1.68 %; IQR = 0.54 % – 2.57 %; n = 20, while for the bicuculline-treated cultures median = 1.11 %; IQR = 0.43 % – 2.00 %; n = 21 (from N = 2 independent experiments, $p > 0.05$). For the $\alpha_2\beta_2\gamma_2$-$GABA_A$ receptor/NL2-expressing HEK293 cells no significant difference was observed between DMSO and bicuculine treatments (median = 4.21 %; IQR = 2.00 % – 7.11 %; n = 20 *vs.* median = 2.28 %; IQR = 1.34 % – 4.22 %; n = 20, respectively; from N = 2 independent experiments, $p > 0.05$).

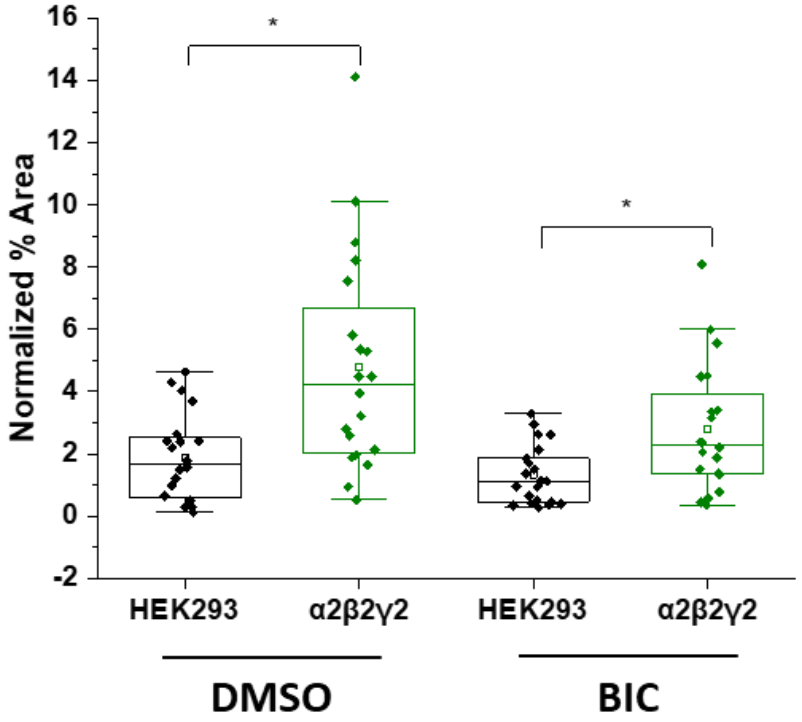

Figure 4.3.13

No significant difference was observed with DMSO or bicuculline treatment in quantitative analysis of the wt/NL2 or $\alpha_2\beta_2\gamma_2$-$GABA_A$ receptor/NL2-expressing HEK293 cells forming contacts with VGAT terminals. The % area and count were normalized with the expression level of NL2. The box and whisker plot shows the mean (square dot with no fill), median (horizontal line), standard deviation of the mean (whiskers) and the outliers (square dot black fill). Data from n = 20 wt/NL2, n = 20 $\alpha_2\beta_2\gamma_2$-$GABA_A$ receptor/NL2-expressing HEK293 cells treated with DMSO, and n = 21 wt/NL2, n = 20 $\alpha_2\beta_2\gamma_2$-$GABA_A$ receptor/NL2-expressing HEK293 cells treated with Bicuculline; N = 2 independent experiments. Shapiro-Wilk normality test was used to test the normal distribution of the data and Kruskal Wallis ANOVA followed by Dunn's test was used to analyze the statistical significance of the difference. (* $p < 0.05$)

For comparison, the extrasynaptic $\alpha_4\beta_3\delta$-$GABA_A$ receptor/NL2-expressing HEK293 cells were also co-cultured with the medium spiny neurons and incubated in the presence of DMSO control or bicuculline for 24 hours. No change in the pattern of synaptic contact formation was observed in the presence of bicuculline (Figure 4.3.14).

Quantification of the % area of co-localized pixels of VGAT and GFP that represents contacts between the presynaptic terminals and HEK293 cells showed significant increase in the presence of $\alpha_4\beta_3\delta$-$GABA_A$ receptors (Figure 4.3.15). However, no difference in the % area was observed between DMSO and Bicuculline-treated co-cultures with either the wt/NL2- or $\alpha_4\beta_3\delta$-$GABA_A$ receptor/NL2-expressing HEK293 cells. For DMSO-treated wt/NL2-HEK293 cells, the median % area was 1.05 % (IQR = 0.52 % – 1.72 %; n = 20), while for the Bicuculline-treated wt/NL2-HEK293 cells the median % area was 0.61 % (IQR = 0.27 % – 1.27 %; n = 20; from N = 2 independent experiments, $p > 0.05$). For DMSO-treated $\alpha_4\beta_3\delta$-$GABA_A$ receptor/NL2-expressing HEK293 cells, the median % area = 2.89 % (IQR = 1.77 % – 4.99 %; n = 20), while for the Bicuculline-treated $\alpha_4\beta_3\delta$-$GABA_A$ receptor/NL2-expressing HEK293 cells, the median % area was 3.23 % (IQR = 1.36 % – 4.79 %; n = 20; from N = 2 independent experiments, $p > 0.05$).

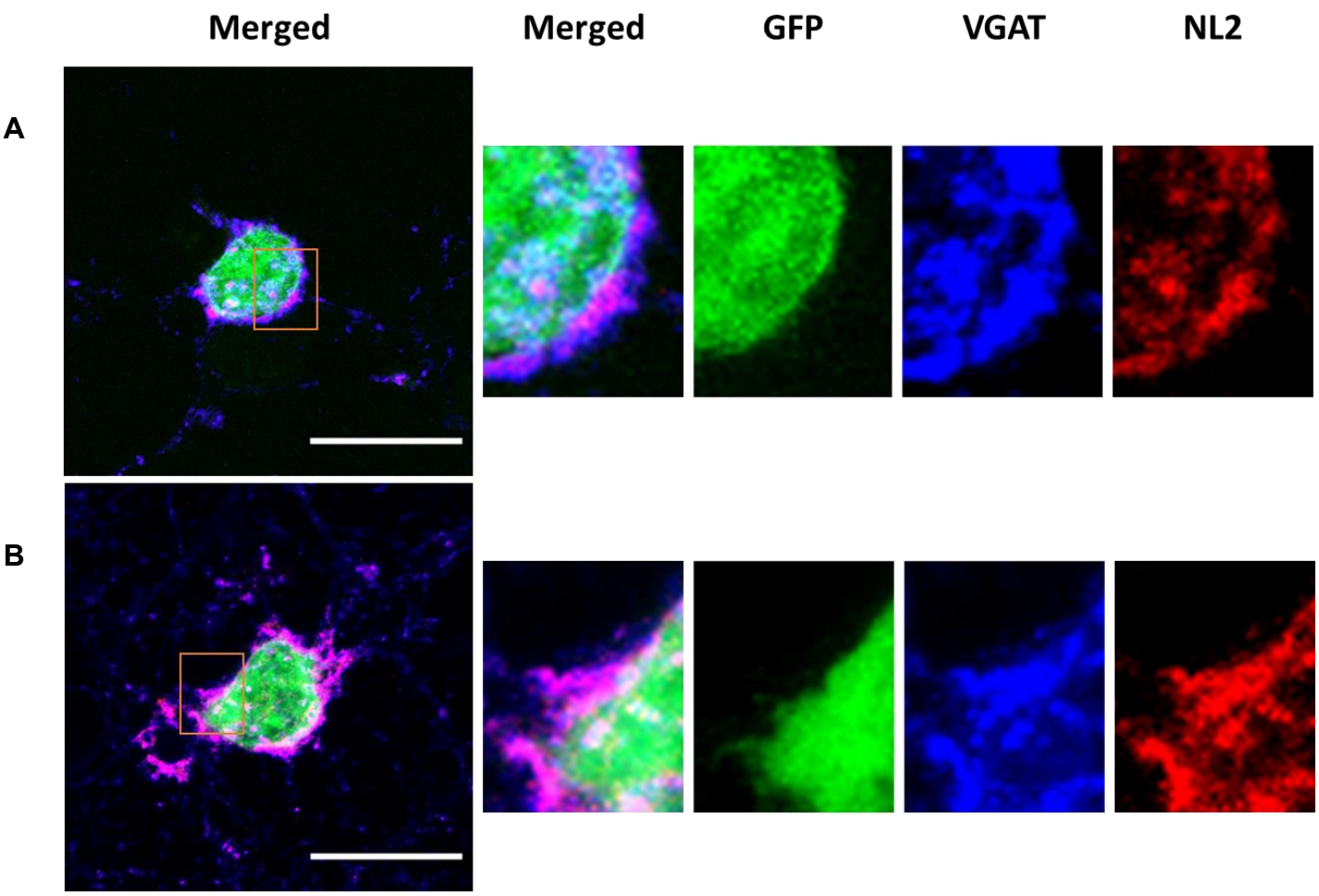

Figure 4.3.14

Synaptic formation in co-culture of $\alpha_4\beta_3\delta$-$GABA_A$ receptor/NL2-expressing HEK293 cells and embryonic medium spiny neurons in the presence of DMSO control or bicuculline (25 μM). HEK293 cell body was visualized with GFP expression (green) and the presynaptic terminals were visualized with VGAT-specific antibody (blue). (A) $\alpha_4\beta_3\delta$-$GABA_A$ receptor/NL2-expressing HEK293 cells in co-culture treated with bicuculline; (B) $\alpha_4\beta_3\delta$-$GABA_A$ receptor/NL2-expressing HEK293 cells in co-culture treated with DMSO; Scale bar = 20 μm. Fluorescent imaging was done using Zeiss 700 confocal microscope at 63 × magnification with image size 512 ×512. Max intensity projection of the z-stack images was shown. The enlarged images are 10 × zoom in.

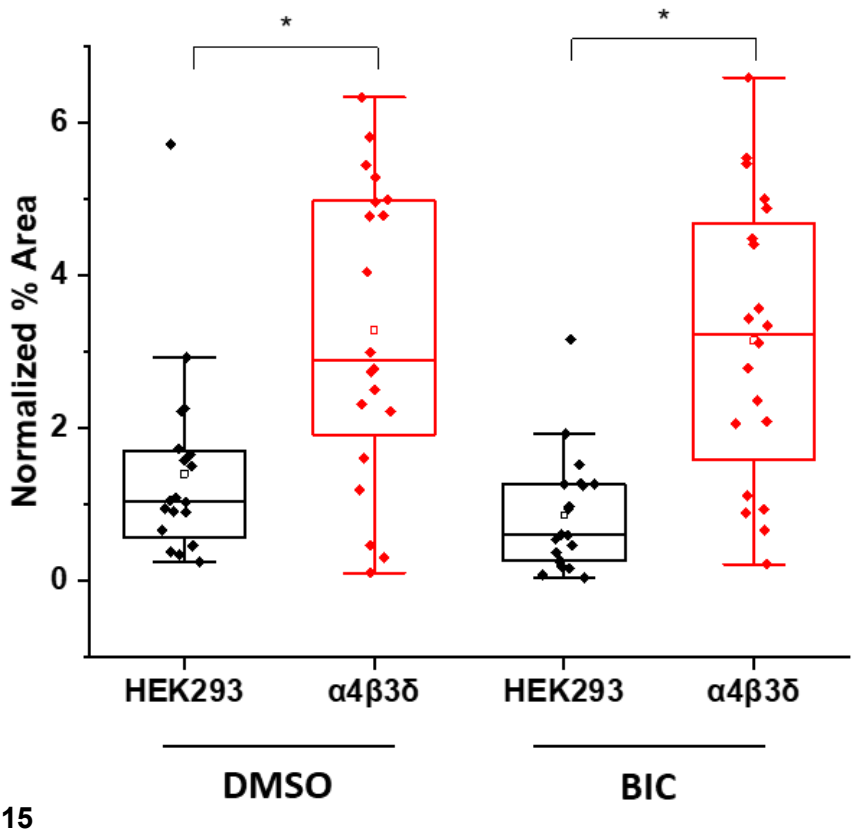

Figure 4.3.15

No significant difference was observed with DMSO or bicuculline treatment in quantitative analysis of the wt/NL2 and $\alpha_4\beta_3\delta$-$GABA_A$ receptor/NL2-expressing HEK293 cells forming contacts with VGAT terminals. The % area for each cell analyzed was normalized with expression level of NL2. The box and whisker plot shows the mean (square dot with no fill), median (horizontal line), standard deviation of the mean (whiskers) and the outliers (square dot black fill). Data from n = 20 wt, n = 20 $\alpha_4\beta_3\delta$-$GABA_A$ receptor-expressing HEK293 cells treated with DMSO, and n = 20 wt, n = 20 $\alpha_4\beta_3\delta$-$GABA_A$ receptor-expressing HEK293 cells treated with bicuculline; N = 2 independent experiments. Shapiro-Wilk normality test was used to test the normal distribution of the data and Kruskal Wallis ANOVA followed by Dunn's test was used to analyze the statistical significance of the difference. (* $p < 0.05$)

These data demonstrate that the level of synapse formation induced by co-expression of $GABA_A$ receptors/NL2 or NL2 alone was not affected by the treatment with the $GABA_A$ receptor antagonist bicuculline, indicating that activation of $GABA_A$ receptors is not required in this process.

The effect of potentiated $GABA_A$ receptor activity on the formation of synapses in the presence of NL2 was investigated by applying diazepam (1 µM) to the co-culture system. In this case, I have only tested the wt/NL2- and $\alpha_2\beta_2\gamma_2$-$GABA_A$ receptor/NL2-expressing HEK293 cells because diazepam requires the presence of the γ_2 subunit to bind to and allosterically upregulate $GABA_A$ receptors (Figure 4.3.16).

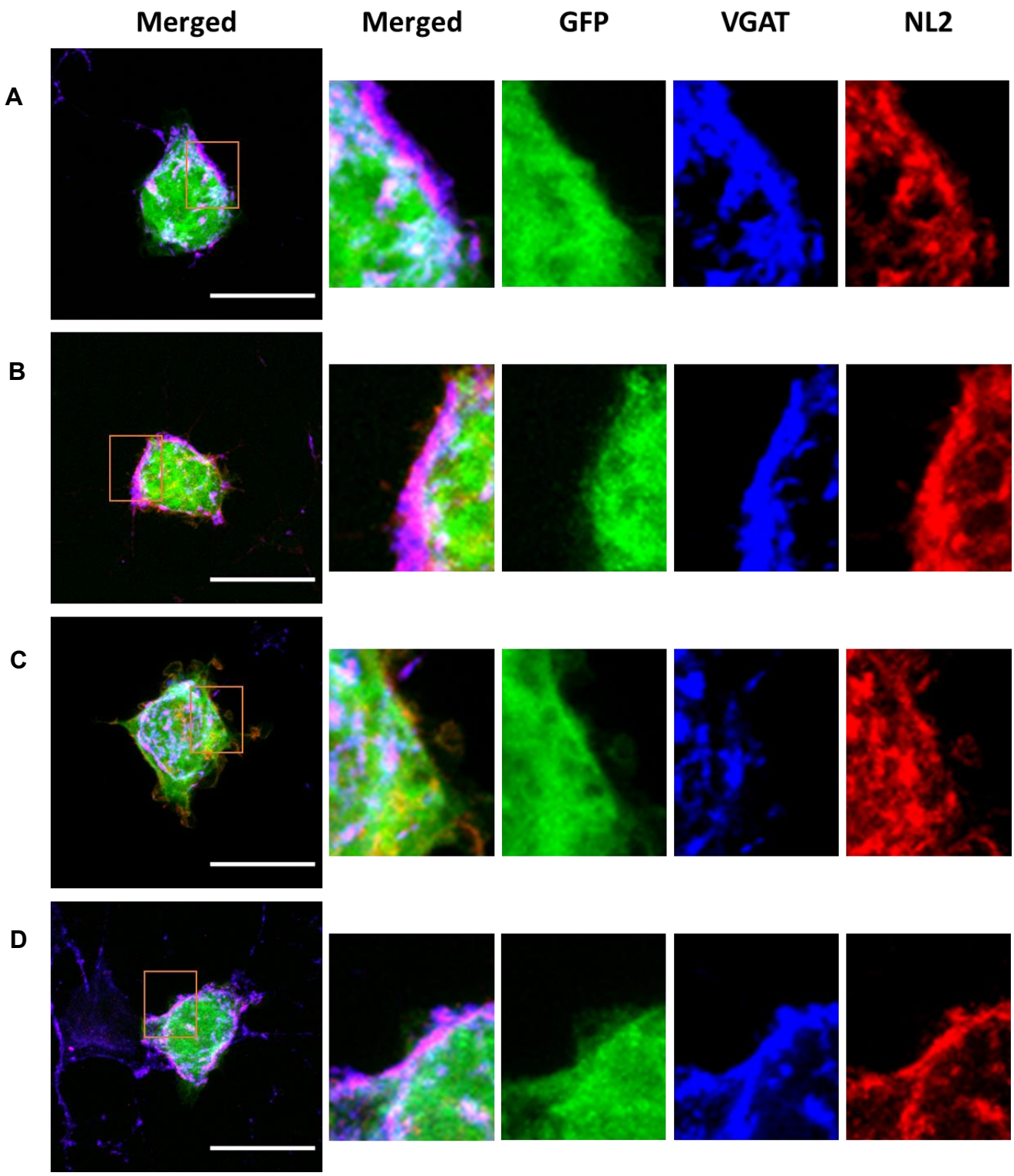

Figure 4.3.16

Synaptic formation in co-culture of $\alpha_2\beta_2\gamma_2$-$GABA_A$ receptor/NL2-expressing HEK293 cells and medium spiny neurons. Co-cultures were treated with (A) DMSO, (B) diazepam (DIA), (C) diazepam + flumazenil (Ro), and (D) flumazenil. $\alpha_2\beta_2\gamma_2$-$GABA_A$ receptor-expressing HEK293 whole cell body was visualized with GFP (green); NL2 was tagged with cherry-tag (red); synaptic terminals were visualized using VGAT antibody (blue); Scale bar = 20 μm. Fluorescent imaging was done using Zeiss 700 confocal microscope at 63 × magnification with image size 512 ×512. Max intensity projection of the z-stack images was shown. The enlarged images are 10 × zoom in.

Quantification of the % area of co-localized pixels of VGAT and GFP that represents contacts between presynaptic terminals and $\alpha_2\beta_2\gamma_2$-$GABA_A$ receptor-expressing HEK293 cells showed a slight increase under diazepam treatment in comparison with DMSO control which was not significant (Diazepam: median = 6.34 %; IQR = 4.62 % – 9.46 %; n = 30 vs. DMSO: median = 4.59 %; IQR = 2.59 % – 8.77 %; n = 30, respectively; from N = 2 independent experiments, $p > 0.05$). Addition of flumazenil, a competitive antagonist of the benzodiazepine binding site, together with diazepam (median = 3.25 %; IQR = 1.55 % – 4.85 %; n = 30; from N = 2 independent experiments) significantly decreased the level of synapse formation compared to diazepam added alone ($p < 0.05$). Addition of flumazenil alone (median = 6.33 %; IQR = 3.05 % – 9.31 %; n = 30; from N = 2 independent experiments) had no statistically significant effect on synapse formation in comparison with the DMSO control, although the median % area was significantly higher than the diazepam and flumazenil added together ($p < 0.05$; Figure 4.3.17).

Together, these results indicate that the level of synapse formation induced by $GABA_A$ receptors and NL2 is not regulated by $GABA_A$ receptor activity. Either inhibition or potentiation of $GABA_A$ receptors does not change the level of GABAergic synapse formation in the presence of NL2.

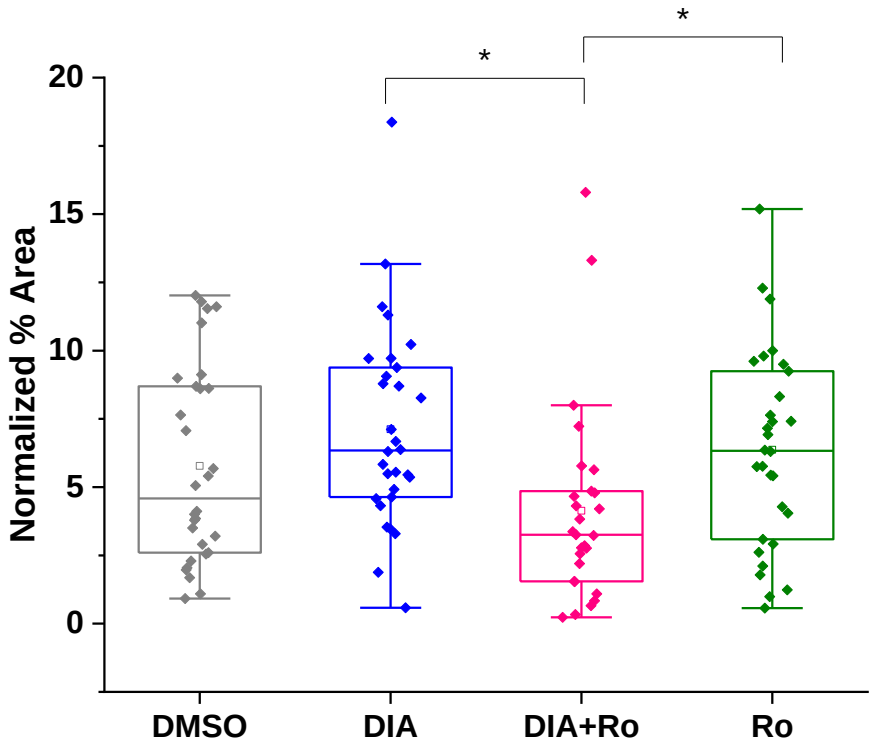

Figure 4.3.17

Quantitative analysis of synaptic contacts formed between the $\alpha_2\beta_2\gamma_2$-$GABA_A$ receptor/NL2-expressing HEK293 cells and medium spiny neurons in the presence of DMSO control, diazepam (DIA, 1 µM), diazepam + flumazenil (DIA + Ro, 1 µM + 25 µM) or flumazenil (Ro, 25 µM). The % area for each cell analyzed was normalized with expression level of NL2. The box and whisker plot shows the mean (square dot with no fill), median (horizontal line), standard deviation of the mean (whiskers) and the outliers (square dot black fill). Data from $\alpha_2\beta_2\gamma_2$-$GABA_A$ receptor/NL2-expressing HEK293 cells treated with DMSO (n = 30), diazepam (n = 30), diazepam + flumazenil (n = 27), and flumazenil (n = 30), from N = 2 independent experiments. Shapiro-Wilk normality test was used to test the normal distribution of the data and Kruskal Wallis ANOVA followed by Dunn's test was used to analyze the statistical significance of the difference. (* $p < 0.05$).

4.3.3 Active GABAergic Synapses are Formed in the Presence of NL2 and γ2 Subunit-Containing $GABA_A$ receptors

Whole-cell recording of the IPSCs of the HEK293 cells in the co-culture model system was performed by our collaborator's lab. The HEK293 cells were cultured with embryonic medium spiny neurons for 48 hours which was shown to be an optimal period of incubation for the electrophysiology experiments. In the absence of NL2, IPSCs were detected in 60 % of the $\alpha_2\beta_2\gamma_2$-$GABA_A$ receptor-expressing HEK293 cells (9 out of 15), in which 8 cells were detected with < 0.1 Hz IPSC and 1 cell with > 0.1 Hz. When NL2 was expressed, IPSCs were detected in 93.3 % $\alpha_2\beta_2\gamma_2$-$GABA_A$ receptor-expressing HEK293 cells (14 out of 15), in which 2 cells were detected with < 0.1 Hz IPSC and 12 cells with > 0.1 Hz (Figure 4.3.18A). In the absence of NL2, no IPSCs were detected in the $\alpha_4\beta_3\delta$-$GABA_A$ receptor-expressing HEK293 cells (11 cells), while in the presence of NL2, IPSCs were detected in only 1 $\alpha_4\beta_3\delta$-$GABA_A$ receptor-expressing HEK293 cell out of 15 (> 0.1 Hz).

These data show that the expression of NL2 increases the frequency of GABAergic IPSCs in the presence of synaptic $\alpha_2\beta_2\gamma_2$-$GABA_A$ receptors but has limited effect in the presence of $\alpha_4\beta_3\delta$-$GABA_A$ receptors.

To investigate which of the $GABA_A$ receptor subunits is necessary for the observed effects, we transfected the B2 clone of the HEK293 cells stably expressing β_3 subunits (Chapter 2, section 2.2.1) with α_4 + γ_2 + NL2 or α_2 + δ + NL2 cDNAs and co-cultured them with the medium spiny neurons for

electrophysiology recordings (Figure 4.3.18A). Compared to the $\alpha_2\beta_2\gamma_2$-$GABA_A$ receptor/NL2-expressing HEK293 cells, a similar level of activity was detected in 7 out of 8 of the $\alpha_4\beta_3\gamma_2$-$GABA_A$ receptor/NL2-expressing HEK293 cells with the frequency > 0.1 Hz. In 8 out of 10 of the $\alpha_2\beta_3\delta$-$GABA_A$ receptor/NL2-expressing HEK293 cells, no IPSCs were detected, indicating that any synaptic contacts formed in these conditions were functionally silent just like in the case of synapses formed with the $\alpha_4\beta_3\delta$-$GABA_A$ receptor-expressing HEK293 cells in the absence of NL2.

The typical recording traces are shown in Figure 4.3.18B. Expression of NL2 resulted in a higher frequency of IPSCs in $\alpha_2\beta_2\gamma_2$-$GABA_A$ receptor-expressing HEK293 cells (Figure 4.3.18B(i) & (ii)). On the contrary, in the presence of NL2, IPSCs were detected in $\alpha_4\beta_3\gamma_2$-$GABA_A$ receptor expressing-HEK293 cells but not in $\alpha_4\beta_3\delta$-$GABA_A$ receptor expressing-HEK293 cells (Figure 4.3.18B(iii)).

These data indicate an important role of the γ_2 subunit in generating GABAergic IPSCs during the formation of functional synapses in this model system.

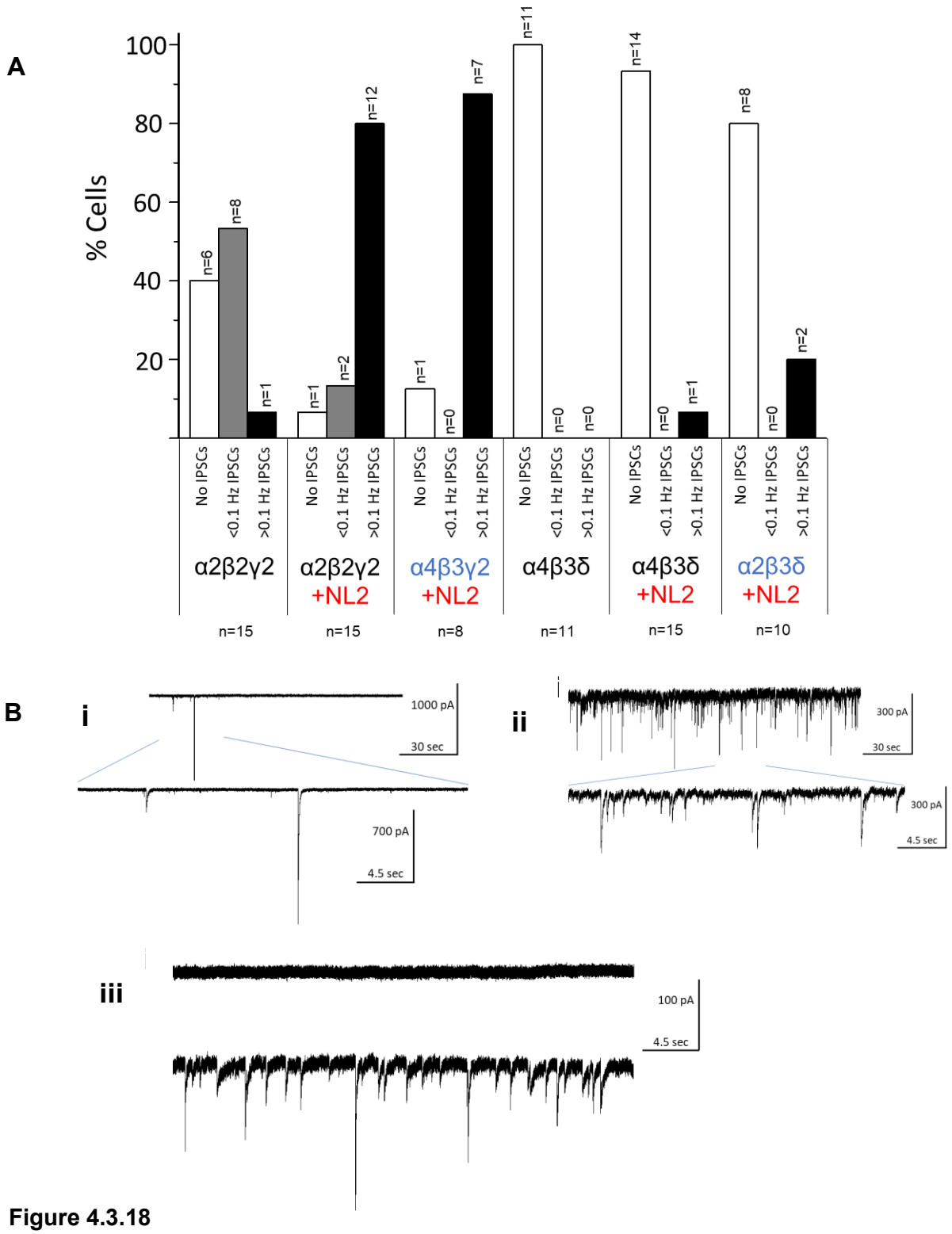

Figure 4.3.18

Whole cell recordings of IPSCs in co-culture of HEK293 cells and embryonic medium spiny neurons. (A) Recorded IPSCs in the presence of different $GABA_A$ receptors. Expression of NL2 increases the frequency of IPSCs in HEK293 cells expressing γ_2 subunit containing $GABA_A$ receptors but has a limited effect in $\alpha_4\beta_3\delta$-$GABA_A$ receptor-expressing HEK293 cell line. (B) Typical recording traces of IPSCs in (i) $\alpha_2\beta_2\gamma_2$-$GABA_A$ receptor-expressing HEK293 cells; (ii) $\alpha_2\beta_2\gamma_2$-$GABA_A$ receptor/NL2-expressing HEK293 cells and (iii) $\alpha_4\beta_3\delta$-$GABA_A$ receptor/NL2 (above) and $\alpha_4\beta_3\gamma_2$-$GABA_A$ receptor/NL2 (below) expressing-HEK293 cells.

4.3.4 Presynaptic GABAergic Terminals Show High Activity in Synapses formed with the $\alpha_2\beta_2\gamma_2$-$GABA_A$ receptor/NL2-expressing HEK293 cells

To investigate further a possible reason for the lack of synaptic transmission in the majority of synapses received by the $\alpha_4\beta_3\delta$-$GABA_A$ receptors/NL2 expressing HEK293 cells, we have carried out the synaptotagmin-antibody uptake assays (Fernández-Alfonso, Kwan and Ryan, 2006), in which the active presynaptic terminals can be fluorescently labelled with the cy5-tagged anti-synaptotagmin 1 vesicle-luminal domain-specific antibodies and imaged using the confocal microscope. In these experiments, we have added cy5-tagged anti-synaptotagmin antibody (1:50, 105311C5, Synaptic Systems) into the co-cultures for 30 minutes at 37 ℃ 5 % CO_2 prior to fixation and processing for immunocytochemistry with the VGAT-specific antibody and confocal imaging. Synaptic contact formation and presynaptic activity were thus recorded in parallel allowing us to quantify the number of active synaptic contacts formed with the wt/NL2-, $\alpha_4\beta_3\delta$-$GABA_A$ receptor/NL2- or $\alpha_2\beta_2\gamma_2$-$GABA_A$ receptor/NL2-expressing HEK293 cells (Figure 4.3.19).

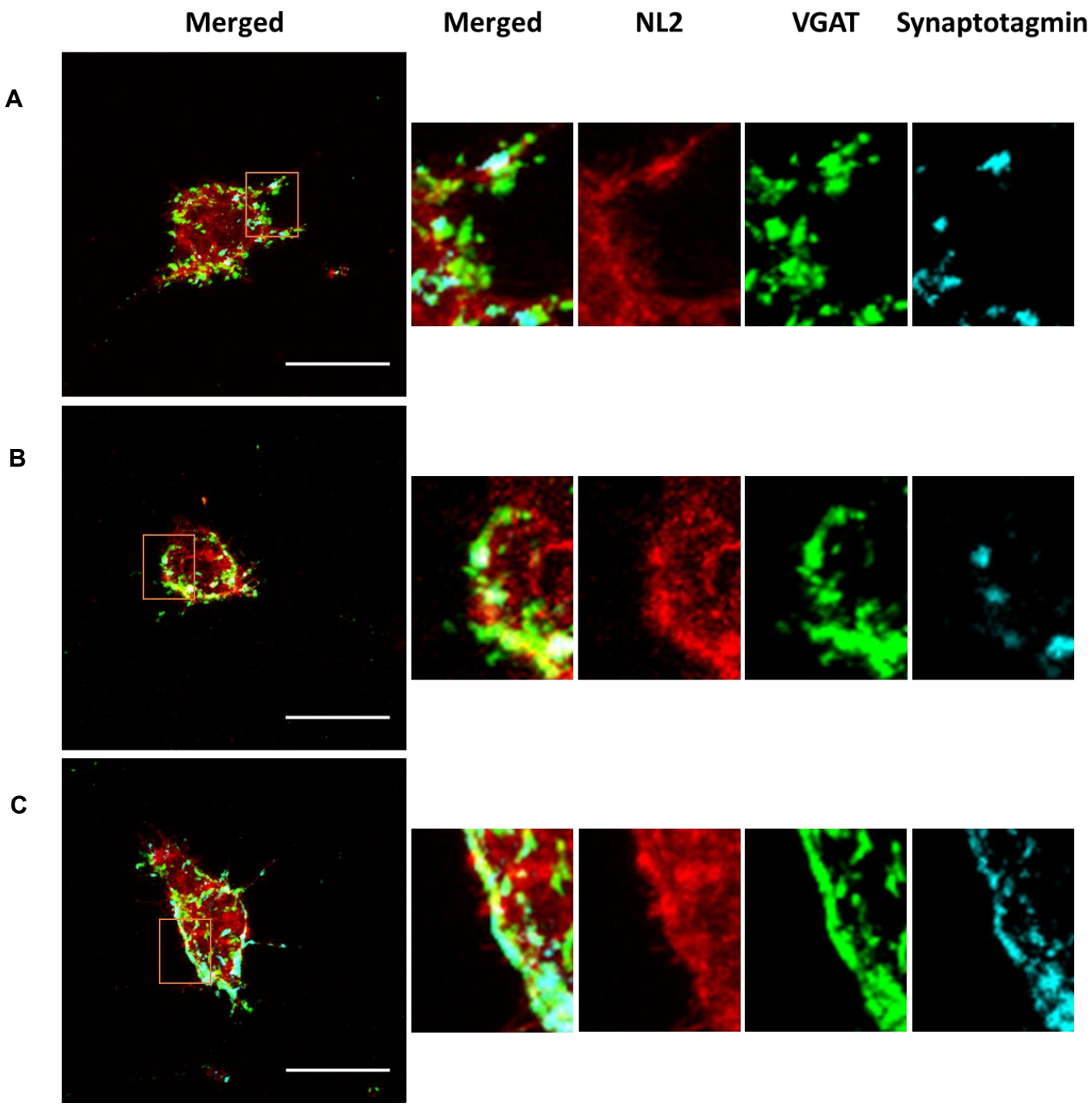

Figure 4.3.19

Detection of active synapses formed between HEK293 cells and embryonic medium spiny neurons in co-culture. (A) wt/NL2 expressing-HEK293 cells, (B) $\alpha_4\beta_3\delta$-$GABA_A$ receptor/NL2-expressing HEK293 cells, and (C) $\alpha_2\beta_2\gamma_2$/NL2-$GABA_A$ receptor-expressing HEK293 cells were incubated in co-culture with medium spiny neurons for 24 hours. Active presynaptic terminals forming synapses were visualized with the cy5-labelled synaptotagmin luminal domain specific antibody (cyan). All presynaptic terminals forming synapses were visualized with the VGAT antibody (green). NL2 was tagged with cherry tag (red). Scale bar = 20 µm. Fluorescent imaging was done using Zeiss 700 confocal microscope at 63 × magnification with image size 512 ×512. Max intensity projection of the z-stack images was shown. The enlarged images are 10 × zoom in.

Quantification of the % area of co-localized pixels that represents contacts between synaptotagmin (Figure 4.3.20A) or VGAT (Figure 4.3.20B) terminals and the wt-HEK293 cells, revealed that NL2 promotes synapse formation in the absence $GABA_A$ receptors and that in some of these synapses, presynaptic terminals are active.

Compared to the wt-HEK293 cell line, the presence of $\alpha_4\beta_3\delta$-$GABA_A$ receptors and NL2 the formation of functional synapses was significantly increased (median = 0.12 %; IQR = 0.03 % - 0.22 %; n = 30 cells; from N = 3 independent experiments, *vs.* median = 0.52 %; IQR = 0.18 % - 0.95 %; n = 21 cells; from N = 2 independent experiments , $p < 0.05$). In the presence of the $\alpha_2\beta_2\gamma_2$-$GABA_A$ receptors, the synergistic effect was further increased significantly compared with the $\alpha_4\beta_3\delta$-$GABA_A$ receptor-expressing HEK293 (median = 1.32 %; IQR = 0.78 % - 2.03 %; n = 21 cells *vs.* median = 0.52 %; IQR = 0.18 % - 0.95 %; n = 21 cells, respectively; from N = 2 independent experiments, $p < 0.05$). The difference between the wt- and $\alpha_2\beta_2\gamma_2$-$GABA_A$ receptor-expressing HEK293 cell lines was also significant ($p < 0.05$) (Figure 4.3.20A).

Compared to the wt-HEK293 cell line, in the presence of $\alpha_4\beta_3\delta$-$GABA_A$ receptors and NL2, the formation of synapses was significantly increased (median = 1.14 %; IQR = 0.54 % - 2.03 %; n = 30 cells, from N = 3 independent experiments, *vs.* median = 2.18 %; IQR = 1.39 % - 4.18 %; n = 21 cells from N = 2 independent experiments respectively; $p < 0.05$). In the presence of the $\alpha_2\beta_2\gamma_2$-$GABA_A$ receptors, the synergistic effect was further increased significantly

compared to the $\alpha_4\beta_3\delta$-$GABA_A$ receptor-expressing HEK293 (median = 4.38 %; IQR = 3.58 % - 6.39 %; n = 21 cells *vs.* median = 2.18 %; IQR = 1.39 % - 4.18 %; n = 21 cells, respectively; from N = 2 independent experiments, $p < 0.05$). The difference between wt- and $\alpha_2\beta_2\gamma_2$-$GABA_A$ receptor-expressing HEK293 cell lines was also significant ($p < 0.05$) (Figure 4.3.20B).

In the presence of NL2, the number of VGAT positive contacts was always higher than the number of synaptotagmin positive contacts, indicating that not all synapses formed incorporated active presynaptic terminals. In the wt-HEK293 cells, the synaptotagmin and VGAT normalized % area was 0.12 % and 1.14 %, respectively (10.53 % were active). In the $\alpha_4\beta_3\delta$-$GABA_A$ receptor expressing-HEK293 cells, the synaptotagmin and VGAT normalized % area was 0.52 % and 2.18 %, respectively (23.9 % were active). In the $\alpha_2\beta_2\gamma_2$-$GABA_A$ receptor expressing-HEK293 cells, the synaptotagmin and VGAT normalized % area was 1.32 % and 4.38 %, respectively (30.1 % were active).

These data demonstrates that in the presence of NL2 and $\alpha_2\beta_2\gamma_2$-$GABA_A$ receptors, more active synapses were formed than in the presence of NL2 alone or with the $\alpha_4\beta_3\delta$-$GABA_A$ receptors.

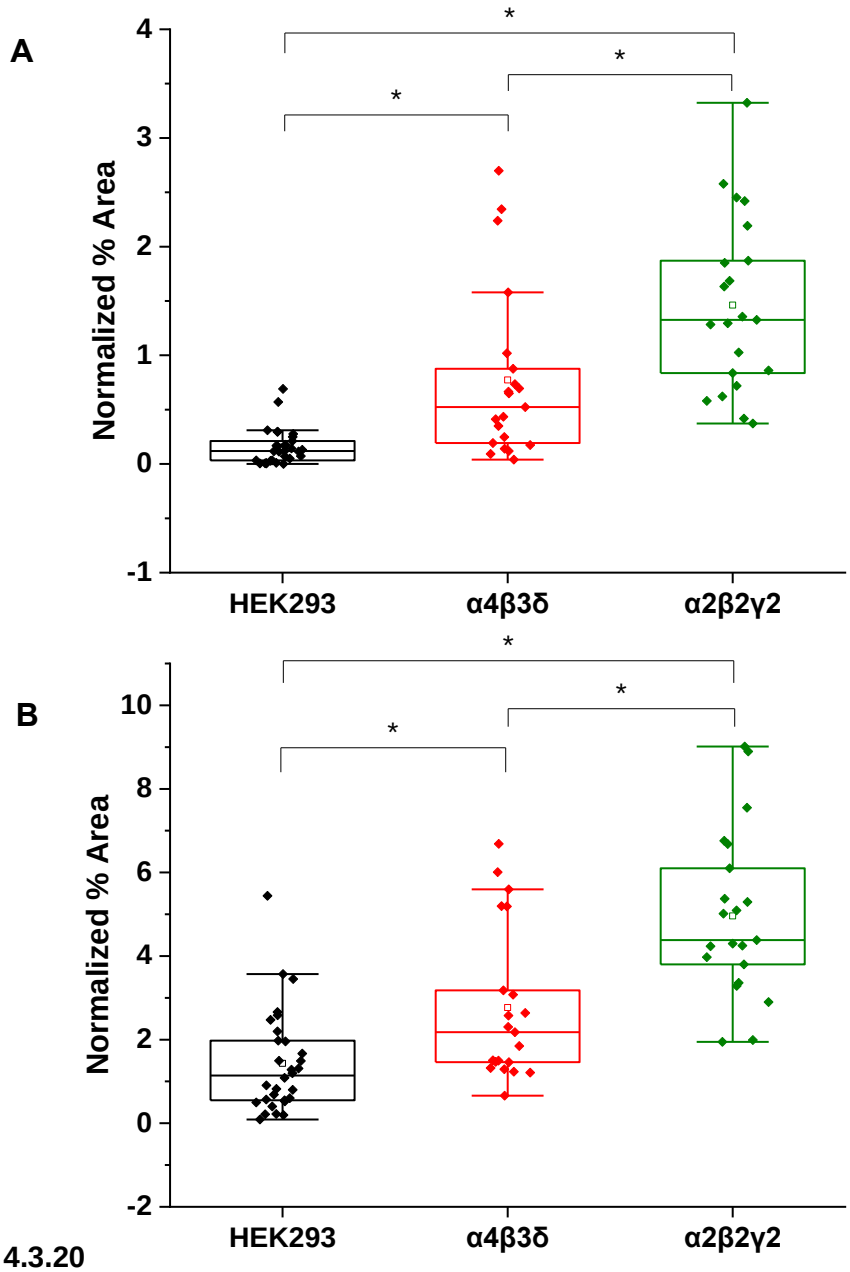

Figure 4.3.20

Quantitative analysis of synaptic contacts received by the wt, $\alpha_4\beta_3\delta$-GABA$_A$ receptor- or $\alpha_2\beta_2\gamma_2$-GABA$_A$ receptor-expressing HEK293 cells in the presence of NL2, in co-culture with medium spiny neurons. The % area was normalized to the expression level of NL2. (A) Normalized % area of Synaptotagmin colocalization indicating that functional synapse formation was further significantly increased in the presence of $\alpha_4\beta_3\delta$-GABA$_A$ receptors and $\alpha_2\beta_2\gamma_2$-GABA$_A$ receptors, with the latter being significantly more potent. (B) Normalized % area of VGAT colocalization indicating that synapse formation was further significantly increased in the presence of $\alpha_4\beta_3\delta$-GABA$_A$ receptors and $\alpha_2\beta_2\gamma_2$-GABA$_A$ receptors, with the latter being significantly more potent. The box and whisker plot shows the mean (square dot with no fill), median (horizontal line), standard deviation of the mean (whiskers) and the outliers (square dot black fill). Data from wt-HEK293 cells (n = 30, from N = 3 independent experiments), $\alpha_4\beta_3\delta$-GABA$_A$ receptor-expressing HEK293 cells (n = 22, from N = 2 independent experiments) and $\alpha_2\beta_2\gamma_2$-GABA$_A$ receptor-expressing HEK293 cells (n = 22, from N = 2 independent experiments). Shapiro-Wilk normality test was used to test the normal distribution of the data and Kruskal Wallis ANOVA followed by Dunn's test was used to analyze the statistical significance of the difference. (* $p < 0.05$).

In order to quantitively analyze these effects, I have plotted the mean intensity of the NL2 signal measured in individual HEK293 cells (x-axis) and the % area of synaptotagmin or VGAT signal overlapping with the NL2 signal on the y-axis (Figure 4.3.21). The intensity of the 12-bit NL2 signal was represented at $\times 10^4$. The slope of the linear regression analysis represents the synaptic contacts induced by a certain amount of NL2 expression which can be defined as a unit in this scenario.

The slopes of the curves representing all VGAT positive synapses induced by a unit of NL2 expression are very different between the wt-HEK293 cells (Slope = 0.94, R^2 = 0.21), $\alpha_4\beta_3\delta$-$GABA_A$ receptor-expressing HEK293 cells (Slope = 2.88, R^2 = 0.41) and $\alpha_2\beta_2\gamma_2$-$GABA_A$ receptor-expressing HEK293 cell (Slope = 4.46, R^2 = 0.57). These results suggests that the number of synapses induced by a unit of NL2 expression in the presence of synaptic $GABA_A$ receptors is almost doubled when compared to the extrasynaptic $GABA_A$ receptors and quadrupled when compared to the wt cells with no $GABA_A$ receptors expressed. Likewise, the slopes of the curves representing active synaptotagmin-positive synapses induced by a unit of NL2 expression are also very different between the wt-HEK293 cells (Slope = 0.14, R^2 = 0.07), the $\alpha_4\beta_3\delta$-$GABA_A$ receptor-expressing HEK293 cells (Slope = 1.05, R^2 = 0.19) and the $\alpha_2\beta_2\gamma_2$-$GABA_A$ receptor-expressing HEK293 cell (Slope = 1.92, R^2 = 0.51). This suggests that the number of active synapse induced by a unit of NL2 expression is ~ 8 times higher when the extrasynaptic receptors are expressed, and ~14 times higher in the presence

of synaptic $GABA_A$ receptors in comparison with the cells expressing NL2 alone.

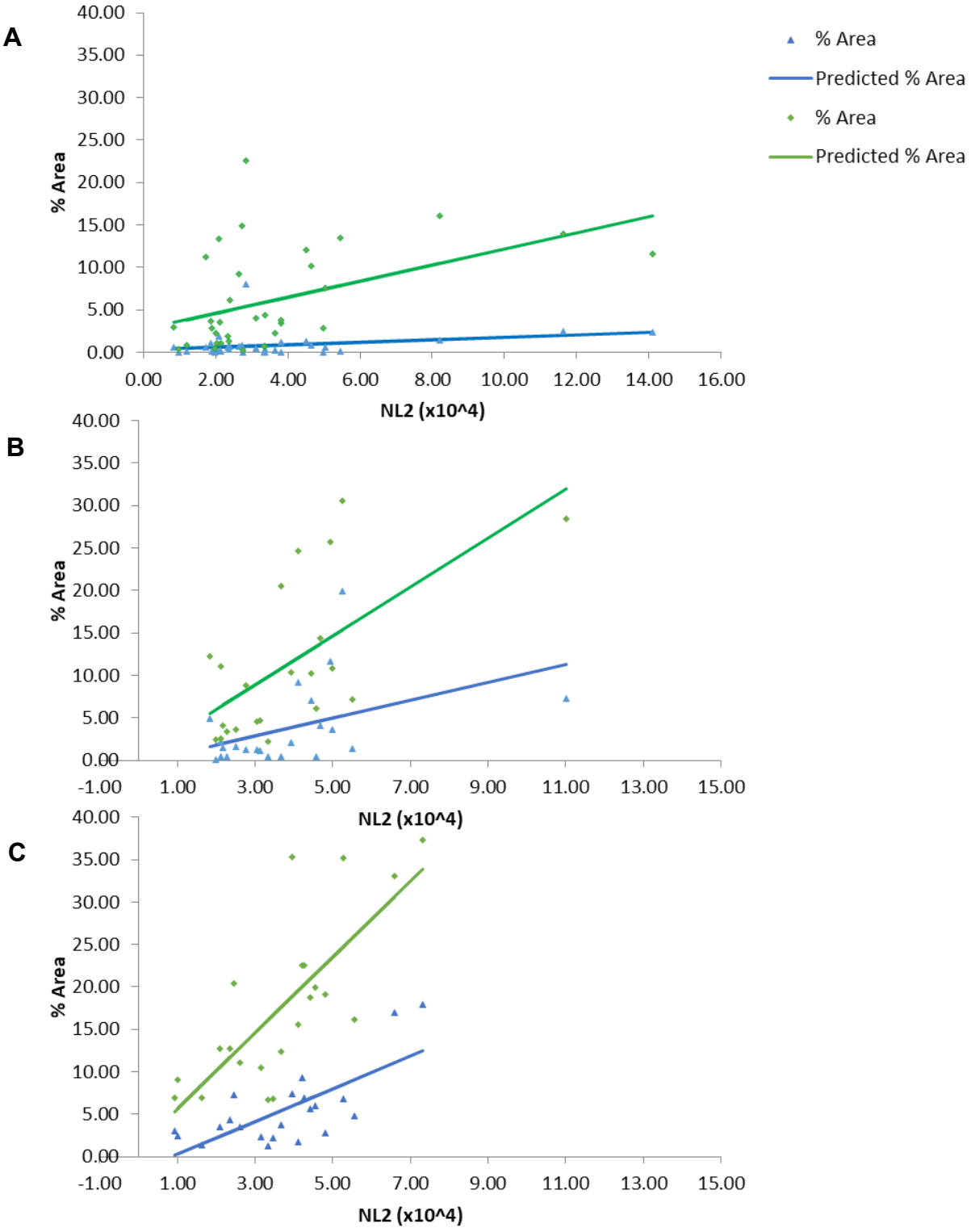

Figure 4.3.21

Linear correlation of the % area of synaptic contacts *vs.* NL2 expression level (× 10^4) in co-culture of medium spiny neurons with (A) wt-HEK293 cells, (B) $\alpha_4\beta_3\delta$-$GABA_A$ receptor-expressing HEK293 cells, and (C) $\alpha_2\beta_2\gamma_2$-$GABA_A$ receptor-expressing HEK293 cells expressing NL2. Solid green squares represent VGAT data points. Solid blue triangles represent synaptotagmin data points. Data from n = 34 wt-HEK293 cells; N = 3 independent experiments; n = 22 $\alpha_4\beta_3\delta$-$GABA_A$ receptor- and n = 22 $\alpha_2\beta_2\gamma_2$-$GABA_A$ receptor-expressing HEK293 cells; N = 2 independent experiments.

4.3.5 Pre-synaptic Terminal Marker Bassoon Shows a Higher Degree of Colocalization with the $\alpha_2\beta_2\gamma_2$-GABA$_A$ Receptors than $\alpha_4\beta_3\delta$-GABA$_A$ Receptors

To analyze the degree of colocalization between the $\alpha_2\beta_2\gamma_2$-GABA$_A$ receptors or $\alpha_4\beta_3\delta$-GABA$_A$ receptor**s** and the presynaptic zone protein Bassoon in synaptic contacts we have carried out super-resolution imaging using Zeiss ELYRA PS.1 SIM (Figure 4.3.22). The $\alpha_2\beta_2\gamma_2$-GABA$_A$ receptor/NL2- or $\alpha_4\beta_3\delta$-GABA$_A$ receptor**/**NL2-expressing HEK293 cells were co-cultured with embryonic medium spiny neurons for 24 hours, fixed and processed for immunocytochemistry and super-resolution imaging with the α_2 subunit or α_4 subunit antibodies specific for the extracellular epitopes, to label receptors at the cell surface, and Bassoon specific antibodies. The z-stack images were rendered to 3-dimensional images for colocalization analysis and Manders coefficients were calculated to show the level of overlapping signals, with M1 indicating the proportion of Bassoon overlapping with the surface GABA$_A$ receptors and M2 indicating the proportion of the surface GABA$_A$ receptors overlapping with Bassoon. The M1 coefficient was significantly higher for the $\alpha_2\beta_2\gamma_2$- than $\alpha_4\beta_3\delta$-GABA$_A$ receptors in synaptic contacts (median = 0.27; IQR = 0.24 – 0.42; n = 8 cells *vs.* median = 0.17; IQR = 0.10 – 0.25; n = 8 cells, respectively; from N = 2 independent experiments, $p < 0.05$) indicating that higher proportion of the $\alpha_2\beta_2\gamma_2$-GABA$_A$ receptors was co-localized with Bassoon and thus in proximity of the presynaptic active zone than in the case of the $\alpha_4\beta_3\delta$-GABA$_A$ receptors (Figure 4.3.22). The M2 coefficient

shows no significant difference between the two cell lines (median = 0.73; IQR = 0.24 – 0.81; n = 8 cells *vs.* median = 0.51; IQR = 0.36 – 0.66; n = 8 cells, respectively; from N = 2 independent experiments, $p > 0.05$,), although the median of M2 for $\alpha_2\beta_2\gamma_2$-$GABA_A$ receptor-expressing HEK293 cells was slightly higher than that for $\alpha_4\beta_3\delta$-$GABA_A$ receptor-expressing HEK293 cells (Figure 4.3.23).

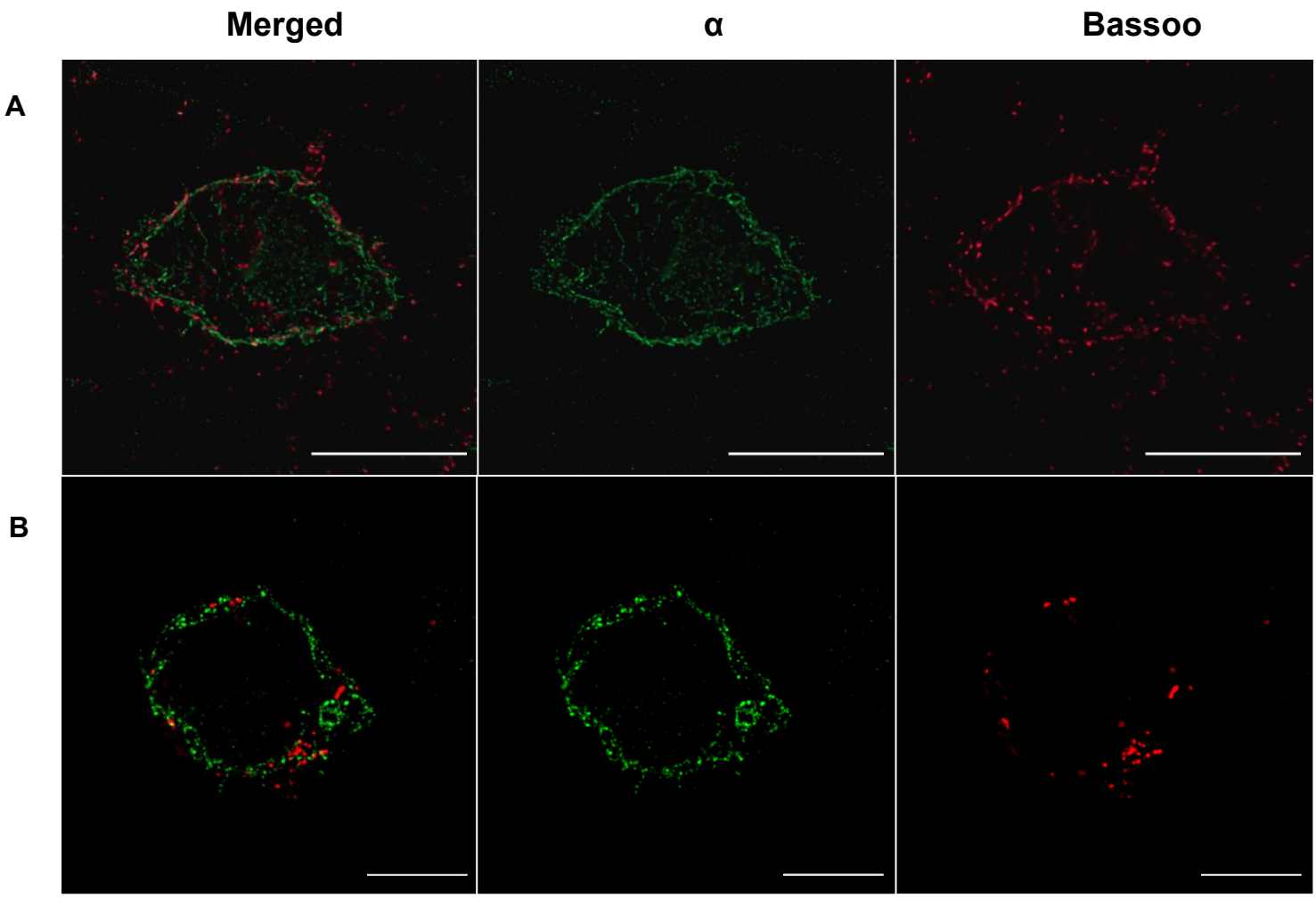

Figure 4.3.22

Co-localization of the presynaptic marker Bassoon and $GABA_A$ receptors in co-culture of (A) $\alpha_2\beta_2\gamma_2$-$GABA_A$ receptor- and (B) $\alpha_4\beta_3\delta$-$GABA_A$ receptor-expressing HEK293 cells with embryonic medium spiny neurons. $GABA_A$ receptor α_2 or α_4 subunits were visualized using antibodies for each subunit (green) and Bassoon was visualized using Bassoon-specific antibody (red). Images were acquired using Zeiss ELYRA PS.1 SIM at 63 x magnification. Scale bar = 10 µm.

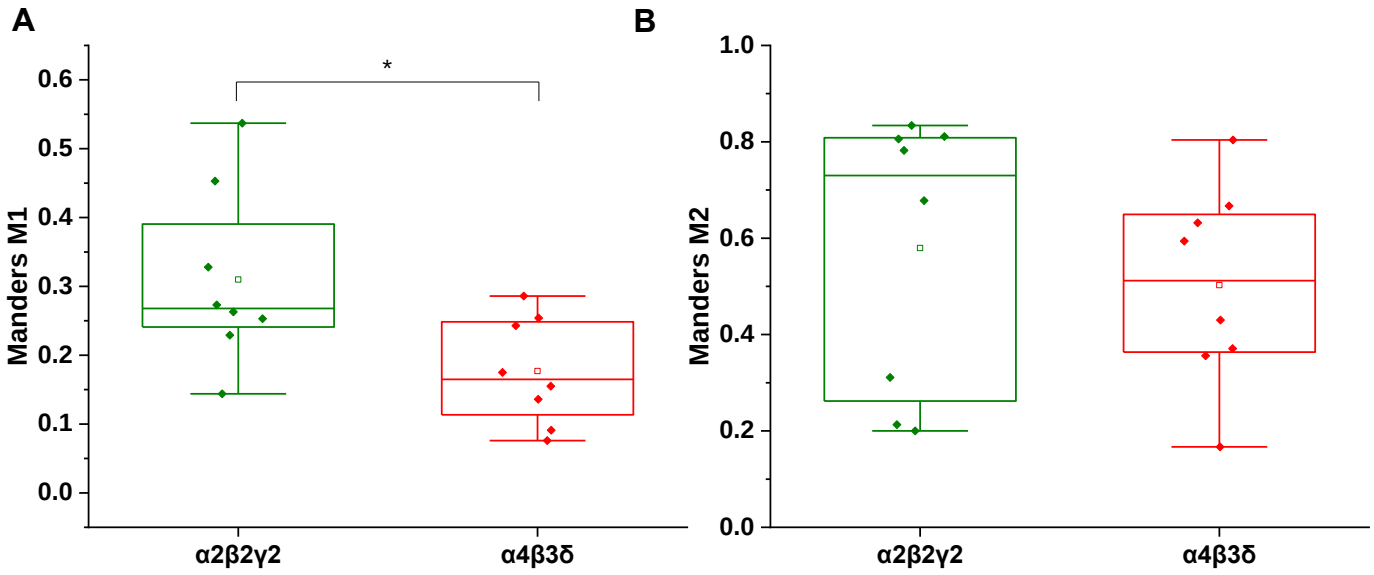

Figure 4.3.23

Quantitative analysis of colocalization between the presynaptic active zone marker Bassoon and $\alpha_2\beta_2\gamma_2$-$GABA_A$ receptors or $\alpha_4\beta_3\delta$-$GABA_A$ receptors using Manders coefficients which indicate (A) M1- the proportion of Bassoon signal that overlaps with $GABA_A$ receptors in synaptic contacts, and (B) M2-the proportion of surface $GABA_A$ receptors that overlaps with Bassoon in two different cell lines in co-culture with the medium spiny neurons. The M1 coefficient is significantly higher for contacts formed with the $\alpha_2\beta_2\gamma_2$-$GABA_A$ receptor/NL2-expressing HEK293 cells than with the $\alpha_4\beta_3\delta$-$GABA_A$ receptor/NL2 expressing HEK293 cells. The M2 coefficient is higher for $\alpha_2\beta_2\gamma_2$-$GABA_A$ receptors than $\alpha_4\beta_3\delta$-$GABA_A$ receptors albeit not statistically significant. Data from n = 8 $\alpha_2\beta_2\gamma_2$-$GABA_A$ receptor/NL2-, and n = 8 $\alpha_4\beta_3\delta$-$GABA_A$ receptor/NL2-expressing HEK293 cells; form N = 2 independent experiments.

4.3.6 $GABA_A$ Receptor γ_2 Subunit Plays an Important Role in NL2-induced GABAergic Synapse Formation

To investigate the mechanisms underlying the observed synergistic effects of $\alpha_2\beta_2\gamma_2$-$GABA_A$ receptors and NL2 in synapse formation, I first wanted to establish which domains of $GABA_A$ receptor subunits may be involved in this process either by interacting directly with NL2 or with any of the presynaptic binding partners of NL2. The extracellular N-terminals domain of $GABA_A$ receptor α_1, β_2 and γ_2 subunits were previously shown to contribute to the GABAergic synapse formation in the absence of NL2 (Brown et al., 2016). Therefore, I wanted to test if these domains may also play a role in the presence of NL2.

4.3.6.1 NL2-Induced Synapse Formation is not Regulated by $GABA_A$ Receptor N-Terminal Extracellular Domains

To test if the N-terminal ECD of $GABA_A$ receptor subunits may play a role in regulating NL2-induced GABAergic synapse formation, 4 µg of either the α_2, β_2 or γ_2 ECD (0.29 – 0.32 µM) purified from the SF9 cells (Brown et al., 2016) were individually applied to the co-culture of $\alpha_2\beta_2\gamma_2$-$GABA_A$ receptor/NL2-expressing HEK293 cells and embryonic medium spiny neurons (Figure 4.3.24). HEK293 cells were transfected to express GFP for the visualization of the cell body. An equivalent amount of untransfected SF9 cell extract (4 µg), taken through the same purification procedure as extracts expressing ECDs, was used as control. ECDs were applied 30 minutes after the HEK293 cells and embryonic medium spiny neurons were cultured together and incubated at 37 ℃ with 5 % CO_2 for 24

hours.

Quantification of the % area of co-localized pixels of VGAT and GFP that represents contacts between presynaptic terminals and $\alpha_2\beta_2\gamma_2$-$GABA_A$ receptor-expressing HEK293 cells showed no significant change with the application of ECDs (Figure 4.3.25). With SF9 extract control, the median was 5.82 % with IQR = 3.96 % - 6.90 % (n = 19 cells from N = 2 independent experiments). The application of β_2 ECD slightly decreased the synapse formation albeit not significantly (median = 4.67 %; IQR = 2.67 % – 7.35 %; n = 20 cells; from N = 2 independent experiments). No change was observed with application of α_2 (median = 6.03 %; IQR = 4.04 % – 7.58 %; n = 20 cells; from N = 2 independent experiments) or γ_2 (median = 6.22 %; IQR = 4.05 % – 7.33 %; n = 20 cells; from N = 2 independent experiments) ECDs.

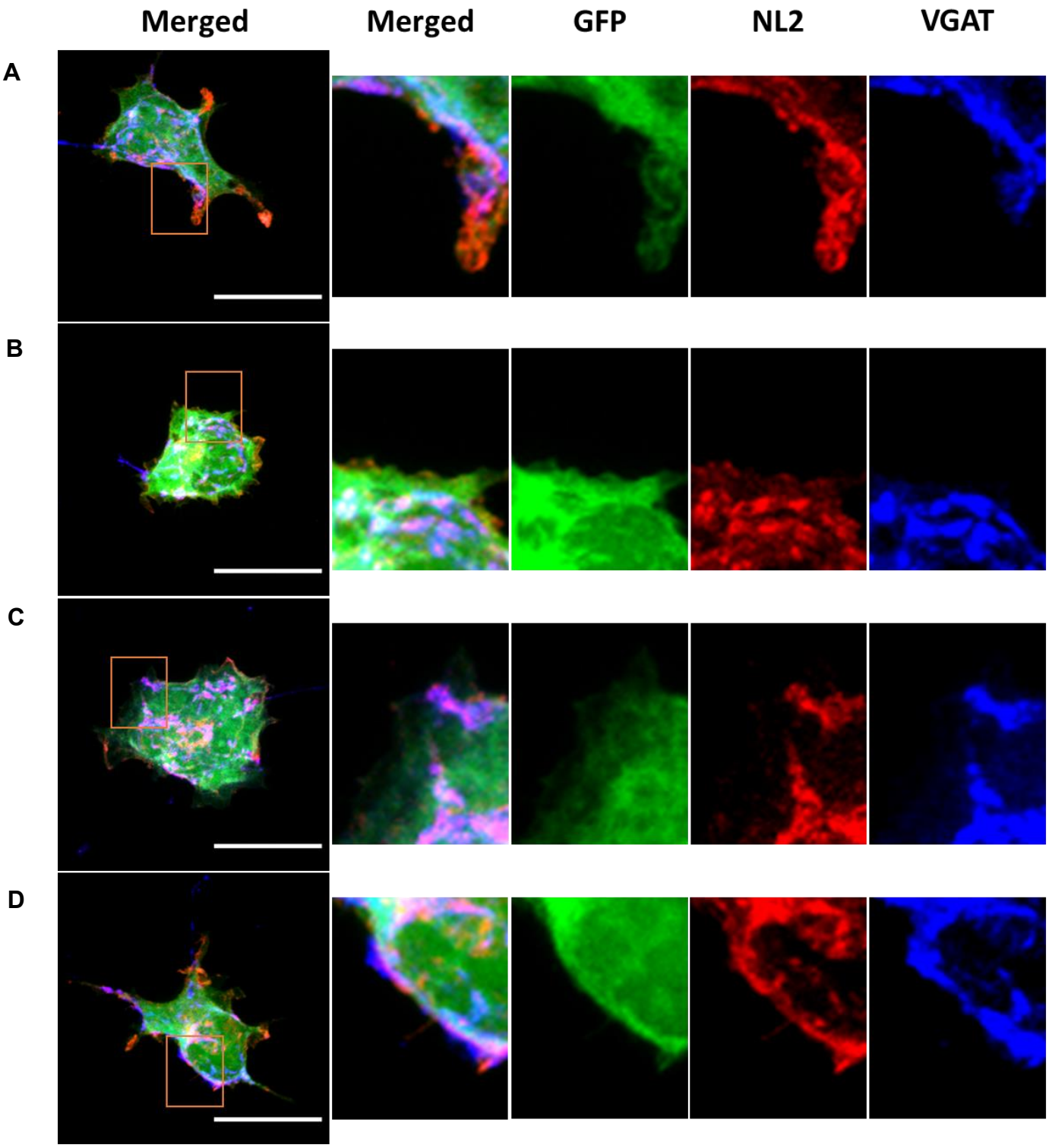

Figure 4.3.24

Synaptic contact formation in co-culture of HEK293 cells and embryonic medium spiny neurons with the addition of $GABA_A$ receptor subunit ECDs. HEK293 cells stably expressing $\alpha_2\beta_2\gamma_2$-$GABA_A$ receptors + $NL2^{cherry}$ + GFP were incubated with medium spiny neurons and (A) SF9 cell extracts (B) α_2 subunit ECD (C) β_2 subunit ECD (D) γ_2 subunit ECD, for 24 hours. HEK293 cell body was visualized with GFP expression (green); NL2 was tagged with cherry-tag (red); and the presynaptic terminals were visualized with VGAT-specific antibody (blue). Scale bar = 20 µm. Fluorescent imaging was done using Zeiss 700 confocal microscope at 63 × magnification with image size 512 × 512. Max intensity projection of the z-stack images was shown. The enlarged images are 10 × zoom in.

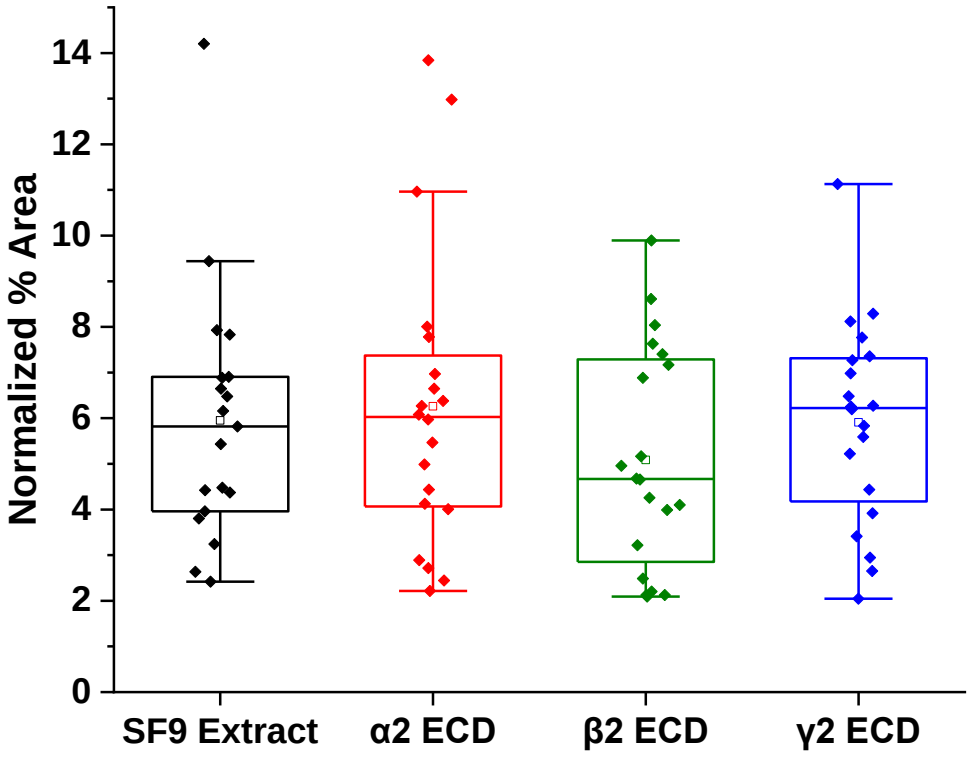

Figure 4.3.25

Quantitative analysis of the % area of synaptic contacts between the $\alpha_2\beta_2\gamma_2$-$GABA_A$ receptor-expressing HEK293 cells and embryonic medium spiny neurons. The % area values were normalized with the expression of NL2. The application of the ECDs exerted no significant effect on the synapse formation. The box and whisker plot shows the mean (square dot with no fill), median (horizontal line), standard deviation of the mean (whiskers) and the outliers (square dot black fill). Data from n = 19 $\alpha_2\beta_2\gamma_2$-$GABA_A$ receptor-expressing HEK293 cells treated with SF9, n = 20 treated with α_2 subunit ECD, n = 20 treated with β_2 subunit ECD, and n = 20 treated with γ_2 subunit ECD; N = 2 independent experiments. Shapiro-Wilk normality test was used to test the normal distribution of the data and Kruskal Wallis ANOVA followed by Dunn's test was used to analyze the statistical significance of the difference. (* $p < 0.05$)

4.3.6.2 $GABA_A$ Receptor γ_2 Subunit Intracellular Loop is Important for Synergistic Effects of $GABA_A$ Receptors and NL2 in Synapse Formation

A chimera of the $GABA_A$ receptor δ subunit ($\delta^{\gamma 2ICL}$) (Hannan et al., 2020), in which the large intracellular loop (TM 3-4) was replaced with the TM 3-4 sequence of the γ_2 subunit, was used to study whether and how the intracellular loop of $GABA_A$ receptor γ_2 subunit may contribute to synapse formation in the presence of NL2. The TM 3-4 loop sequence shows a low level of similarity between the δ and γ_2 subunits (~ 45%) (Hannan et al., 2020). B2 clone of HEK293 cells stably expressing the β_3 subunit was transfected to express $NL2^{cherry}$ and α_2 + γ_2, α_2 + $\delta^{\gamma 2ICL}$, or α_2 + δ subunits and cultured with embryonic medium spiny neurons at 37 ℃ with 5 % CO_2 for 24 hours (Figure 4.3.26).

Quantification of the % area of co-localized pixels that represents contacts between presynaptic Bassoon and NL2 on HEK293 cell surface demonstrated a significant increase in synapse formation in the presence of $\alpha_2\beta_3\delta^{\gamma 2ICL}$- when compared to $\alpha_2\beta_3$δ-$GABA_A$ receptors (median = 2.42 %; IQR = 1.12 % – 4.06 %; n = 32 cells *vs.* median = 1.42 %; IQR = 0.78 % – 2.49 %; n = 30 cells, respectively; from N = 2 independent experiments, $p < 0.05$). The presence of γ_2 subunit resulted in significantly higher level of synaptic contacts (median = 2.72 %; IQR = 1.63 % – 5.15 %; n = 31 cells; from N = 2 independent experiments) than δ subunit but not significantly different from δ chimera subunit (Figure 4.3.27).

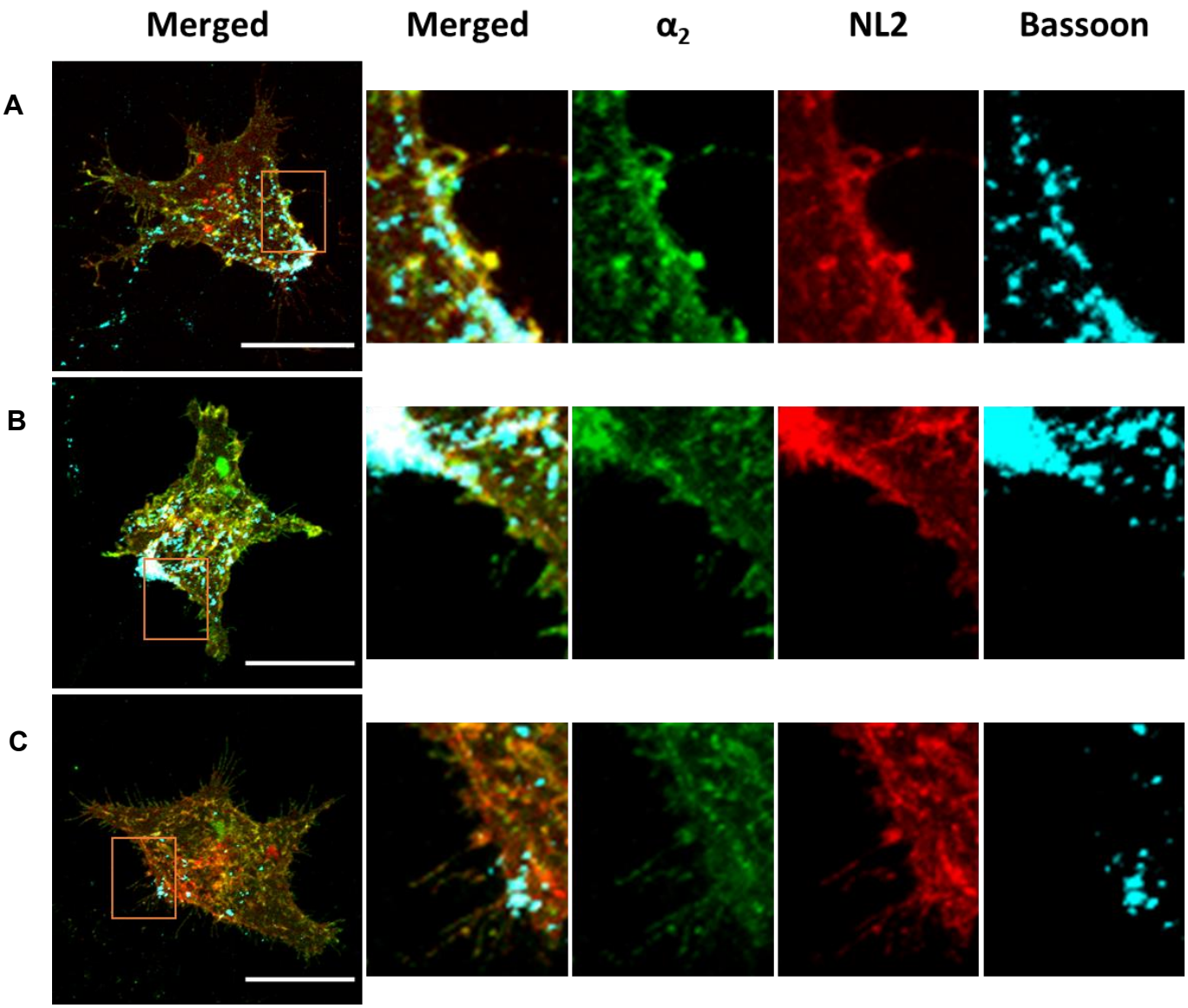

Figure 4.3.26

Synaptic contact formation in co-culture of HEK293 cells and embryonic medium spiny neurons. HEK293 cells expressing NL2 + (A) $\alpha_2\beta_3\gamma_2$-$GABA_A$ receptors, (B) $\alpha_2\beta_3\delta^{\gamma 2ICL}$-$GABA_A$ receptors or (C) $\alpha_2\beta_3\delta$-$GABA_A$ receptors were incubated in co-culture with medium spiny neurons for 24 hours. NL2 was tagged with pcherry (red); synaptic terminals were labelled with Bassoon antibody (cyan); and $GABA_A$ receptors were visualized with α_2 subunit specific antibody (green). Scale bar = 20 μm. Fluorescent imaging was done using Zeiss 700 confocal microscope at 63 × magnification with image size 512 × 512. Max intensity projection of the z-stack images was shown. The enlarged images are 10 × zoom in.

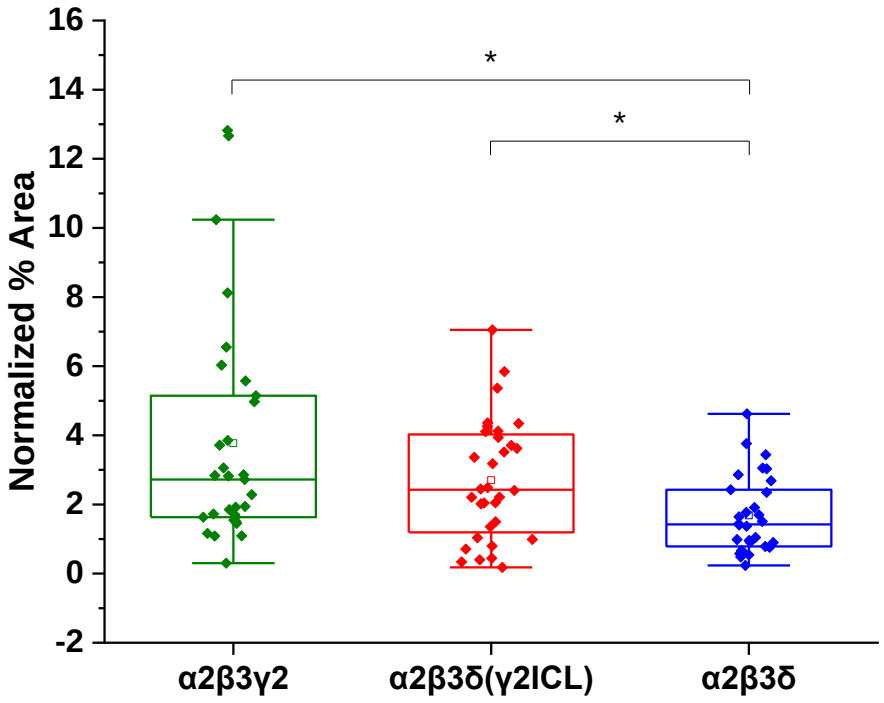

Figure 4.3.27

Quantitative analysis of the % area of synaptic contacts between HEK293 cells expressing $\alpha_2\beta_3\gamma_2$-$GABA_A$ receptors, $\alpha_2\beta_3\delta^{\gamma 2ICL}$-$GABA_A$ receptors or $\alpha_2\beta_3\delta$-$GABA_A$ receptors and embryonic medium spiny neurons. The % area values were normalized with the expression of NL2. The normalized % area is significantly higher in $\alpha_2\beta_3\gamma_2$ and $\alpha_2\beta_3\delta^{\gamma 2ICL}$ group when compared to $\alpha_2\beta_3\delta^{\gamma 2ICL}$ than $\alpha_2\beta_3\delta$ group. The box and whisker plot shows the mean (square dot with no fill), median (horizontal line), standard deviation of the mean (whiskers) and the outliers (square dot black fill). Data from n = 31 $\alpha_2\beta_3\gamma_2$-$GABA_A$ receptor-, n = 32 $\alpha_2\beta_3\delta^{\gamma 2ICL}$-$GABA_A$ receptor-, and n = 30 $\alpha_2\beta_3\delta$-$GABA_A$ receptor-expressing HEK293 cells; N = 2 independent experiments. Shapiro-Wilk normality test was used to test the normal distribution of the data and Kruskal Wallis ANOVA followed by Dunn's test was used to analyze the statistical significance of the difference. (* $p < 0.05$)

4.3.6.3 $GABA_A$ Receptors and NL2 Interact via Their Intracellular Domain to Promote Synapse Formation

Neurexin-Neuroligin 2 interaction is important for the formation of functional GABAergic synapses (Südhof, 2018). However, initiation of GABAergic synapses is not solely dependent on this interaction (Varoqueaux et al., 2006). Given that synapses can be initiated by $GABA_A$ receptors in the absence of NL2 but also further increased when $GABA_A$ receptors and NL2 are co-expressed, I have hypothesized that Neurexin, NL2 and $GABA_A$ receptors may interact with each other during this process to initiate, stabilize and/or maintain functional GABAergic synapses.

To test this hypothesis, I have first attempted to co-immunoprecipitate these proteins from the brain lysates. Adult male rat cortex was lysed under non-denaturing conditions and incubated with Dithiobis (succinimidyl propionate) (DSP, Thermo Fisher) to cross-link and preserve protein-protein interactions. Co-immunoprecipitation was carried out with a $GABA_A$ receptor α_1 subunit C-terminal-specific antibody as described in the section 4.2.5. Protein complexes were resolved using SDS-PAGE and immunoblotting was carried out in the presence of NL2-specific antibody (1:1000; 129203, Synaptic Systems). A band corresponding to the molecular weight of NL2 was detected in immunoprecipitates of the α_1 subunit while no band was detected with the non-immune control IgG (Figure 4.3.28). This confirms that NL2 forms complexes with $GABA_A$ receptors in the brain.

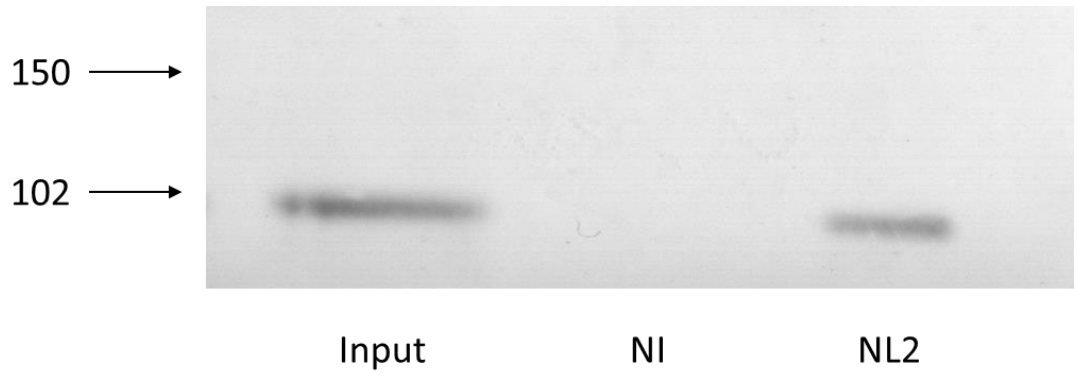

Figure 4.3.28

NL2 interacts with the α_1 subunit-containing $GABA_A$ receptors in the adult male rat cortex extracts detected by co-immunoprecipitation. Immunoprecipitation was carried out with the α_1 subunit C-terminal-specific antibody. Input contained 100 µg lysates. For immunoprecipitation, 2.5 mg protein was used. NL2 was detected using a specific primary antibody followed by alkaline phosphatase-conjugated secondary antibody and NBT/BCIP color substrate reaction. Representative blot of N = 2 independent experiments.

Because detection of Neurexins was low in total brain lysates used for co-immunoprecipitation, I used the synaptic membrane enriched fraction (P2) of brain lysates to attempt to co-immunoprecipitate $GABA_A$ receptors with Neurexins. The enrichment of $GABA_A$ receptor α_1 subunit, NL2 and Neurexins, but not $GABA_A$ receptor α_4 subunit was first demonstrated by immunoblotting in cortical lysate fractions (Figure 4.3.29A-C).

Using the P2 fraction, Neurexins were immunoprecipitated with $GABA_A$ receptors using the α_2 subunit C-terminal-specific antibody (Figure 4.3.30) and detected by a Neurexin1/2/3-specific antibody (1:800; 175003, Synaptic Systems). A very faint band was detected corresponding to the molecular weight of α-Neurexin, which suggests that $GABA_A$ receptor-Neurexin interaction may not be as strong as interaction with NL2.

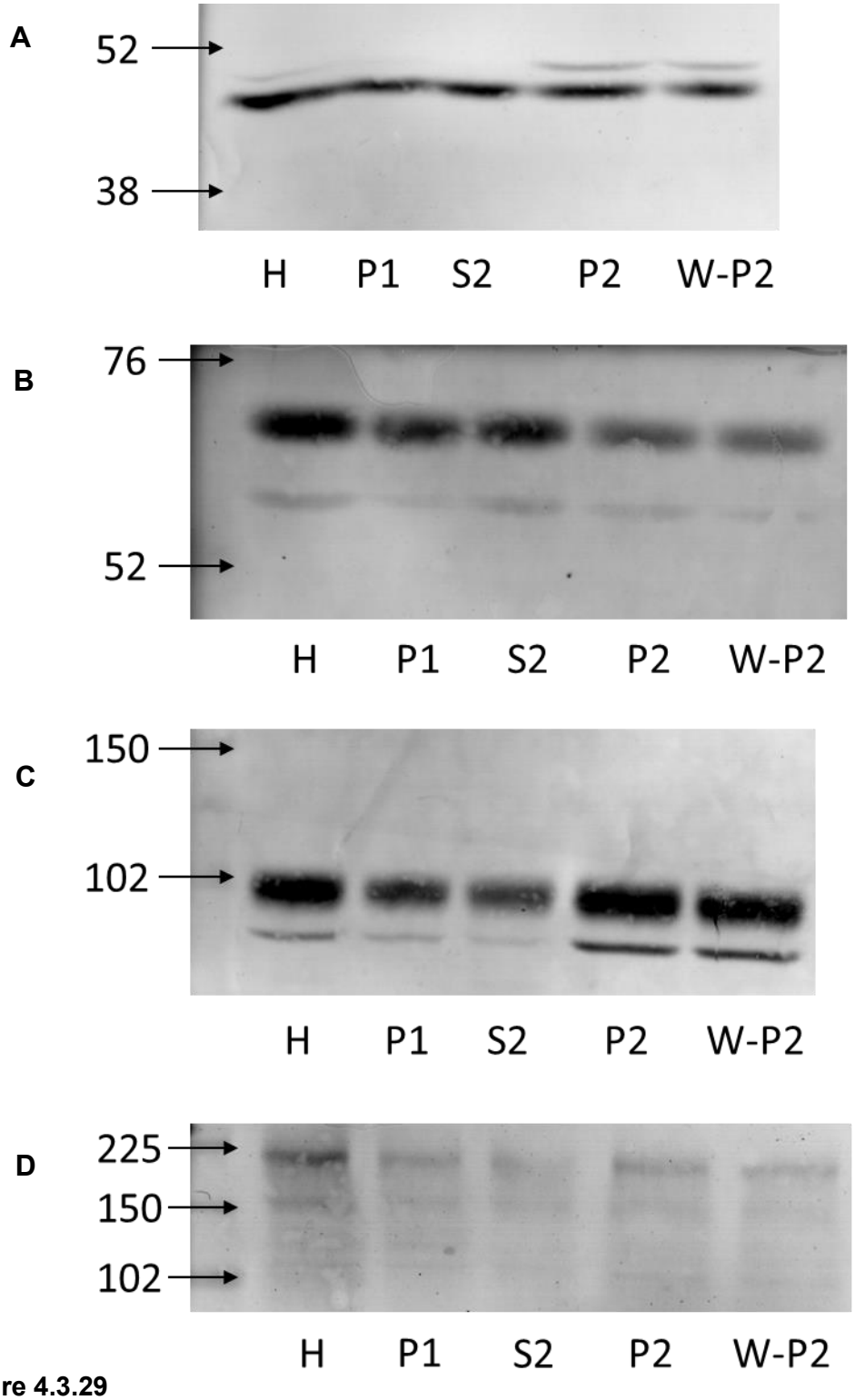

Figure 4.3.29

Characterization of (A) $GABA_A$ receptor α_1 subunit, (B) $GABA_A$ receptor α_4 subunit, (C) NL2, and (D) Neurexin expression in P2 synaptosome fraction in adult male rat cortex extracts. For each fraction 100 µg protein was loaded. Expression of each protein was visualized using alkaline phosphatase conjugated secondary antibody and NBT/BCIP color substrate reaction. H-Homogenate; P-Pellet; S-Supernatant; H-Washed with HBM.

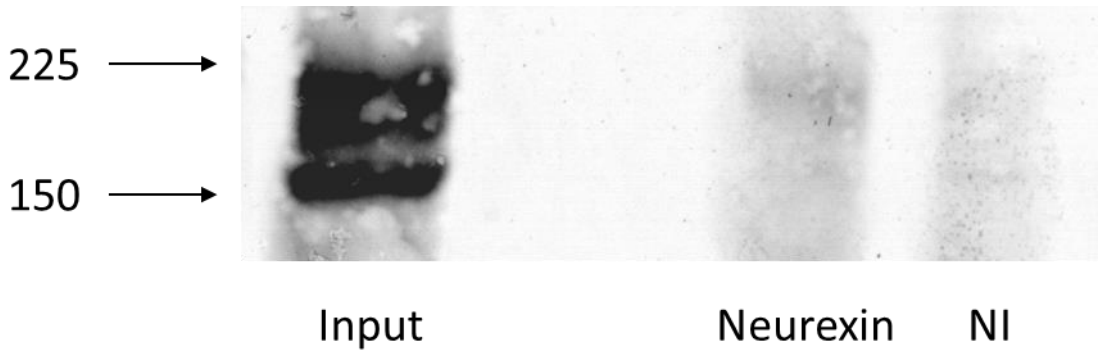

Figure 4.3.30

Neurexin interacts with the α_2 subunit containing $GABA_A$ receptors in P2 synaptosome fraction of the adult male rat cortex extracts detected by co-immunoprecipitation. Input contained 200 µg lysates. For immunoprecipitation, 1 mg of protein was used. Neurexin was visualized using Neurexin1/2/3-specific primary antibody followed by alkaline phosphatase conjugated secondary antibody and NBT/BCIP color substrate reaction. Representative blot of N = 2 independent experiments.

To confirm the interaction between $GABA_A$ receptors and NL2, I used lysates of HEK293 cells transiently transfected with myc-tagged $GABA_A$ receptor α_2, β_3 and γ_2 subunits and NL2. Co-immunoprecipitation was carried out using myc-specific antibody (10 µg per reaction; 05-724, Millipore), followed by immunoblotting with NL2-specific antibody (1:1000; 129203, Synaptic Systems). A band corresponding to NL2 was detected in lanes with proteins pulled down with the myc antibody (Figure 4.3.31), but not in lanes with the control, non-specific IgG. This indicates that $GABA_A$ receptors and NL2 interact in HEK293 cells possibly even in the absence of Gephyrin and Collybistin which were previously shown to mediate interaction between $GABA_A$ receptors and NL2 (Poulopoulos et al., 2009).

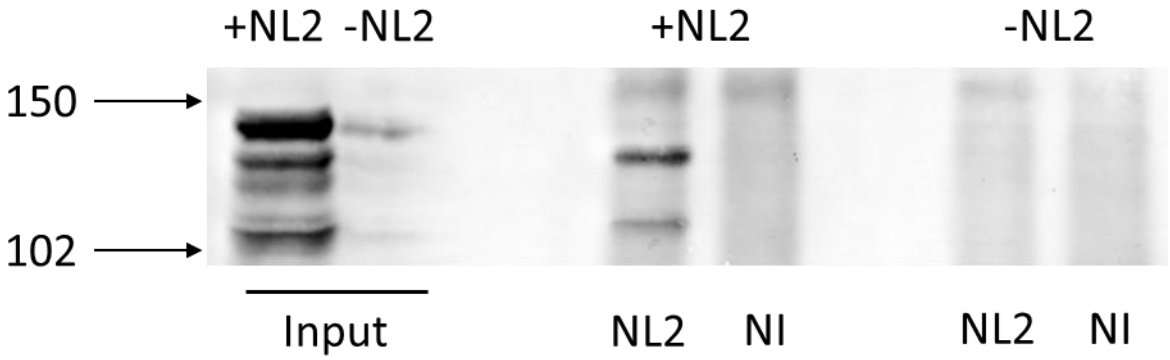

Figure 4.3.31
NL2 interacts with the $\alpha_2\beta_3\gamma_2$-$GABA_A$ receptors in HEK293 cell lysates detected by co-immunoprecipitation. The $GABA_A$ receptor subunits were myc tagged. The immunoprecipitation was carried out with myc-specific antibody. Input contained 100 µg lysates. For immunoprecipitation 2.5 mg protein was used. NL2 was visualized using a specific primary antibody followed by an alkaline phosphatase-conjugated secondary antibody and NBT/BCIP color substrate reaction. Representative blot of N = 2 independent experiments.

To further investigate the interaction between $GABA_A$ receptors and NL2, $NL2^{HA}$ and $GABA_A$ receptor subunits-α_2, β_3 and γ_2 cDNAs were transfected to HEK293 cells as described in section 4.2.3, of which all $GABA_A$ receptor subunits were tagged with myc sequence. HA-specific antibody was used to pull down protein complex from the lysate for immunoprecipitation, followed by immunoblotting with β_3 subunit-specific antibody (1:400; UCL112) or NL2-specific antibody (1:1000; 129203, Synaptic Systems). A band corresponding to NL2 was detected from the pulled down protein confirming the immunoprecipitation of NL2 by HA-specific antibody (Figure 4.3.32A). A band corresponding to the β_3 subunit was also detected in the same pull down (Figure 4.3.32B), confirming that NL2 and $GABA_A$ receptors interact with each other in HEK293 cells.

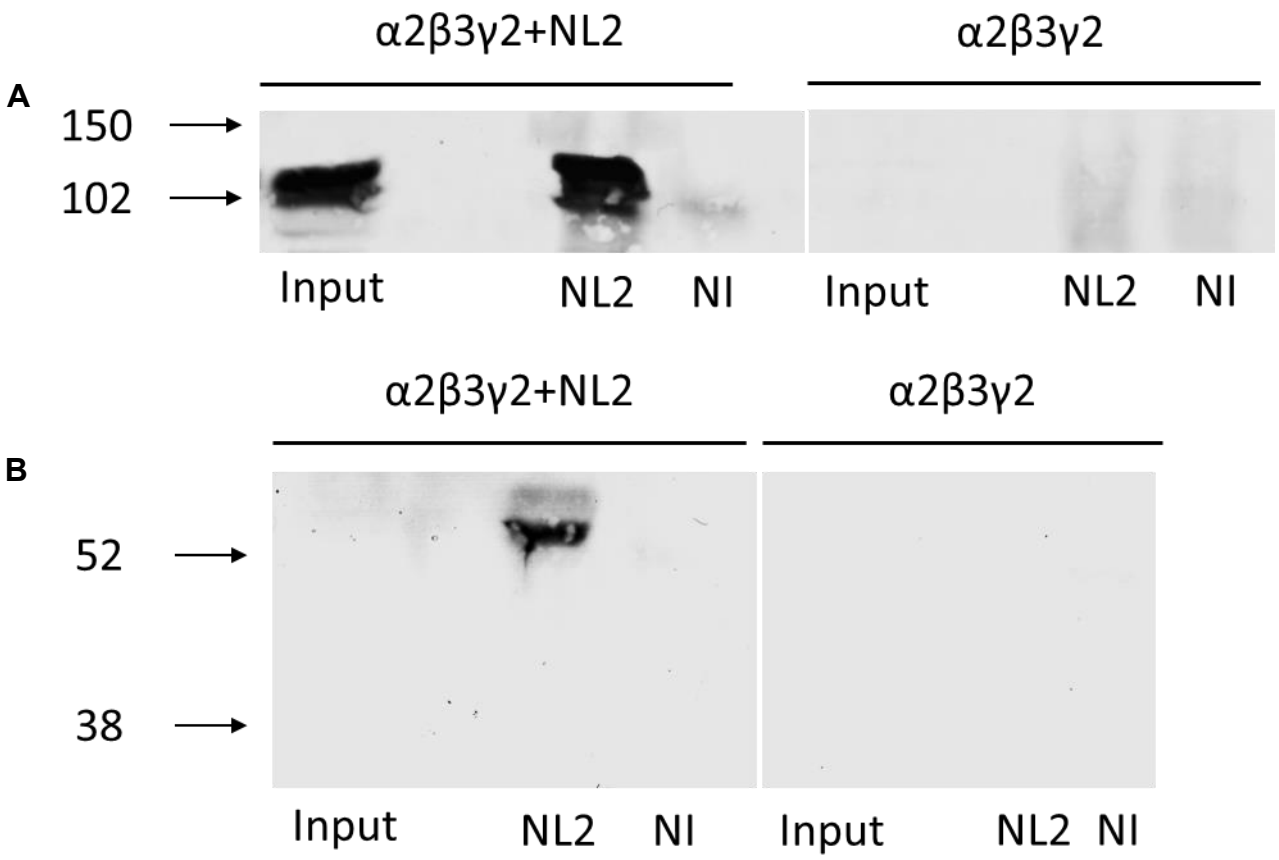

Figure 4.3.32

NL2 interacts with the $\alpha_2\beta_3\gamma_2$-$GABA_A$ receptors in HEK293 cell lysates detected by co-immunoprecipitation. The $GABA_A$ receptor subunits were myc tagged. NL2 was HA tagged. The immunoprecipitation was carried out with HA-specific antibody. (A) Detection of NL2 using specific primary antibody from proteins pulled down using HA-tag antibody. (B) Detection of β_3 specific antibody from proteins pulled down with HA-tag antibody. Input contained 100 µg lysates. For immunoprecipitation 2.5 mg protein was used. NL2 and $GABA_A$ receptor β_3 subunit were visualized using alkaline phosphatase-conjugated secondary antibody and NBT/BCIP color substrate reaction. Representative blot of N = 2 independent experiments.

Our results shown in Figures 4.3.11 and 4.3.26 have demonstrated the importance of the γ_2 subunit and, in particular, the TM3-4 intracellular loop of this subunit for the synergistic effects of $GABA_A$ receptors and NL2 in synapse formation. In order to test if these synergistic effects may be mediated by direct interaction between NL2 and $GABA_A$ receptors, transfection experiments were designed to compare the binding of NL2 to $\alpha_2\beta_3\gamma_2$-, $\alpha_2\beta_3\delta^{\gamma 2ICL}$ - or $\alpha_2\beta_3\delta$-$GABA_A$ receptors in HEK293 cells, conditions that showed clear difference in efficacy of synaptic contact formation (Figure 4.3.33).

The NL2 and α_2 + β_3 + $\gamma_{2,}$, α_2 + β_3 +$\delta^{\gamma 2ICL}$, or α_2 + β_3 +δ subunit cDNAs were transfected into HEK293 cells as described in section 4.2.3. The β_3 subunit was myc tagged. Myc-specific antibody (10 µg per reaction; 05-724, Millipore) was used to pull down protein complexes from the lysates and β_3 subunit-specific antibody (1:400; UCL112) or NL2-specific antibody (1:1000; 129203, Synaptic Systems) were used to detect presence of these proteins by immunoblotting.

In the $\alpha_2\beta_3\gamma_2$-$GABA_A$ receptor/NL2 expressing HEK293 cells, a clear band corresponding to the right molecular weight for NL2 was detected while no band was detected in $\alpha_2\beta_3\delta$-$GABA_A$ receptor/NL2 expressing HEK293 cells (Figure 4.3.32A). In the $\alpha_2\beta_3\delta^{\gamma 2ICL}$-$GABA_A$ receptor/NL2 expressing HEK293 cells, a band corresponding the right molecular weight for NL2 was detected, albeit relatively faint compared to the band detected in $\alpha_2\beta_3\gamma_2$-$GABA_A$ receptor/NL2 expressing HEK293 cells (Figure 4.3.32A). The β_3 subunit-specific antibody confirmed the presence of $GABA_A$ receptors in immunoprecipitates (Figure 4.3.32B).

These data together with confocal analysis in section 4.3.4.2, suggest that synapse formation may require direct interactions between NL2 and $GABA_A$ receptors. The TM 3-4 intracellular loop of the γ_2 subunit was shown to play an essential role in this interaction, given that the δ subunit chimera with TM 3-4 loop replaced by the equivalent sequence from the γ_2 subunit significantly increased this interaction as well as facilitated synapse formation.

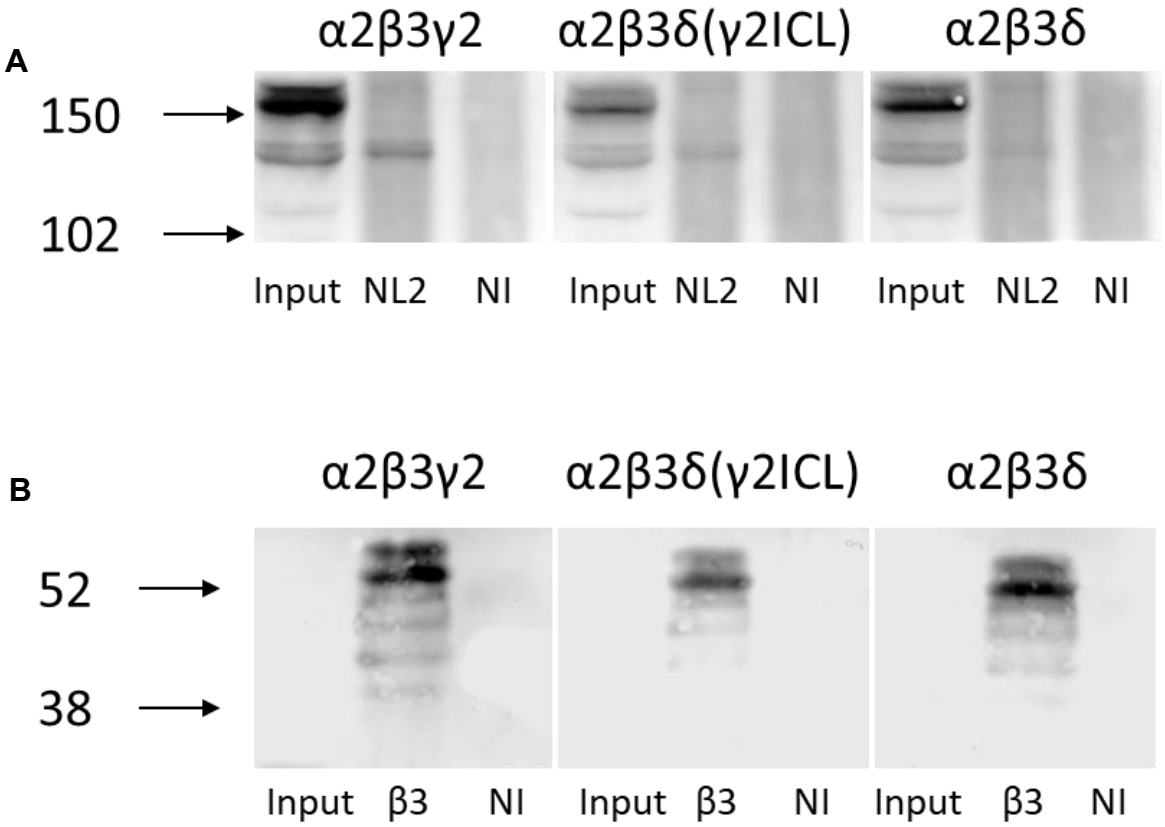

Figure 4.3.33

NL2-$GABA_A$ receptor interaction in the presence of the γ_2 subunit intracellular TM 3-4 loop domain detected by co-immunoprecipitation. The β_3 subunit was myc tagged. The immunoprecipitation was carried out with the myc-specific antibody. (A) Detection using the NL2-specific antibody from proteins pulled down using the myc-specific antibody. (B) Detection using the β_3 subunit-specific antibody from proteins pulled down using the myc-specific antibody. Input contained 100 µg lysates. For immunoprecipitation 2.5 mg protein was used. NL2 and $GABA_A$ receptor β_3 subunit were visualized using alkaline phosphatase conjugated secondary antibody and NBT/BCIP color substrate reaction. Representative blot of N = 2 independent experiments.

4.4 Discussion

Regulation of GABAergic synapse formation and function is achieved by multiple factors. The complexity and diversity of the proteins present in the pre- and postsynaptic membranes and the synaptic cleft bring a huge difficulty to the study of GABAergic synapses. A well-established co-culture model system of HEK293 cells and embryonic rat medium spiny neurons has been used in our lab to study the role of $GABA_A$ receptors and the associating proteins in the GABAergic synapses (Brown et al., 2014). The co-culture model system provides a platform to study the effects of individual proteins or interaction between a small number of proteins on the formation and function of the GABAergic synapse, although this method overlooks the effects of multiprotein complexes and is thus considered as an overly simplified system. With the expression of proteins in HEK293 cells, and the presynaptic proteins by the embryonic rat medium spiny neurons, the synaptogenesis process can be investigated using immunocytochemistry and microscopic imaging.

To investigate the role of different $GABA_A$ receptors in the formation of GABAergic synapses, HEK293 cell lines stably expressing typical synaptic $\alpha_2\beta_2\gamma_2$-$GABA_A$ receptors and typical extrasynaptic $\alpha_4\beta_3\delta$-$GABA_A$ receptors were tested in parallel. It has been shown that certain subtypes of $GABA_A$ receptors, which are mainly synaptically localized, are able to initiate inhibitory synapse formation and that this process is mediated by their N-terminal ECDs (Fuchs et al., 2013; Brown et al., 2016). The significant increase in synapse formation in

the presence of $\alpha_2\beta_2\gamma_2$-$GABA_A$ receptors (Figure 4.3.5) is consistent with these findings. In comparison, the $\alpha_4\beta_3\delta$-$GABA_A$ receptors were shown to have no effect on GABAergic synapse formation under the same conditions (Figure 4.3.2). The expression of $\alpha_4\beta_3\delta$-$GABA_A$ receptors in HEK293 cells resulted in a general distribution of $\alpha_4\beta_3\delta$-$GABA_A$ receptors on the cell surface. Although the δ subunit has been shown to restrict the extrasynaptic localization of the δ-containing $GABA_A$ receptors in neurons (Martenson et al., 2017), a great proportion of $\alpha_4\beta_3\delta$-$GABA_A$ receptors are likely to be present in the synaptic domain in any given time in our co-cultures in the absence of a full repertoire of postsynaptic proteins. In contrast, the γ_2 subunit-containing $GABA_A$ receptors which are restricted to the synaptic domains in neurons appear to be more abundant in the postsynaptic domain in co-cultures although not exclusively present here (Figure 4.3.22). At the same time, these receptors have the ability to induce the formation of synaptic contacts if in a combination with certain α and β subunits (Brown et al., 2016).

Previous work from our lab has revealed synaptogenic effects of the $\alpha_2\beta_2\gamma_2$-$GABA_A$ receptors and possible synergistic effects of $GABA_A$ receptors and NL2 in GABAergic synapse formation (Fuchs et al., 2013). The current experiments have confirmed these synergistic effects but also showed that synaptic contact formation can be increased even in the presence of the $\alpha_4\beta_3\delta$-$GABA_A$ receptors, although significantly less than in the presence of the $\alpha_2\beta_2\gamma_2$-$GABA_A$ receptors (Figure 4.3.8). These effects are not affected by the activity of $GABA_A$ receptors (Figure 4.3.12 - 4.3.17), as previously observed in the absence of NL2 (Brown et

al., 2016). However, electrophysiological recordings showed that no signal transmission was detected in these NL2/$\alpha_4\beta_3\delta$-$GABA_A$ receptor-induced synapses (Figure 4.3.18). Therefore, the localization of the $\alpha_2\beta_2\gamma_2$- and $\alpha_4\beta_3\delta$-$GABA_A$ receptors in the presence of NL2 was investigated with SIM super-resolution imaging, which showed that a significantly higher proportion of synaptic contacts were observed to contain the $\alpha_2\beta_2\gamma_2$-$GABA_A$ receptors than $\alpha_4\beta_3\delta$-$GABA_A$ receptors in the co-culture (Figure 4.3.23A). This is in line with the findings that the $\alpha_2\beta_2\gamma_2$-$GABA_A$ receptors are more potent in inducing synapse formation than the $\alpha_4\beta_3\delta$-$GABA_A$ receptors in the presence of NL2 (Figure 4.3.8). The difference in the proportion of the $\alpha_2\beta_2\gamma_2$- and $\alpha_4\beta_3\delta$-$GABA_A$ receptors that were co-localized with the presynaptic active zone protein Bassoon was also reduced but not significant level (Figure 4.3.23B). This suggests that the vast majority of the GABAergic synapses formed with $\alpha_4\beta_3\delta$-$GABA_A$ receptor/NL2 expressing-HEK293 cells lacked the functional postsynaptic $GABA_A$ receptors which are able to mediate IPSCs in response to GABA. These results have raised a question about what may be the reason for the lack of postsynaptic responses given that extrasynaptic $\alpha_4\beta_3\delta$-$GABA_A$ receptors, with higher GABA affinity (Brown et al., 2002), are expected to mediate postsynaptic electrophysiological responses if present in the vicinity of GABA-releasing presynaptic terminals. One possible explanation could be that the presynaptic release of GABA may be impaired in synapses formed in the presence of the $\alpha_4\beta_3\delta$-$GABA_A$ receptors and NL2. Synaptotagmin-specific antibody was therefore used to label active

presynaptic terminals that undergo synaptic vesicle exocytosis and release of GABA in these co-cultures (Figure 4.3.19). While most of the presynaptic terminals were active in the presence of NL2 and $\alpha_2\beta_2\gamma_2$-$GABA_A$ receptors, significantly lower proportion of the presynaptic terminals were active in the presence of NL2 alone or with $\alpha_4\beta_3\delta$-$GABA_A$ receptors (Figure 4.3.20). Therefore, the lack of IPSCs detected in co-cultures in the presence of NL2 and $\alpha_4\beta_3\delta$-$GABA_A$ receptors can be partially explained by a reduction in GABA release from presynaptic terminals. This suggests a role of the $\alpha_2\beta_2\gamma_2$-$GABA_A$ receptors in facilitating the functional maturation of presynaptic terminals in addition to their "structural" role in inducing synaptic contact formation. In summary, while both $\alpha_2\beta_2\gamma_2$- and $\alpha_4\beta_3\delta$-$GABA_A$ receptors show synergistic effects when co-expressed with NL2, the induced synapses are fully functional, *i.e.* releasing sufficient amount of GABA, in the presence of the $\alpha_2\beta_2\gamma_2$-$GABA_A$ receptors and NL2.

The role of the γ_2 subunit in combination with certain α and β subunits, in inducing functional GABAergic synapse innervation on HEK293 cells in co-culture has been characterized previously (Brown et al., 2016). This is in agreement with the fact that the γ_2 subunit is specifically concentrated in synapses in most of the brain regions (Somogyi et al., 1996). Although the $\alpha_2\beta_3\gamma_2$-$GABA_A$ receptors were not as effective as other synaptic $GABA_A$ receptor subtypes tested in the absence of NL2 (Brown et al., 2016), in the current study, these receptors were significantly more active than $\alpha_2\beta_3\delta$-, $\alpha_4\beta_3\gamma_2$-, or $\alpha_4\beta_3\delta$-$GABA_A$ receptors in inducing synapse formation in the presence of NL2 (Figure

4.3.11). This suggests a different underlying mechanism in inducing GABAergic synapse formation in the presence of NL2. This is further supported by my findings that application of purified N-terminal ECDs of α_2, β_2 and γ_2 subunits did not affect the synaptic contact formation in the presence of NL2 (Figure 4.3.24), although these proteins were able to reduce synapse formation in the absence of NL2 (Brown et al., 2016). Therefore, in the presence of NL2, the formation of GABAergic synapses is independent of the ECDs of $GABA_A$ receptor subunits in the co-culture. On the contrary, the intracellular loop between TM 3-4 of the γ_2 subunit was shown to be important for synergistic effects between $GABA_A$ receptors and NL2 in inducing synapse formation (Figure 4.3.26). The co-immunoprecipitation of NL2 and γ_2 or δ^{ICL2} subunit, but not δ subunit, suggests that this synergistic effect is dependent on the interaction between NL2 and $GABA_A$ receptor via the intracellular loop of the γ_2 subunit (Figure 4.3.33). The diffusion of the δ subunit was shown to be predominantly constrained outside the GABAergic synapses possibly due to the intracellular loop TM3-4 interacting with an unknown protein which is restricted to the extrasynaptic domain. This constraint can be largely relieved by replacing this loop with the γ_2 equivalent (Hannan et al., 2020). Therefore, the intracellular loop TM3-4 of the γ_2 subunit is crucial for the synaptic localization of $GABA_A$ receptors possibly due to binding to NL2 in the GABAergic synapses. This is in agreement with the findings that the δ subunit prevents the $GABA_A$ receptor assembly with GARLH4 and NL2, which is preferable with the γ_2 subunit (Martenson et al., 2017). GARLH4 has been

recently identified to facilitate the synaptic localization of the γ_2 subunit-containing $GABA_A$ receptors as an auxiliary protein in a complex with the γ_2 subunit-containing $GABA_A$ receptors and NL2 (Yamasaki et al., 2017). However, using GARLH specific antibody, the expression of GARLH was not detected in HEK293 cells (not shown) from which overexpressed $GABA_A$ receptor and NL2 could be co-immunoprecipitated (Figure 4.3.31 – Figure 4.3.33). This result indicated while the auxiliary chaperone protein GARLH4 can facilitate $GABA_A$ receptor and NL2 interaction, it may not be necessary for it to occur. NL2 may interact with $GABA_A$ receptors directly via binding of their intracellular domains, as well as via GARLH4. Therefore, GARLH4 may be important for stabilizing $GABA_A$ receptor-NL2 interactions at synaptic contacts and holding them together (Martenson et al., 2017). However, a direct interaction between the γ_2 subunits and NL2 requires to be tested further.

The interaction between α-Neurexin and α_2 subunit-containing $GABA_A$ receptors was demonstrated using co-immunoprecipitation (Figure 4.3.30), but the results were inconsistent which suggests that this interaction may be indirect possibly occurring via $GABA_A$ receptor interaction with NL2. Although, β-Neurexin has been shown to directly bind to the α_1 subunit N-terminal ECD *in vitro* (Zhang et al., 2010), this interaction has not been confirmed *in vivo*. While knock-out of α-Neurexin has been shown to have a limited effect on GABAergic synapse formation, the impairment in both spontaneous and evoked vesicular release of GABA was clearly demonstrated (Missler et al., 2003). Moreover, the knock-out

of NL2 was also shown to impair GABAergic synaptic transmission without affecting synapse numbers (Zhang et al., 2015). These suggest that NL2 may play an essential role in facilitating the presynaptic vesicle release by binding to Neurexin as an “on” switch of the synaptic transmission activities. Moreover, this induction of the presynaptic activity may require the γ_2 subunit-containing $GABA_A$ receptors in interaction with NL2 via their intracellular domains.

In summary, this study has revealed a different mechanism underlying the formation of $GABA_A$ receptor-induced GABAergic synapses in the presence of NL2-Neurexin complex in the co-culture. A synergistic effect between $GABA_A$ receptors and NL2 was confirmed, with the synaptic $\alpha_2\beta_2\gamma_2$-$GABA_A$ receptors being more prominent than the extrasynaptic $\alpha_4\beta_3\delta$-$GABA_A$ receptors. The synergistic effect may be facilitated by interaction between the TM3-4 intracellular loop of the γ_2 subunit and NL2, which may influence indirectly the NL2 interaction with the presynaptic Neurexins leading to activation of the presynaptic release of GABA. How these mechanisms operate together with other proteins shown to be important for synapse formation and synaptic clustering of $GABA_A$ receptors, such as Gephyrin or GARLH4, requires further investigations.

5. GABAergic Synapse Formation can be Initiated by Pikachurin and Diazepam Binding Inhibitor

5.1 Introduction

5.1.1 Cell Adhesion Molecules in GABAergic Synapses

GABAergic synapse is categorized as Gray's type II synapse which contains relatively simple postsynaptic density (PSD) with a similar size to the presynaptic active zone (Sassoè-Pognetto et al., 2011). Although the number of proteins present in GABAergic synapses may not be as high as in glutamatergic synapses, many of these proteins play an important role in inducing GABAergic synapse formation and functional maturation (Sassoè-Pognetto et al., 2011; Lu, Bromley-Coolidge and Li, 2017; Südhof, 2018). The establishment of a functional GABAergic synapse requires precise recognition and connection between the presynaptic neuronal terminal with specific region of the postsynaptic neuronal membrane. However, the molecular and cellular mechanisms for the formation of GABAergic synapses have not been fully elucidated.

5.1.1.1 Dystroglycan

Dystroglycan is the key component of the DGC which is essential for the connection of the neuronal actin cytoskeleton and the extracellular matrix in the brain (Henry and Campbell, 1996). Dystroglycan is composed of two subunits: extracellular α-dystroglycan which binds to a variety of proteins including Laminins, Neurexins and Pikachurin (Bello et al., 2015), and β-Dystroglycan,

which anchors the α-Dystroglycan. The Dystroglycan gene is widely expressed within the human body and it can be found in cardiac and skeletal muscles, brain, kidney, liver, lung, diaphragm, placenta, pancreas and stomach (Ibraghimov-Beskrovnaya et al., 1992). In the brain, Dystroglycan can be found in neurons of the cerebral cortex, hippocampus, olfactory bulb, basal ganglia, thalamus, hypothalamus, brainstem and cerebellum and has been shown to be essential for the early development of the basal lamina as a receptor for Laminins (Bello et al., 2015).

In the early development of the brain, Dystroglycan is important for the proliferation and differentiation of the neuroepithelial cells as these processes are influenced by the impaired Dystroglycan function (Schröder et al., 2007) which can lead to a range of brain abnormalities, from a mild cognitive impairment to neuronal migration disorders (Waite, Brown and Blake, 2012). In the mature brain, Dystroglycan is closely associated with GABAergic synapses in which it is essential for the formation of DGC while it is not detectable in glutamatergic synapses (Lévi et al., 2002). Dystroglycan plays an essential role in the clustering of GABAergic postsynaptic proteins such as α_1-containing $GABA_A$ receptors, NL2 and Gephyrin, and is required for the maintenance of functional GABAergic synapses (Briatore et al., 2020).

5.1.1.2 Pikachurin

In the retina, a complex formed between Dystroglycan and Pikachurin is essential for the formation of the photoreceptor ribbon synaptic structures (Sato et al., 2008,

Omori et al., 2012). The mRNA of Pikachurin and the expressed protein were also detected in the brain (Sato et al., 2008, Allen Brain Atlas). Pikachurin is an extracellular matrix-like protein which was initially identified as a presynaptic Dystroglycan ligand containing three Laminin globular (G) domains (Sato et al., 2008).

Expression of Dystroglycan is essential for localization of Pikachurin to the synapses and *vice versa* (Omori et al., 2012). Laminin was shown to facilitate the expression and stability of the DGC and Pikachurin complex in the retinal synapses as well as formation and stabilization of these synapses (Hunter et al., 2017). Moreover, a postsynaptic receptor GPR179 has been identified recently as a binding partner for Dystroglycan-Pikachurin complex, which is essential for the synaptic organization in the retina (Orlandi et al., 2018). The transsynaptic interaction between GPR179 and DGC via Pikachurin plays an essential role in coordinating the structure and signal transmission at synapses formed by ON-bipolar neurons and the presynaptic photoreceptors in the retina (Dunn, Orlandi and Martemyanov, 2019). A previous proteomic screen for proteins that bind to $GABA_A$ receptor subunits in our lab revealed that Pikachurin can bind to the N-terminal extracellular domain of $GABA_A$ receptor α_2 subunit. This binding was subsequently confirmed in *in vitro* binding assays and co-immunoprecipitation of Pikachurin and α_2 subunit from cortical and striatal lysates (Jessica Arama, PhD Thesis). These results suggest that Pikachurin may play an important role in the formation and maintenance of GABAergic synapses.

5.1.1.3 Diazepam Binding Inhibitor

Diazepam binding inhibitor (DBI) is a ~10 kDa polypeptide that inhibits the binding of diazepam to $GABA_A$ receptors (Ala and MI, 1983, Barbaccia et al., 1991). DBI is secreted in the unconventional secretory pathway named exophagy (Abrahamsen and Stenmark, 2010), in which the cytosolic DBI lacking a signal peptide is sequestered into the autophagosomes transported to the cell membrane and released into the extracellular space (Abrahamsen and Stenmark, 2010). The major source of DBI in the brain are glia cells but neuronal cells can also secrete DBI (Kavaliers and Hirst, 1986).

In the brain, DBI is a precursor for two biologically active peptides: octadecaneuropeptide (ODN) and triakontatetraneuropeptide (TTN) (Costa and Guidotti, 1991, Slobodyansky et al., 1989). Both products of DBI bind to the benzodiazepine binding sites (Farzampour, Reimer and Huguenard, 2015). ODN plays an important role in protecting the neurons and astrocytes from cell death caused by oxidative stress (Masmoudi-Kouki et al., 2018) and TTN stimulates the biosynthesis of the neurosteroids from pregnenolone (Do-Rego et al., 1998).

The effects of DBI on $GABA_A$ receptors appear to depend on where in the CNS these proteins interact: DBI can act as a negative allosteric modulator in the spinal cord neurons and neural progenitors in the subventricular zone (SVZ) of the lateral ventricles (Alfonso et al., 2012), or as a positive allosteric modulator in the thalamic reticular nucleus (Christian et al., 2013). DBI has been shown to promote stem cell proliferation and expansion by reducing the ambient GABA

signals which inhibit proliferation (Alfonso et al., 2012). DBI has also been shown to be present in the neurogenic niche for both excitatory and inhibitory neurons where it affects the neurogenesis by exerting regulation on the stem cells (Dumitru et al., 2017).

However, while the allosteric modulation effect of DBI on $GABA_A$ receptors has been intensively studied, whether and how DBI influences the formation of GABAergic synapses has not been described. That DBI may play a part in the regulation of GABAergic synapses was inferred based on the fact that the long-term exposure of neurons to Diazepam leads to a loss of GABAergic synapses (Nicholson et al., 2018). We have therefore hypothesized that DBI, by inhibiting Diazepam binding to the benzodiazepine binding sites on the $GABA_A$ receptors, may have a protective role in preventing this loss and any other structural changes caused by the prolonged exposure of neurons to benzodiazepines.

5.1.2 Aim and Hypothesis

The aim of this chapter was to test the effect of Pikachurin, Dystroglycan and DBI on the formation of GABAergic synapses in the co-culture model. These proteins are all found to express within the GABAergic synapses and can interact with $GABA_A$ receptors. I have hypothesized that the formation of GABAergic synapses requires the presence and functional activities of Pikachurin and Dystroglycan, and that DBI may have a protective role on maintaining and thus have a positive effect on the GABAergic synapse formation. Therefore, the role of each of these proteins in GABAergic synapse formation were test using a well-

established co-culture model system of embryonic medium spiny neurons and HEK293 cells, stably expressing synaptic $\alpha_2\beta_2\gamma_2$-$GABA_A$ receptors.

5.2 Materials and Methods

5.2.1 Effectene Transfection

Embryonic rat medium spiny neuronal culture was prepared as described in the Chapter 20 section 2.1.2. HEK293 cells (wt or stably expressing the $\alpha_2\beta_2\gamma_2$-$GABA_A$ receptors) were plated on the 6-well plate (3×10^5 cells / well) 24 hours before transfection. After 24-hour incubation of cells in the 37℃ 5% CO_2 humidified incubator, a total of 200 ng cDNAs (GFP + Pikachurin^{cherry} / dystroglycan^{myc} / DBI^{myc}; Table 5.1) was mixed in 252.6 µl EC buffer (Qiagen) with 8.1 µl enhancer (Qiagen) for 5 minutes at room temperature after 1-second vortex. Effectene (Qiagen) was then added into the mixture (25.25 µl per 5 µg DNA) and vortexed. After 10-minute incubation at room temperature, the mixture of DNA - Effectene was added into the wells drop-by-drop. The transfected cells were incubated in the 37 ℃ 5 % CO_2 humidified incubator for 24 hours before they were detached and plated on poly-L-lysine (0.1 mg / ml) coated glass coverslips (VWR) in 24-well plates or added to rat medium spiny neurons already growing on glass coverslips for 12-13 days, to form the co-cultures.

Table 5.1 The cDNA constructs of trans-synaptic proteins used in co-cultures.

Construct	Protein	Reference
pCAG-Pikachurin-FL-mCherry	Pikachurin	Omori et al., 2012
pCMV6-myc-DDK-Dag1	Dystroglycan	OriGene
pCMV6-myc-DDK-DBI	Diazepam binding inhibitor	OriGene

5.2.2 Immunocytochemistry and Confocal Microscope Imaging

The transfected HEK293 cells were incubated at 37 ℃ with 5 % CO_2 for 24 hours and subsequently transferred to the neuronal culture. The co-culture was incubated at 37 ℃ with 5 % CO_2 for 24 hours and the fixed using 4 % PFA solution for 10 minutes at room temperature. GABAergic presynaptic terminals were labelled with VGAT-specific antibody (1:500; 131013, Synaptic Systems). HEK293 cells were labelled with GFP. Expression of Pikachurin was visualized with the cherry tag on the construct while Dystroglycan and DBI were labelled with a myc-specific antibody (1:500; 05-724, Merck Millipore). AlexaFluoro™ secondary antibodies (Abcam) were applied at dilution of 1:750. Images were acquired using LSM700 confocal microscope (Carl Zeiss) using 63× oil immersion objective and analyzed as described in Chapter 2 section 2.4.

5.3 Results

In order to investigate how expression of various trans-synaptic proteins affects synapse formation, the constructs containing the cDNA of these proteins were transfected together with the GFP cDNA into the HEK293-wt cells or HEK293 cells stably expressing $\alpha_2\beta_2\gamma_2$-$GABA_A$ receptors.

After 24 hours of incubation, the cells were transferred into 14 DIV rat (E17-19) embryonic medium spiny neuron cultures and further incubated for 24 hours in 37 ℃ in the 5 % CO_2 humidified incubator before they were fixed and subjected to immunolabeling with the primary and fluorescently-labelled secondary antibodies as described in section 5.2.2. Fluorescent images were acquired by Zeiss confocal microscope LSM 710. Cell bodies were visualized by GFP at the λ = 488 nm, expressed trans-synaptic proteins were visualized at the λ = 555 nm, and synaptic terminals labelled with VGAT-specific antibodies were visualized at the λ = 647 nm (Cy5 secondary antibody). The cells imaged were located near at least one or several medium spiny neuron projections. During acquisition z-stack of a single cell was obtained using 63× lens. The interval between each z-stack was 0.70 µm.

5.3.1 Pikachurin Promotes GABAergic Synapse Formation

After transfection into HEK293 cells and expression in co-cultures. Pikachurin was detected in synapses formed by VGAT terminals and HEK293 cells (Figure 5.3.1). Pikachurin was also detected in association with other VGAT positive terminals which were not directly associated with HEK293 cells, which suggests that Pikachurin can be secreted by HEK293 cells into the medium (Figure 5.3.2). In the presence of Pikachurin, the number of contacts formed between the VGAT-labelled presynaptic terminals of medium spiny neurons and HEK293 cells was increased, and this was noted in the case of both the wt-HEK293 and $\alpha_2\beta_2\gamma_2$-$GABA_A$ receptor-expressing HEK293 cells (Figure 5.3.1.).

Quantification of the % area of co-localized pixels that represents contacts between VGAT terminals and HEK293 cells using ImageJ demonstrated a significant increase in co-cultures where expression of Pikachurin was detected. In co-cultures with the wt-HEK283 cells, the median % area was 0.05 % (IQR = 0.03 - 0.13 %; n = 20 cells from N=2 independent experiments) in the absence of Pikachurin, while the median % area in the presence of Pikachurin was 0.15 % (IQR = 0.04 - 0.23 %; n = 22 cells, from N = 2 independent experiments, $p < 0.05$, Figure 5.3.3A). In co-cultures with the $\alpha_2\beta_2\gamma_2$-$GABA_A$ receptor-expressing HEK293 cells, the median % area was 0.25 % (IQR = 0.08 - 0.54 %; n = 19 cell from N=2 independent experiments) in the absence of Pikachurin, while median % area in the presence of Pikachurin was 0.48 % (IQR = 0.31 – 0.91 %; n = 19, from N = 2 independent experiments, $p < 0.05$, Figure 5.3.3A). In addition, the %

area of co-localization was significantly increased in the presence of Pikachurin and $\alpha_2\beta_2\gamma_2$-$GABA_A$ receptors as opposed to Pikachurin alone ($p < 0.05$, Figure 5.3.3A).

Quantification of the count of co-localized pixel puncta between VGAT terminals and HEK293 cells using ImageJ also demonstrated a significant increase in co-cultures where expression of Pikachurin was detected. In co-cultures with the wt-HEK283 cells, the median count was 24 (IQR = 16 - 68; n = 20 cells from N = 2 independent experiments) in the absence of Pikachurin, while the median count in the presence of Pikachurin was 65 (IQR = 34 - 114; n = 22 cells, from N = 2 independent experiments, $p < 0.05$, Figure 5.3.3B). In co-cultures with $\alpha_2\beta_2\gamma_2$-$GABA_A$ receptor-expressing HEK293 cells, the median count was 53 (IQR = 29 - 93; n = 19 cell from N=2 independent experiments) in the absence of Pikachurin, while median count in the presence of Pikachurin was 124 (IQR = 52 - 466; n = 19, from N = 2 independent experiments, $p < 0.05$, Figure 5.3.3B). Moreover, the count of co-localized pixel puncta was significantly increased in the presence of Pikachurin and $\alpha_2\beta_2\gamma_2$-$GABA_A$ receptors than Pikachurin alone ($p < 0.05$, Figure 5.3.3B).

These experiments indicate that overexpression of Pikachurin facilitates the formation of synaptic contacts between the medium spiny neurons and HEK293 cells in the presence or absence of $\alpha_2\beta_2\gamma_2$-$GABA_A$ receptors. However, the effect of Pikachurin expression on contact formation appears to be more pronounced when HEK293 cells also express $GABA_A$ receptors.

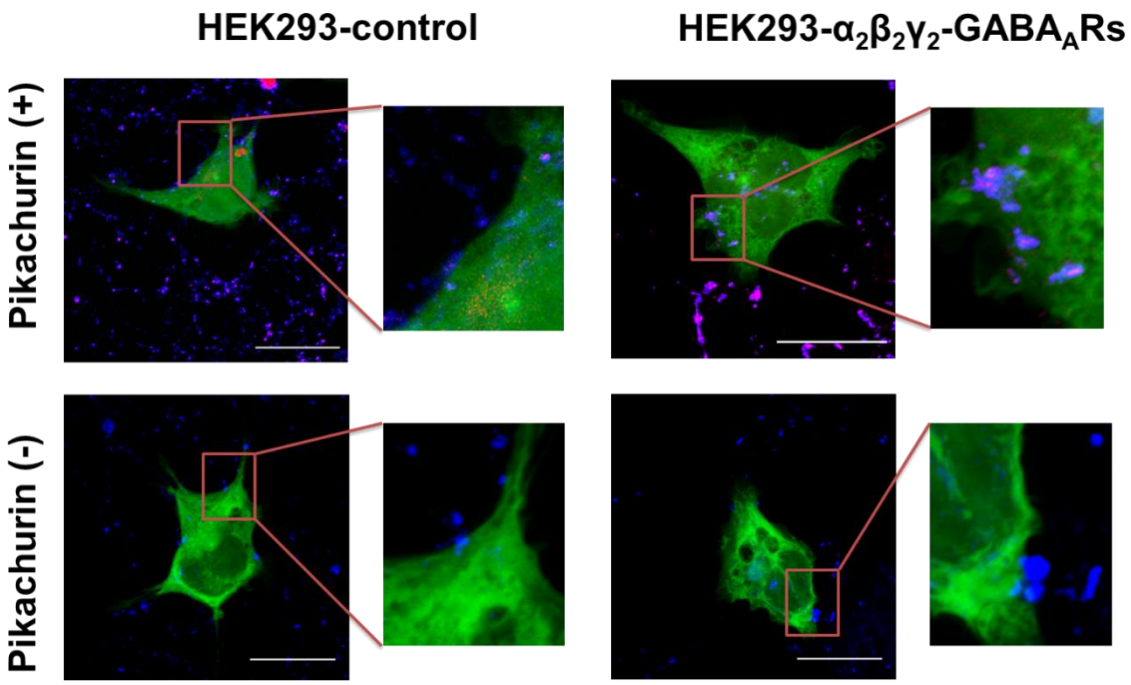

Figure 5.3.1

Synaptic contact formation in co-culture of HEK293 cells and medium spiny neurons. HEK293 cells (wt or stably expressing $\alpha_2\beta_2\gamma_2$-$GABA_A$ receptors) expressing GFP alone and GFP + Pikachurin were incubated in co-culture with medium spiny neurons for 24 hours. The HEK293 cells were visualized by GFP (green); Pikachurin was tagged with p-cherry (red); and synaptic terminals were labelled with VGAT antibody (blue). Scale bar = 20 μm. Fluorescent imaging was done using Zeiss 710 confocal microscope at 63 × magnification with image size 512 × 512. Max intensity projection of the z-stack images was shown. The enlarged images are 12 × zoom in.

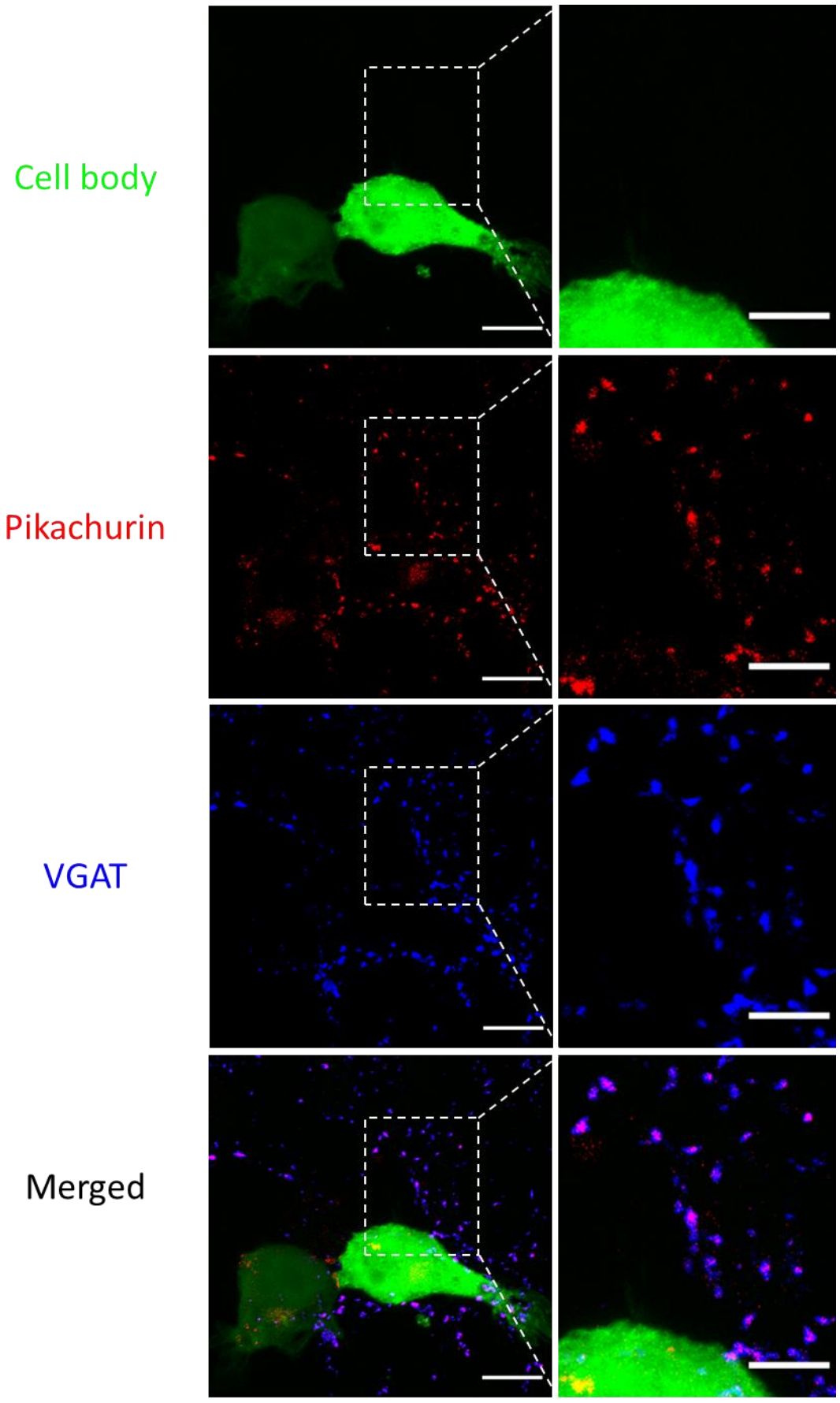

Figure 5.3.2
Typical fluorescent image that shows co-localization of Pikachurin secreted by HEK293-wt and VGAT positive terminals of co-cultured medium spiny neurons. Scale bar = 10 µm (5 µm in enlarged image). Fluorescent imaging was done using Zeiss 710 confocal microscope at 63 × magnification with image size 512 × 512. Max intensity projection of the z-stack images was shown.

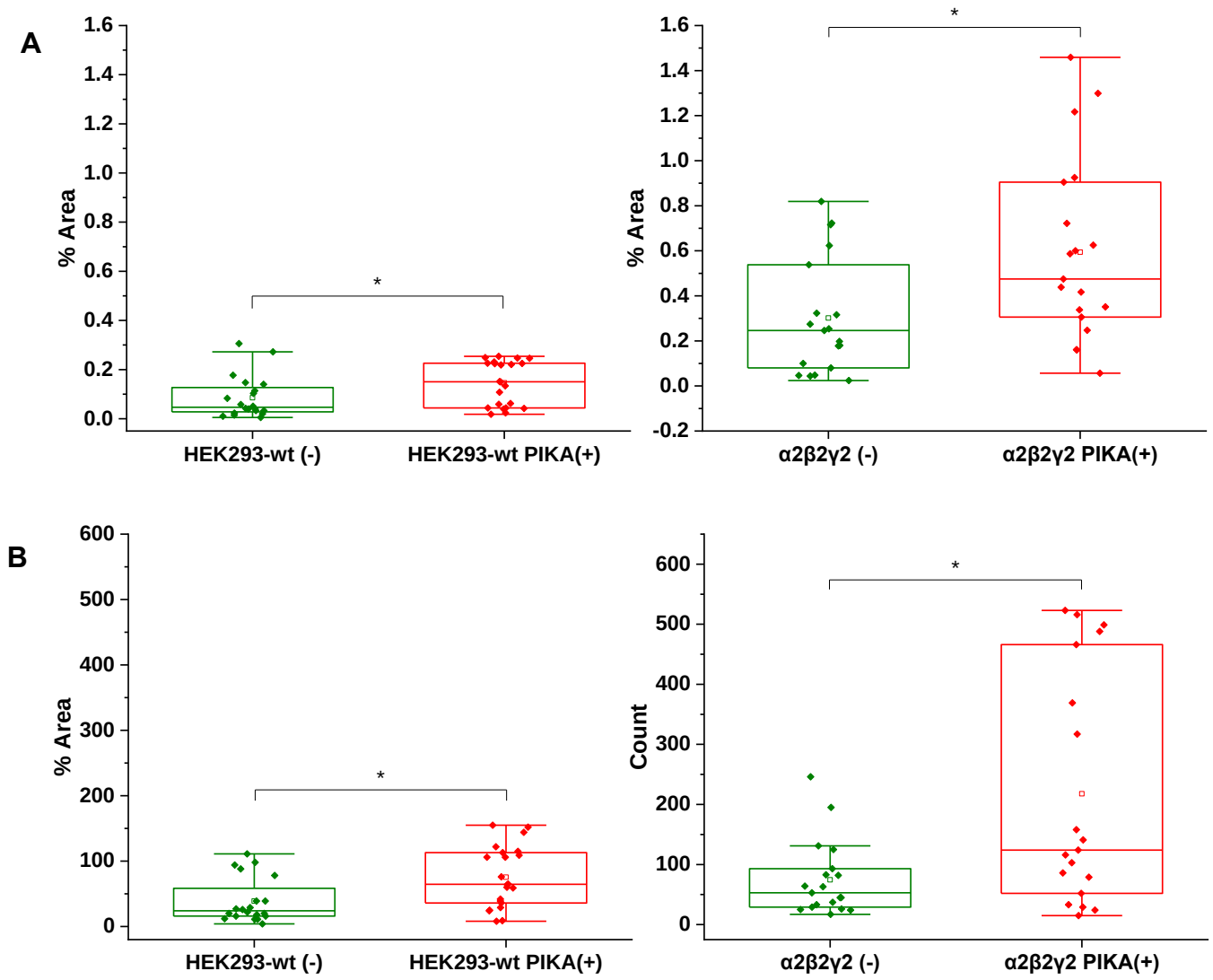

Figure 5.3.3

Expression of Pikachurin promotes synaptic contact formation between medium spiny neurons and the wt- or $\alpha_2\beta_2\gamma_2$-$GABA_A$ receptor-expressing HEK293 cells in co-culture. Quantitative analysis of HEK293 cell in contact with VGAT terminals. (A) % Area of co-localization. (B) Count of co-localization. The box and whisker plot shows the mean (square dot with no fill), median (horizontal line) and standard deviation of the mean (whiskers). Data from N = 2 independent experiments with n = 20 wt-HEK293 cells, n = 22 wt-HEK293 cells expressing Pikachurin, n = 19 $\alpha_2\beta_2\gamma_2$-$GABA_A$ receptor-expressing HEK293 cells and n = 19 $\alpha_2\beta_2\gamma_2$-$GABA_A$ receptor-expressing HEK293 cells expressing Pikachurin. Shapiro-Wilk normality test was used to test the normal distribution of the data and Mann-Whitney test was used to analyze the statistical significance of the difference. (* $p < 0.05$)

5.3.2 Dystroglycan Exerts No Effect on the Formation of GABAergic Synapses

Dystroglycan, the key component of the DGC, is essential for the connection between the actin skeleton of the neuron and the extracellular matrix (Henry and Campbell, 1996). It has been shown to play an essential role in stabilizing GABAergic synapses but whether it induces the formation of GABAergic synapse is unknown. Moreover, it was found that Dystroglycan is essential in the structure maintenance of the ribbon synapses by docking Pikachurin (Dunn, Orlandi and Martemyanov, 2019).

Myc-tagged Dystroglycan (at the N-terminal extracellular domain) was expressed in the wt- or $\alpha_2\beta_2\gamma_2$-$GABA_A$ receptors-expressing HEK293 cell line and the cells were co-cultured with the medium spiny neurons for 24 h. The cells were fixed and processed for immunocytochemistry and confocal imaging using a myc-specific antibody to label Dystroglycan at the cell surface and VGAT antibody to label GABAergic terminals. Dystroglycan was detected at the surface of HEK293 cells (Figure 5.3.4, dystroglycan channel), however, showing no co-localization with the VGAT terminals forming contacts with HEK cells. Moreover, there was no apparent difference in synaptic contact formation between the medium spiny neurons and either wt- or $GABA_A$ receptor-expressing HEK293 cells in the absence or presence of Dystroglycan (Figure 5.3.4).

Quantification of the % area of co-localized pixels that represents contacts between VGAT terminals and HEK293 cells using ImageJ demonstrated no

significant change in co-cultures where expression of Dystroglycan was detected. In co-cultures with wt-HEK283 cells, the median % area was 0.15 % (IQR = 0.10 - 0.29 %; n = 24 cells from N=2 independent experiments) in the absence of Dystroglycan, while the median % area in the presence of Dystroglycan was 0.19 % (IQR = 0.08 - 0.34 %; n = 22 cells, from N = 2 independent experiments, Figure 5.3.5A). In co-cultures with $\alpha_2\beta_2\gamma_2$-$GABA_A$ receptor-expressing HEK293 cells, the median % area was 0.16 % (IQR = 0.05 - 0.40 %; n = 27 cell from N=2 independent experiments) in the absence of Dystroglycan, while median % area in the presence of Dystroglycan was 0.22 % (IQR = 0.12 – 0.46 %; n = 27, from N = 2 independent experiments, Figure 5.3.5A).

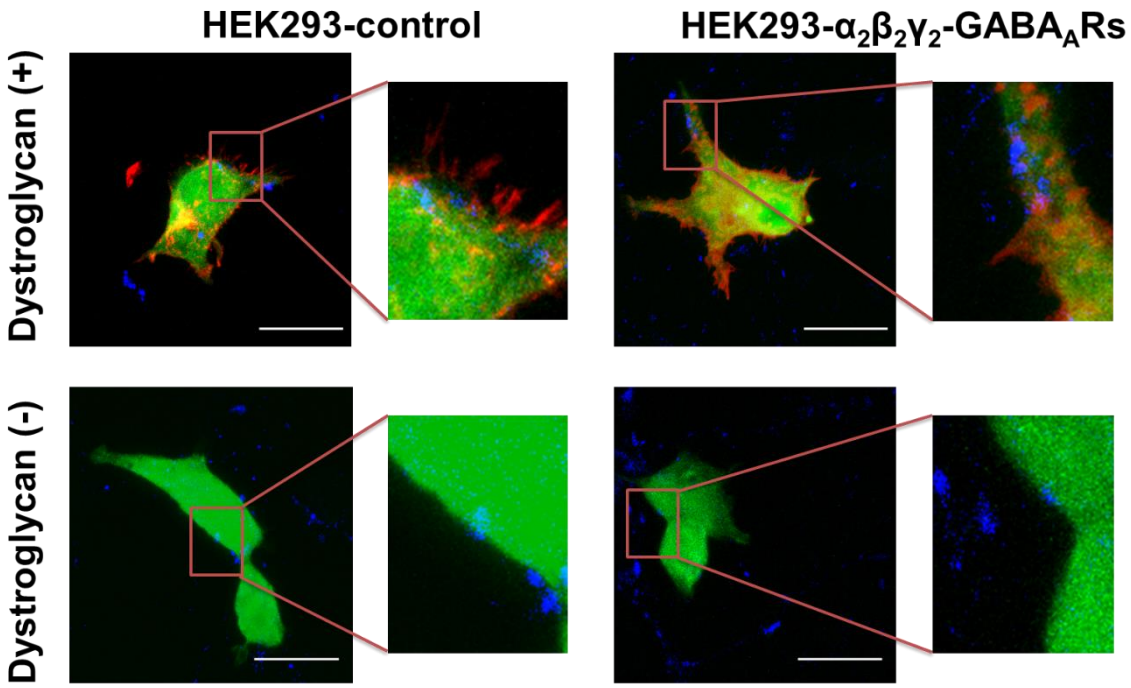

Figure 5.3.4

Synaptic contact formation in co-culture of HEK293 cells and medium spiny neurons. HEK293 cells (wt or stably expressing $\alpha_2\beta_2\gamma_2$-$GABA_A$ receptors) expressing GFP alone or GFP + dystroglycan were incubated in co-culture with medium spiny neurons for 24 hours. The HEK293 cells were visualized by GFP (green); Dystroglycan was tagged with myc-tag which was visualized by myc antibody (red); and synaptic terminals of medium spiny neurons were labeled with VGAT antibody (blue). Scale bar = 20 μm. Fluorescent imaging was done using Zeiss 710 confocal microscope at 63 × magnification with image size 512 × 512. Max intensity projection of the z-stack images was shown. The enlarged images are 12 × zoom in.

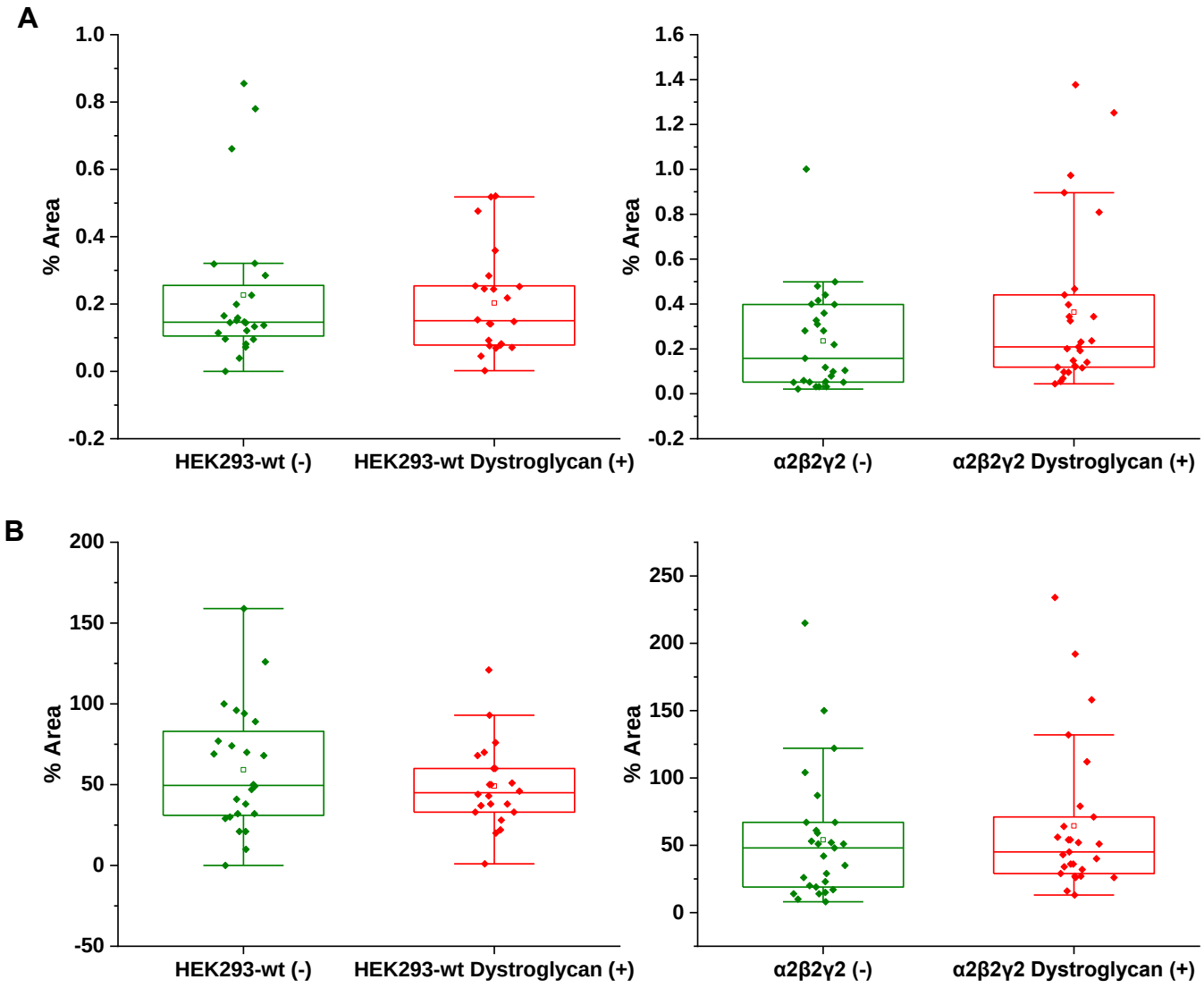

Figure 5.3.5

Expression of Dystroglycan has no effect on synaptic contact formation between the medium spiny neurons and wt- or $\alpha_2\beta_2\gamma_2$-$GABA_A$ receptor-expressing HEK293 cells in co-culture. Quantitative analysis of HEK293 cell in contact with VGAT terminals. (A) % Area of co-localization. (B) Count of co-localization. The box and whisker plot shows the mean (square dot with no fill), median (horizontal line) and standard deviation of the mean (whiskers). Data from N = 2 independent experiments with n = 24 wt-HEK293 cells and, n = 22 wt-HEK293 cells expressing Dystroglycan, n = 27 $\alpha_2\beta_2\gamma_2$-$GABA_A$ receptor-expressing HEK293 cells and n = 27 $\alpha_2\beta_2\gamma_2$-$GABA_A$ receptor-expressing HEK293 cells also expressing Dystroglycan. Shapiro-Wilk normality test was used to test the normal distribution of the data and Mann-Whitney test was used to analyze the statistical significance of the difference.

Quantification of the count of co-localized pixel puncta that represents the number of contacts between VGAT terminals and HEK293 cells using ImageJ also demonstrated no change in co-cultures where expression of Dystroglycan was detected. In co-cultures with wt-HEK283 cells, the median count was 50 (IQR = 31 - 86; n = 24 cells from N=2 independent experiments) in the absence of Dystroglycan, while the median count in the presence of Dystroglycan was 45 (IQR = 33 - 45; n = 22 cells, from N = 2 independent experiments, Figure 5.3.5B). In co-cultures with $\alpha_2\beta_2\gamma_2$-$GABA_A$ receptor-expressing HEK293 cells, the median count was 48 (IQR = 19 - 67; n = 27 cell from N = 2 independent experiments) in the absence of Dystroglycan, while median count in the presence of Dystroglycan was 45 (IQR = 29 - 71; n = 27, from N = 2 independent experiments, Figure 5.3.5B).

Because Dystroglycan is expressed on the surface of HEK293 cells instead of being secreted into the culture medium like Pikachurin, the level of expression of Dystroglycan may affect the formation of synapses. Therefore, the data were normalized with the level of expression of Dystroglycan. The expression level of dystroglycan was quantified by the sum of mean intensity of Dystroglycan signal in each stack of the z-stack images at level of 10^4. In this way, I have analyzed the formation of GABAergic synapses induced by a certain amount of Dystroglycan in the presence or absence of $GABA_A$ receptors in the co-culture. However, even after this adjustment, the size of area with co-localized pixels that represents contacts between VGAT terminal and HEK293 cells was not

significantly different in the absence or presence of Dystroglycan (median = 1.93 %; IQR = 0.38 – 3.55 %; n = 24 cells *vs.* median = 1.89 %; IQR = 0.56 – 5.11 %; n = 28 cells from N = 2 independent experiments, respectively; $p > 0.05$, Figure 5.3.6A). The count of co-localized pixels that represents contacts between VGAT terminal and HEK293 cells was not significantly different in the absence or presence of Dystroglycan either (median = 0.42; IQR = 0.17 – 0.92; n = 22 *vs.* median = 0.38; IQR = 0.19 – 0.74; n = 27, from N = 2 independent experiments, respectively; $p > 0.05$, Figure 5.3.6B).

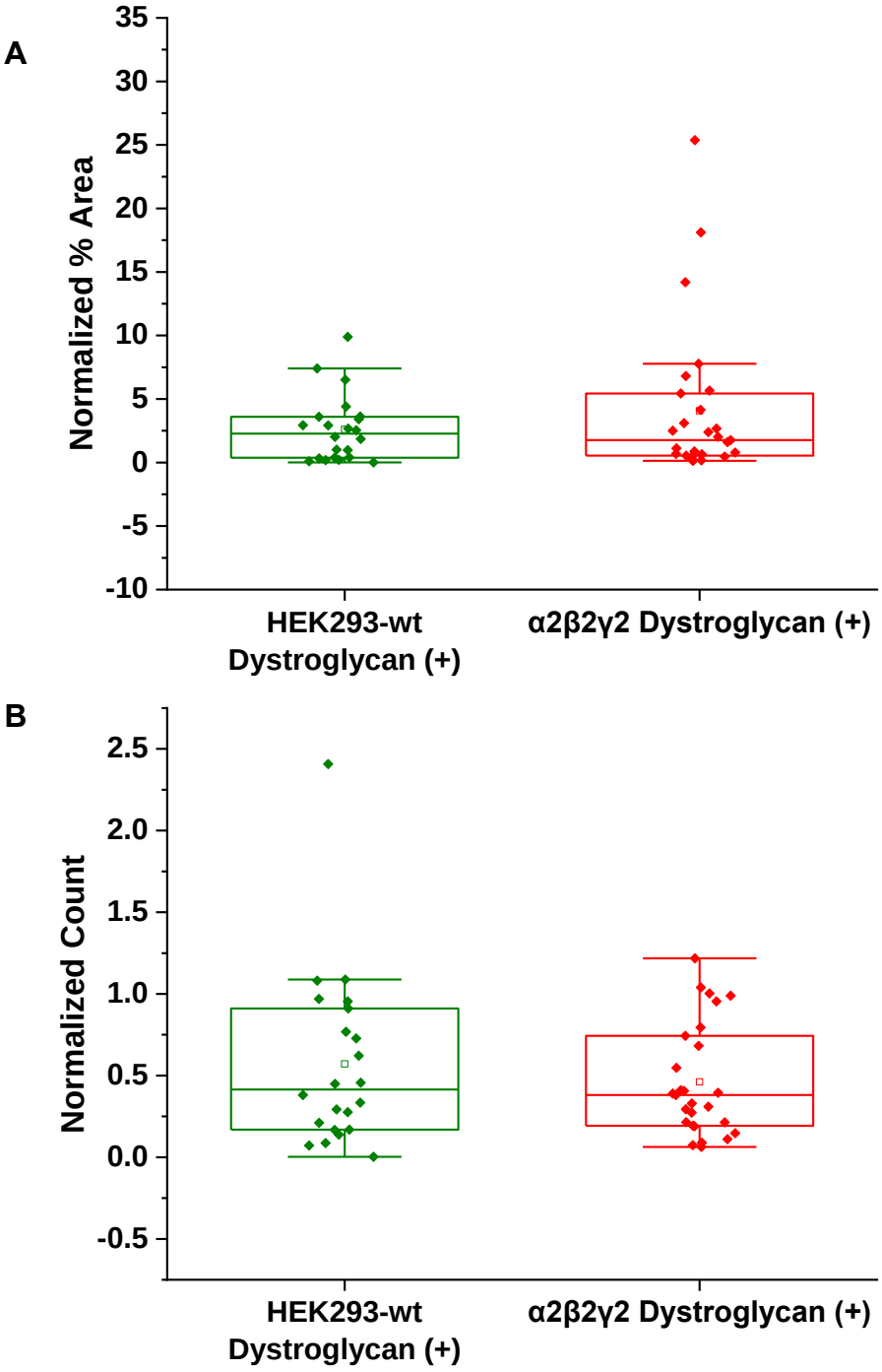

Figure 5.3.6

No significant difference was observed in quantitative analysis of HEK293 (wt and $\alpha_2\beta_2\gamma_2$) cell in contact with VGAT terminals in the presence of Dystroglycan. The % area was normalized by the expression level of Dystroglycan in HEK293 cells. (A) Normalized % area of co-localization. (B) Normalized count of co-localization. The box and whisker plot shows the mean (square dot with no fill), median (horizontal line), standard deviation of the mean (whiskers) and the outliers (square dot black fill). Data from N = 2 independent experiments with n = 22 wt-HEK293 cells expressing Dystroglycan and n = 27 $\alpha_2\beta_2\gamma_2$-$GABA_A$ receptor-expressing HEK293 cells expressing Dystroglycan. Shapiro-Wilk normality test was used to test the normal distribution of the data and Mann-Whitney test was used to analyze the statistical significance of the difference.

Furthermore, as Pikachurin was found to be a ligand of dystroglycan, which promotes the formation of synapses in the retina (Sato et al., 2008), these two proteins were transfected together into HEK293 cells for investigation of a possible cumulative effect they may have on GABAergic synapse formation in the co-culture model used above (Figure 5.3.7). Confocal imaging revealed that Dystroglycan was expressed on the surface of HEK293 cells while Pikachurin was secreted, with very little co-localization detected between these two proteins (Figure 5.3.7). Quantitative analysis of the % area of co-localized pixels between the presynaptic marker VGAT and HEK293 cells shows that co-expression of Pikachurin and Dystroglycan significantly increased synaptic contact formation in the presence of $\alpha_2\beta_2\gamma_2$-$GABA_A$ receptors (median = 0.79 %; IQR = 0.40 – 1.50 %; n = 44 *vs.* median = 1.32 %; IQR = 0.68 – 2.19 %; n = 44, from N = 3 independent experiments, $p < 0.05$, Figure 5.3.8A). However, with the wt-HEK293 cell, the level of synapse formation was not significantly different in the absence or presence of Dystroglycan and Pikachurin (median = 0.57 %; IQR = 0.35 – 1.09 %; n = 44 *vs.* median = 0.52 %; IQR = 0.36 – 1.04 %; n = 43, from N = 3 independent experiments, $p > 0.05$, Figure 5.3.8A). In addition, the % area of co-localization was significantly increased in the presence of Pikachurin, Dystroglycan, and $\alpha_2\beta_2\gamma_2$-$GABA_A$ receptors as opposed to Pikachurin and Dystroglycan alone ($p < 0.05$, Figure 5.3.8A).

Quantitative analysis of the count of co-localized pixel puncta between the presynaptic marker VGAT wt-HEK293 cells shows no significant difference in the

absence or presence of Dystroglycan and Pikachurin (median = 62; IQR = 42 - 88; n = 44 *vs.* median = 66; IQR = 33 - 92; n = 43, from N = 3 independent experiments, p > 0.05, Figure 5.3.8B). With the $\alpha_2\beta_2\gamma_2$-$GABA_A$ receptor expressing-HEK293 cells, the level of synapse formation was not significantly different in the absence or presence of Dystroglycan and Pikachurin (median = 43; IQR = 23 - 88; n = 44 *vs.* median = 70; IQR = 42 - 98; n = 43, from N = 3 independent experiments, p > 0.05, Figure 5.3.8A).

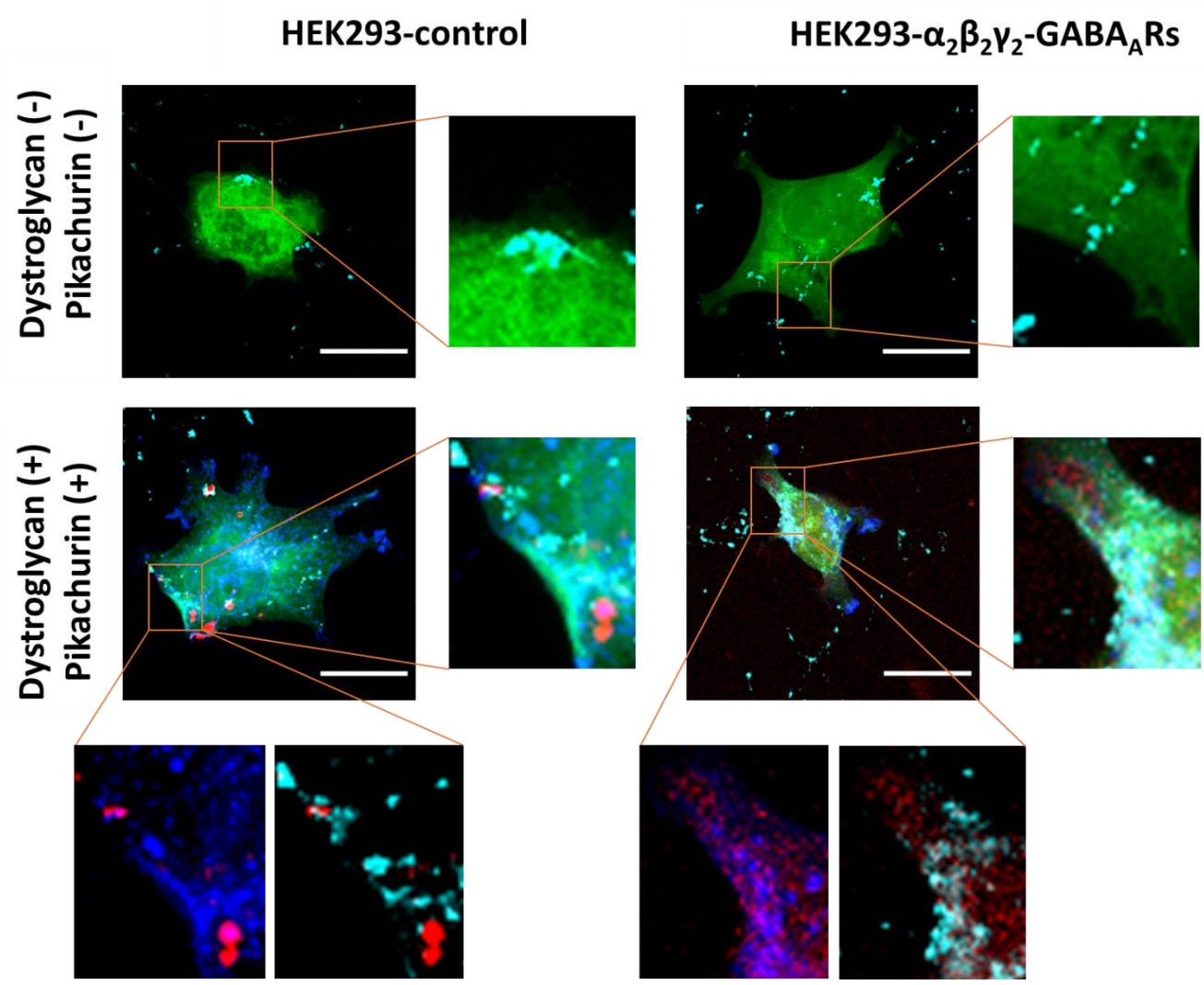

Figure 5.3.7

Synaptic contact formation in co-culture of HEK293 cells and medium spiny neurons. HEK293 cells (wt or $\alpha_2\beta_2\gamma_2$-$GABA_A$ receptor cell line) expressing GFP alone and GFP + dystroglycan + pikachurin were incubated in co-culture with medium spiny neurons for 24 hours. The HEK293 cells were visualized by GFP (green); Dystroglycan was tagged with myc-tag which is visualized with myc antibody (blue); pikachurin was tagged with p-cherry (red) and synaptic terminals of medium spiny neurons were labelled with VGAT antibody (cyan). Pikachurin signal is more punctate in the absence of $\alpha_2\beta_2\gamma_2$-$GABA_A$ receptor than in the presence of $\alpha_2\beta_2\gamma_2$-$GABA_A$ receptor. Scale bar = 20 μm. Fluorescent imaging was done using Zeiss 880 confocal microscope at 63 x magnification with image size 512 × 512. Max intensity projection of the z-stack images was shown. The enlarged images are 12 × zoom in.

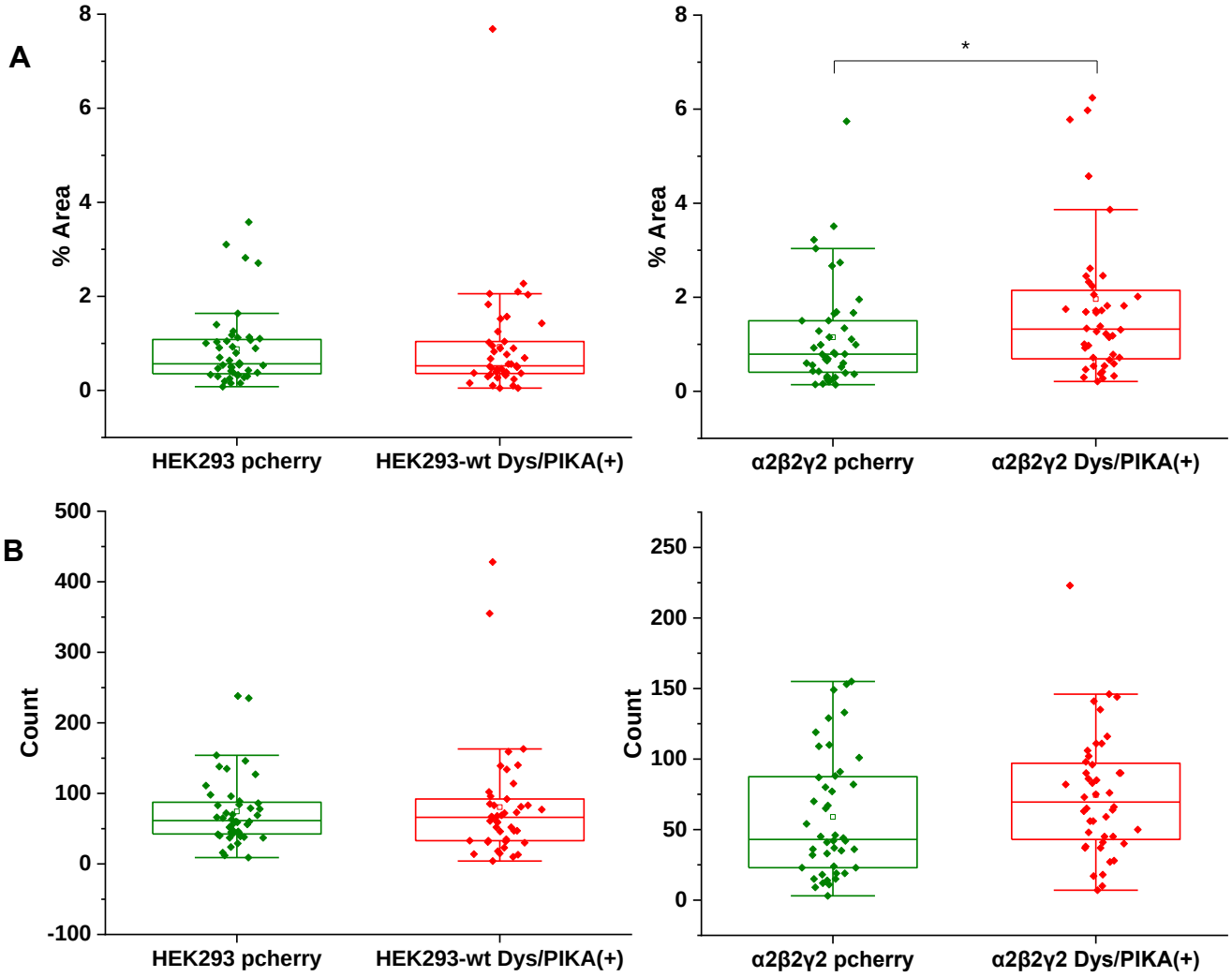

Figure 5.3.8

Expression of Pikachurin and Dystroglycan significantly increases synaptic contacts formed between the medium spiny neurons and HEK293 cells in the presence of $\alpha_2\beta_2\gamma_2$-$GABA_A$ receptors. Quantitative analysis of (A) % area and (B) Count of co-localized pixel puncta between VGAT terminals and HEK293 cells. The box and whisker plot shows the mean (square dot with no fill), median (horizontal line), standard deviation of the mean (whiskers) and the outliers (square dot black fill). Data from N = 3 independent experiments with n = 44 wt-HEK293 cells, n = 43 wt-HEK293 cells expressing Pikachurin and dystroglycan, n = 44 $\alpha_2\beta_2\gamma_2$-$GABA_A$ receptor-expressing HEK293 cells and n = 44 $\alpha_2\beta_2\gamma_2$-$GABA_A$ receptor-expressing HEK293 cells expressing Pikachurin and dystroglycan. Shapiro-Wilk normality test was used to test the normal distribution of the data and Mann-Whitney test was used to analyze the statistical significance of the difference. (* $p < 0.05$)

These experiments indicate that Dystroglycan does not induce formation of GABAergic synapses on its own or in the presence of $\alpha_2\beta_2\gamma_2$-$GABA_A$ receptors in our co-culture model. In addition, when co-expressed with Pikachurin, Dystroglycan appears to abolish the positive effects of Pikachurin on synapse formation in the case of wt-HEK293 cells and diminish these effects in the case of $GABA_A$ receptor-expressing HEK293 cells. However, the effects of Pikachurin were still statistically significant in the latter case. Still, these effects were no longer significant when the number of co-localized pixel puncta were quantified which was due to high variability in size between individual HEK293 cells. This discrepancy could be explained by differences in how these two parameters were calculated. In the case of the *% Area* of co-localization, the size of each individual HEK293 cell is taken into calculation while that is not the case when the *Count* of co-localized pixels is estimated because this simply represents the total number of sites where the pixels in two channels are co-localized. However, it is very well known that after transfection the shape and size of HEK293 cells can vary significantly (Ooi et al., 2016), and thus the surface area where the contacts can be formed. Therefore, the significance observed with the *% Area* analysis is not always also observed with the *Count* analysis especially when the factor of difference is lower than 2 ×.

5.3.3 DBI Promotes Formation of GABAergic Synapses

Long-term treatment with Diazepam has been reported to induce the loss of GABAergic synapses in cortical neuronal cultures (Nicholson et al., 2018). As DBI inhibits the binding of Diazepam to $GABA_A$ receptors, we hypothesized that DBI may have a protective role in these processes. Therefore, it was of interest to study how the expression of DBI may influence the formation of GABAergic synapses in our co-culture model system.

DBI cDNA is myc-tagged at the N-terminus, therefore, anti-myc primary antibody was used to label DBI via its extracellular domain. DBI was shown to express at certain locations on the cell surface (Figure 5.3.9, red channel), but the majority of the label was detected in the cytoplasm of HEK293 cells (Figure 5.3.9). The merged channels show that more synaptic contacts (co-localization of cell body and VGAT) are formed with the cells expressing DBI.

Expression of DBI significantly increased the GABAergic synaptic contacts formed between the wt-HEK293 cells and medium spiny neurons (median = 0.12 %; IQR = 0.05 - 0.17 %; n = 38 *vs.* median = 0.19 %; IQR = 0.11 - 0.31 %; n = 39, from N = 3 independent experiments, $p < 0.05$, Figure 5.3.10A). In the presence of $\alpha_2\beta_2\gamma_2$-$GABA_A$ receptors, the GABAergic synapse formation was also increased by DBI (median = 0.09 %; IQR = 0.05 - 0.23 %; n = 30 *vs.* median = 0.27 %; IQR = 0.17 - 0.44 %; n = 36, from N = 3 independent experiments, $p < 0.05$, Figure 5.3.10A).

Quantitative analysis of the number of colocalized pixel puncta (Count) between the VGAT and wt-HEK293 cells showed no significant difference in the absence or presence of DBI (median = 34; IQR = 17 - 68; n = 38 *vs.* median = 43; IQR = 25 - 76; n = 39, from N = 2 independent experiments, $p > 0.05$, Figure 5.3.10B). However, in the presence of $\alpha_2\beta_2\gamma_2$-$GABA_A$ receptors, the count of co-localized pixels was significantly increased by DBI (median = 35; IQR = 24 - 60; n = 30 *vs.* median = 77; IQR = 49 - 121; n = 37, from N = 2 independent experiments, $p < 0.05$, Figure 5.3.10B).

These data indicate that DBI promotes the formation of GABAergic synaptic contacts between the medium spiny neurons and HEK293 cells, and that this effect is further potentiated when synaptic $\alpha_2\beta_2\gamma_2$-$GABA_A$ receptors are also expressed on the surface of HEK293 cells.

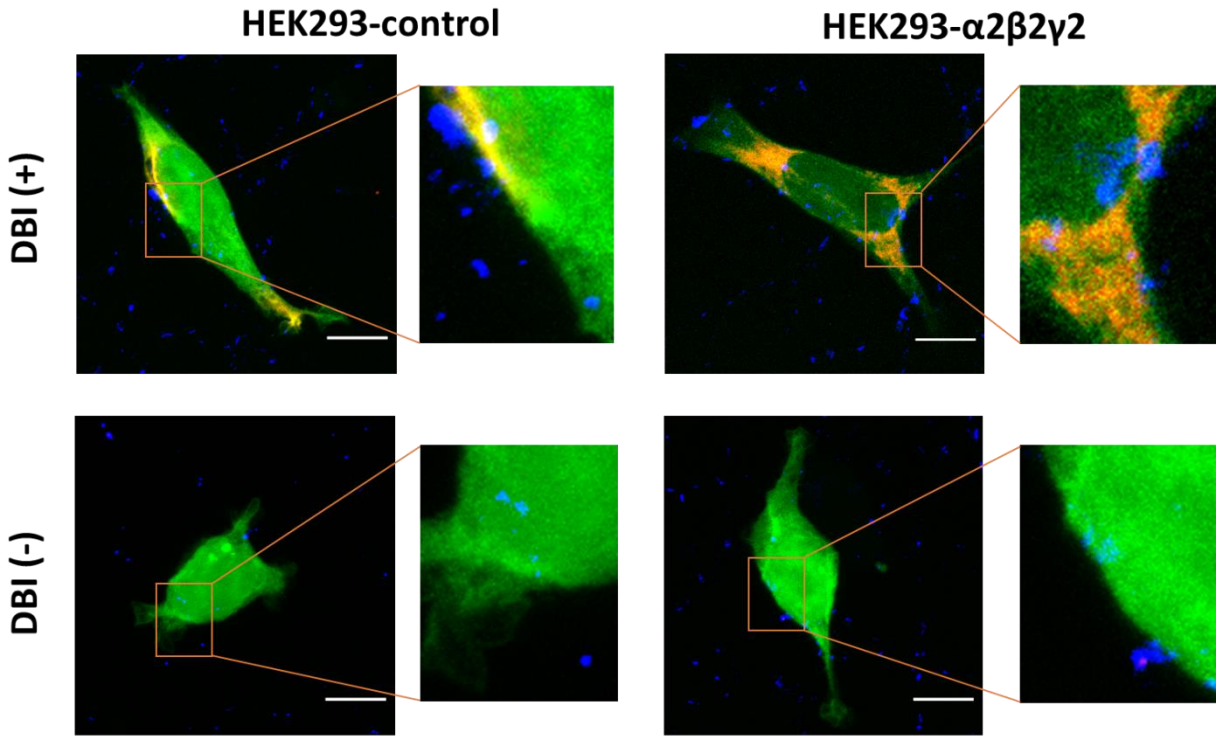

Figure 5.3.9

Synaptic contact formation in co-culture of HEK293 cells and medium spiny neurons. HEK293 cells (wt or $\alpha_2\beta_2\gamma_2$-$GABA_A$ receptor cell line) expressing GFP alone and GFP + DBI were incubated in co-culture with medium spiny neurons for 24 hours. The whole cell body was visualized by GFP (green); DBI was tagged with myc-tag which was visualized with the myc antibody (red); and synaptic terminals of medium spiny neurons were labelled with VGAT antibody (blue). Scale bar = 20 μm. Fluorescent imaging was done using Zeiss 710 confocal microscope at 63 × magnification with image size 512 × 512. Max intensity projection of the z-stack images was shown. The enlarged images show segments which were enlarged 12 ×.

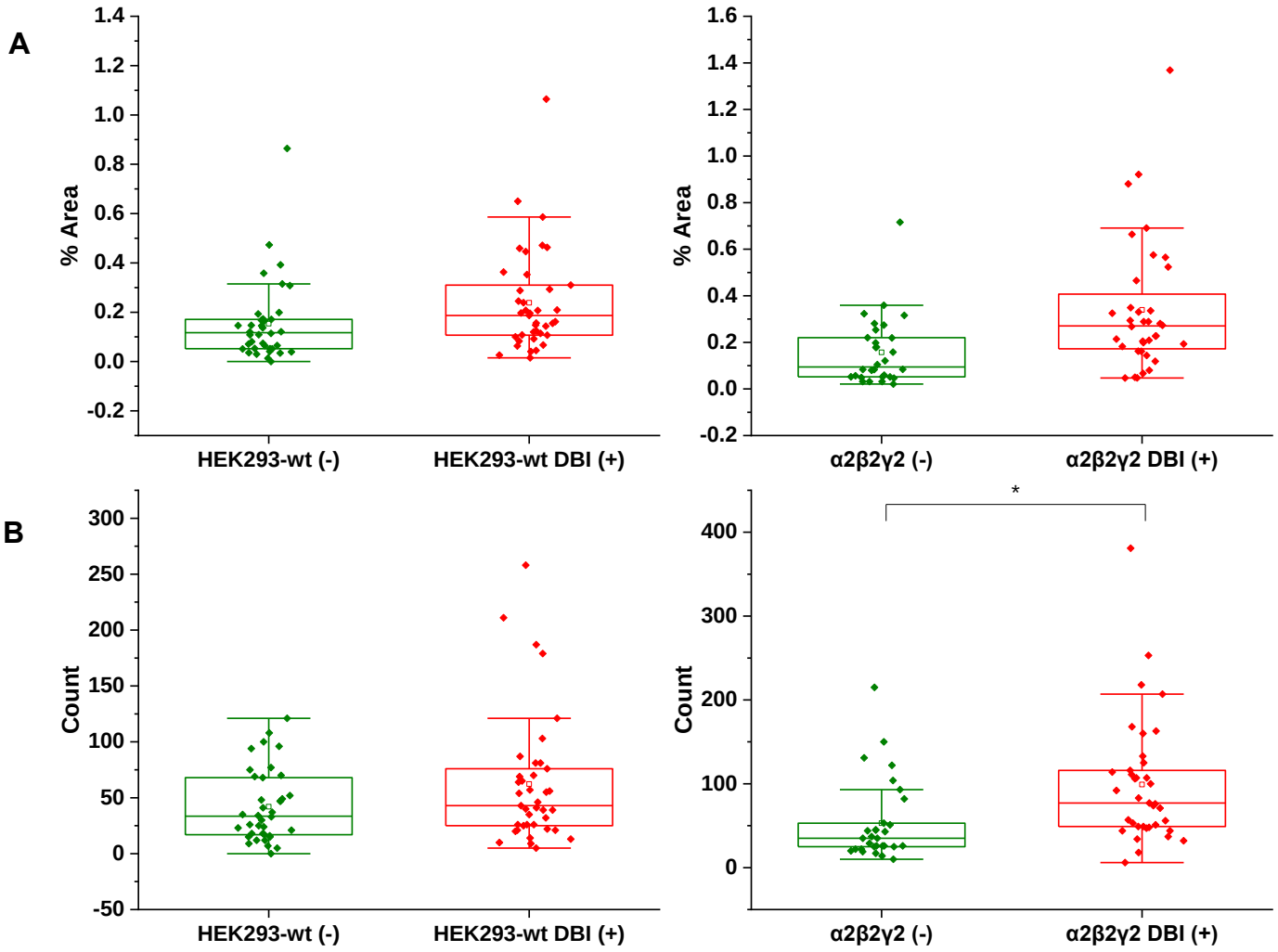

Figure 5.3.10

Expression of DBI significantly potentiates the formation of synaptic contacts between the medium spiny neurons and HEK293 (wt and $\alpha_2\beta_2\gamma_2$) cells. Quantitative analysis of (A) % area, and (B) count of HEK293 cell in contact with VGAT terminals. The box and whisker plot shows the mean (square dot with no fill), median (horizontal line), standard deviation of the mean (whiskers) and the outliers (square dot black fill). Data from N = 3 independent experiments with n = 38 wt-HEK293 cells, n = 39 wt-HEK293 cells expressing DBI, n = 30 $\alpha_2\beta_2\gamma_2$-$GABA_A$ receptor-expressing HEK293 cells and n = 36 $\alpha_2\beta_2\gamma_2$-$GABA_A$ receptor-expressing HEK293 cells expressing DBI. Shapiro-Wilk normality test was used to test the normal distribution of the data and Mann-Whitney test was used to analyze the statistical significance of the difference. (* $p < 0.05$)

5.4 Discussion

The formation and maintenance of GABAergic synapses is regulated by a variety of cell adhesion molecules. However, the specific function of each of these proteins remains largely unclear. We focused on three plausible cell adhesion molecules that are present at GABAergic synapses and interact with $GABA_A$ receptors: Pikachurin, Dystroglycan and DBI. The role of Dystroglycan and Pikachurin as cell adhesion molecules that form complexes and interact with other proteins to mediate the formation and normal function of the ribbon synapses has been well characterized in the retina (Sato et al., 2008, Omori et al., 2012), and both proteins have been shown to be present in the brain (Sato et al., 2008). Preliminary experiments from our lab have demonstrated that Pikachurin can interact with $GABA_A$ receptor α_2 subunit. While both Pikachurin and Dystroglycan are components of the ECM in the brain synapses (Bello et al., 2015), how these two proteins participate in synapse formation is currently unknown. DBI is an endogenous ligand for the benzodiazepine binding site of the $GABA_A$ receptors that displaces the binding of Diazepam (Ala and MI, 1983). Prolonged Diazepam exposure has been shown to reduce the expression of $GABA_A$ receptors via calcium-dependent internalization from the neuronal cell surface, which leads to disassembly of GABAergic synapses (Nicholson et al., 2018). Therefore, we hypothesized that DBI may work in the opposite direction to Diazepam and facilitate GABAergic synapse formation.

5.4.1 Pikachurin Promotes GABAergic Synapse Formation

While playing an essential role in the retinal ribbon synaptic formation and maintenance, the role of Pikachurin in the brain is currently unknown. Confocal images of the co-cultures showed a significant increase in the contact formation between the medium spiny neurons and HEK293 cells expressing Pikachurin both in the absence and presence of $\alpha_2\beta_2\gamma_2$-$GABA_A$ receptors (Figure 5.3.3). These data suggest that Pikachurin might function as an adhesion molecule in the GABAergic synapses. A significantly higher level of synapse formation was observed in the presence of the $\alpha_2\beta_2\gamma_2$-$GABA_A$ receptors (Figure 5.3.3). This suggests a synergistic effect of $GABA_A$ receptors and Pikachurin in inducing GABAergic synapse formation. This synergistic effect might be subunit-specific, however, this will require further experimentations, such as a comparison between different $GABA_A$ receptor subtypes .

Moreover, a significant amount of Pikachurin was found co-localized with VGAT in our co-culture (Figure 5.3.2). This indicates that Pikachurin is largely secreted into the extracellular space where it can interact with the presynaptic proteins. Although further analysis is needed to characterize these interactions, this suggests that Pikachurin might act as a “guide” that facilitates the adhesion of nerve terminals to the postsynaptic membrane. In the retina, Pikachurin is secreted by photoreceptors to facilitate the formation and function of ribbon synapses by physically connecting the presynaptic DGC and the GPR179 (Sato et al., 2008; Orlandi et al., 2018). Therefore, it is likely that α_2-containing $GABA_A$

receptors act as the postsynaptic ligand for Pikachurin in this process. However, the fact that Pikachurin can promote synapse formation in the absence of $GABA_A$ receptors as well (Figure 5.3.3) suggests that $GABA_A$ receptors are not likely to be the only player in this context.

5.4.2 Dystroglycan only Promotes GABAergic Synapse Formation when Co-expressed with Pikachurin and $\alpha_2\beta_2\gamma_2$-$GABA_A$ Receptors

Because Pikachurin was shown to promote the ribbon synapse formation in the retina as a component of the DGC, we tested the effect of co-expression of Pikachurin and Dystroglycan, the key component of the DGC, on the GABAergic synapse formation. The DGC plays an essential role in connecting the cytoskeleton to the extracellular matrix. Unlike Pikachurin which is secreted into the surrounding environment, Dystroglycan is expressed on the cell surface (Figure 5.3.4). Dystroglycan is selectively expressed in inhibitory synapses in the brain and is essential for clustering of GABAergic postsynaptic proteins (Lévi et al., 2002). However, no significant change in synapse formation was observed in the presence of Dystroglycan (Figure 5.3.5 & Figure 5.3.6). It has been recently shown that the deletion of Dystroglycan impairs the formation of inhibitory synapses in cerebellar Purkinje cells (Briatore et al., 2020). Conditional knockout of Dystroglycan in pyramidal cells can result in loss of GABAergic CCK-positive interneuron innervation of these cells and CCK-positive interneuron cell death and failure. The remaining CCK-positive interneurons axonal terminals were retargeted to the striatum where expression of Dystroglycan was retained in

(Miller and Wright, 2021). In a separate study, deletion of Dystroglycan also reduced the CCK-positive interneuron innervation of pyramidal cells in the hippocampus and neocortex, while the parvalbumin (PV)-positive cells were not affected (Früh et al., 2016). This can be explained by the expression of different proteins by these two types of cells. Albeit Dystroglycan interaction with both Neurexins and Neuroligins (Briatore et al., 2020) in the brain has been reported, the specificity of Dystroglycan inducing GABAergic interneuronal innervation suggests that other presynaptic cell adhesion molecules can be involved in this process. Overall, these findings demonstrate that Dystroglycan plays an important role in the GABAergic synapse formation and targeting of the GABAergic axons *in vivo*. However, in our co-culture model system, no such effect was observed with the expression of Dystroglycan in the absence or presence of $\alpha_2\beta_2\gamma_2$-$GABA_A$ receptors. In the basal ganglia, Dystroglycan is sparsely found in the Striatum but not in the Substantia Nigra (Zaccaria et al., 2001) which the medium spiny neurons predominantly innervate (Tepper, Abercrombie and Bolam, 2007). These together suggest that Dystroglycan may not be relevant to synapses formed by the medium spiny neurons. Moreover, it has been shown that the clustering of the postsynaptic Gephyrin at GABAergic synapses is not dependent on Dystroglycan (Lévi et al., 2002). The same was reported for the clustering of $GABA_A$ receptor α_2 or γ_2 subunits at GABAergic synapses (Früh et al., 2016). Together, these studies suggest that Dystroglycan effects on GABAergic synapse formation require the presence of interactors.

With co-expression of Dystroglycan and Pikachurin, the level of synapse formation was significantly increased in the presence of $GABA_A$ receptors (Figure 5.3.8). Without the expression of the $\alpha_2\beta_2\gamma_2$-$GABA_A$ receptors, no significant change in the synapse formation was observed (Figure 5.3.8). It seems that the expression of Dystroglycan reverses the synaptogenic effects of Pikachurin. Our analysis shows that in the presence of the $\alpha_2\beta_2\gamma_2$-$GABA_A$ receptors, the median % Area of contacts was 1.93 × higher than controls when Pikachurin was expressed alone. However, when Dystroglycan was co-expressed with Pikachurin, the median % Area of synaptic contacts was 1.68 × higher than controls. Also, in the presence of Pikachurin alone, the median % Area of synaptic contacts was 3.16 × higher with HEK293 cells expressing $\alpha_2\beta_2\gamma_2$-$GABA_A$ receptors than wt-HEK293 cells, but in the presence of Dystroglycan and Pikachurin, the factor was slightly lower (2.53 ×). Together, expression of Dystroglycan seems to reduce, if anything, the synaptogenic effects of Pikachurin but not fully eliminate them. This is likely due to the binding of Dystroglycan and Pikachurin, which may affect Pikachurin interaction with other postsynaptic ligands such as $GABA_A$ receptors. Moreover, Dystroglycan interaction with Neurexin seems to be inhibited by NL2 (Reissner et al., 2014), which suggests that the earlier expressed Dystroglycan may function as an inducer of synapses which is subsequently replaced by NL2 during functional maturation of synapses (Moore et al., 2002). This suggests a relatively low affinity of Dystroglycan-Neurexin interaction (Reissner et al., 2014). In the retina, Dystroglycan is linked to the Laminin via its binding of Agrin (Sato et al.,

2008), and is linked to GPR179 to stabilize the ribbon synapse via Pikachurin interaction (Orlandi et al., 2018). Thus, Pikachurin might play a similar structural role in the brain to bridge Dystroglycan to the presynaptic transmembrane proteins, likely Neurexins, to induce the formation of GABAergic synapses. However, this requires further investigation and identification of a presynaptic ligand for Dystroglycan which may play a key role in these processes. For example, fluorescent labeling of Dystroglycan, Pikachurin and Neurexin in the co-culture model system can allow quantitative assessment of Dystroglycan and Neurexin co-colocalization in the presence or absence of Pikachurin.

The formation of GABAergic synapses is a highly organized and regulated process that leads to pre- and post-synaptic specialization, and functional maturation. Although Dystroglycan is essential for maintaining the structure of GABAergic synapses, our results indicate that Dystroglycan, alone or in the presence of $GABA_A$ receptors, is not sufficient to induce the GABAergic synapse formation.

5.4.3 DBI Promotes GABAergic Synapse Formation

Previous studies of DBI have focused primarily on its role in allosteric modulation of $GABA_A$ receptors which has a great effect on signal transmission (Christian et al., 2013) and neurogenesis (Dumitru, Neitz, Alfonso and Monyer, 2017). Recently, it has been revealed that loss of DBI exerts opposite effects in different subregions of the mouse Hippocampus. The inhibitory signals were enhanced in the CA1 pyramidal neurons but attenuated in the Dentate Gyrus granule cells

(Courtney and Christian, 2018). One of the possible explanations for this is the difference in the type of $GABA_A$ receptors expressed in these subregions (Hörtnagl et al., 2013). Therefore, we hypothesized that DBI might affect GABAergic signal transmission by interacting with specific subtypes of $GABA_A$ receptors. We, therefore, cultured the $\alpha_2\beta_2\gamma_2$-$GABA_A$ receptors expressing HEK293 cells with the medium spiny neurons. The confocal images show that DBI was predominantly accumulated in the HEK293 cell cytoplasm (Figure 5.3.9), however, a significant increase in contact formation was observed (Figure 5.3.10). Surprisingly, an increase in synapse formation was also observed with the wt-HEK293 cell line expressing DBI, although the count analysis, which does not consider the change in the size of HEK293 cells after transfection, showed no significant change (Figure 5.3.10).

There are two possible reasons for this result. The first possibility is that DBI interacts with the presynaptic $GABA_A$ receptors to exert an allosteric modulation and thus induce the innervation. When HEK293 cells express the $\alpha_2\beta_2\gamma_2$-$GABA_A$ receptors, DBI also binds to the postsynaptic receptors, which further promote the synapse formation process. The second possibility is that DBI is cleaved in the culture and the proteolyzed products interact with the pre- or postsynaptic ligands, which induce the innervation process. As the cleavage products of DBI mostly interact with benzodiazepine binding sites as well (Bormann, 1991), this effect is likely to be further promoted by the expression of the $\alpha_2\beta_2\gamma_2$-$GABA_A$ receptors on the surface of HEK293 cells. DBI has been shown to promote

postnatal neurogenesis events (Alfonso et al., 2012; Dumitru, Neitz, Alfonso and Monyer, 2017) and protect the central nervous system from oxidative stress-induced cell death (Masmoudi-Kouki et al., 2019). Therefore, we also hypothesize that DBI may be part of a protective mechanism that prevents or reverses the long term benzodiazepine-induced loss of GABAergic synapses. To investigate the putative protection mechanism, future experiments with DBI treatment will be needed. Purified DBI from the culture medium will be applied to the culture model of the medium spiny neurons and the $\alpha_2\beta_2\gamma_2$-$GABA_A$ receptor-expressing HEK293 cells at the same time as Diazepam treatment to investigate if the GABAergic synapses can be rescued. Moreover, electrophysiological experiments will be conducted to test the allosteric modulation of $GABA_A$ receptors by DBI in the co-culture model, which will investigate if DBI regulates the strength of GABAergic signal transmission.

Together, these data have revealed that not all proteins present in GABAergic synapses play a role in their formation and suggest diverse mechanisms involved in this process. Future work will be to study the mechanisms by which Pikachurin and DBI induce GABAergic synapse formation and establish their role using both *in vitro* and *in vivo* approaches.

6. Discussion

Synapses are the key elements of neural circuits. The normal function of the brain depends on the precise maintenance of the excitation/inhibition balance which is mainly determined by the activity of Glutamatergic and GABAergic synapses. GABAergic synapse formation is a highly regulated and dynamic process (Wierenga, Becker and Bonhoeffer, 2008; Wierenga, 2017) and it involves multiple steps: the recognition of the pre- and postsynaptic neurons, adhesion of the pre- and postsynaptic membranes, and functional maturation of the synapse. Currently, little is known about the cellular and molecular mechanisms underlying these events, despite identification and detailed characterization of various synaptic adhesion proteins specifically expressed in GABAergic synapses. The interactions of the synaptic adhesion proteins have been extensively studied and proposed to be key mediators of GABAergic synapse formation (Lu, 2017; Sudhof, 2017, 2021).

The major challenge to the understanding of the role of $GABA_A$ receptors in GABAergic synapse formation *in vivo* is the diversity of $GABA_A$ receptors expressed in the CNS, and the heterogeneity of the proteins expressed in the GABAergic synapses. Using a reduced system of embryonic medium spiny neurons and HEK293 cells expressing proteins of interest, the role of $GABA_A$ receptors in inducing functional GABAergic synapses has been characterized (Fuchs et al., 2013; Brown et al., 2014, 2016).

The current study aimed to investigate the regulation of GABAergic synapses

by $GABA_A$ receptors and their interaction with proteins expressed in GABAergic synapses including NL2, Dystroglycan, Pikachurin, and DBI.

6.1 Creation and Characterization of the Extrasynaptic $\alpha_4\beta_3\delta$-$GABA_A$ receptor expressing-HEK293 cell line

A HEK293 cell line stably expressing extrasynaptic $\alpha_4\beta_3\delta$-$GABA_A$ receptors, which are the most abundant form of the extrasynaptic $GABA_A$ receptors in the brain (Sur et al., 1999; Belelli et al., 2009), was created to use as a control for the study of the synaptic $GABA_A$ receptors in the synaptogenesis events in co-culture with medium spiny neurons. The δ subunit has been shown to restrict the $GABA_A$ receptors from diffusing into the postsynaptic membranes (Martenson et al., 2017). These extrasynaptic $GABA_A$ receptors are important for the tonic inhibition in the brain (Chandra et al., 2006; Liang et al., 2007). In comparison to the synaptogenic effects exhibited by the synaptic $\alpha_2\beta_2\gamma_2$-$GABA_A$ receptors (Figure 4.3.5), fully functional $\alpha_4\beta_3\delta$-$GABA_A$ receptors, which were activated by bath-applied GABA (Figure 3.3.10), did not induce the formation of synapses (Figure 4.3.2). This result is consistent with the previous findings that the synaptogenic effect of $GABA_A$ receptors requires the presence of the γ_2 subunit (Brown et al., 2016).

6.2 Subunit-Dependent $GABA_A$ Receptor-NL2 Synergistic Effects in GABAergic Synaptogenesis

The postsynaptic transmembrane adhesion protein NL2 has been shown to

induce the formation of GABAergic synapses, but it was more effective in the presence of $GABA_A$ receptors (Fuchs et al., 2013). Here, I have characterized a subunit-dependent synergistic effect of $GABA_A$ receptors and NL2 in promoting GABAergic synapse formation and functional maturation, which is more prominent in the presence of the synaptic $GABA_A$ receptors than extrasynaptic $GABA_A$ receptors (Figure 4.3.8 & Figure 4.3.18). This synergistic effect was not dependent on the activity of $GABA_A$ receptors (Figure 4.3.12 – Figure 4.3.17), which is consistent with the findings in the absence of NL2 (Brown et al., 2016). However, the importance of GABA in inducing GABAergic synapse formation by stimulating the assembly of postsynaptic specializations has been well characterized in pure neuronal cultures and *in vivo* (Oh, Lutzu, Castillo and Kwon, 2016; Burlingham et al., 2022). Together, these findings suggest that the activity of $GABA_A$ receptors plays a pivotal role in the recruitment of GABAergic postsynaptic specializations but not in the adhesion of the pre- and postsynaptic membranes. Furthermore, the $GABA_A$ receptor subunit ECDs were shown to mediate the induction of GABAergic synapses by $GABA_A$ receptors (Brown et al., 2016), but did not appear to be involved in NL2-guided mechanisms (Figure 4.3.25), which suggests an alternative mechanism. Moreover, by comparing the synaptogenic effects of NL2 in the presence of different $GABA_A$ receptor subunit combinations ($\alpha_2\beta_3\delta$, $\alpha_2\beta_3\gamma_2$, $\alpha_4\beta_3\delta$, or $\alpha_4\beta_3\gamma_2$), it became apparent that the γ_2 and α_2 subunits were required for this process (Figure 4.3.11). However, in the previous study, the $\alpha_2\beta_3\gamma_2$-$GABA_A$ receptors alone were not as potent as other

subunit combinations in inducing synaptogenesis (Brown et al., 2016). This further implies a different mechanism underlying the synaptogenesis effects of $GABA_A$ receptors in the presence of NL2.

Intriguingly, although the synergistic effect was also observed in the presence of $\alpha_4\beta_3\delta$-$GABA_A$ receptors, the synapses showed no activity as revealed in the whole-cell recordings (Figure 4.3.18). Moreover, the super-resolution imaging revealed a lower level, but not a complete absence, of the $\alpha_4\beta_3\delta$-$GABA_A$ receptors from the synaptic contacts (Figure 4.3.23). In parallel, the presynaptic terminals were more active in releasing GABA in the presence of the $\alpha_2\beta_2\gamma_2$-$GABA_A$ receptors than $\alpha_4\beta_3\delta$-$GABA_A$ receptors (Figure 4.3.20 & Figure 4.3.21). Together, in the presence of the $\alpha_4\beta_3\delta$-$GABA_A$ receptors and NL2, the lower presynaptic activity and postsynaptic $GABA_A$ receptor density may be the reasons for the lack of effective GABA-mediated transmission in these synaptic contacts.

The fact that application of $GABA_A$ receptor subunit ECDs did not affect the induction of synapses by $GABA_A$ receptors and NL2 led to the hypothesis that the intracellular domains of $GABA_A$ receptors may play a role and indeed this was demonstrated in our experiments. It is however surprising that the interaction between the intracellular domains of NL2 and γ_2 subunit in our experiments did not require the auxiliary protein GARLH4 (Yamasaki et al., 2017). The expression of this protein was not detected in our HEK293 cell lines. This suggests that GARLH4 may not be only protein that may facilitate the recruitment of $GABA_A$

receptors to the NL2 (Martenson et al., 2017) or that these proteins undergo a direct interaction via their intracellular domains. The importance of the γ_2 subunit TM3-4 loop was further demonstrated by using the δ chimera – $\delta^{\gamma 2ICL}$. In the presence of this chimeric subunit, the synapse formation was increased almost to the same level as with the γ_2 subunit (Figure 4.3.26). In agreement with these results were our biochemical experiments in which similar level of binding to NL2 was detected when the chimera was compared to γ_2 subunit (Figure 4.3.33).

Despite the prominent effect of NL2 on GABAergic synapses in the co-culture, the fact that knockout of NL2 impairs the GABAergic transmission but has little effect on the number of GABAergic synapses (Zhang et al., 2015; Chanda et al., 2017) suggests the role of other transsynaptic interactions in the initiation of the GABAergic synaptogenesis. These interactions must precede the NL2-Neurexin interaction which then plays a pivotal role in maintaining the structure of GABAergic synapses and their functional maturation. Neurexin interaction with $GABA_A$ receptors may be a candidate for this synaptogenic interaction due to the direct interaction of Neurexins and the α_1 subunit-containing $GABA_A$ receptors (Zhang et al., 2010), but this requires further experimentation. In my experiments,α Neurexin was co-immunoprecipitated with the α_2 subunit-containing $GABA_A$ receptors from the enriched synaptic membrane fraction, but this binding was weak and likely indirect, i.e. mediated by NL2 (Figure 4.3.30).

Therefore, I propose here, that a tripartite complex formed by the γ_2 subunit-containing $GABA_A$ receptors, Neurexins, and NL2 may play an essential role in

the formation of functional GABAergic synapses. The Neurexins are the core of this complex because the deletion of Neurexins can lead to both decreased number of GABAergic synapses and decreased presynaptic Ca^{2+}-dependent GABA release (Chen et al., 2017). Unlike NL2 and other postsynaptic adhesion proteins that are recruited to the synaptic domain during development, the Neurexins are expressed long before the formation of the synapses in the brain, which suggests they may be involved in the initial synaptogenesis (Daly and Ziff, 1997). Co-expression of $GABA_A$ receptors and NL2 on the postsynaptic membrane and their interaction with Neurexins drives the functional maturation of the presynaptic terminals. The $GABA_A$ receptor-NL2 interaction is mediated by the γ_2 subunit via its intracellular loop, which possibly triggers the Neurexin-dependent presynaptic Ca^{2+} influx and thus allows the release of GABA. However, how $GABA_A$ receptors facilitate this process remains unknown. I propose here that $GABA_A$ receptors may stabilize the NL2-Neurexin interaction via the γ_2 subunit TM3-4 intracellular loop, which provides the structural stability of the complex while the postsynaptic density, *i.e.* the scaffolding proteins including Gephyrin and Collybistin, are assembled. To confirm this hypothesis, further experimentations will be required. For instance, characterization of the $GABA_A$ receptor-Neurexin-NL2 interactions at different developmental stages by co-immunoprecipitation may reveal important temporal aspects of the tripartite complex formation. Furthermore, whether $GABA_A$ receptors can interact with Neurexin and/or NL2 via their extracellular and intracellular domains could also

be investigated using biochemical tools.

An important question that remains to be explored is why synapses formed in the presence of NL2 and $\alpha_4\beta_3\delta$-$GABA_A$ receptors are functionally silent. The IPSCs largely disappeared while the $\alpha_4\beta_3\delta$-$GABA_A$ receptor exhibited a synergistic effect with NL2 in promoting GABAergic synapse formation, albeit less prominent than the $\alpha_2\beta_2\gamma_2$-$GABA_A$ receptor (Figure 4.3.8). The $\alpha_4\beta_3\delta$-$GABA_A$ receptors possesses a higher affinity for GABA than the synaptic $\alpha_2\beta_2\gamma_2$-$GABA_A$ receptor and slow desensitization (Mortensen, Patel and Smart, 2012), therefore they are expected to be activated by GABA even at much lower levels. The current results indicate that the presynaptic activities were not fully diminished in the presence of the $\alpha_4\beta_3\delta$-$GABA_A$ receptors, albeit lower than those induced by $\alpha_2\beta_2\gamma_2$-$GABA_A$ receptors (Figure 4.3.20 & Figure 4.3.21). One possible explanation is that the lower presynaptic release probability in these synapses and the free diffusion of the $\alpha_4\beta_3\delta$-$GABA_A$ receptors in and out of synapses decreased the overall probability of GABA reaching the $GABA_A$ receptors. This can also possibly explain a sporadic IPSCs recorded in very few $\alpha_4\beta_3\delta$-$GABA_A$ receptor/NL2 expressing-HEK293 cells in our electrophysiology experiments (Figure 4.3.18).

6.3 Synaptogenic Effects of Proteins Expressed in GABAergic Synapses: Pikachurin, Dystroglycan, and DBI

Although the co-culture model system has been considered as a reduced system that is far from the *in vivo* conditions, it provides an efficient platform for

investigating the role of specific proteins in the GABAergic synapse formation because it allows a precise control of the protein expression. In the current study, I expressed Pikachurin, Dystroglycan, and DBI individually in HEK293 cells and quantified the innervation of these cells by the embryonic medium spiny neurons. Both Pikachurin and DBI were able to induce GABAergic synapse formation either in the presence or absence of $GABA_A$ receptors (Figure 5.3.3 & Figure 5.3.10). Pikachurin and DBI are secreted proteins and both interact with the $GABA_A$ receptors so it was surprising to see an increase in GABAergic synapse formation caused by them in the absence of $GABA_A$ receptors. This suggests that there may be other proteins that interact with Pikachurin or DBI to mediate synaptic adhesion. The mechanism underlying the formation of GABAergic synapses may differ between these two proteins. DBI, or its proteolyzed products (Bormann, 1991), binds to the Benzodiazepine binding site of $GABA_A$ receptors, which induces an allosteric modulation of $GABA_A$ receptors that enhances their synaptogenic effects. To investigate this, the advances in the cryo-EM may help to resolve the exact conformation change of $GABA_A$ receptors binding with DBI and to compare with the models of $GABA_A$ receptors binding with other ligands such as Diazepam. DBI could be a part of a protection mechanism in the brain in response to the synaptic loss induced by Diazepam (Nicholson et al., 2018). Pikachurin, as suggested by its role in the retina (Orlandi et al., 2018), may act as an adhesion molecule that structurally bridges the pre- and postsynaptic membranes via interacting with transmembrane proteins such as $GABA_A$

receptors or Dystroglycan.

Dystroglycan alone did not have any effect on GABAergic synapse formation (Figure 5.3.6). However, co-expression of Dystroglycan with Pikachurin was able to induce the formation of GABAergic synapses in the presence of $GABA_A$ receptors (Figure 5.3.8). This is in agreement with the finding that Pikachurin, in physical interaction with Dystroglycan, promotes the formation of ribbon synapses in the retina (Sato et al., 2008; Orlandi et al., 2018). However, in the current study, it appeared that the expression of Dystroglycan reduced the synaptogenic effect of Pikachurin, which suggests that the Pikachurin interaction with the postsynaptic protein such as $GABA_A$ receptor was affected by the Pikachurin binding to Dystroglycan (described in Chapter 5 section 5.4.2). Dystroglycan has been shown to express early in development as Neurexins, which suggests a possible role in inducing the initial GABAergic synapse formation (Moore et al., 2002). This is supported by direct *in vivo* evidence that deletion of Dystroglycan impairs the formation of inhibitory synapses by several types of interneurons (Früh et al., 2016; Briatore et al., 2020; Miller and Wright, 2021). The contradiction between these studies and the current study which is supported by the *in vivo* evidence from Dystroglycan knockout mice (Früh et al., 2016) suggests that Dystroglycan may exert distinct effects on synaptogenesis in different brain regions.

6.4 Limitation and Future Experiment Plan

Currently, we are still far from being able to draw a whole picture of the

mechanisms underlying the formation of GABAergic synapses. However, it is well acknowledged that the synaptic adhesion proteins that are expressed in GABAergic synapses may play pivotal roles in the GABAergic synaptogenesis process. What we do not know is how these various proteins coordinate this dynamic process.

The current study has characterized the specific role of synaptic $GABA_A$ receptors and their interactions with distinct proteins expressed in the GABAergic synapses. It is evident that not all proteins found in GABAergic synapses show synaptogenic properties. Within the proteins investigated in the current study, all proteins that showed a synaptogenic effect had a more prominent effect in the presence of $GABA_A$ receptors. Although these proteins showed an ability to induce innervations in the co-culture model system, it cannot be directly concluded that they would induce the initiation of GABAergic synapse formation *in vivo*. In the co-culture model system, the HEK293 cells expressing no exogenous proteins can receive sporadic innervations by the medium spiny neurons (Figure 4.3.1A & Figure 4.3.4A). Indeed, more than 30 % of molecules that are active in inducing innervations in the co-cultures demonstrated no evidence for their function in initiating the synapse formation process in vivo (Sudhof, 2018). Therefore, it is difficult to conclude from a co-culture experiment whether or not the same properties will be retained in vivo and that a protein will take part in GABAergic synapse formation.

To support the current *in vitro* study demonstrating the complex formed by

$GABA_A$ receptor, Neurexin, and NL2, the loss-of-function models can be generated by acute knockout of specific proteins such as NL2. The knockout of NL2 in several brain regions impairs inhibitory transmission but does not affect the presynaptic neurotransmitter release (Poulopoulos et al., 2009; Zhang et al., 2015; Panzanelli, Früh and Fritschy, 2017). This is in line with the current finding that the impaired transmission may be caused by impaired Neurexin-mediated presynaptic Ca^{2+} influx, which can be investigated by evaluating the level of presynaptic VGCCs and their activities in the acute NL2 knockout model. Furthermore, co-immunoprecipitation of $GABA_A$ receptors and Neurexins can be compared between knockout and wt mice, followed by *in vitro* binding of the recombinant $GABA_A$ receptors and Neurexins, to characterize the binding affinities and interaction sites in each of these molecules.

The next step in the study of Pikachurin and DBI effects on synapses could be performed using the medium spiny neuronal cultures. The role of these proteins in synapse formation could be confirmed by characterizing changes in the number of neuronal synapses following application of purified Pikachurin or DBI. A possible protection mechanism of DBI can be tested by applying DBI after Diazepam treatment to cultured neurons culture and analyzing changes in the level of GABAergic innervation. These experiments could be followed by *in vitro* binding assays and proteomics to isolate and characterize possible binding partners of Pikachurin in neuronal synapses.

The specific roles of Dystroglycan in synaptogenesis by different types of

GABAergic cells could be attributed to specific pre- or postsynaptic components. In Cerebellar Purkinje cells, in which deletion of Dystroglycan impairs GABAergic innervation, Dystroglycan mediates the clustering of the postsynaptic proteins including $GABA_A$ receptors, NL2, and Gephyrin (Briatore et al., 2020). Therefore, it would be beneficial to establish a profile of Dystroglycan interaction with different types of $GABA_A$ receptors, which will contribute to the understanding of Dystroglycan functions in synaptogenesis. The type of $GABA_A$ receptors that may interact with Dystroglycan and possibly contribute to the GABAergic synapse formation can be determined by immunolabelling and confocal microscopy in either the cultured neurons or in vivo.

In conclusion, my studies have characterized roles of several GABAergic expressing proteins, including $GABA_A$ receptors, NL2, Pikachurin, Dystroglycan, and DBI, in formation of GABAergic synapses *in vitro*. These results contribute to the knowledge about $GABA_A$ receptor-related regulation of the GABAergic synaptogenesis. However, the co-culture model system is not a perfect imitation of the real brain environment, which can be supported by more *in vivo* and *in vitro* experiments.

7. Reference

Abrahamsen, H. and Stenmark, H. (2010). Protein Secretion: Unconventional Exit by Exophagy. *Current Biology*, 20(9), pp.R415-R418.

AIa, K. and MI, F. (1983). Detection of an endogenous inhibitor of benzodiazepine receptor binding. *Bulletin of Experimental Biology and Medicine*, 96(7), pp.64-5.

Alfonso, J., Le Magueresse, C., Zuccotti, A., Khodosevich, K. and Monyer, H. (2012). Diazepam Binding Inhibitor Promotes Progenitor Proliferation in the Postnatal SVZ by Reducing GABA Signaling. *Cell Stem Cell*, 10(1), pp.76-87.

Allen Brain Atlas. [online] Available at: http://portal.brain-map.org/ [Accessed 31 Mar. 2019]. Hunter, D., Manglapus, M., Bachay, G., Claudepierre, T., Dolan, M., Gesuelli, K. and Brunken, W. (2017). CNS synapses are stabilized trans-synaptically by laminins and laminin-interacting proteins. *Journal of Comparative Neurology*, 527(1), pp.67-86.

Anders, N. and Jürgens, G. (2008). Large ARF guanine nucleotide exchange factors in membrane trafficking. *Cellular and Molecular Life Sciences*, 65(21), pp.3433-3445.

Anderson, G., Aoto, J., Tabuchi, K., Földy, C., Covy, J., Yee, A., Wu, D., Lee, S., Chen, L., Malenka, R. and Südhof, T. (2015). β-Neurexins Control Neural Circuits by Regulating Synaptic Endocannabinoid Signaling. *Cell*, 162(3), pp.593-606.

Aoto, J., Földy, C., Ilcus, S., Tabuchi, K. and Südhof, T. (2015). Distinct circuit-dependent functions of presynaptic neurexin-3 at GABAergic and glutamatergic synapses. *Nature Neuroscience*, 18(7), pp.997-1007.

Arama, J., Abitbol, K., Goffin, D., Fuchs, C., Sihra, T., Thomson, A. and Jovanovic, J. (2015). GABAA receptor activity shapes the formation of inhibitory synapses between developing medium spiny neurons. *Frontiers in Cellular Neuroscience*, 9(290).

Bang, M. and Owczarek, S. (2013). A Matter of Balance: Role of Neurexin and Neuroligin at the Synapse. *Neurochemical Research*, 38(6), pp.1174-1189.

Barbaccia, M., Costa, E., Ferrero, P., Guidotti, A., Roy, A., Sunderland, T., Pickar,

D., Paul, S. and Goodwin, F. (1991). Diazepam-binding inhibitor. A brain neuropeptide present in human spinal fluid: studies in depression, schizophrenia, and Alzheimer's disease. *Archives Of General Psychiatry*, 43(12), pp.1143-7.

Barclay, A. (2003). Membrane proteins with immunoglobulin-like domains—a master superfamily of interaction molecules. *Seminars in Immunology*, 15(4), pp.215-223.

Baur, R., Minier, F. and Sigel, E. (2006). A $GABA_A$ receptor of Defined Subunit Composition and positioning: Concatenation of Five Subunits. *FEBS Letters*, 580(6), pp.1616–1620.

Bayés, À., van de Lagemaat, L., Collins, M., Croning, M., Whittle, I., Choudhary, J. and Grant, S. (2010). Characterization of the proteome, diseases and evolution of the human postsynaptic density. *Nature Neuroscience*, 14(1), pp.19-21.

Bedford, F., Kittler, J., Muller, E., Thomas, P., Uren, J., Merlo, D., Wisden, W., Triller, A., Smart, T. and Moss, S. (2001). GABAA receptor cell surface number and subunit stability are regulated by the ubiquitin-like protein Plic-1. *Nature Neuroscience*, 4(9), pp.908-916.

Belelli, D., Harrison, N.L., Maguire, J., Macdonald, R.L., Walker, M.C., and Cope, D.W. (2009). Extrasynaptic $GABA_A$ receptors: Form, pharmacology, and function. *Journal of Neuroscience*, 41, pp.12757–12763.

Belelli, D., Peden, D., Rosahl, T., Wafford, K. and Lambert, J. (2005). Extrasynaptic GABAA Receptors of Thalamocortical Neurons: A Molecular Target for Hypnotics. *Journal of Neuroscience*, 25(50), pp.11513-11520.

Bello, V., Moreau, N., Sirour, C., Hidalgo, M., Buisson, N. and Darribère, T. (2015). The dystroglycan: Nestled in an adhesome during embryonic development. *Developmental Biology*, 401(1), pp.132-142.

Ben-Ari, Y., Gaiarsa, J., Tyzio, R. and Khazipov, R. (2007). GABA: A Pioneer Transmitter That Excites Immature Neurons and Generates Primitive Oscillations. *Physiological Reviews*, 87(4), pp.1215-1284.

Bennett, M.V.L. and Zukin, R.Suzanne. (2004). Electrical Coupling and Neuronal Synchronization in the Mammalian Brain. *Neuron*, 41(4), pp.495–511.

Bianchi, M., Haas, K. and Macdonald, R. (2002). α1 and α6 subunits specify distinct desensitization, deactivation and neurosteroid modulation of GABAA receptors containing the δ subunit. *Neuropharmacology*, 43(4), pp.492-502.

Bolsover, S., Shephard, E. and White, H. (2011). *Cell Biology: A Short Course*. 3rd ed. Hoboken, New Jersy: John Wiley & Sons, p.230.

Bomalaski, M., Claflin, E., Townsend, W. and Peterson, M. (2017). Zolpidem for the Treatment of Neurologic Disorders. *JAMA Neurology*, 74(9), p.1130.

Bormann, J., (1991). Electrophysiological characterization of diazepam binding inhibitor (DBI) on GABAA receptors. *Neuropharmacology*, 30(12), pp.1387-1389.

Bourgeois, J. and Rakic, P. (1993). Changes of synaptic density in the primary visual cortex of the macaque monkey from fetal to adult stage. *The Journal of Neuroscience*, 13(7), pp.2801-2820.

Bradford, M. (1976). A rapid and sensitive method for the quantitation of microgram quantities of protein utilizing the principle of protein-dye binding. *Analytical Biochemistry*, 72(1-2), pp.248-254.

Bradley, C.A., Taghibiglou, C., Collingridge, G.L. and Wang, Y.T. (2008). Mechanisms Involved in the Reduction of GABAA Receptor α1-Subunit Expression Caused by the Epilepsy Mutation A322D in the Trafficking-competent Receptor. *Journal of Biological Chemistry*, 283(32), pp.22043–22050.

Brady, M. and Jacob, T. (2015). Synaptic localization of α5 GABA (A) receptors via gephyrin interaction regulates dendritic outgrowth and spine maturation. *Developmental Neurobiology*, 75(11), pp.1241-1251.

Briatore, F., Pregno, G., Di Angelantonio, S., Frola, E., De Stefano, M., Vaillend, C., Sassoè-Pognetto, M. and Patrizi, A. (2020). Dystroglycan Mediates Clustering of Essential GABAergic Components in Cerebellar Purkinje Cells. *Frontiers in Molecular*

Neuroscience, 13.

Brickley, S. and Mody, I. (2012). Extrasynaptic GABAA Receptors: Their Function in the CNS and Implications for Disease. *Neuron*, 73(1), pp.23-34.

Briggs, D.C., Yoshida-Moriguchi, T., Zheng, T., Venzke, D., Anderson, M.E., Strazzulli, A., Moracci, M., Yu, L., Hohenester, E. and Campbell, K.P. (2016). Structural Basis of Laminin Binding to the LARGE Glycans on Dystroglycan. *Nature Chemical Biology*, 12(10), pp.810–814.

Brown, L., Fuchs, C., Nicholson, W., Anne Stephenson, F., Thomson, A. and Jovanovic, J., (2014). Inhibitory Synapse Formation in a Co-culture Model Incorporating GABAergic Medium Spiny Neurons and HEK293 Cells Stably Expressing $GABA_A$ Receptors. *Journal of Visualised Experiments*, 93(e52115).

Brown, L., Nicholson, M., Arama, J., Mercer, A., Thomson, A. and Jovanovic, J. (2016). γ-Aminobutyric Acid Type A (GABAA) Receptor Subunits Play a Direct Structural Role in Synaptic Contact Formation via Their N-terminal Extracellular Domains. *Journal of Biological Chemistry*, 291(27), pp.13926-13942.

Brown, N., Kerby, J., Bonnert, T.P., Whiting, P.J. and Wafford, K.A. (2002). Pharmacological Characterization of a Novel Cell Line Expressing Human α4β3δ GABAA Receptors. *British Journal of Pharmacology*, 136(7), pp.965–974.

Brünig, I., Suter, A., Knuesel, I., Lüscher, B. and Fritschy, J.-M. (2002). GABAergic Terminals Are Required for Postsynaptic Clustering of Dystrophin But Not of $GABA_A$ Receptors and Gephyrin. *The Journal of Neuroscience*, 22(12), pp.4805–4813.

Budreck, E. and Scheiffele, P. (2007). Neuroligin-3 is a neuronal adhesion protein at GABAergic and glutamatergic synapses. *European Journal of Neuroscience*, 26(7), pp.1738-1748.

Burlingham, S.R., Wong, N.F., Peterkin, L., Lubow, L., Dos Santos Passos, C., Benner, O., Ghebrial, M., Cast, T.P., Xu-Friedman, M.A., Südhof, T.C. and Chanda, S. (2022). Induction of Synapse Formation by De Novo Neurotransmitter Synthesis. *Nature Communications*, 13(1).

Calcaterra, N. and Barrow, J. (2014). Classics in Chemical Neuroscience: Diazepam (Valium). *ACS Chemical Neuroscience*, 5(4), pp.253-260.

Cestari, I., Min, K., Kulli, J. and Yang, J. (2000). Identification of an Amino Acid Defining the Distinct Properties of Murine β1 and β3 Subunit-Containing GABAA Receptors. *Journal of Neurochemistry*, 74(2), pp.827-838.

Chanda, S., Hale, W., Zhang, B., Wernig, M. and Südhof, T. (2017). Unique versus Redundant Functions of Neuroligin Genes in Shaping Excitatory and Inhibitory Synapse Properties. *The Journal of Neuroscience*, 37(29), pp.6816-6836.

Chandra, D., Jia, F., Liang, J., Peng, Z., Suryanarayanan, A., Werner, D., Spigelman, I., Houser, C., Olsen, R., Harrison, N. and Homanics, G. (2006). GABAA receptor α4 subunits mediate extrasynaptic inhibition in thalamus and dentate gyrus and the action of gaboxadol. *Proceedings of the National Academy of Sciences*, 103(41), pp.15230-15235.

Chapman, E. (2008). How Does Synaptotagmin Trigger Neurotransmitter Release?. *Annual Review of Biochemistry*, 77(1), pp.615-641.

Charych E.I., Yu W., Miralles C.P., Serwanski D.R., Li X., Rubio M., De Blas A.L. (2004). The brefeldin A-inhibited GDP/GTP exchange factor 2, a protein involved in vesicular trafficking, interacts with the beta subunits of the GABA receptors. *Journal of Neurochemistry*, 90(1), pp.173–189.

Charych, E., Liu, F., Moss, S. and Brandon, N. (2009). GABAA receptors and their associated proteins: Implications in the etiology and treatment of schizophrenia and related disorders. *Neuropharmacology*, 57(5-6), pp.481-495.

Che Has, A., Absalom, N., van Nieuwenhuijzen, P., Clarkson, A., Ahring, P. and Chebib, M. (2016). Zolpidem is a potent stoichiometry-selective modulator of α1β3 GABAA receptors: evidence of a novel benzodiazepine site in the α1-α1 interface. *Scientific Reports*, 6(1).

Chen, L.Y., Jiang, M., Zhang, B., Gokce, O. and Südhof, T.C. (2017). Conditional Deletion of All Neurexins Defines Diversity of Essential Synaptic Organizer Functions for

Neurexins. *Neuron*, 94(3), pp.611-625.e4.

Cherubini, E., Gaiarsa, J. and Ben-Ari, Y. (1991). GABA: an excitatory transmitter in early postnatal life. *Trends in Neurosciences*, 14(12), pp.515-519.

Christian, C., Herbert, A., Holt, R., Peng, K., Sherwood, K., Pangratz-Fuehrer, S., Rudolph, U. and Huguenard, J. (2013). Endogenous Positive Allosteric Modulation of GABAA Receptors by Diazepam binding inhibitor. *Neuron*, 78(6), pp.1063-1074.

Chung, W.-S., Allen, N.J. and Eroglu, C. (2015). Astrocytes Control Synapse Formation, Function, and Elimination. *Cold Spring Harbor Perspectives in Biology*, [online] 7(9).

Connolly, C., Krishek, B., McDonald, B., Smart, T. and Moss, S., (1996). Assembly and Cell Surface Expression of Heteromeric and Homomeric γ-Aminobutyric Acid Type A Receptors. *Journal of Biological Chemistry*, 271(1), pp.89-96.

Connor, J., Boileau, A. and Czajkowski, C., (1998). A GABAA Receptor α1 Subunit Tagged with Green Fluorescent Protein Requires a β Subunit for Functional Surface Expression. *Journal of Biological Chemistry*, 273(44), pp.28906-28911.

Costa, E. and Guidotti, A. (1991). Diazepam binding inhibitor (DBI): A peptide with multiple biological actions. *Life Sciences*, 49(5), pp.325-344.

Costes, S., Daelemans, D., Cho, E., Dobbin, Z., Pavlakis, G. and Lockett, S., (2004). Automatic and Quantitative Measurement of Protein-Protein Colocalization in Live Cells. *Biophysical Journal*, 86(6), pp.3993-4003.

Craig, A. and Kang, Y. (2007). Neurexin–neuroligin signaling in synapse development. *Current Opinion in Neurobiology*, 17(1), pp.43-52.

Culligan, K. and Ohlendieck, K. (2000). Characterization of the brain dystrophin-glycoprotein complex. *Biochemical Society Transactions*, 28(1), pp.A31-A31.

Dale, H. (1935). Pharmacology and Nerve-Endings (Walter Ernest Dixon Memorial Lecture): (Section of Therapeutics and Pharmacology). *The Lancet*, 225(5816), p.387.

Daly, C. and Ziff, E.B. (1997). Post-Transcriptional Regulation of Synaptic Vesicle

Protein Expression and the Developmental Control of Synaptic Vesicle Formation. *The Journal of Neuroscience*, 17(7), pp.2365–2375.

Davenport, E., Pendolino, V., Kontou, G., McGee, T., Sheehan, D., López-Doménech, G., Farrant, M. and Kittler, J. (2017). An Essential Role for the Tetraspanin LHFPL4 in the Cell-Type-Specific Targeting and Clustering of Synaptic GABA A Receptors. *Cell Reports*, 21(1), pp.70-83.

Davis, L. and Radke, G., (1987). Measurement of protein using flow injection analysis with bicinchoninic acid. *Analytical Biochemistry*, 161(1), pp.152-156.

Deng, L., Kaeser, P., Xu, W. and Südhof, T., (2011). RIM Proteins Activate Vesicle Priming by Reversing Autoinhibitory Homodimerization of Munc13. *Neuron*, 69(2), pp.317-331.

Distler JH, Jungel A, Kurowska-Stolarska M, Michel BA, Gay RE, Gay S, Distler, O., (2005). Nucleofection: A new, highly efficient transfection method for primary human keratinocytes*. *Experimental Dermatology*, 14(4), pp.315–320.

Dobie, F.A., Craig, A.M. (2011). Inhibitory synapse dynamics: coordinated presynaptic and postsynaptic mobility and the major contribution of recycled vesicles to new synapse formation. *Journal of Neuroscience*, 31(29), pp.10481–10493.

Dong, N., Qi, J. and Chen, G. (2007). Molecular reconstitution of functional GABAergic synapses with expression of neuroligin-2 and GABAA receptors. *Molecular and Cellular Neuroscience*, 35(1), pp.14-23.

Do-Rego, J., Mensah-Nyagan, A., Feuilloley, M., Ferrara, P., Pelletier, G. and Vaudry, H. (1998). The endozepine triakontatetraneuropeptide diazepam-binding inhibitor [17–50] stimulates neurosteroid biosynthesis in the frog hypothalamus. *Neuroscience*, 83(2), pp.555-570.

Douglas, K., Piccirillo, C. and Tabrizian, M., (2008). Cell line-dependent internalization pathways and intracellular trafficking determine transfection efficiency of nanoparticle vectors. *European Journal of Pharmaceutics and Biopharmaceutics*, 68(3), pp.676-687.

Duan, J., Pandey, S., Li, T., Castellano, D., Gu, X., Li, J., Tian, Q. and Lu, W. (2019). Genetic Deletion of GABAA Receptors Reveals Distinct Requirements of Neurotransmitter Receptors for GABAergic and Glutamatergic Synapse Development. *Frontiers in Cellular Neuroscience*, 13.

Duggan, M. and Stephenson, F., 1990. Biochemical evidence for the existence of gamma-aminobutyrate A receptor iso-oligomers. *Journal of Biological Chemistry*, 265(7), pp.3831-3835.

Dumitru, I., Neitz, A., Alfonso, J. and Monyer, H. (2017). Diazepam Binding Inhibitor Promotes Stem Cell Expansion Controlling Environment-Dependent Neurogenesis. *Neuron*, 94(1), pp.125-137.e5.

Dunn, H., Orlandi, C. and Martemyanov, K., (2019). Beyond the Ligand: Extracellular and Transcellular G Protein–Coupled Receptor Complexes in Physiology and Pharmacology. *Pharmacological Reviews*, 71(4), pp.503-519.

Essrich, C., Lorez, M., Benson, J., Fritschy, J. and Lüscher, B. (1998). Postsynaptic clustering of major GABAA receptor subtypes requires the γ2 subunit and gephyrin. *Nature Neuroscience*, 1(7), pp.563-571.

Farrant, M., Nusser, Z., (2005). Variations on an inhibitory theme: Phasic and tonic activation of GABA A receptors. *Nature Reviews Neuroscience*, 6, pp.215-229.

Farzampour, Z., Reimer, R. and Huguenard, J. (2015). Endozepines. *Diversity and Functions of GABA Receptors: A Tribute to Hanns Möhler, Part A*, pp.147-164.

Fernández-Alfonso, T., Kwan, R. and Ryan, T. (2006). Synaptic Vesicles Interchange Their Membrane Proteins with a Large Surface Reservoir during Recycling. *Neuron*, 51(2), pp.179-186.

Fritschy, J. M., Panzanelli, P., Kralic, J. E., Vogt, K. E., and Sassoe-Pognetto, M. (2006). Differential dependence of axo-dendritic and axo-somatic GABAergic synapses on GABAA receptors containing the alpha1 subunit in Purkinje cells. *Journal of Neuroscience*, 26(12), 3245–3255.

Früh, S., Romanos, J., Panzanelli, P., Bürgisser, D., Tyagarajan, S.K., Campbell, K.P., Santello, M. and Fritschy, J.M. (2016). Neuronal Dystroglycan Is Necessary for Formation and Maintenance of Functional CCK-Positive Basket Cell Terminals on Pyramidal Cells. *The Journal of Neuroscience*, 36(40), pp.10296–10313.

Fuchs, C., Abitbol, K., Burden, J., Mercer, A., Brown, L., Iball, J., Anne, S. F., Thomson, A. and Jovanovic, J. (2013). $GABA_A$ receptors can initiate the formation of functional inhibitory GABAergic synapses. *European Journal of Neuroscience*, 38(8), pp.3146-3158.

Gallagher, JP., Higashi, H. & Nisiii, S. (1978). Characterization and ionic basis of GABAinduced depolarizations recorded in vitro from cat primary afferent neurones. *Journal of Physiology,* 275, pp.263-282.

Ge, Y., Kang, Y., Cassidy, R., Moon, K., Lewis, R., Wong, R., Foster, L. and Craig, A. (2018). Clptm1 Limits Forward Trafficking of GABAA Receptors to Scale Inhibitory Synaptic Strength. *Neuron*, 97(3), pp.596-610.e8.

George, T. and Tripp, J. (2019). *Alprazolam*. [online] Ncbi.nlm.nih.gov. Available at: https://www.ncbi.nlm.nih.gov/books/NBK538165/#article-17404.s1 [Accessed 16 Mar. 2019].

Ghit, A., Assal, D., Al-Shami, A. and Hussein, D., (2021). GABAA receptors: structure, function, pharmacology, and related disorders. *Journal of Genetic Engineering and Biotechnology*, 19(1).

Gomez-Castro, F., Zappettini, S., Pressey, J., Silva, C., Russeau, M., Gervasi, N., Figueiredo, M., Montmasson, C., Renner, M., Canas, P., Gonçalves, F., Alçada-Morais, S., Szabó, E., Rodrigues, R., Agostinho, P., Tomé, A., Caillol, G., Thoumine, O., Nicol, X., Leterrier, C., Lujan, R., Tyagarajan, S., Cunha, R., Esclapez, M., Bernard, C. and Lévi, S. (2021). Convergence of adenosine and GABA signaling for synapse stabilization during development. *Science*, 374(6568).

Goto H., Terunuma M., Kanematsu T., Misumi Y., Moss S.J., Hirata M. (2005). Direct interaction of N-ethylmaleimide-sensitive factor with GABA(A) receptor beta

subunits. *Molecular and Cellular Neuroscience,* 30(2), pp.197–206.

Gottschling, C., Wegrzyn, D., Denecke, B. and Faissner, A. (2019). Elimination of the four extracellular matrix molecules tenascin-C, tenascin-R, brevican and neurocan alters the ratio of excitatory and inhibitory synapses. *Scientific Reports*, 9(1).

Gracheva, E.O., Hadwiger, G., Nonet, M.L. and Richmond, J.E. (2008). Direct interactions between C. elegans RAB-3 and Rim provide a mechanism to target vesicles to the presynaptic density. *Neuroscience Letters*, 444(2), pp.137–142.

Graf, E.R., Zhang, X., Jin, S.-X., Linhoff, M.W. and Craig, A.M. (2004). Neurexins Induce Differentiation of GABA and Glutamate Postsynaptic Specializations via Neuroligins. *Cell*, 119(7), pp.1013–1026.

Gray, G. (1969). Electron Microscopy of Excitatory and Inhibitory Synapses: a Brief Review. *Progress in Brain Research*, 31, pp.141-155.

Groeneweg, F., Trattnig, C., Kuhse, J., Nawrotzki, R. and Kirsch, J. (2018). Gephyrin: a key regulatory protein of inhibitory synapses and beyond. *Histochemistry and Cell Biology*, 150(5), pp.489-508.

Guidotti, A., Forchetti, C., Corda, M., Konkel, D., Bennett, C. and Costa, E. (1983). Isolation, characterization, and purification to homogeneity of an endogenous polypeptide with agonistic action on benzodiazepine receptors. *Proceedings of the National Academy of Sciences*, 80(11), pp.3531-3535.

Haenggi, T. and Fritschy, J., (2006). Role of dystrophin and utrophin for assembly and function of the dystrophin glycoprotein complex in non-muscle tissue. *Cellular and Molecular Life Sciences*, 63(14), pp.1614-1631.

Han, W., Li, J., Pelkey, K., Pandey, S., Chen, X., Wang, Y., Wu, K., Ge, L., Li, T., Castellano, D., Liu, C., Wu, L., Petralia, R., Lynch, J., McBain, C. and Lu, W. (2019). Shisa7 is a GABA A receptor auxiliary subunit controlling benzodiazepine actions. *Science*, 366(6462), pp.246-250.

Hannan, S., Minere, M., Harris, J., Izquierdo, P., Thomas, P., Tench, B. and Smart,

T., (2020). GABAAR isoform and subunit structural motifs determine synaptic and extrasynaptic receptor localisation. *Neuropharmacology*, 169, p.107540.

Hausrat, T., Muhia, M., Gerrow, K., Thomas, P., Hirdes, W., Tsukita, S., Heisler, F., Herich, L., Dubroqua, S., Breiden, P., Feldon, J., Schwarz, J., Yee, B., Smart, T., Triller, A. and Kneussel, M. (2015). Radixin regulates synaptic GABAA receptor density and is essential for reversal learning and short-term memory. *Nature Communications*, 6(1).

Henry, M. and Campbell, K., (1996). Dystroglycan: an extracellular matrix receptor linked to the cytoskeleton. *Current Opinion in Cell Biology*, 8(5), pp.625-631.

Hoon, M., Soykan, T., Falkenburger, B., Hammer, M., Patrizi, A., Schmidt, K., Sassoe-Pognetto, M., Lowel, S., Moser, T., Taschenberger, H., Brose, N. and Varoqueaux, F., (2011). Neuroligin-4 is localized to glycinergic postsynapses and regulates inhibition in the retina. *Proceedings of the National Academy of Sciences*, 108(7), pp.3053-3058.

Hörtnagl, H., Tasan, R.O., Wieselthaler, A., Kirchmair, E., Sieghart, W. and Sperk, G. (2013). Patterns of mRNA and Protein Expression for 12 GABAA Receptor Subunits in the Mouse Brain. *Neuroscience*, [online] 236, pp.345–372.

Ibraghimov-Beskrovnaya, O., Ervasti, J., Leveille, C., Slaughter, C., Sernett, S. and Campbell, K. (1992). Primary structure of dystrophin-associated glycoproteins linking dystrophin to the extracellular matrix. *Nature*, 355(6362), pp.696-702.

Jacob, T., Bogdanov, Y., Magnus, C., Saliba, R., Kittler, J., Haydon, P. and Moss, S. (2005). Gephyrin Regulates the Cell Surface Dynamics of Synaptic GABAA Receptors. *Journal of Neuroscience*, 25(45), pp.10469-10478.

Jacob, T., Moss, S. and Jurd, R. (2008). GABAA receptor trafficking and its role in the dynamic modulation of neuronal inhibition. *Nature Reviews Neuroscience*, 9(5), pp.331-343.

Johnston, G.A.R. (1996). GABAC receptors: Relatively Simple transmitter-gated Ion channels? *Trends in Pharmacological Sciences*, 17(9), pp.319–323.

Jones A, Korpi ER, McKernan RM, Pelz R, Nusser Z, Ma¨ kela¨ R, Mellor JR, Pollard S, Bahn S, Stephenson FA, Randall AD, Sieghart W, Somogyi P, Smith AJ, Wisden W. (1997). Ligand-gated ion channel subunit partnerships: GABAA receptor alpha6 subunit gene inactivation inhibits delta subunit expression. *Journal of Neuroscience*, 17, pp.1350–1362.

Jordan, M. and Wurm, F. (2004). Transfection of Adherent and Suspended Cells by Calcium Phosphate. *Methods*, 33(2), pp.136–143.

Kavaliers, M. and Hirst, M. (1986). An octadecaneuropeptide (ODN) derived from diazepam binding inhibitor increases aggressive interactions in mice. *Brain Research*, 383(1-2), pp.343-349.

Keller, C., Yuan, X., Panzanelli, P., Martin, M., Alldred, M., Sassoè-Pognetto, M. and Lüscher, B. (2004). The γ2 Subunit of GABAA Receptors Is a Substrate for Palmitoylation by GODZ. *Journal of Neuroscience*, 24(26), pp.5881-5891.

Khazipov, R., Ragozzino, D. and Bregestovski, P., (1995). Kinetics and Mg2+ block of N-methyl- d-aspartate receptor channels during postnatal development of hippocampal CA3 pyramidal neurons. *Neuroscience*, 69(4), pp.1057-1065.

Kilpatrick C.L., Murakami S., Feng M., Wu X., Lal R., Chen G., Du K., Luscher B. (2016). Dissociation of Golgi-associated DHHC-type Zinc Finger Protein (GODZ)- and Sertoli Cell Gene with a Zinc Finger Domain-β (SERZ-β)- Mediated Palmitoylation by Loss of Function Analyses in Knockout Mice. *Journal of Biological Chemistry*, 291(53), pp.2737l–27386.

Kim, H., Kim, D., Kim, J., Lee, H.-Y., Park, D., Kang, H., Matsuda, K., Sterky, F.H., Yuzaki, M., Kim, J.Y., Choi, S.-Y., Ko, J. and Um, J.W. (2020). Calsyntenin-3 interacts with both α- and β-neurexins in the regulation of excitatory synaptic innervation in specific Schaffer collateral pathways. *Journal of Biological Chemistry*, 295(27), pp.9244–9262.

Kim, J.J., Gharpure, A., Teng, J., Zhuang, Y., Howard, R.J., Zhu, S., Noviello, C.M., Walsh, R.M., Lindahl, E. and Hibbs, R.E. (2020). Shared Structural Mechanisms of General Anaesthetics and Benzodiazepines. *Nature*, [online] 585(7824), pp.303–308.

Kins, S., Betz, H. and Kirsch, J., (2000). Collybistin, a newly identified brain-specific GEF, induces submembrane clustering of gephyrin. *Nature Neuroscience*, 3(1), pp.22-29.

Kittler, J., Chen, G., Kukhtina, V., Vahedi-Faridi, A., Gu, Z., Tretter, V., Smith, K., McAinsh, K., Arancibia-Carcamo, I., Saenger, W., Haucke, V., Yan, Z. and Moss, S. (2008). Regulation of synaptic inhibition by phospho-dependent binding of the AP2 complex to a YECL motif in the GABAA receptor γ2 subunit. *Proceedings of the National Academy of Sciences*, 105(9), pp.3616-3621.

Kittler, J., Delmas, P., Jovanovic, J., Brown, D., Smart, T. and Moss, S. (2000). Constitutive Endocytosis of GABAA Receptors by an Association with the Adaptin AP2 Complex Modulates Inhibitory Synaptic Currents in Hippocampal Neurons. *The Journal of Neuroscience*, 20(21), pp.7972-7977.

Kneussel, M., Brandstätter, J., Gasnier, B., Feng, G., Sanes, J.R. and Betz, H. (2001). Gephyrin-Independent Clustering of Postsynaptic GABAA Receptor Subtypes. *Molecular and Cellular Neuroscience*, 17(6), pp.973–982.

Kneussel, M., Brandstätter, J., Laube, B., Stahl, S., Müller, U. and Betz, H. (1999). Loss of Postsynaptic $GABA_A$ Receptor Clustering in Gephyrin-Deficient Mice. *Journal of Neuroscience*, 19(21), pp.9289-9297.

Knudsen, J. (1991). Acyl-CoA-binding and transport, an alternative function for diazepam binding inhibitor (DBI), which is identical with acyl-CoA-binding protein. *Neuropharmacology*, 30(12), pp.1405-1410.

Koehnke, J., Jin, X., Budreck, E., Posy, S., Scheiffele, P., Honig, B. and Shapiro, L., (2008). Crystal structure of the extracellular cholinesterase-like domain from neuroligin-2. *Proceedings of the National Academy of Sciences*, 105(6), pp.1873-1878.

Krasowski, M., Rick, C., Harrison, N., Firestone, L. and Homanics, G., (1998). A Deficit of Functional GABAA Receptors in Neurons of β3 Subunit Knockout Mice. *Neuroscience Letters*, 240(2), pp.81-84.

Krishek B.J., Moss S.J., Smart T.G. (1996). Homomeric beta 1 gamma-

aminobutyric acid A receptor-ion channels: evaluation of pharmacological and physiological properties. *Molecular Pharmacology*, 49(3), pp.494– 504.

Kuzirian, M. and Paradis, S. (2011). Emerging themes in GABAergic synapse development. *Progress in Neurobiology*, 95(1), pp.68-87.

Laverty, D., Desai, R., Uchański, T., Masiulis, S., Stec, W.J., Malinauskas, T., Zivanov, J., Pardon, E., Steyaert, J., Miller, K.W. and Aricescu, A.R. (2019). Cryo-EM Structure of the Human α1β3γ2 GABAA Receptor in a Lipid Bilayer. *Nature*, 565(7740), pp.516–520.

Leal-Ortiz, S., Waites, C., Terry-Lorenzo, R., Zamorano, P., Gundelfinger, E. and Garner, C., (2008). Piccolo modulation of Synapsin1a dynamics regulates synaptic vesicle exocytosis. *Journal of Cell Biology*, 181(5), pp.831-846.

Lee, K., Kim, Y., Lee, S., Qiang, Y., Lee, D., Lee, H., Kim, H., Je, H., Südhof, T. and Ko, J. (2012). MDGAs Interact Selectively with Neuroligin-2 but not other Neuroligins to Regulate Iinhibitory Synapse Development. *Proceedings of the National Academy of Sciences*, 110(1), pp.336-341.

Leil T.A., Chen Z.W., Chang C.S., Olsen R.W. (2004). GABAA receptor-associated protein traffics GABAA receptors to the plasma membrane in neurons. *Journal of Neuroscience*, 24(50), pp.11429–11438.

Leinekugel, X., Tseeb, V., Ben-Ari, Y. and Bregestovski, P. (1995). Synaptic GABAA activation induces Ca2+ rise in pyramidal cells and interneurons from rat neonatal hippocampal slices. *The Journal of Physiology*, 487(2), pp.319-329.

Lenzi, D. and von Gersdorff, H. (2001). Structure suggests function: the case for synaptic ribbons as exocytotic nanomachines. *BioEssays*, 23(9), pp.831–840.

Leonard, R., Labarca, C., Charnet, P., Davidson, N. and Lester, H., (1988). Evidence That the M2 Membrane-Spanning Region Lines the Ion Channel Pore of the Nicotinic Receptor. *Science*, 242(4885), pp.1578-1581.

Lévi, S., Grady, R., Henry, M., Campbell, K., Sanes, J. and Craig, A., (2002).

Dystroglycan Is Selectively Associated with Inhibitory GABAergic Synapses But Is Dispensable for Their Differentiation. *The Journal of Neuroscience*, 22(11), pp.4274-4285.

Levinson, J., Li, R., Kang, R., Moukhles, H., El-Husseini, A. and Bamji, S., (2010). Postsynaptic scaffolding molecules modulate the localization of neuroligins. *Neuroscience*, 165(3), pp.782-793.

Li, H.Q., and N.C. Spitzer. (2020). Exercise enhances motor skill learning by neurotransmitter switching in the adult midbrain. *Nature Communications*, 11(1), 2195.

Liang, J., Suryanarayanan, A., Chandra, D., Homanics, G., Olsen, R. and Spigelman, I., (2007). Functional Consequences of GABAA Receptor α4 Subunit Deletion on Synaptic and Extrasynaptic Currents in Mouse Dentate Granule Cells. *Alcoholism: Clinical and Experimental Research*, 32(1), pp.19-26.

Lobo, I. and Harris, R. (2008). GABAA receptors and alcohol. *Pharmacology Biochemistry and Behavior*, 90(1), pp.90-94.

Loebrich, S., Bähring, R., Katsuno, T., Tsukita, S., & Kneussel, M. (2006). Activated radixin is essential for GABAA receptor alpha5 subunit anchoring at the actin cytoskeleton. *The EMBO Journal*, 25(5), pp.987–999.

Lorenz-Guertin, J. and Jacob, T. (2017). GABA type a receptor trafficking and the architecture of synaptic inhibition. *Developmental Neurobiology*, 78(3), pp.238-270.

Lu, W., Bromley-Coolidge, S. and Li, J., (2017). Regulation of GABAergic synapse development by postsynaptic membrane proteins. *Brain Research Bulletin*, 129, pp.30-42.

Lukasiewicz, P.D. (1996). GABAC Receptors in the Vertebrate Retina. *Molecular Neurobiology*, 12(3), pp.181–194.

Luo, F., Sclip, A., Jiang, M. and Südhof, T.C. (2020). Neurexins Cluster Ca2+ Channels within the Presynaptic Active Zone. *The EMBO Journal*, 39(7).

Maher, B. and Westbrook, G. (2008). Co-Transmission of Dopamine and GABA in

Periglomerular Cells. *Journal of Neurophysiology*, 99(3), pp.1559-1564.

Malenka, R. C., and Bear, M. F. (2004). LTP and LTD: an embarrassment of riches. *Neuron*, 44(1), pp.5–21.

Manders, E., Stap, J., Brakenhoff, G., van Driel, R. and Aten, J., (1992). Dynamics of three-dimensional replication patterns during the S-phase, analysed by double labeling of DNA and confocal microscopy. *Journal of Cell Science*, 103(3), pp.857-862.

Martenson, J. S., Yamasaki, T., Chaudhury, N. H., Albrecht, D., & Tomita, S. (2017). Assembly rules for $GABA_A$ receptor complexes in the brain. *eLife*, *6*, e27443.

Masiulis, S., Desai, R., Uchański, T., Serna Martin, I., Laverty, D., Karia, D., Malinauskas, T., Zivanov, J., Pardon, E., Kotecha, A., Steyaert, J., Miller, K. and Aricescu, A. (2019). GABAA receptor signalling mechanisms revealed by structural pharmacology. *Nature*, 565(7740), pp.454-459.

Masmoudi-Kouki, O., Hamdi, Y., Ghouili, I., Bahdoudi, S., Kaddour, H., Leprince, J., Castel, H., Vaudry, H., Amri, M., Vaudry, D. and Tonon, M., (2019). Neuroprotection with the Endozepine Octadecaneuropeptide, ODN. *Current Pharmaceutical Design*, 24(33), pp.3918-3925.

Mayer, S., Kumar, R., Jaiswal, M., Soykan, T., Ahmadian, M., Brose, N., Betz, H., Rhee, J. and Papadopoulos, T., (2013). Collybistin activation by GTP-TC10 enhances postsynaptic gephyrin clustering and hippocampal GABAergic neurotransmission. *Proceedings of the National Academy of Sciences*, 110(51), pp.20795-20800.

Mayford, M., Siegelbaum, S. A., and Kandel, E. R. (2012). Synapses and memory storage. *Cold Spring Harbor Perspectives in Biology,* 4(6), a005751.

Mele, M., Leal, G. and Duarte, C. (2016). Role of GABAAR trafficking in the plasticity of inhibitory synapses. *Journal of Neurochemistry*, 139(6), pp.997-1018.

Miller, D. and Wright, K., (2021). Neuronal Dystroglycan regulates postnatal development of CCK/cannabinoid receptor-1 interneurons. *Neural Development*, 16(1).

Miller, P. and Aricescu, A. (2014). Crystal structure of a human GABAA receptor. *Nature*, 512(7514), pp.270-275.

Missler, M., Südhof, T. C. & Biederer, T. Synaptic cell adhesion. (2012). *Cold Spring Harbor Perspectives in Biology*, 4(4), a005694.

Missler, M., Zhang, W., Rohlmann, A., Kattenstroth, G., Hammer, R., Gottmann, K. and Südhof, T. (2003). α-Neurexins couple Ca2+ channels to synaptic vesicle exocytosis. *Nature*, 423(6943), pp.939-948.

Mohler, H., Knoflach, F., Paysan, J., Motejlek, K., Benke, D., Lüscher, B. and Fritschy, J., (1995). Heterogeneity of GABAA-receptors: cell-specific expression, pharmacology, and regulation. *Neurochemical Research*, 20(5), pp.631-636.

Moore, S., Saito, F., Chen, J., Michele, D., Henry, M., Messing, A., Cohn, R., Ross-Barta, S., Westra, S., Williamson, R., Hoshi, T. and Campbell, K., (2002). Deletion of brain dystroglycan recapitulates aspects of congenital muscular dystrophy. *Nature*, 418(6896), pp.422-425.

Mortensen, M., and Smart, T. G. (2006). Extrasynaptic αβ subunit $GABA_A$ receptors on rat hippocampal pyramidal neurons. *J. Physiol. (Lond.)* 577, 841–856.

Mortensen, M., Patel, B. and Smart, T. (2012). GABA Potency at GABAA Receptors Found in Synaptic and Extrasynaptic Zones. *Frontiers in Cellular Neuroscience*, 6(1), pp.1-10.

Mukherjee, J., Kretschmannova, K., Gouzer, G., Maric, H.-M. ., Ramsden, S., Tretter, V., Harvey, K., Davies, P.A., Triller, A., Schindelin, H. and Moss, S.J. (2011). The Residence Time of GABAARs at Inhibitory Synapses Is Determined by Direct Binding of the Receptor α 1 Subunit to Gephyrin. *Journal of Neuroscience*, 31(41), pp.14677–14687.

Mukherjee, K., Yang, X., Gerber, S., Kwon, H., Ho, A., Castillo, P., Liu, X. and Südhof, T. (2010). Piccolo and bassoon maintain synaptic vesicle clustering without directly participating in vesicle exocytosis. *Proceedings of the National Academy of*

Sciences, 107(14), pp.6504-6509.

Nelson, R., Schaffner, A.E., Li, Y.-X. and Walton, M.K. (1999). Distribution of GABAC-like Responses among Acutely Dissociated Rat Retinal Neurons. *Visual Neuroscience*, 16(1), pp.179–190.

Nguyen, Q. and Nicoll, R. (2018). The GABAA Receptor β Subunit Is Required for Inhibitory Transmission. *Neuron*, 98(4), pp.718-725.e3.

Nicholson, M., Sweeney, A., Pekle, E., Alam, S., Ali, A., Duchen, M. and Jovanovic, J. (2018). Diazepam-induced loss of inhibitory synapses mediated by PLCδ/ Ca2+/calcineurin signalling downstream of GABAA receptors. *Molecular Psychiatry*, 23(9), pp.1851-1867.

Nusser Z, Sieghart W, Somogyi P. (1998). Segregation of different GABAA receptors to synaptic and extrasynaptic membranes of cerebellar granule cells. *Journal of Neuroscience*, 18, pp.1693–1703.

Nusser, Z., Sieghart, W. and Somogyi, P. (1998). Segregation of Different GABAAReceptors to Synaptic and Extrasynaptic Membranes of Cerebellar Granule Cells. *The Journal of Neuroscience*, 18(5), pp.1693-1703.

O'Neill, N. and Sylantyev, S. (2018). Spontaneously opening GABAA receptors play a significant role in neuronal signal filtering and integration. *Cell Death & Disease*, 9(8).

O'Sullivan G.A., Kneussel M., Elazar Z., Betz H. (2005). GABARAP is not essential for GABA receptor targeting to the synapse. *European Journal of Neuroscience*, 22(10), pp.2644–2648.

Oh, W., Lutzu, S., Castillo, P. and Kwon, H. (2016). De novo synaptogenesis induced by GABA in the developing mouse cortex. *Science*, 353(6303), pp.1037-1040.

Olsen, R. and Sieghart, W. (2008). International Union of Pharmacology. LXX. Subtypes of γ-Aminobutyric $Acid_A$ Receptors: Classification on the Basis of Subunit Composition, Pharmacology, and Function. Update. *Pharmacological Reviews*, 60(3),

pp.243-260.

Omori, Y., Araki, F., Chaya, T., Kajimura, N., Irie, S., Terada, K., Muranishi, Y., Tsujii, T., Ueno, S., Koyasu, T., Tamaki, Y., Kondo, M., Amano, S. and Furukawa, T. (2012). Presynaptic Dystroglycan-Pikachurin Complex Regulates the Proper Synaptic Connection between Retinal Photoreceptor and Bipolar Cells. *Journal of Neuroscience*, 32(18), pp.6126-6137.

Ooi, A., Wong, A., Esau, L., Lemtiri-Chlieh, F. and Gehring, C. (2016). A Guide to Transient Expression of Membrane Proteins in HEK-293 Cells for Functional Characterization. *Frontiers in Physiology*, 7(300).

Orlandi, C., Omori, Y., Wang, Y., Cao, Y., Ueno, A., Roux, M., Condomitti, G., de Wit, J., Kanagawa, M., Furukawa, T. and Martemyanov, K. (2018). Transsynaptic Binding of Orphan Receptor GPR179 to Dystroglycan-Pikachurin Complex Is Essential for the Synaptic Organization of Photoreceptors. *Cell Reports*, 25(1), pp.130-145.e5.

Orlandi, C., Omori, Y., Wang, Y., Cao, Y., Ueno, A., Roux, M.J., Condomitti, G., de Wit, J., Kanagawa, M., Furukawa, T. and Martemyanov, K.A. (2018). Transsynaptic Binding of Orphan Receptor GPR179 to Dystroglycan-Pikachurin Complex Is Essential for the Synaptic Organization of Photoreceptors. *Cell Reports*, 25(1), pp.130-145.e5.

Panzanelli, P., Früh, S. and Fritschy, J. (2017). Differential role of GABAA receptors and neuroligin 2 for perisomatic GABAergic synapse formation in the hippocampus. *Brain Structure and Function*, 222(9), pp.4149-4161.

Panzanelli, P., Gunn, B.G., Schlatter, M.C., Benke, D., Tyagarajan, S.K., Scheiffele, P., Belelli, D., Lambert, J.J., Rudolph, U. and Fritschy, J.-M. (2011). Distinct mechanisms regulate $GABA_A$receptor and gephyrin clustering at perisomatic and axo-axonic synapses on CA1 pyramidal cells. *The Journal of Physiology*, 589(20), pp.4959–4980.

Paolicelli, R., Bolasco, G., Pagani, F., Maggi, L., Scianni, M., Panzanelli, P., Giustetto, M., Ferreira, T., Guiducci, E., Dumas, L., Ragozzino, D. and Gross, C. (2011). Synaptic Pruning by Microglia Is Necessary for Normal Brain Development. *Science*, 333(6048), pp.1456-1458.

Papadopoulos, T., Eulenburg, V., Reddy-Alla, S., Mansuy, I., Li, Y. and Betz, H. (2008). Collybistin is required for both the formation and maintenance of GABAergic postsynapses in the hippocampus. *Molecular and Cellular Neuroscience*, 39(2), pp.161-169.

Patrizi, A., Scelfo, B., Viltono, L., Briatore, F., Fukaya, M., Watanabe, M., et al. (2008). Synapse formation and clustering of neuroligin-2 in the absence of GABAA receptors. *Proceedings of the National Academy of Sciences of the United States of American*, 105(35), pp.13151–13156.

Pennacchietti, F., Vascon, S., Nieus, T., Rosillo, C., Das, S., Tyagarajan, S.K., Diaspro, A., Del Bue, A., Petrini, E.M., Barberis, A. and Cella Zanacchi, F. (2017). Nanoscale Molecular Reorganization of the Inhibitory Postsynaptic Density is a Determinant of GABAergic Synaptic Potentiation. *The Journal of Neuroscience*, 37(7), pp.1747–1756.

Perucca, E. (2005). An Introduction to Antiepileptic Drugs. *Epilepsia*, 46, pp.31-37.

Pettem, K., Yokomaku, D., Takahashi, H., Ge, Y. and Craig, A. (2013b). Interaction between Autism-linked MDGAs and Neuroligins Suppresses Inhibitory Synapse Development. *Journal of Cell Biology*, 200(3), pp.321-336.

Pettem, Katherine L., Yokomaku, D., Luo, L., Linhoff, Michael W., Prasad, T., Connor, Steven A., Siddiqui, Tabrez J., Kawabe, H., Chen, F., Zhang, L., Rudenko, G., Wang, Y., Brose, N. and Craig, A. (2013a). The Specific α-Neurexin Interactor Calsyntenin-3 Promotes Excitatory and Inhibitory Synapse Development. *Neuron*, 80(1), pp.113–128.

Phulera, S., Zhu, H., Yu, J., Claxton, D.P., Yoder, N., Yoshioka, C. and Gouaux, E. (2018). Cryo-EM Structure of the benzodiazepine-sensitive α1β1γ2S tri-heteromeric GABAA Receptor in Complex with GABA. *eLife*, 7.

Pilgram, G., Potikanond, S., Baines, R., Fradkin, L. and Noordermeer, J. (2009). The Roles of the Dystrophin-Associated Glycoprotein Complex at the Synapse. *Molecular Neurobiology*, 41(1), pp.1-21.

Poulopoulos, A., Aramuni, G., Meyer, G., Soykan, T., Hoon, M., Papadopoulos, T., Zhang, M., Paarmann, I., Fuchs, C., Harvey, K., Jedlicka, P., Schwarzacher, S., Betz, H., Harvey, R., Brose, N., Zhang, W. and Varoqueaux, F. (2009). Neuroligin 2 Drives Postsynaptic Assembly at Perisomatic Inhibitory Synapses through Gephyrin and Collybistin. *Neuron*, 63(5), pp.628-642.

Poulopoulos, A., Soykan, T., Tuffy, L., Hammer, M., Varoqueaux, F. and Brose, N., (2012). Homodimerization and isoform-specific heterodimerization of neuroligins. *Biochemical Journal*, 446(2), pp.321-330.

Prior, P., Schmitt, B., Grenningloh, G., Pribilla, I., Multhaup, G., Beyreuther, K., Maulet, Y., Werner, P., Langosch, D., Kirsch, J. and Betz, H. (1992). Primary structure and alternative splice variants of gephyrin, a putative glycine receptor-tubulin linker protein. *Neuron*, 8(6), pp.1161–1170.

Pritchett, D.B., Sontheimer, H., Shivers, B.D., Ymer, S., Kettenmann, H., Schofield, P.R., and Seeburg, P.H., (1989). Importance of a novel Gabaa receptor subunit for benzodiazepine pharmacology. *Nature*, 338(6216), pp.582–585.

Reissner, C., Runkel, F. and Missler, M. (2013). Neurexins. *Genome Biology*, 14(9), p.213.

Reissner, C., Stahn, J., Breuer, D., Klose, M., Pohlentz, G., Mormann, M. and Missler, M. (2014). Dystroglycan Binding to α-Neurexin Competes with Neurexophilin-1 and Neuroligin in the Brain. *Journal of Biological Chemistry*, 289(40), pp.27585–27603.

Root, D.H., Mejias-Aponte, C.A., Zhang, S., Wang, H.-L., Hoffman, A.F., Lupica, C.R. and Morales, M. (2014). Single Rodent Mesohabenular Axons Release Glutamate and GABA. *Nature Neuroscience*, 17(11), pp.1543–1551.

Root, D.H., Zhang, S., Barker, D.J., Miranda-Barrientos, J., Liu, B., Wang, H.-L. and Morales, M. (2018). Selective Brain Distribution and Distinctive Synaptic Architecture of Dual Glutamatergic-GABAergic Neurons. *Cell Reports*, 23(12), pp.3465–3479.

Rubenstein, J.L.R. and Merzenich, M.M. (2003). Model of autism: Increased Ratio of excitation/inhibition in Key Neural Systems. *Genes, Brain and Behavior*, [online] 2(5),

pp.255–267.

Sabo, S., Gomes, R. and McAllister, A. (2006). Formation of Presynaptic Terminals at Predefined Sites along Axons. *Journal of Neuroscience*, 26(42), pp.10813-10825.

Saliba R.S., Michels G., Jacob T.C., Pangalos M.N., Moss S.J. (2007). Activity-dependent ubiquitination of GABA(A) receptors regulates their accumulation at synaptic sites. *Journal of Neuroscience*, 27(48), pp.13341–13351.

Sander, B., Tria, G., Shkumatov, A.V., Kim, E.-Y., Grossmann, J.G., Tessmer, I., Svergun, D.I. and Schindelin, H. (2013). Structural characterization of gephyrin by AFM and SAXS reveals a mixture of compact and extended states. *Acta Crystallographica Section D Biological Crystallography*, 69(10), pp.2050–2060.

Sassoè-Pognetto, M., Frola, E., Pregno, G., Briatore, F. and Patrizi, A. (2011). Understanding the Molecular Diversity of GABAergic Synapses. *Frontiers in Cellular Neuroscience*, 5.

Sato, S., Omori, Y., Katoh, K., Kondo, M., Kanagawa, M., Miyata, K., Funabiki, K., Koyasu, T., Kajimura, N., Miyoshi, T., Sawai, H., Kobayashi, K., Tani, A., Toda, T., Usukura, J., Tano, Y., Fujikado, T. and Furukawa, T. (2008). Pikachurin, a dystroglycan ligand, is essential for photoreceptor ribbon synapse formation. *Nature Neuroscience*, 11(8), pp.923-931.

Scheiffele, P., Fan, J., Choih, J., Fetter, R. and Serafini, T. (2000). Neuroligin Expressed in Nonneuronal Cells Triggers Presynaptic Development in Contacting Axons. *Cell*, 101(6), pp.657-669.

Schröder, J., Tegeler, M., Groβhans, U., Porten, E., Blank, M., Lee, J., Esapa, C., Blake, D. and Kröger, S. (2007). Dystroglycan regulates structure, proliferation and differentiation of neuroepithelial cells in the developing vertebrate CNS. *Developmental Biology*, 307(1), pp.62-78.

Schuemann, A., Klawiter, A., Bonhoeffer, T., Wierenga, C.J. (2013). Structural plasticity of GABAergic axons is regulated by network activity and GABAA receptor activation. *Frontiers in Neural Circuits*, 7(113).

Schweizer, C., Balsiger, S., Bluethmann, H., Mansuy, I., Fritschy, J., Mohler, H. and Luscher, B. (2003). The γ2 subunit of GABAA receptors is required for maintenance of receptors at mature synapses. *Molecular and Cellular Neuroscience*, 24(2), pp.442-450.

Shivers, B. D., Killisch, I., Sprengel, R., Sontheimer, H., Köhler, M., Schofield, P. R., & Seeburg, P. H. (1989). Two novel GABAA receptor subunits exist in distinct neuronal subpopulations. *Neuron*, *3*(3), pp.327–337.

Shoar, N. and Saadabadi, A. (2019). *Flumazenil*. [online] Ncbi.nlm.nih.gov. Available at: https://www.ncbi.nlm.nih.gov/books/NBK470180/ [Accessed 15 Feb. 2019].

Sieghart, W. (2015). Allosteric Modulation of GABAA Receptors via Multiple Drug-Binding Sites. *Diversity and Functions of GABA Receptors: A Tribute to Hanns Möhler, Part A*, pp.53-96.

Sieghart, W. and Sperk, G. (2002). Subunit Composition, Distribution and Function of GABA-A Receptor Subtypes. *Current Topics in Medicinal Chemistry*, 2(8), pp.795-816.

Sigel, E. and Ernst, M. (2018). The Benzodiazepine Binding Sites of GABA A Receptors. *Trends in Pharmacological Sciences*, 39(7), pp.659-671.

Sigel, E. and Steinmann, M. (2012). Structure, Function, and Modulation of GABAA Receptors. *Journal of Biological Chemistry*, 287(48), pp.40224-40231.

Slobodyansky, E., Guidotti, A., Wambebe, C., Berkovich, A. and Costa, E. (1989). Isolation and Characterization of a Rat Brain Triakontatetraneuropeptide, a Posttranslational Product of Diazepam Binding Inhibitor: Specific Action at the Ro 5-4864 Recognition Site. *Journal of Neurochemistry*, 53(4), pp.1276-1284.

Soghomonian, J. and Martin, D. (1998). Two isoforms of glutamate decarboxylase: why?. *Trends in Pharmacological Sciences*, 19(12), pp.500-505.

Sola, M., Bavro, V.N., Timmins, J., Franz, T., Ricard-Blum, S., Schoehn, G., Ruigrok, R.W.H., Paarmann, I., Saiyed, T., O'Sullivan, G.A., Schmitt, B., Betz, H. and Weissenhorn, W. (2004). Structural basis of dynamic glycine receptor clustering by gephyrin. *The EMBO Journal*, 23(13), pp.2510–2519.

Somogyi, P., Fritschy, J.-M., Benke, D., Roberts, J.D.B. and Sieghart, W. (1996). The γ2 Subunit of the GABA a Receptor Is Concentrated in Synaptic Junctions Containing the α1 and B 23 Subunits in Hippocampus, Cerebellum and Globus Pallidus. *Neuropharmacology*, 35(9-10), pp.1425–1444.

Song, J., Ichtchenko, K., Sudhof, T. and Brose, N. (1999). Neuroligin 1 is a postsynaptic cell-adhesion molecule of excitatory synapses. *Proceedings of the National Academy of Sciences*, 96(3), pp.1100-1105.

Sontheimer, H., Shivers, B. D., Ymer, S., Kettenmann, H., Schofield, P. R., & Seeburg, P. H. (1989). Importance of a novel GABA(A) receptor subunit for benzodiazepine pharmacology. *Nature*, *338*(April), pp.582–585.

Soykan, T., Schneeberger, D., Tria, G., Buechner, C., Bader, N., Svergun, D., Tessmer, I., Poulopoulos, A., Papadopoulos, T., Varoqueaux, F., Schindelin, H. and Brose, N. (2014). A conformational switch in collybistin determines the differentiation of inhibitory postsynapses. *The EMBO Journal*, 33(18), pp.2113-2133.

Specht, Christian G., Izeddin, I., Rodriguez, Pamela C., El Beheiry, M., Rostaing, P., Darzacq, X., Dahan, M. and Triller, A. (2013). Quantitative Nanoscopy of Inhibitory Synapses: Counting Gephyrin Molecules and Receptor Binding Sites. *Neuron*, 79(2), pp.308–321.

Spitzer, N.C. (2017). Neurotransmitter Switching in the Developing and Adult Brain. *Annual Review of Neuroscience*, 40, pp.1–19.

Strata, P. and Harvey, R. (1999). Dale's Principle. *Brain Research Bulletin*, 50(5-6), pp.349–350.

Studer, R., von Boehmer, L., Haenggi, T., Schweizer, C., Benke, D., Rudolph, U. and Fritschy, J.-M. (2006). Alteration of GABAergic Synapses and Gephyrin Clusters in the Thalamic Reticular Nucleus of GABAAreceptor α3 subunit-null Mice. *European Journal of Neuroscience*, 24(5), pp.1307–1315.

Südhof, T. (2012). The Presynaptic Active Zone. *Neuron*, 75(1), pp.11-25.

Südhof, T. (2017). Synaptic Neurexin Complexes: A Molecular Code for the Logic of Neural Circuits. *Cell*, 171(4), pp.745-769.

Südhof, T. (2018). Towards an Understanding of Synapse Formation. *Neuron*, 100(2), pp.276-293.

Südhof, T. (2021). The cell biology of synapse formation. *Journal of Cell Biology*, 220(7).

Sugita, S., Saito, F., Tang, J., Satz, J., Campbell, K. and Südhof, T.C. (2001). A Stoichiometric Complex of Neurexins and Dystroglycan in Brain. *Journal of Cell Biology*, 154(2), pp.435–446.

Sumita, K., Sato, Y., Iida, J., Kawata, A., Hamano, M., Hirabayashi, S., Ohno, K., Peles, E. and Hata, Y. (2007). Synaptic scaffolding molecule (S-SCAM) membrane-associated guanylate kinase with inverted organization (MAGI)-2 is associated with cell adhesion molecules at inhibitory synapses in rat hippocampal neurons. *Journal of Neurochemistry*, 100(1), pp.154-166.

Sur, C., Farrar, S., Kerby, J., Whiting, P., Atack, J. and McKernan, R. (1999). Preferential Coassembly of α4 and δ Subunits of the γ-Aminobutyric AcidA Receptor in Rat Thalamus. *Molecular Pharmacology*, 56(1), pp.110-115.

Suter, T.A.C.S. and Jaworski, A. (2019). Cell Migration and Axon Guidance at the Border between Central and Peripheral Nervous System. *Science*, 365(6456), p.eaaw8231.

Takács, V., Cserép, C., Schlingloff, D., Pósfai, B., Szőnyi, A., Sos, K., Környei, Z., Dénes, Á., Gulyás, A., Freund, T. and Nyiri, G. (2018). Co-transmission of acetylcholine and GABA regulates hippocampal states. *Nature Communications*, 9(1).

Takahashi, H., Katayama, K., Sohya, K., Miyamoto, H., Prasad, T., Matsumoto, Y., Ota, M., Yasuda, H., Tsumoto, T., Aruga, J. and Craig, A.M. (2012). Selective control of inhibitory synapse development by Slitrk3-PTPδ trans-synaptic interaction. *Nature Neuroscience*, 15(3), pp.389–398.

Tepper, J.M., Abercrombie, E.D. and Bolam, J.P. (2007). Basal Ganglia Macrocircuits. *Progress in Brain Research*, 16, pp.3-7.

Thomas, P. and Smart, T. (2005). HEK293 cell line: A vehicle for the expression of recombinant proteins. *Journal of Pharmacological and Toxicological Methods*, 51(3), pp.187-200.

Tretter, V., Jacob, T., Mukherjee, J., Fritschy, J., Pangalos, M. and Moss, S. (2008). The Clustering of GABAA Receptor Subtypes at Inhibitory Synapses is Facilitated via the Direct Binding of Receptor alpha2 Subunits to Gephyrin. *Journal of Neuroscience*, 28(6), pp.1356-1365.

Tretter, V., Kerschner, B., Milenkovic, I., Ramsden, S., Ramerstorfer, J., Saiepour, L., Maric, H., Moss, S., Schindelin, H., Harvey, R., Sieghart, W. and Harvey, K. (2011). Molecular Basis of the γ-Aminobutyric Acid A Receptor α3 Subunit Interaction with the Clustering Protein Gephyrin. *Journal of Biological Chemistry*, 286(43), pp.37702-37711.

Tyagarajan, S.K., Fritschy, J.M. (2014). Gephyrin: a master regulator of neuronal function? *Nature Reviews Neuroscience*, 15(3), pp.141–156.

Ullrich, B., Ushkaryov, Y.A. and Südhof, T.C. (1995). Cartography of neurexins: More than 1000 Isoforms Generated by Alternative Splicing and Expressed in Distinct Subsets of Neurons. *Neuron*, 14(3), pp.497–507.

Um, J., Pramanik, G., Ko, J., Song, M.-Y., Lee, D., Kim, H., Park, K.-S., Südhof, Thomas C., Tabuchi, K. and Ko, J. (2014). Calsyntenins Function as Synaptogenic Adhesion Molecules in Concert with Neurexins. *Cell Reports*, 6(6), pp.1096–1109.

Ushkaryov, Y., Petrenko, A., Geppert, M. and Südhof, T. (1992). Neurexins: Synaptic Cell Surface Proteins Related to the α-Latrotoxin Receptor and Laminin. *Science*, 257(5066), pp.50-56.

Varoqueaux, F., Aramuni, G., Rawson, R.L., Mohrmann, R., Missler, M., Gottmann, K., Zhang, W., Südhof, T.C. and Brose, N. (2006). Neuroligins Determine Synapse Maturation and Function. *Neuron*, 51(6), pp.741–754.

Varoqueaux, F., Jamain, S. and Brose, N. (2004). Neuroligin 2 is exclusively localized to inhibitory synapses. *European Journal of Cell Biology*, 83(9), pp.449-456.

Waite, A., Brown, S. and Blake, D. (2012). The dystrophin–glycoprotein complex in brain development and disease. *Trends in Neurosciences*, 35(8), pp.487-496.

Wang, H., Bedford, F., Brandon, N., Moss, S. and Olsen, R. (1999). GABAA-receptor-associated protein links GABAA receptors and the cytoskeleton. *Nature*, 397(6714), pp.69-72.

Wang, R., Dong, J., Wang, L., Dong, X., Anenberg, E., Jiang, P., Zeng, L. and Xie, Y. (2019). A negative regulator of synaptic development: MDGA and its links to neurodevelopmental disorders. *World Journal of Pediatrics*, 15(5), pp.415-421.

Wierenga, C. (2017). Live imaging of inhibitory axons: Synapse formation as a dynamic trial-and-error process. *Brain Research Bulletin*, 129, pp.43-49.

Wierenga, C., Becker, N. and Bonhoeffer, T. (2008). GABAergic synapses are formed without the involvement of dendritic protrusions. *Nature Neuroscience*, 11(9), pp.1044-1052.

Wisden, W., Herb, A., Wieland, H., Keinänen, K., Lüddens, H., & Seeburg, P. H. (1991). Cloning, pharmacological characteristics and expression pattern of the rat GABAA receptor α4 subunit. *FEBS Letters*, *289*(2), pp.227–230.

Wlodarczyk, A., Sylantyev, S., Herd, M., Kersante, F., Lambert, J., Rusakov, D., Linthorst, A., Semyanov, A., Belelli, D., Pavlov, I. and Walker, M. (2013). GABA-Independent GABAA Receptor Openings Maintain Tonic Currents. *Journal of Neuroscience*, 33(9), pp.3905-3914.

Wong, L., Tae, H. and Cromer, B. (2015). Assembly, trafficking and function of α1β2γ2 GABAA receptors are regulated by N-terminal regions, in a subunit-specific manner. *Journal of Neurochemistry*, 134(5), pp.819-832.

Woo, J., Kwon, S., Nam, J., Choi, S., Takahashi, H., Krueger, D., Park, J., Lee, Y., Bae, J., Lee, D., Ko, J., Kim, H., Kim, M., Bae, Y., Chang, S., Craig, A. and Kim, E.,

(2013). The adhesion protein IgSF9b is coupled to neuroligin 2 via S-SCAM to promote inhibitory synapse development. *Journal of Cell Biology*, 201(6), pp.929-944.

Wooltorton J.R., Moss S.J., Smart T.G. (1997). Pharmacological and physiological characterization of murine homomeric beta3 GABA(A) receptors. *European Journal of Neuroscience*, 9(11), pp.2225–2235.

Wu, B. and Zhang, C., (2011). Neurexins and neuroligins: new partners for GABAA receptors at synapses. *Frontiers in Biology*, 6(3).

Wu, X., Wu, Z., Ning, G., Guo, Y., Ali, R., Macdonald, R., De Blas, A., Luscher, B. and Chen, G., (2012). γ-Aminobutyric Acid Type A (GABAA) Receptor α Subunits Play a Direct Role in Synaptic Versus Extrasynaptic Targeting. *Journal of Biological Chemistry*, 287(33), pp.27417-27430.

Xiang, S., Kim, E., Connelly, J., Nassar, N., Kirsch, J., Winking, J., Schwarz, G. and Schindelin, H., (2006). The Crystal Structure of Cdc42 in Complex with Collybistin II, a Gephyrin-interacting Guanine Nucleotide Exchange Factor. *Journal of Molecular Biology*, 359(1), pp.35-46.

Yamada, J., Okabe, A., Toyoda, H., Kilb, W., Luhmann, H.J. and Fukuda, A. (2004). Cl^-uptake Promoting Depolarizing GABA Actions in Immature Rat Neocortical Neurones Is Mediated by NKCC1. *The Journal of Physiology*, 557(3), pp.829–841.

Yamasaki, T., Hoyos-Ramirez, E., Martenson, J., Morimoto-Tomita, M. and Tomita, S. (2017). GARLH Family Proteins Stabilize GABA A Receptors at Synapses. *Neuron*, 93(5), pp.1138-1152.e6.

Yasumura Y., Kawakita M., (1963). The research for the SV40 by means of tissue culture technique. *Nippon Rinsho*, 21, pp.1201-1219

Ye, J., Zou, G., Zhu, R., Kong, C., Miao, C., Zhang, M., Li, J., Xiong, W. and Wang, C. (2021). Structural basis of GABARAP-mediated GABAA receptor trafficking and functions on GABAergic synaptic transmission. *Nature Communications*, 12(1).

Yim, Y.S., Kwon, Y., Nam, J., Yoon, H.I., Lee, K., Kim, D.G., Kim, E., Kim, C.H. and

Ko, J. (2013). Slitrks control excitatory and inhibitory synapse formation with LAR receptor protein tyrosine phosphatases. *Proceedings of the National Academy of Sciences*, 110(10), pp.4057–4062.

Yoon, B. and Lee, C. (2014). GABA as a rising gliotransmitter. *Frontiers in Neural Circuits*, 8.

Zaccaria, M.L., Di Tommaso, F., Brancaccio, A., Paggi, P. and Petrucci, T.C. (2001). Dystroglycan Distribution in Adult Mouse brain: a Light and Electron Microscopy Study. *Neuroscience*, 104(2), pp.311–324.

Zarnowska ED., Keist R., Rudolph U. and Pearce RA. (2009). GABAA receptor alpha5 subunits contribute to $GABA_{A,}$slow synaptic inhibition in mouse hippocampus. *Journal of Neurophysiol*, 101(3), pp.1179-91.

Zhang, B., Chen, Lulu Y., Liu, X., Maxeiner, S., Lee, S.-J., Gokce, O. and Südhof, Thomas C. (2015). Neuroligins Sculpt Cerebellar Purkinje-Cell Circuits by Differential Control of Distinct Classes of Synapses. *Neuron*, 87(4), pp.781–796.

Zhang, C., Atasoy, D., Araç, D., Yang, X., Fucillo, M., Robison, A., Ko, J., Brunger, A. and Südhof, T. (2010). Neurexins Physically and Functionally Interact with GABAA Receptors. *Neuron*, 66(3), pp.403-416.

Zhang, N., Wei, W., Mody, I. and Houser, C. (2007). Altered Localization of GABAA Receptor Subunits on Dentate Granule Cell Dendrites Influences Tonic and Phasic Inhibition in a Mouse Model of Epilepsy. *Journal of Neuroscience*, 27(28), pp.7520-7531.

Zhen, M. and Jin, Y. (2004). Presynaptic Terminal Differentiation: Transport and Assembly. *Current Opinion in Neurobiology*, 14(3), pp.280–287.

Zhu, S., Noviello, C., Teng, J., Walsh, R., Kim, J. and Hibbs, R. (2018). Structure of a human synaptic GABAA receptor. *Nature*, 559(7712), pp.67-72.

Zuber, B. and Lučić, V. (2019). Molecular architecture of the presynaptic terminal. *Current Opinion in Structural Biology*, 54, pp.129–138.

Zuber, B., Nikonenko, I., Klauser, P., Muller, D. and Dubochet, J. (2005). The

Mammalian Central Nervous Synaptic Cleft Contains a High Density of Periodically Organized Complexes. *Proceedings of the National Academy of Sciences*, [online] 102(52), pp.19192–19197.